Universitat Autònoma de Barcelona

RAD51 AS FUNCTIONAL BIOMARKER TO SELECT TUMORS FOR PARP INHIBITOR TREATMENT

Marta Castroviejo Bermejo

RAD51 AS FUNCTIONAL BIOMARKER TO SELECT TUMORS FOR PARP INHIBITOR TREATMENT

DOCTORAL THESIS

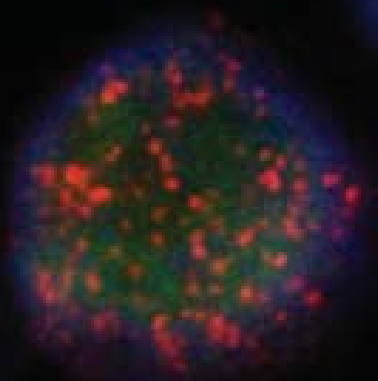

Marta Castroviejo Bermejo

Barcelona, 2019

RAD51 as functional biomarker to select tumors for PARP inhibitor treatment

DOCTORAL THESIS

Marta Castroviejo Bermejo

Experimental Therapeutics Group

Vall d'Hebron Institute of Oncology (VHIO)

Director: Dr. Violeta Serra Elizalde and Dr. Mercè Martí Ripoll

Tutor: Dr. José Miguel Lizcano de Vega

PhD program in Biochemistry, Molecular Biology and Biomedicine

Departament of Biochemistry and Molecular Biology

Universidad Autónoma de Barcelona (UAB)

Barcelona, 2019

The directors **Dr. Violeta Serra Elizalde** and **Dr. Mercè Martí Ripoll** and the tutor **Dr. José Miguel Lizcano de Vega**,

Certify:

That the experimental work and the writing of the memory of this doctoral thesis entitled "RAD51 as functional biomarker to select tumors for PARP inhibitor treatment" have been performed by Marta Castroviejo Bermejo under their supervision and consider that it is suitable to be presented for the degree of Doctor of Philosophy (PhD) in Biochemistry, Molecular Biology and Biomedicine by Universidad Autónoma de Barcelona

Barcelona, 2019

PhD Candidate

Marta Castroviejo Bermejo

Directors

Dr. Violeta Serra Elizalde and **Dr. Mercè Martí Ripoll**

Tutor

Dr. José Miguel Lizcano de Vega

Al tío Nano

ACKNOWLEDGEMENTS

Decía Newton que pudo mirar tan lejos porque se aupó a hombros de gigantes. Yo escribo hoy estas líneas para dejar aquí, en público, los nombres de todos aquellos que, de una u otra manera, me han cedido sus hombros durante este camino para hacerlo posible.

Mi primer agradecimiento es para alguien tan especial que cualquier palabra de gratitud se queda corta: **Xabi**, con quien comparto los miedos y las alegrías, las preocupaciones y las certezas. Por tu paciencia, inteligencia y generosidad. Por comprenderme siempre y compartir conmigo todas las historias que vivo, pienso y a veces incluso sueño, también la de nuestra vida.

A mi **padre**, por ser siempre mi maestro y guía en la ciencia del alma. A mi **madre**, por ser ejemplo de tenacidad, valentía y superación. A mi **hermana**, porque quizás lo primero que me enseñaste fue a leer, pero a eso se añade una larga lista en continuo crecimiento, de la que destacaría tu enorme empatía y generosidad. A los tres, juntos, por rodearme siempre, como el bosque a un árbol, y atarme al suelo incluso cuando sopla el viento. Por hacerme comprender que no tengo en el mundo otro deber que la alegría.

A toda mi **familia**, Castroviejos, Bermejos, Rodríguez y "pegados", por confiar en mí más que yo misma, desde bien pequeñita, y no dejar de hacerlo nunca. A todos los que estáis y a los que faltan, cuyo hueco es imposible llenar, pero que dejan paso a la ilusión de los que llegan nuevos. Porque no he podido pasar todo el tiempo que quisiera con vosotros durante esta vorágine profesional, pero, aún estando lejos, siempre estáis presentes en mis valores y en cada acto, en cada decisión diaria que tomo.

No puedo dejar de dar un gracias largo y extenso, como las horas que hemos compartido, a mis compañeros del laboratorio de Terapias Experimentales. A **Martis**, por tu pasión hacia lo que haces y el impulso creativo de tu genial humor. A **Albert**, por acogerme con tanto cariño (a pesar de ser de Logroño) y por esas miradas de complicidad previas a un ataque de risa. Y de risas va la cosa cuando pienso en ti, **Judit**; gracias por tu alegría inagotable y, sobre todo, contagiosa, que hace que no pase un solo día sin dibujar una sonrisa. A **Alba**, por darme tu ejemplo de trabajo y honradez, y por sostener esta mesa aun cuando las patas se tambaleaban. A **Moniqueta**, por siempre ofrecer tu ayuda y caminar junto a mí en esta etapa. A **Olguita**, por divertirnos con tus despistes. A **Guzmi**, por tu trabajo, ayuda y comprensión. Y también a los recién llegados, como **Laia**; aunque me hacen sentir que el tiempo pasa muy deprisa, alegran a cualquiera con la ilusión y ganas con las que aterrizan.

A **Violeta**, por tu generosidad al aceptarme en el equipo y durante todo mi aprendizaje, por tu asesoramiento y experiencia, por tu paciencia para leer y corregir mis extensos textos. Siempre me ha emocionado el apoyo y comprensión que he recibido de ti durante estos años, por lo que siempre, siempre, te deberé un mayúsculo ¡GRACIAS!

A **Cristi**, por confiar en mí como aprendiz, permitir que absorbiera como una esponja tu conocimiento y por ser ejemplo de incansable y vibrante esfuerzo y valentía. En estos años he intentado darte el mejor homenaje que puede tributarse a las personas buenas, imitarlas.

A **Bene**, mi hermanita italiana. Llegaste inundando todo con tu ilusión y así te convertiste en la fuerza que me empujó a seguir luchando cuando quise rendirme. Gracias por enseñarme que, con esfuerzo e ilusión, todo es posible; o no, pero eso no es lo importante.

Y a toda la gente del **VHIO**, por estar siempre tan unidos compartiendo la aventura científica (y no tan científica). En especial quiero agradecer a los *runners*, que despertaron en mí esa afición, pilar hoy de mi vida, y con los que he recorrido kilómetros muy especiales.

Sin mis estudios no habría podido realizar este proyecto y por eso doy gracias a mis profesores, en especial aquellos que supieron avivar en mí la pasión por aprender. Mis compañeros de clase, mis amigos del colegio, instituto y carrera. A mi **Anus**, por nuestra complicidad, siempre y en todo. A mi **Nunu**, por desprender esa bonita ilusión tuya por cada cosa que haces. A **Miguel**, **Lidoy**, **Iria** e **Itsaso**, por acompañarme y hacer de mis años de estudiante una etapa preciosa de mi vida.

Y no puedo dejar de mencionar a mi gente de Logroño. A mi **Aji**, desde pequeñita a mi lado y siempre en él. A los **tenistas**, por aguantarme esas tardes en las que repasaba mis exámenes mientras ensayaba la derecha. A mis compañeros de carreras, el equipo **Ferrer**, que se alegran tanto o más de mis logros en la ciencia que de los del asfalto.

También quiero agradecer a todos los pacientes, profesionales sanitarios, donantes, instituciones e investigadores, que juntos trabajan para hacer del cáncer una enfermedad curable, y sin los cuales este trabajo no tendría sentido. Quiero dar las gracias especialmente a la Junta Provincial de Barcelona de la Asociación Española Contra el Cáncer por apostar por mi proyecto y hacerlo posible.

Y por qué no, acabaré agradeciéndome a mí misma, por esos momentos oscuros y noches de duda; porque cuando pensaba que no podía continuar, valió la pena intentarlo y ahora puedo decir: sí, pudiste.

INDEX

ABBREVIATIONS

53BP1	p53 binding protein 1
ABC	ATP-binding cassette
ABCB1	ATP-binding cassette B member 1
ANOVA	Analysis of variance
ATCC	American type culture collection
ATM	Ataxia telangiectasia-mutated protein kinase
ATR	ATM and Rad3-related protein kinase
AUC	Area under the curve
BARD1	BRCA1-associated RING domain protein 1
BC	Breast cancer
BCL-2	B-cell lymphoma 2
BCL-XL	B-cell lymphoma-extra large
BER	Base excision repair
BRCA1	Breast cancer growth suppressor protein 1
BRCA2	Breast cancer growth suppressor protein 2
BRCT	BRCA1 C-terminal domain
BRIP1	BRCA1-interacting protein C-terminal helicase 1
BSA	Bovine serum albumin
BWA	Burrows-Wheeler Alignment
CCNB1	Cyclin B1
CDK1	Cyclin-dependent kinase 1
CDK12	Cyclin-dependent kinase 12
CDK2	Cyclin-dependent kinase 2
CGAS	Cyclic GMP-AMP (cGAMP) synthase
CHD4	Chromodomain helicase DNA 4
CHEK1	Checkpoint Kinase 1
CHEK1i	Checkpoint Kinase 1 inhibitor
CHK1	Checkpoint Kinase 1
CHK2	Checkpoint Kinase 2
CI	Confidence Interval
COSMIC	Catalogue of somatic mutations in cancer

CR	Complete response
CRPC	Castration resistant prostate cancer
CtBP	C-terminal binding protein
CtIP	CtBP-interacting protein
DAB	3,3'-Diaminobenzidine
DAPI	4',6-diamino-2-fenilindo
DDR	DNA damage response
DLBCL	Diffuse large B-cell lymphoma
DMEM	Dulbecco modified Eagles minimal essential medium
DMSO	Dimethyl sulfoxide
DNA	Deoxyribonucleic acid
DNA-PK	DNA-activated protein kinase
DSB	Double strand brake
ECL	Enhanced chemiluminescence
EDTA	Ethylenediaminetetraacetic acid
ELK	Embryonic leucine zipper kinase
EMA	European Medicines Agency
EMT	Epithelial-to-mesenchymal transition
ER	Estrogen receptor
ERBB2	Erythroblastic oncogene B2
EXO1	Exonuclease 1
EZH2	Enhancer of zester homolog 2
FAM175A	Family with sequence similarity 175 member A
FAM35A	Family with sequence similarity 35 member A
FANC	Fanconi anemia complementation group
FANCD2	Fanconi anemia complementation group D2
FBS	Fetal bovine serum
FDA	Food and Drug Administration
FFPE	Formalin-fixed and paraffin-embedded
FGF	Fibroblast growth factors
FRAP	Fluorescence recovery after photobleaching

fs	frameshift
GAPDH	Glyceraldehyde 3-phosphate dehydrogenase
GFP	Green fluorescent protein
H2AX	Histone 2AX
HBOC	Hereditary breast and ovarian cancer
HER2	Human epidermal growth factor receptor 2
HGSOC	High grade serous ovarian cancer
HH3	Histone H3
HRD	Homologous recombination deficiency
HRP	Horseadish peroxidase
HRR	Homologous recombination repair
HSP90	Heat shock protein 90
IF	Immunofluorescence
IGF-1	Insulin-like growth factor 1
IGF-1R	Insulin-like growth factor 1 receptor
IR	Ionizing radiation
LKB1	Liver kinase B1
LMNA	Lamin A
LOH	Loss of heterozygosity
LST	Large-scale transitions
MDC1	Mediator of DNA damage checkpoint 1
MDR1	Multidrug resistance protein 1
MELK	Maternal embryonic leucine zipper kinase
MHC	Major histocompatibility complex
MHC-I	Major histocompatibility complex class I
MLL3	Mixed-lineage leukemia protein 3
MLL4	Mixed-lineage leukemia protein 4
MLPA	Multiplex ligation-dependent probe amplification
MS-MLPA	Methylation-specific MLPA
MRE11	Meiotic recombination 11
MYT1	Myelin Transcription Factor 1

n	Number of replicates
Na_2VO_4	Sodium orthovanadate
NaCl	Sodium chloride
NaF	Sodium fluoride
NBN	Nibrin
NBS1	Nijmegen breakage syndrome protein 1
NES	Nuclear export signal
NF2	Neurofibromin 2
NGS	Next generation sequencing
NHEJ	Non-homologous end-joining
c-NHEJ	Conservative NHEJ
alt-NHEJ	Alternative NHEJ
NLS	Nuclear localization sequence
NMRI	Naval Medical Research Institute
NOD/SCID	Non-obese diabetic / Severe combined immunodeficiency
NK	Natural killer
OC	Ovarian cancer
OR	Odds Ratio
ORF	Open reading frame
p value	Probability value
P/S	Penicillin / Streptomycin
p21	Protein 21
p27	Protein 27
p53	Protein 53
PALB2	Partner and localizer of BRCA2
PAR	Poly-ADP ribose
PARG	Poly-ADP ribose glycohydrolase
PARP	Poly-ADP ribose polymerase
PAXIP1	PAX Interacting Protein 1
PBS	Phosphate buffered saline
PBST	Phosphate buffered saline-Tween

PC	Prostate cancer
PCR	Polymerase chain reaction
RT-PCR	Real time PCR
PD	Progressive disease
PDL1	Programmed death-ligand 1
PDX	Patient derived xenograft
PFS	Progression free survival
PgP	P-glycoprotein
PgR	Progesterone receptor
pH	Potential of hydrogen
PI3K	Phosphatidylinositol 3-kinase
PMSF	Phenylmethane sulfonyl fluoride
PR	Partial response
PRCC	Proline rich mitotic checkpoint control factor
PTIP	PAX transactivation domain-interacting protein
PVDF	Polyvinylidene difluoride
RAP80	Receptor associated protein 80
RECIST	Response Evaluation Criteria In Solid Tumors
mRECIST	Modified RECIST
RIF1	Rap1-interacting protein 1
RING	Really Interesting New Gene
RIPA	Radioimmunoprecipitation assay
RNA	Ribonucleic acid
miRNA	Micro RNA
mRNA	Messenger RNA
siRNA	Small interfering RNA
RNF8	RING finger protein 8
ROC	Receiver operating characteristic
RPA	Replication protein A
RPPA	Reverse phase protein array
RRM2	Ribonucleotide reductase subunit M2

s	seconds
SCLC	Small cell lung cancer
SD	Stable disease
SDS-PAGE	Sodium dodecyl sulfate polyacrylamide gel electrophoresis
SEM	Standard error of the mean
SHFM1	Split hand/split foot protein 1
SHLD1	Shieldin complex subunit 1
SHLD2	Shieldin complex subunit 2
SHLD3	Shieldin complex subunit 3
SL	Synthetic Lethality
SLFN11	Schlafen Family Member 11
SSB	Single strand brake
TAI	Telomeric allelic imbalance
TBS	Tris buffered saline
TBST	TBS Tween
TGF-β	Transforming growth factor beta
TNBC	Triple negative breast cancer
TOPBP1	Topoisomerase 2-binding protein 1
TP53	Tumor protein 53
Treg	T regulatory
TSP-1	Thrombospondin 1
Tyr	Tyrosine
UV	Ultraviolet
VEGF-A	Vascular endothelial growth factor A
WEE1	Small cell protein, a mitotic inhibitor kinase
WES	Whole-exome sequencing
WT	Wild type
XRCC1	X-ray repair cross-complementing group 1
YFP	Yellow fluorescent protein
Zeb1	Zinc finger E-box binding homeobox 1
Zeb2	Zinc finger E-box binding homeobox 2

ABSTRACT

Poly(ADP-ribose) polymerase (PARP) inhibitors (PARPi) are effective anticancer drugs in cancers with defective homologous recombination DNA repair (HRR), including cancers with mutations in *BRCA1* and *BRCA2 (BRCA1/2),* which also display enhanced sensitivity to DNA damaging chemotherapy such as platinum salts. Several mechanisms of PARPi resistance have been described in tumors with germline mutations in *BRCA1/2* (gBRCA) and there are also other tumors with wild type *BRCA1/2* (non-BRCA) that benefit from PARPi treatment. Therefore, there is a need to develop robust biomarkers to better select HRR-deficient tumors and extend the use of PARP inhibition in new indications, as well as identify PARPi-resistant tumors and study combination treatment options that enhance clinical efficacy and utility of PARPi.

We evaluated the activity of the PARPi olaparib in patient-derived tumor xenografts (PDXs) from patients with breast or ovarian cancer, both with and without gBRCA mutation, exhibiting differential response to PARPi. We studied the *in vivo* mechanisms of PARPi resistance and sensitivity in these models and tested the formation of RAD51 nuclear foci by immunofluorescence as biomarker of HRR functionality and PARPi response in PDXs and routine clinical samples. We also tested the antitumor activity of the WEE1i AZD1775 and the ATMi AZD0156 as single agent and in combination with PARPi in PDXs. The measurement of replication stress biomarkers was assessed to study the mechanisms of action of these treatment strategies.

Within the gBRCA PDXs panel, no *BRCA1/2* secondary mutations were found in the PARPi resistant models. BRCA1 nuclear foci were detected in six out of ten PARPi-resistant PDXs, in keeping with expression of hypomorphic BRCA1 isoforms. Loss of 53BP1 and FAM35A were identified in three PDXs, one of which concomitantly expressed an hypomorphic BRCA1 protein. The common feature in all PDXs with primary or acquired PARPi resistance was the formation of RAD51 nuclear foci. Consistently, lack of RAD51 foci was always associated with clinical response to PARPi in patients treated with these agents. When studying the mechanisms of PARPi sensitivity in the non-gBRCA PDX cohort, *BRCA1* promoter hypermethylation and alterations in HRR-related genes were found in PARPi-sensitive models. Again, the unique common feature in all PDXs that exhibited tumor

regression upon PARPi treatment is the absence of RAD51 nuclear foci. The RAD51 assay could be performed in untreated samples and was highly discriminative of PARPi sensitivity versus PARPi resistance in different PDX cohorts and outperformed the Myriad's myChoice® HRD genomic test. In routine clinical samples from patients with hereditary breast and ovarian cancer (HBOC) syndrome, all PALB2-related tumors were classified as HRR-deficient by the RAD51 score. In PDXs, PARPi resistance in BRCA1-altered tumors could be reverted upon combination of PARPi with WEE1 or ATM inhibitors and both combination strategies resulted in exacerbated induction of replication stress (RS) in combination-sensitive PDXs.

With the results obtained in this thesis, it can be concluded that gBRCA tumors achieve PARPi resistance by several mechanisms that restore HRR function, all detected by the presence of RAD51 nuclear foci. This functional assay also enables the identification of PARPi-sensitive non-gBRCA tumors independently of the mechanisms of HRR-deficiency, thereby being a promising biomarker to better select patients for PARP inhibition and broaden the population who may benefit from this therapy. Our study also supports the clinical development of PARPi combinations such as those with WEE1 and ATM inhibitors and highlighted the induction of RS as the major mechanisms of action of these drugs.

RESUMEN

Los inhibidores de la enzima Poly (ADP-ribosa) polimerasa (PARPi) son efectivos en el tratamiento de cánceres que presentan defectos en la reparación del ADN por recombinación homóloga (HRR), incluyendo aquellos con mutaciones en los genes *BRCA1* y *BRCA2* (*BRCA1/2*), los cuales presentan también una mayor sensibilidad a quimioterapias que producen daño en el ADN, como las sales de platino. Se han descrito distintos mecanismos de resistencia a los PARPi en tumores con mutaciones germinales en *BRCA1/2* (gBRCA), mientras que, por otro lado, existen otros tumores sin mutaciones en *BRCA1/2* (no-BRCA) que se benefician del tratamiento con PARPi. Así, existe la necesidad de desarrollar un biomarcador robusto que permita una mejor selección de tumores deficientes en HRR para extender el uso de los PARPi a nuevas indicaciones, al mismo tiempo que se identifican tumores resistentes a la inhibición de PARP para estudiar terapias en combinación que mejoren la eficacia y uso de los PARPi en la clínica.

En este trabajo se evaluó la actividad del PARPi olaparib en xenoimplantes de tumores derivados de pacientes (PDX, *patient derived tumor xenografts*) con cáncer de mama u ovario, tanto gBRCA como no-gBRCA, mostrando una respuesta diferencial a la inhibición de PARP. En los modelos PDXs se estudiaron los mecanismos de resistencia y sensibilidad a PARPi *in vivo,* así como la utilidad de una técnica de inmunofluorescencia para detectar focos nucleares de RAD51 como biomarcador de la funcionalidad de HRR y respuesta a PARPi, tanto en PDXs como en muestras clínicas de rutina. Además, se investigó la actividad antitumoral del inhibidor de WEE1 AZD1775 y del inhibidor de ATM AZD0156 en monoterapia y en combinación con PARPi. Se investigaron los mecanismos de acción de estas estrategias terapéuticas utilizando distintos marcadores de estrés replicativo (RS, *replication stress*).

Entre los modelos PDX gBRCA resistentes a PARPi no se encontraron mutaciones secundarias en *BRCA1/2* como mecanismo de resistencia a la terapia. Sin embargo, se reportó la formación de focos nucleares de BRCA1 en seis de los diez modelos resistentes a PARPi, en concordancia con la expresión de proteínas BRCA1 hipomórficas. En tres PDX resistentes a PARPi, se identificó la pérdida de 53BP1 y FAM35A como mecanismo de resistencia, estando presente de forma conjunta con la expresión de una proteína BRCA1 hipomórfica en uno de los modelos. La única característica común a todos los PDXs

resistentes a PARPi, ya sea resistencia primaria o adquirida, fue la capacidad de formación de focos nucleares de la proteína RAD51. De acuerdo con estos resultados, la ausencia de focos de RAD51 se asoció con respuesta clínica a PARPi en muestras de pacientes tratadas con estos agentes. Cuando se estudiaron los mecanismos de sensibilidad a PARPi en la colección de PDXs no-gBRCA, se observó la presencia de hipermetilación del promotor de BRCA1 y alteraciones en otros genes relacionados con HRR en modelos sensibles a PARPi. Sin embargo, de nuevo la única característica común a todos los PDXs respondedores al tratamiento fue la ausencia de focos nucleares de RAD51. El ensayo de RAD51 se pudo realizar en muestras no tratadas y mostró ser altamente discriminativo entre sensibilidad y resistencia a PARPi, superando la capacidad predictiva del test genético myChoice® HRD de Myriad. En muestras clínicas de rutina procedentes de pacientes con síndrome de cáncer de mama y ovario hereditario (HBOC, *hereditary breast and ovarian cancer*), todos los tumores relacionados con mutaciones en *PALB2* se clasificaron como deficientes en HRR por el ensayo de RAD51. Finalmente, se demostró que la resistencia a la terapia con PARPi en tumores con alteraciones en *BRCA1* puede revertirse combinando estos agentes con un inhibidor de WEE1 o de ATM, y en ambas estrategias terapéuticas se reportó una mayor inducción de estrés replicativo en los PDX sensibles a la combinación.

Los resultados obtenidos en esta tesis doctoral permiten concluir que los tumores gBRCA logran la resistencia a PARPi mediante diferentes mecanismos que restauran la función de reparación del ADN por HRR, lo cual puede detectarse por la capacidad de formación de focos nucleares de la proteína RAD51. Este ensayo funcional también permite identificar tumores no-BRCA sensibles a PARPi, de forma independiente del mecanismo que produce la deficiencia en HRR. Por tanto, el ensayo de RAD51 representa un biomarcador prometedor para mejorar la selección de pacientes que puedan beneficiarse del tratamiento con PARPi, así como ampliar la población candidata a recibir esta terapia más allá de los cánceres relacionados con mutaciones en *BRCA1/2*. Los resultados reportados en este trabajo también impulsan el desarrollo clínico de estrategias terapéuticas que combinen los PARPi con inhibidores de WEE1 y ATM, destacando la inducción de estrés replicativo como principal mecanismo de acción de estos fármacos.

INTRODUCTION

1. CARCINOGENESIS

Human organisms are composed of multiple cells that continuously interact to ensure a normal function and development. In mature, healthy human cells, differentiation is irreversible and cells replicate and die to maintain the integrity of the different tissues, which are constantly renewed. When an aged cell can no longer function normally, it activates an effectively suicide called apoptosis to die and keep tissues healthy. On the other hand, tissue stem cells retain the ability to differentiate into different types of mature cells and are the responsible to ensure the cellular turnover[1].

Normal cell cycle

The cell cycle is a highly regulated process by which a cell divides. In each cycle of cell division, the DNA is replicated by copying its nucleotide sequence in a process that is vulnerable to introduce errors. Furthermore, cells are constantly exposed to DNA damaging factors, both exogenous (radiation, chemicals) and endogenous (free radicals), which may cause DNA damage that needs to be repaired to prevent the transmission and avoid the accumulation of cells with these lesions. To get this objective, a normal cell cycle is monitored at checkpoints that sense errors in the DNA sequence and stop the progression through the cell cycle until all damages are repaired. However, the processes involved in DNA repair are not always perfect and eventually, cells with errors in the DNA, called mutations, may appear.

Key cellular processes relevant for cancer

Cancer develops when the processes that regulate cell behavior fail as a result of mutations that transform a normal cell into a cancer cell. This cell becomes therefore the ancestor of a group of cells that share its functional abnormalities. Mutant genes associated with carcinogenesis are often categorized as tumor suppressor genes or oncogenes.

Tumor suppressor genes are critically important genes that codify for proteins involved in suppression of cell proliferation and cell growth (e.g. p53, p21 and p27), maintain cell differentiation, edit and repair DNA damage (e.g. BRCA1 and BRCA2) and promote apoptosis (e.g. FOCO family). All these processes are key in preventing the cell cycle progression with errors, so if these genes are inactivated through a "loss-of-function" alteration, either by mutation or through epigenetic changes, cancer development is a greater possibility[2].

On the other hand, oncogenes are abnormally functioning versions of genes (called proto-oncogenes) that are typically involved in the activation of growth, replication and survival signals as well as the inhibition of apoptosis[3,4]. "Gain-of-function" alterations on proto-oncogenes promote the activation of the oncogenes, which results in unregulated proliferation, growth advantage and prolonged survival. This group of genes include growth factors (e.g. *IGF-1*) and growth factor receptors (e.g. *ERBB2*, *IGF-1R*), signal transducers (e.g. *PI3KCA*, *AKT1*), transcription factors (e.g. *ER*, *Fos*, *c-Jun*), chromatin remodelers and apoptosis regulators (e.g. *BCL-2*, *BCL-XL*)[3].

As each normal cell has two copies of the same gene, a mutation in just one copy is sufficient for activation of an oncogene to induce aberrant cancer behavior. However, both copies must be altered to lose the function of tumor suppressor genes and have a carcinogenic impact. Therefore, oncogenes are typically viewed as dominant mutations, while cancer-causing mutations in tumor suppressor genes are considered to be recessive mutations.

Cancer-associated mutations have also been classified as "drivers" mutations, which provide selective growth advantage, and "passenger" mutations that contribute to tumorigenesis and clonal selection but do not provides any selective growth advantage[5–7]. Thus, an initial "driver" mutation produces the development of a dysplasic lesion from a normal cell, but it is still benign. Tumor progression to malignant in situ carcinoma and invasive tumor result from the accumulation of passenger mutations that provide the cell with the characteristic biologic features of cancer cells[6–8].

Over the last years it has become clear that, despite the variety of possible mutations that can combine to promote cancer, most cancers display a much narrower range of functional changes. These phenotypical characteristics that unifies the molecular pathways contributing to the fundamental properties of cancer cells have been termed the "hallmarks of cancer"[4,9]. Some of the "hallmarks of cancer" are evident early in the course of carcinogenesis while others may not characterize premalignant conditions but the last step of carcinogenesis[6,10–15] (**Fig.1**). The current model identifies eight phenotypical characteristics, which are all involved with disordered control of cell function, along with two more fundamental enabling characteristics[4,6,9]:

- **Sustained proliferative signaling**. While normal cells require growth signals that activate proliferation, malignant cells acquire the capacity to proliferate without these external stimuli. Mechanisms by which cancer cells acquire this capacity include the activation of oncogenes, self-production of growth factors, stimulation of tumor-associated stroma to also produce more growth factors or amplification of mitogen receptors. As a consequence, cell proliferation is sustained and uncontrolled, leading to tumor development.

- **Resisting cell death.** Cancer cells evade the process of apoptosis despite the presence of errors in the DNA or specific signals that induce the programmed-cell death. This characteristic of tumor cells is achieved by the alteration of any components of the apoptotic machinery, both the sensors of extracellular signals and intracellular condition, and effectors that signal and execute the cell death program.

- **Evading growth suppressors.** Besides the capacity of sustained proliferation, cancer cells also negatively regulate cell proliferation by circumventing programs that many times depend on the activity of tumor suppressor proteins (e.g. RB, p53). As a consequence, cancer cells lose the balance between proliferation, senescence and apoptosis. Other mechanism related with this evasion capability is the inhibition of cell-to-cell contact that leads to lose the capacity of cells to maintain tissue architecture (e.g. the product of the *NF2* gene, suppression of *LKB1* expression). Finally, corruption of the TGF-β pathway allows cancer cells to evade its antiproliferative effects and promotes malignancy.

- **Enabling replicative immortality.** Normal cells are able to pass through only a limited number of successive cell division cycles, a limitation that is associated with two barriers: senescence, a typically irreversible entrance into a non-proliferative state, and crisis, which involves cell death. It is well accepted that telomeres degradation in each cell division is responsible of the replicative limit of normal cells. In contrast, cancer cells become immortal, so telomeres maintenance is necessary and, therefore, telomerase activity appears to be a common feature.

- **Inducing angiogenesis.** Tumors, as normal tissues, require sustained uptake of nutrients and oxygen and also evacuate metabolic wastes and carbon dioxide. Therefore, while tumor mass enlarges, the formation of new vasculature is necessary to supply these necessities and angiogenesis is activated. This angiogenic state is governed by changing the balance between angiogenic inducers (e.g. VEGF-A, FGF) and inhibitors (e.g. TSP-1).

- **Activating invasion and metastasis.** When carcinomas arising from epithelial tissues progress to local invasion and metastasis, cancer cells alter their shape and attachment to other cells and extracellular matrix. The acquisition of the abilities to invade, resist apoptosis and disseminate has been called the "epithelial-mesenchymal transition" (EMT), a multifaceted program that can be activated transiently or stably by carcinoma cells during invasion and metastasis. Alteration of different proteins (e.g. E-cadherin, N-cadherin, Snail, Slug, Twist, Zeb1/2), together with the crosstalk between cancer cells and stromal cells, permit these cellular changes, and the travel and invasion of other tissues.

- **Avoiding immune destruction.** It is proposed that cells are continuously monitored by the immune system to recognize and eliminate every incipient cancer cell. According with this, tumor cells need to avoid the immune surveillance to survive, so cancer cells are able to trigger negative signals (e.g. TGF-β) on immune cells and reverse activation and infiltration of cytotoxic immune cells[4,16–18]. Other common features in cancer cells related with this emerging hallmark are the recruitment of immunosuppressive cells such as regulatory T cells (Tregs), the downregulation of major histocompatibility complex class I (MHC-I) and the expression of ligands for inhibitory receptors present in immune cells[19,20].

- **Deregulating cellular energetics.** The uncontrolled cell proliferation of a tumor requires the reprogramming of energy metabolism to fuel the rapid cell growth. Thus, even in the presence of oxygen, cancer cells can limit the energy metabolism to glycolysis, that results in the production of intermediates used in pathways such as amino acid and nucleoside generation, and, therefore, facilitates the biosynthesis of macromolecules and organelles required to cell proliferation. Moreover, it has been proposed the existence of a symbiotic relation between cancer cells, which produce lactate, and other cell population that use this lactate in the citric acid cycle. This cooperation between cells that differ in their energy-generating pathways helps to support the continuous tumor growth.

- **Enabling characteristic: genomic instability and mutation.** Acquisition of the multiple capacities described above is highly dependent on genomic alterations in cancer cells. In the course of acquiring the multiple hallmarks, cancer cells increase the rates of mutation through both increasing the sensitivity to mutagenic agents and altering the genomic maintenance machinery[21–24]. Thus, it is though that instability of the genome by defects in its maintenance and repair, is selectively advantageous for the acquisition of hallmark capabilities and tumor progression.

- **Enabling characteristic: tumor-promoting inflammation.** Paradoxically, the tumor-associated inflammatory response can enhance tumorigenesis and progression by helping in the acquisition of hallmark capabilities. Various mechanisms can contribute to this event, including bioactive molecules such as growth and proangiogenic factors, matrix-modifying enzymes that facilitates angiogenesis and metastasis, and the activation of hallmark-facilitating programs such as EMT[25–28].

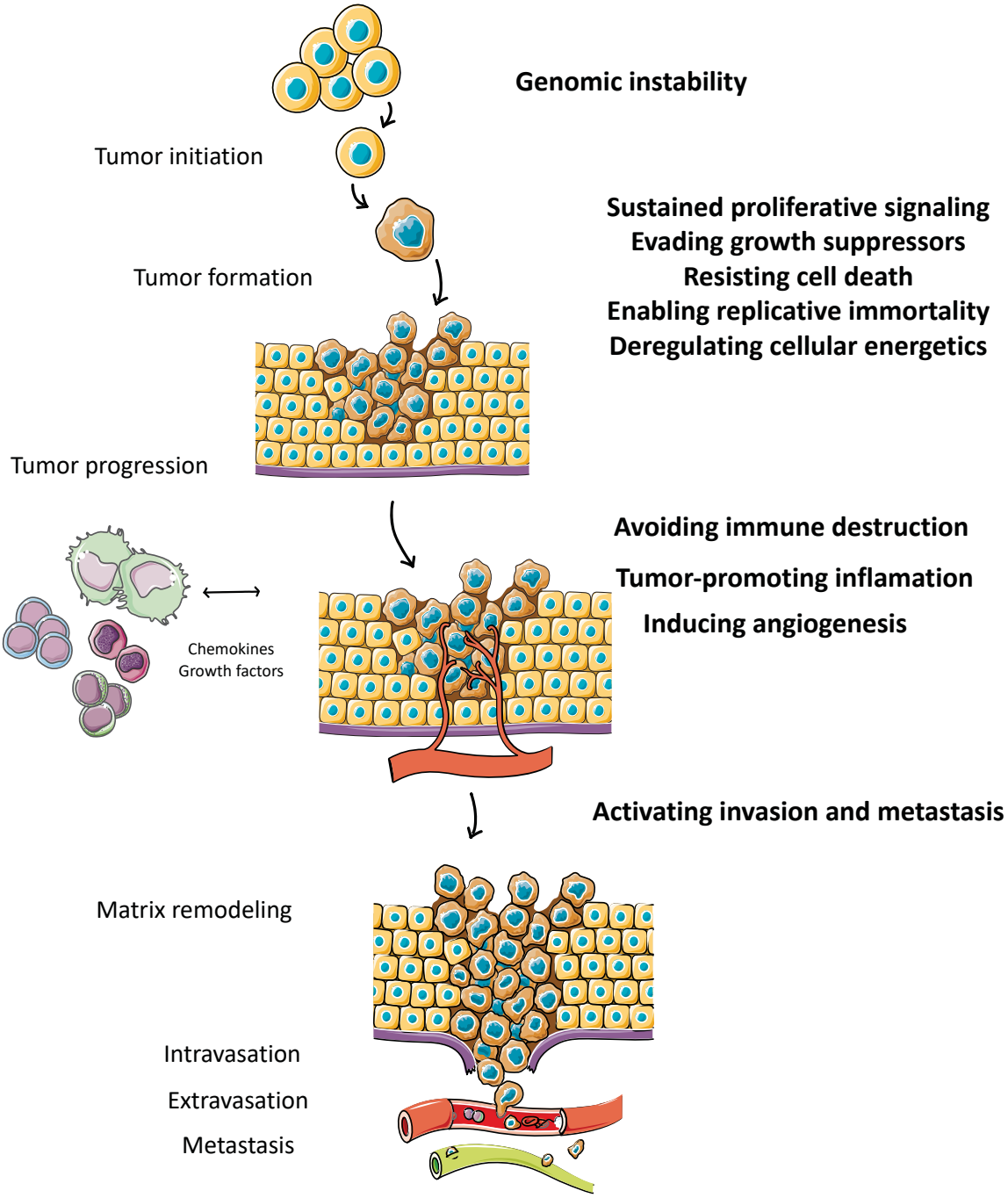

Figure 1 | **Stages of cancer development and the hallmarks of cancer.** The figure indicates the different stages of cancer development (on the left) and its relation with the acquisition of the hallmarks of cancer (on the right). Based on [15].

2. DNA DAMAGE RESPONSE

Tens of thousands of DNA damage events occur in our cells every day and there are different mechanisms to deal with them[29,30]. If these lesions are not repaired or are repaired incorrectly, mutations and genome aberrations that threaten cell viability appear[30]. Defects in DNA repair lead to genomic instability, that is a hallmark of cancer, providing a way to accumulate the sufficient genetic alterations needed to form a cancer cell[21,24].

Cells have various systems to protect against genomic aberrations. The cellular signaling events and enzyme activities that senses DNA damage and sets a response to protect the cell are collectively termed the DNA damage response (DDR)[31,32]. This term include events that lead to cell cycle arrest, regulation of DNA replication, and the repair or bypass of DNA damage[23]. There are many different types of DNA lesions that evoke responses by different repair pathways[33,34] (**Fig.2**). It was estimated that up to 450 genes encode for proteins involved in the DDR[35], including nucleases, helicases, polymerases, topoisomerases, recombinases, ligases, glycosylases, demethylases, kinases and phosphatases[29] (**Fig.2**). As mentioned above, DDR deregulation may lead to cancer through various mechanisms, including increased levels of replication stress and endogenous damage and the dysregulation of one or more DDR pathways, driving genomic instability.

Repair pathway	NHEJ	HR	alt-NHEJ/ MMEJ	SSA	ICL repair	SSB repair	BER	TLS	NER	MMR
Source of DNA damage	IR, radiomimetics, Topo II inhibitors	X-linking agents, replication inhibitors, antimetabolites, Topo I inhibitors			X-linking agents	IR, ROS, radiomimetics Topo I inhibitors H_2O_2, alkylating agents	Alkylating agents	UV, alkylating agents	Alkylating agents, X-linkers	DNA Pol proofreading errors
Damage sensors	Ku70/Ku80	MRN	PARP	MRN	FA core complex (FANCA, B, C, E, F, G, L and M)	PARP	DNA glycosylases, APE	PCNA	XPC DDB2 CSA	MSH2, MSH3, MSH6, MLH1, PMS2
Signaling/ mediator proteins	DNAPK	ATM, ATR MK2, CtIP, BRCA1/BARD1 BRCA2, PALB2, RPA		CtIP	FANCD1 [BRCA2] D2, I J [BRIP1] N [PALB2] O [RAD51C] P [SLX4]			RAD6 RAD18	XPA, XPF RPA	
Effector proteins	XRCC4 XLF LIG4 APLF Artemis PAXX WRN	RAD51 MUS81/EME1 SLX1/SLX4 RTEL1 BLM TOPOIII POLQ PARI RECQL5 FANCJ, BLM	XRCC1 LIG3, LIG1 CtIP POLQ	RAD52, others?	Shared with HR, TLS, and NER	XRCC1 PNKP POLβ FEN1, TDP1 Aprataxin, LIG1, LIG3A	As for SSB repair	REV1, POLH POLI, POLK	XPG ERCC1 POLE POLD1 LIG1, LIG3	EXO1 POLD LIG1

Figure 2 | **DNA damage response (DDR) pathways and proteins.** The figure shows the predominant sensors, signaling and effector proteins for major DDR pathways. Pathways of double strand break (DSB) repair are in the blue area and pathways of single strand break (SSB) repair are in the red area. Adapted from [34].

Homologous recombination repair

Probably the most dangerous type of DNA damage is a double strand break (DSB), which poses a serious threat to cell viability and genome stability[36]. DSBs result naturally from replication forks collapse, programmed genome rearrange, V(D)J recombination, class-switch recombination and meiosis. However, DSBs also result from physical stress and exogenous agents such as ionizing radiation (IR), chemical agents and ultraviolet (UV) light or certain chemotherapeutic drugs[37]. Homologous recombination repair (HRR) and non-homologous end-joining (NHEJ) represent two different pathways to repair DNA DSBs. HRR is considered to be a conservative, error-free repair pathway that depends on the presence of a undamaged sister DNA chromatid[23,38]. NHEJ pathways (both conservative c-NHEJ, and

alternative alt-NHEJ) are not dependent on the presence of replicated DNA and are less accurate, potentially introducing DNA rearrangements[39–41]. What repair pathway is used varies within the different phases of the cell cycle. As cells in G1 have not a sister chromatid DNA available, DSBs will be repaired by NHEJ pathways, while during S and G2 phases of the cell cycle, when an intact sister chromatid can serve as DNA template, cells upregulated HRR[42]. Chromatin context, transcriptional status and extent of end resections also contribute to the selection of DNA repair, either by HRR or by NHEJ[34].

DDR pathways normally involve sensors that detect DNA damage, effectors that execute repair and activate cell cycle checkpoints, and signaling mediators that recruit and activate the effectors. For DSBs repair, Ku heterodimer (comprising the Ku70/Ku80 protein heterodimer) and the MRE11-RAD50-NBS1 complex (MRN) are the predominant sensor protein complexes. Ku serves as a platform for the recruitment of c-NHEJ proteins, while the MRN complex trigger the activation of the DNA damage signaling kinase ataxia telangiectasia mutated (ATM) and the promotion of HRR[23,29–32,36,37,42].

In DSBs repair by HRR, the phosphorylation of histone H2AX (γH2AX) acts as a mediator of DNA damage checkpoint protein 1 (MDC1) and RING finger protein 8 (RNF8) that allow the BRCA1-abraxas-RAP80 complex to associate with ubiquitylated histones near the sites of DNA damage. The BRCA1-CtBP-interacting protein (CtIP) complex associates with the MRN complex and initiates DSB resection (cutting back) of 5’ DNA either side of the DSB, a process that results in the exposure of two regions of single-stranded DNA (ssDNA) on either side of the break. BRCA1 phosphorylation by CHK2 is then necessary for the following cascade events, when BRCA1 interacts with the BRCA2-PALB2 complex allowing the formation of RAD51 nucleoprotein filaments that have the ability to invade the DNA double helix on an intact, homologous DNA strand. DNA polymerases use the homologous DNA sequence as a template and the invaded ssDNA as a primer to synthesize new DNA. Finally, DNA ligases and endonucleases resolve the complex DNA structures and the DSB is repaired. Other proteins are implicated in the HRR pathway as facilitators, such as the BRCA1-interacting protein C-terminal helicase 1 (BRIP1) and DNA topoisomerase 2-binding protein 1 (TOPBP1), among others[42] (**Fig.3**).

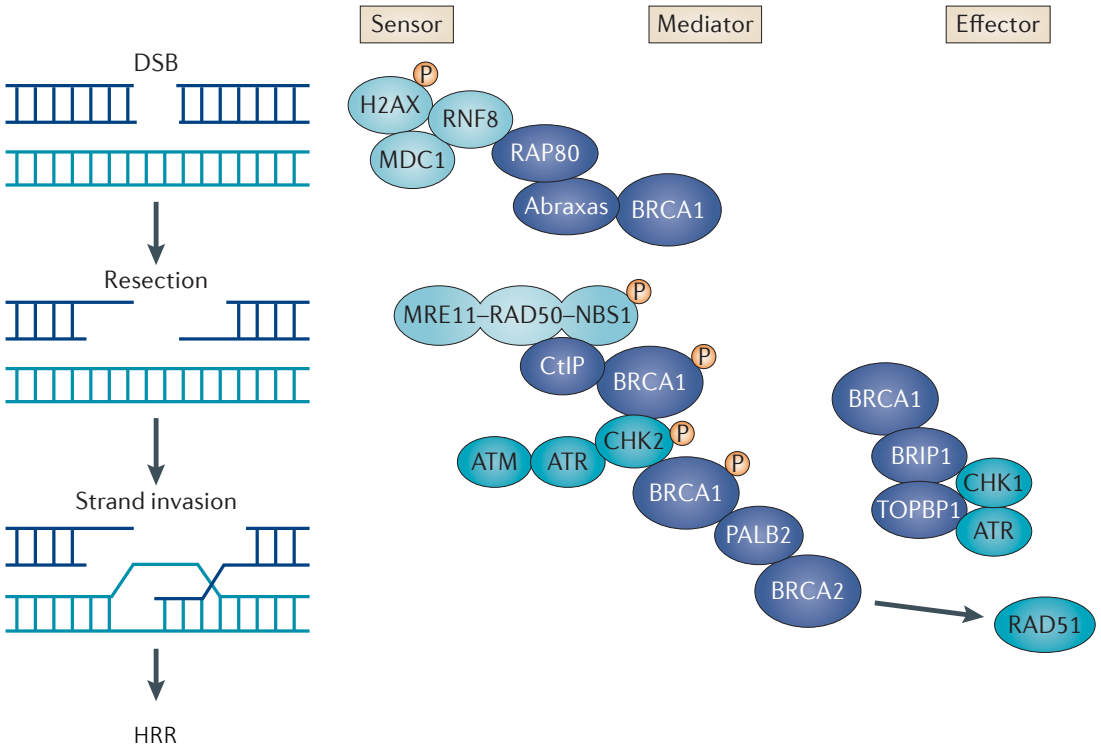

Figure 3 | **DNA double-strand break (DSB) repair by homologous recombination repair (HRR).** In response to DNA DSBs, sensors (light blue) detect the damage, and signaling mediators recruit or activate effectors that repair the damage. BRCA1-containing macro-complexes (dark blue) are crucial mediators of the DNA damage response. Adapted from[42].

BRCA1 domains and binding partners

BRCA1 is a very pleiotropic protein that links DNA damage sensing and DDR effector proteins[42]. Through its ability to form complexes with other proteins, BRCA1 has different roles within the DDR pathways, including cell cycle checkpoint control and DNA repair. Thus, BRCA1 is considered as a master regulator of genome integrity and, therefore, a tumor suppressor protein[43].

The human *BRCA1* gene is located on chromosome 17q21[44] and encodes a protein of 1863 amino acids[43]. BRCA1 interacts with other proteins involved in different functions through its various functional domains, with a highly conserved N-terminal and C-terminal domains (**Fig.4**).

The N-terminal RING domain of BRCA1 is a motif found in many E3 ubiquitin ligases and is required for the heterodimerization with BRCA1-associated RING domain protein 1 (BARD1)[45,46]. *In vivo*, BRCA1 exists in association with BARD1 through the N-terminal RING domain[47]. This heterodimer generates polyubiquitin chains at unconventional K6 linkages that do not appear to signal for protein degradation but mediate downstream signaling events[48–52]. The BRCA1-BARD1 heterodimer has been implicated with the maintenance of genomic stability and tumor suppression through its involvement in DNA damage signaling, DNA repair and transcriptional regulation.

The C-terminal sequence of BRCA1 contain two tandem copies of the BRCA1 C-terminal (BRCT) domain, which is a common motif found in many human DDR proteins[42,47]. The BRCT domains of BRCA1 are implicated in the ability to regulate various cellular processes that confers its tumor-suppressing activity by interactions with numerous cell cycle checkpoint and repair proteins, chromatin remodeling factors and components of transcriptional machineries[43,53–56]. In response to DNA damage, the BRCT domains of BRCA1 form a phospho-recognition surface that binds phosphorylated proteins, preferentially phosphoserine in SXXF motifs, including abraxas, CtIP and BRIP1[42,43,57,58]. The BRCA1-abraxas complex is associated with BRCA1 recruitment to DNA damage sites, while the BRCA1-BRIP1 complex, together with TOPBP1, is associated with DNA repair during replication[42,59]. The BRCA1-CtIP complex promotes ATR activation and HRR by association with the MRN complex and facilitating DNA DSBs resection[60].

The C-terminal region of BRCA1 also contains a coiled-coil domain that mediates its association with PALB2 to form the BRCA1-PALB2-BRCA2-RAD51 complex, which is specifically involved in DSB repair by HRR[61–63]. There is also a SQDC domain that contain various ATM/ATR phosphorylation sites. This phosphorylation is important for the activation of BRCA1-mediated G2/M- and S-phase checkpoint.

Finally, the central region of BRCA1, within the exon 11 of the protein, contains a CHK2 phosphorylation site and the nuclear localization sequences (NLS). This central part of BRCA1 is also important for its interaction with other DDR proteins, including RAD50 and RAD51[42].

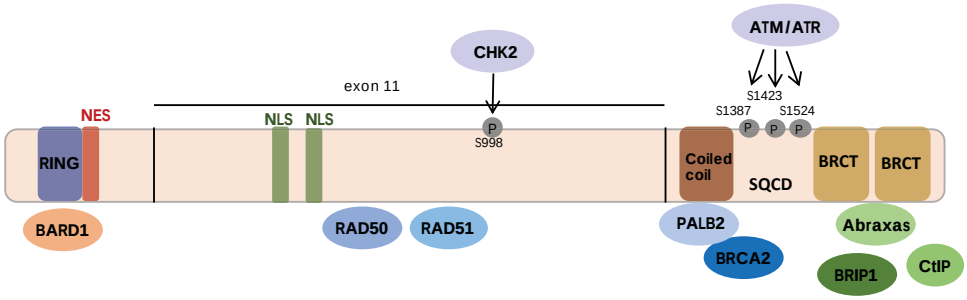

Figure 4 | **BRCA1 domains organization and interaction partners**. Schematic diagram of BRCA1 with its functional domains and the sites where other BRCA-interacting proteins binds. Phosphorylation sites important for DNA damage signaling are also shown, as well as the kinases responsible for their modification. NLS, nuclear localization sequence; NES, nuclear export signal. Based on [42,43].

The association between pathogenic mutations in the conserved N-terminal and C-terminal domains and the development of several types of tumors, including prostate, ovarian and breast cancer, indicates that both the formation of BRCA1/BARD1 heterodimer and the BRCT phosphorecognition are important for and confer the tumor suppression activity of BRCA1[43,47,64–69].

3. BREAST CANCER

Breast cancer (BC) is the one of the most common cancers worldwide[70] and the leading cause of cancer related deaths among women from industrialized countries[71]. BC is a heterogeneous disease and for many decades, was clinically classified into three groups according only to histological type, grade and expression of hormone receptors[72,73]: the estrogen receptor (ER) positive group, the HER2 (also called ERBB2) amplified group, and the triple-negative breast cancers (TNBCs), lacking expression of ER, HER2 and progesterone receptor (PgR)[70]. Later, it has been demonstrated a systematic variation between the expression profiles of breast cancer[74,75], allowing it classification into five main groups: luminal A and B, normal breast-like, HER2 and basal-like carcinomas[75–78]. However, practically and economics established as the current criteria the classification in four different subtypes of BC based on the available clinic-pathological and surrogate immunochemistry (IHC)-based test[79] (**Fig.5**).

While treatments for ER and HER2 positive breast tumors have been improved with targeted therapies, the treatment of patients with TNBC has been challenging due to the heterogeneity of the disease and the absence of well-defined molecular targets[80]. TNBCs were a group with a more aggressive clinical behavior, relatively poor prognosis and lacked effective targeted treatments, so there were only chemotherapy options[81] (**Fig.5**).

Germline BRCA

Family history of BC is associated with a higher risk of the disease. Some inherited mutations, particularly in the *BRCA1* and *BRCA2* genes, result in a very high risk of breast cancer. As mentioned, *BRCA1* and *BRCA2* are tumor suppressor genes which encode proteins involved in repair DSBs by HRR[42,57]. Lack of function of either gene impairs high-fidelity DNA repair and results in the use of non-conservative, potentially mutagenic repair mechanisms, such as NHEJ and strand annealing[82], leading to genomic instability, which is a recognized hallmark of cancer[4,34,83]. As a consequence, germline mutations in *BRCA1* or *BRCA2* (gBRCA) cause hereditary breast and ovarian cancer syndrome (HBOC), meaning

that mutation carriers have an increased risk of breast or ovarian cancer (OC) as compared to the general population[44,84,85]. Although mutations in *BRCA1/2* are the predominant cause of HBOC syndrome, it also includes mutations in other DDR genes, such as *ATM*, *CHK2* and *PALB2*[42,86].

As a consequence of their defective HRR function, gBRCA tumors harbor increased sensitivity to DNA damaging agents, including conventional chemotherapeutics such as anthracyclines or platinum salts, which cause DNA crosslinks that lead to DSBs during DNA replication[87–90]. Such features of familial gBRCA cancers have also led to intense interest in the therapeutic development of specific inhibitors of a range of components of the DDR network, such as the Poly (ADP-ribose) polymerase (PARP) inhibitors (PARPi)[34,91].

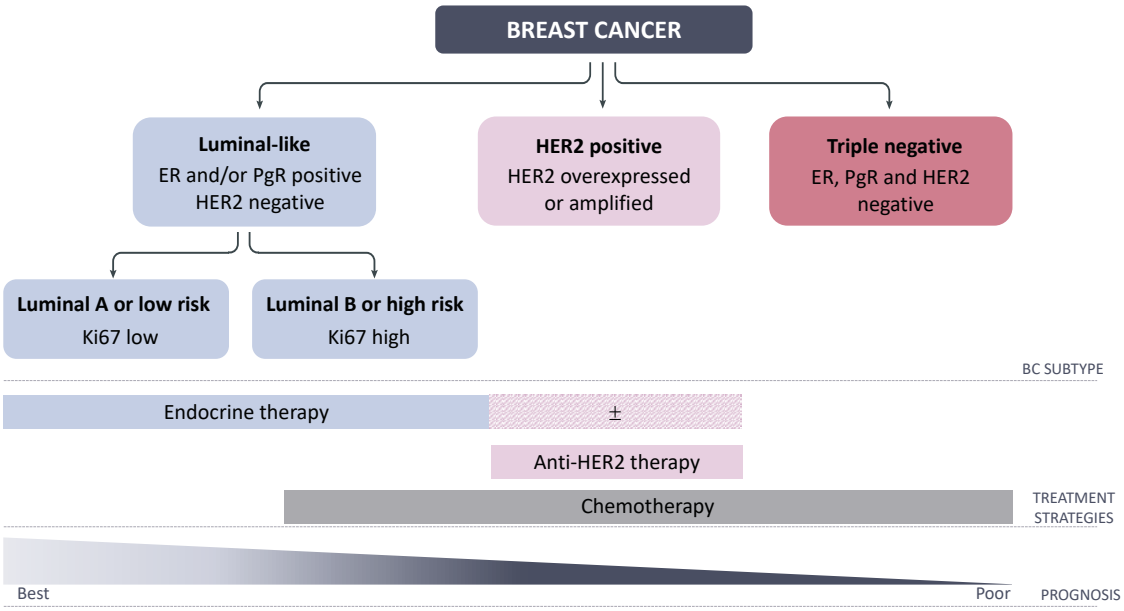

Figure 5 | **Breast cancer subtypes, principles of systemic therapy recommendations and prognosis**. Summary of the breast cancer subtypes classification using conventional IHC for the detection of ER, PgR and HER2 as well as current general treatment strategies and prognosis. ER, estrogen receptor; PgR, progesterone receptor.

4. PARP INHIBITION

The PARP family has 17 members with many diverse functions, of which PARP1 has the predominant role in DNA repair, with PARP2 and to a lesser extent PARP3 also being implicated in the DDR[29,34,92]. The PARP enzymes play an expansive and multifaceted role in the DDR acting in the detection of DNA damage, recruitment of repair factors and also in the regulation of biochemical activities[93]. PARP1 is well known for its role in DNA base excision repair (BER) and repair of DNA SSBs, but also have a role in DNA DSBs repair[94,95] and in fork protection[96], participating in multiple DNA repair pathways that include nucleotide excision repair (NER), c-NHEJ, alt-NHEJ, HRR and DNA mismatch repair (MMR)[93]. PARP enzymes catalyze the addition of Poly (ADP-ribose) (PAR) chains on proteins to recruit DDR factors and remodeling the chromatin structure around the damaged DNA[92,97]. This PARylation also represents a mechanism of regulating PARP1 assembly on DNA, as PARP1 eventually PARylates itself (autoPARylation) and this automodification is required for its dissociation from repaired DNA[98,99].

The understanding of PARP1 function in DDR boosted the development of PARP inhibitors with the original rationale of sensitize tumor cells to DNA damaging treatments, including chemotherapy and radiotherapy. In 2005, two different groups described a synthetic lethal (SL) interaction between PARP inhibition and *BRCA1* or *BRCA2* mutation[88,89,100]. The concept of synthetic lethality was first described by Bridges in 1922 and the term was coined by Dobzhansky in 1946[101]. This phenomenon occurs when two non-lethal mutations have no effect when occur individually, but lead to cell death in combination[89,101,102]. This is consistent with the idea that in *BRCA1/2*-mutated tumors (BRCA), the cancer cells would depend on other DDR pathways for survival, as those depending on PARP1 activity, whereas normal cells (that maintain fully functional HRR) would not. The reliance of BRCA-mutant cells on SSBs repair for survival leads to the accumulation of SSBs upon PARP inhibition that cause the collapse of replication forks and DSBs[98,103]. This was originally proposed as the mechanism underlying the SL interaction between PARP inhibition and BRCA mutation. However, this model has been modified as a result of data suggesting that some PARPis also cause PARP trapping onto DNA by preventing autoPARylation and PARP1

release. This trapped PARP1 protein causes replication-dependent DSBs that also needs HRR to be repaired and therefore significantly contributes to the sensitivity to PARP inhibition of BRCA-mutant cells[104,105] (**Fig.6**).

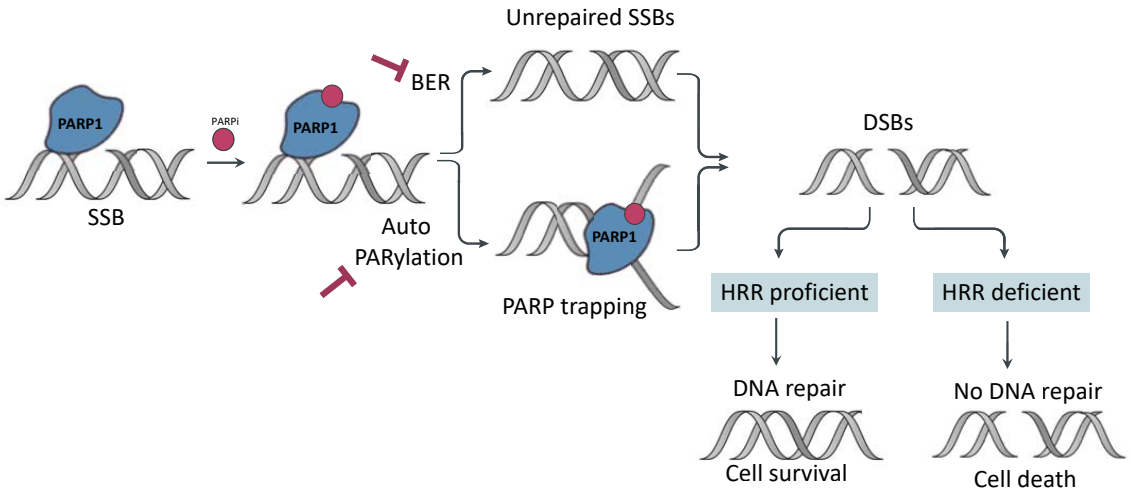

Figure 6 | **Mechanisms of action of PARPi and sensitivity of HRR-deficient cells.** PARP inhibitors (PARPi) impair the repair of single strain breaks (SSBs) by the inhibition of base excision repair (BER) pathway and also cause PARP trapping by inhibiting auto-PARylation and PARP release from DNA. These two effects lead to unresolved DNA double strand breaks (DSBs) that can kill homologous recombination repair (HRR)-deficient cells.

Drug discovery efforts have led to the development of various PARPi, including veliparib, rucaparib, olaparib and niraparib, and a more potent second generation of PARPi such as talazoparib[100]. The clinical development of PARPi in patients with gBRCA mutations stemmed from the robust preclinical data that demonstrated exquisite sensitivity of BRCA-mutated cells and tumors to PARP blockade[106,107]. Cells carrying mutations in *BRCA1/2* are up to 1000 times more sensitive to PARPi than wild type cells[106] and these observations provided the impetus for PARPi to be tested in the clinic[105]. Clinical trials assessing PARP inhibitors have shown to be well tolerated agents, with multiple durable antitumor responses in the advanced setting of specific ovarian, breast or castration-resistant prostate cancers (CRPC)[108–110]. Later-phase clinical trials confirmed the patient benefit, eventually leading to the approval of four different PARP inhibitors for the use in the treatment of ovarian and breast cancer[111] (**Table 1**).

Table 1 | **Regulatory agencies approval of PARP inhibitors.**

PARPi	Approved Indications
Olaparib (Lynparza™, Astrazeneca) [112–116]	EMA (2014): maintenance treatment of patients with relapsed, platinum-sensitive, *BRCA1/2*-mutated (germline or somatic), high-grade serous epithelial ovarian, fallopian tube or primary peritoneal cancer who are in response to platinum-based chemotherapy. FDA (2014): treatment of germline *BRCA1/2*-mutated advanced ovarian cancer with three or more prior lines of chemotherapy. FDA (2017): maintenance treatment of patients with recurrent epithelial ovarian, fallopian tube or primary peritoneal cancer who are in response to platinum-based chemotherapy. EMA (2018): maintenance treatment of patients with platinum-sensitive relapsed high-grade epithelial ovarian, fallopian tube or primary peritoneal cancer who are in response to platinum-based chemotherapy, regardless of BRCA status. FDA (2018): treatment of patients with germline *BRCA1/2*-mutated, HER2-negative metastatic breast cancer with previous chemotherapy treatment.
Rucaparib (Rubraca™, Clovis Oncology) [117–119]	FDA (2016): treatment of patients with deleterious *BRCA1/2* mutation (germline or somatic)-associated epithelial ovarian, fallopian tube or primary peritoneal cancer who have been treated with to two or more chemotherapies. FDA (2018): maintenance treatment of patients with recurrent, advanced epithelial ovarian, fallopian tube or primary peritoneal cancer who are in response to platinum-based chemotherapy. EMA (2018): treatment of patients with platinum-sensitive, relapsed or progressive, *BRCA1/2*-mutated (germline or somatic) high-grade epithelial ovarian, fallopian tube or primary peritoneal cancer with two or more prior lines of platinum-based chemotherapy and do not tolerate further platinum-based chemotherapy.
Niraparib (Zejula™, Tesaro) [120]	FDA (2017): maintenance treatment of patients with recurrent epithelial ovarian, fallopian tube or primary peritoneal cancer who are in response to platinum-based chemotherapy. EMA (2017): maintenance treatment of patients with platinum-sensitive relapsed high-grade serous epithelial ovarian, fallopian tube or primary peritoneal cancer who are in response to platinum-based chemotherapy.
Talazoparib (Talzenna™, Pfizer Inc.) [121]	FDA (2018): treatment of patients with deleterious or suspected deleterious germline *BRCA1/2*-mutated, HER-2 negative locally advanced or metastatic breast cancer.

The use of PARP inhibitors is also being explored in patients with early-stage gBRCA BC, which will provide data to address whether PARPi can improve outcomes in BC if given in an earlier line setting[122–125]. In metastatic *BRCA1/2*- or *ATM*-mutated CRPC, olaparib received FDA breakthrough therapy designation after taxane-based chemotherapy and at least one newer hormonal agent, followed by rucaparib[126,127]. The therapeutic reach of PARPi is expanding to other cancer types, with clinical trials in pancreatic, endometrial, urothelial, colorectal, glioblastoma, small-cell and non-small-cell lung and gastroesophageal cancers[128].

Mechanisms of PARPi resistance

As explained, PARP inhibition has shown to be an effective treatment for BRCA-mutated cancers, but not all trials have been so positive. One of the findings from clinical trials with single agent PARPi is the presence of a subset of gBRCA breast or ovarian cancer patients that do not benefit from treatment with these agents (primary resistance), partially limiting the power of gBRCA condition as a biomarker of response[129,130]. In addition, development of secondary or acquired resistance in responders is a common event and many patients will inevitably progress to these drugs[112,128,131]. The resistance to PARPi have mostly been investigated in parallel to platinum salts and work by several groups using *in vitro* models, transgenic mice and human tumor samples essentially delineates three general mechanisms of resistance to PARPi[128,131–139]: (a) those dependent on the recovery of HRR, either by BRCA-independent (indirect) or BRCA-dependent mechanisms (direct); (b) those involved in the activation of signaling pathways that decrease replication stress and cell cycle progression and (c) miscellaneous alterations not related with DDR (**Fig.7**).

Mechanisms of PARPi resistance that restore HRR functionality

RESISTANCE THROUGH SECONDARY MUTATIONS

Secondary genetic reversion events that restore the mutated gene function of *BRCA1* or *BRCA2* may derive acquired resistance to PARPi[134,139,140]. These secondary intragenic mutations occur either by genetic events that cancel the frameshift caused by the original mutation and restore de open-reading frame (ORF) or by genetic reversion of the inherited mutation, restoring at least a nearly full-length protein. These secondary mutations have been identified in platinum- and/or PARPi-resistant cell lines and patient-derived cells[109,113,139]. Moreover, this mechanism of resistance has been identified in *BRCA1/2*-mutated tumors from patients who have developed clinical resistance to PARPi across multiple cancer types[34,128]. Secondary mutations have been also discovered in other DDR genes, including *RAD51C*, *RAD51D* and *PALB2*, restoring the wild type sequence and/or function of the protein and HRR capacity, therefore inducing clinical resistance to

PARPi[34,128,141]. Nevertheless, larger studies are needed to better understand the clinical prevalence of this mechanisms of resistance in the context of PARP inhibition.

RESISTANCE THROUGH HYPOMORPHIC BRCA1 PROTEINS

As mentioned, the analysis of different missense mutations in *BRCA1* suggests that the different domains of the protein are not equally important for HRR capacity and response to DNA damaging therapies[142], being more essential a conserved N- and C-terminus of the BRCA1 protein[139]. As a result, *BRCA1*-mutated tumors respond differently to PARPi therapy depending on the specific mutation they have. The p.BRCA1-C61G mutation disrupts the N-terminal RING domain of BRCA1 and cancers carrying this alterations respond poorly and rapidly develop resistance to PARPi[139,143]. To explain this fact, it has been determined that both murine and human breast cancer cells with BRCA1 mutated in the RING domain could express a hypomorphic protein lacking the N-terminus through downstream translation initiation. This RING-less BRCA1 isoform may recover the functionality of HRR and, as a consequence, it mediates resistance to PARPi[143]. BRCA1 protein with mutations in the C-terminal domain BRCT is commonly subject to protease-mediated degradation because an improperly folding. In this scenario, the chaperone HSP90 may stabilize the BRCT domain of these BRCA1 mutant proteins allowing the interaction with PALB2-BRCA2-RAD51 and, therefore, the consecution of HRR conferring platinum and PARPi resistance[131,144]. Finally, there is evidence that cancer cells harboring mutations in the exon 11 of *BRCA1* remove the deleterious *BRCA1* mutation thorough alternative mRNA splicing, giving rise to the hypomorphic BRCA1-Δexon11 isoform, which retains residual activity and contribute to therapeutic resistance to platinum compounds and PARPi[145,146].

RESISTANCE THROUGH REVERSION OF EPIGENETIC SILENCING

HRR capacity restoration and PARPi resistance can also be caused by epigenetic changes in HRR-related genes, such as reversal of *BRCA1* promoter hypermethylation[139]. This mechanism can occur in those tumors that are primary sensitive to PARP inhibition through low *BRCA1* expression caused by extensive promoter methylation. The loss of promoter

methylation lead to re-expression of *BRCA1* gene at comparable levels to HRR proficient tumors and, therefore, these tumors become PARPi-resistant. Methylation may be decreased as a result of an active demethylation event, but also from tumor heterogeneity in which the tumor cells with less promoter methylation undergo positive selection upon exposure to PARPi[139]. Reversal of *BRCA1* hypermethylation was observed in acquired platinum resistant ovarian cancers, further demonstrating that cancer cells may re-express silenced *BRCA1* as a resistance mechanism[147].

RESISTANCE THROUGH REMOVAL OF A BARRIER TO DNA END RESECTION

Several mechanisms of PARPi resistance by loss of DDR proteins that suppress DNA end resection and inhibit HRR have been described[139]. These proteins include 53BP1, REV7, RIF1, PTIP and Artemis. More recently, the shielding complex composed of c20orf196 (SHLD1 or RINN3), FAM35A (SHLD2 or RINN2) and FLJ26957 (SHLD3 or RINN1), which has been identified as REV7 binding proteins, also confers PARPi resistance upon depletion[133,135,155–157,139,148–154]. Similarly, loss of members of the CTC1-STN1-TEN1 (CST) complex were found to confer PARPi resistance in BRCA1-deficient cells by the restoration of end resection[158]. This mechanisms of PARPi resistance has been discovered through the observation that the requirement of BRCA1 for HRR was alleviated by removing of 53BP1, which blocks CtIP-mediated DNA end resection and commits DNA repair to c-NHEJ[159]. Loss of some of the proteins involved in the suppression of DNA end resection confers PARPi resistance in BRCA1-deficient cancer cells, but do not rescue BRCA2-deficient cells[148,149,157]. Although there is already preclinical evidence, it is important to determine the real role of functional impairment of these proteins as a mechanism of PARPi resistance in human tumors.

Mechanisms of PARPi resistance independent from HRR functionality

RESISTANCE THROUGH MITIGATION OF REPLICATION STRESS AND SLOWED CELL CYCLE PROGRESSION

Stabilization of stalled replication forks implies replication fork reversal, protection and restart and is gaining attention in the field of DDR, being identified as a mechanism of PARPi resistance that is often combined with slowing of cell cycle progression[128,160–165]. BRCA1, BRCA2 and other FANC proteins (RAD51, FANCD2 or FANCA) play a role in the protection of the stalled replication fork in addition to its function in HRR[166,167]. Thus, in their absence, reversed forks are extensively degraded through uncontrolled resection by EXO1 and MRE11 nucleases[165,166,168,169]. PARP1 is also implicated in fork protection from MRE11-dependent degradation[96], which explains the promotion of toxic fork restart and DSBs in BRCA-deficient cells treated with PARPi[170]. Thus, as alternative to HRR restoration, tumor cells can also achieve resistance to PARPi by protecting replication forks. Fork degradation by MRE11 nuclease in BRCA-deficient cells is promoted by PTIP, CHD4 and RAD52[160,169]. Loss of these protective factors, PARP1 and MRE11 reduced accumulation of chromosomal aberrations in BRCA2-deficient cells treated with platinum and/or PARPi, which is consistent with a reduction of toxic effects from fork degradation[169,171]. In another study, *BRCA2*-mutant cells with reduced expression of PTIP were shown to become PARPi-resistant by fork protection through reduction of the recruitment of the MRE11 nuclease to stalled forks[160]. In addition, BRCA2-deficient cells became resistant to PARPi and platinum salts by decreased activity of EZH2 and the consequent downregulated recruitment to stalled forks of a different nuclease, MUS81[172]. Notably, loss of EZH2 did not impact MRE11-mediated fork degradation, indicating that the EZH2/MUS81 axis function independently to MRE11[173]. Finally, the overexpression of miR-493-5p showed to prevent fork degradation by downregulating MRE11 and EXO1 and is preset in platinum and PARPi-resistant *BRCA2*-mutated OC patients[164]. Altogether, these data consolidate that replication fork protection contributes to PARPi resistance in *BRCA2*-mutated cancers. Importantly, the mentioned alterations that lead to fork protection showed no impact on HRR capacity, which implies that restoration of HRR functionality and fork protection are mutually exclusive and represent two different and independent mechanisms of PARPi resistance[173–175].

OTHER MECHANISMS OF RESISTANCE

Apart from the mechanisms of PARPi resistance related with the rewiring of the DDR, pharmacological events may also be relevant. In this sense, increased expression of ATP-binding cassette (ABC) transporters, such as the P-glycoprotein (PgP) efflux pump (also known as multidrug resistance protein 1 (MDR1)) have shown to reduce the efficacy of different drugs by enhancing their translocation outside the cell[139,176]. Of note, upregulation of the *ABCB1* gene (that encodes PgP pump) was found in approximately 8% of recurrence samples from high grade serous OC (HGSOC)[147].

As PARP inhibition blocks the enzymatic activity of PARP enzymes, decreased expression of these proteins, together with mutations in the catalytic, DNA- or drug-binding domains, may be another mechanism of resistance to PARPi[128,144]. Downregulation or mutations in PARP1 remove the ability to trap PARP1 onto DNA, therefore conferring resistance in BRCA tumors[177,178]. Similarly, mechanisms that increase PARylation of PARP enzymes, such as loss of PARG, may lead to PARPi resistance by decreased PARP trapping through release of PARP1 from DNA[128].

The Schlafen family member 11 (SLFN11) has been proposed as predictive biomarker of sensitivity to PARPi monotherapy in small cell lung cancer (SCLC)[179]. In fact, high protein levels of SLFN11 predicted sensitivity to platinum based agents and PARPi in preclinical models and clinical trials[180,181] and, therefore, SLFN11 inactivation can confer PARPi resistance, probably through increased dependence on the ATR-CHK1 checkpoint[179,182,183].

Finally, extensive tumor desmoplasia has also been suggested as a mechanism of PARPi resistance in BRCA tumor cells without reversion of HRR capacity, and has been associated with chemoresistance and suboptimal drug uptake in prostate cancer (PC)[147].

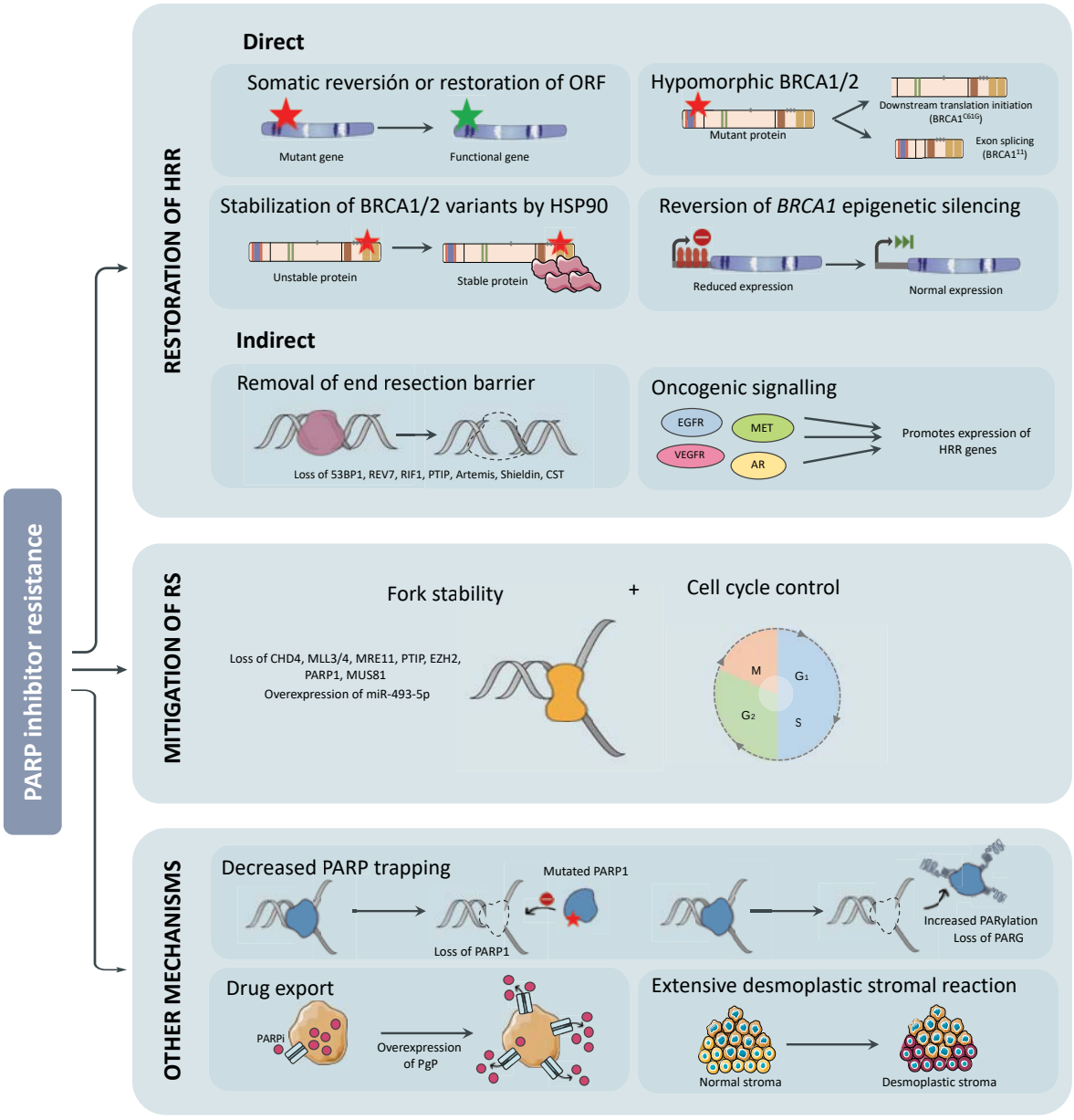

Figure 7 | **Mechanisms of resistance to PARP inhibitors.** Resistance to PARPi can be inherited or acquired and the potential mechanisms of PARPi resistance can be classified in three main categories: (i) restoration of homologous recombination repair (HRR) through both direct and indirect mechanisms, (ii) mitigation of replication stress (RS) commonly together with slower cell cycle progression, and (iii) mechanisms not currently related with a DDR pathway but still alter the response to PARPi. Based on[128].

PARPi beyond BRCA

As PARPi have demonstrated clinical efficacy in gBRCA tumors, research has focused on identifying additional patient populations who may benefit from these drugs[184,185]. Basal-like TNBC and *BRCA1*-mutated tumors have clinicopathological and molecular similarities, such as sensitivity to platinum-based chemotherapy, mutations in *TP53*, diminished BRCA1 protein expression[82,186] and a pattern of genomic instability characterized by allelic loss[77,187], so similar etiology is proposed for these groups of BC[81,188–190]. Some of these similarities are related with the presence of homologous recombination deficiency (HRD) also in non-familial cancers. This phenotype is called BRCAness, which refers to sporadic (germline *BRCA1/2* wild type) cancers sharing traits with familial BRCA tumors, in particular the HRR defect[82,185], which can arise through a range of genomic, epigenetic or post-translational alterations[82].

Within the different mechanisms of causing HRD, studies with *BRCA1/2* wild type tumor cell lines that have defects in other HRR-related genes demonstrated that PARPi sensitivity is likely not restricted to BRCA cancers. These genes included *ATM*, *ATR*, *CHEK1, CHEK2*, *SHFM1* (also known as *DSS1*), *RAD51*, *NBS1* and the Fanconi anemia complementation (*FANC*) family[70,100,101,191–194]. Moreover, it is known that a much longer list of HRR-related genes could alter the response to PARPi[195–199] and genetic and epigenetic somatic mutations in genes involved in HRR occur in a wide spectrum of tumors, leading to HRD in sporadic cancers[100,191,200]. In fact, it has been shown that up to 10% of all cancers harbor HRR-related alterations[201]. Within cancer types, approximately 50% of OC and 40% of TNBC are characterized to harbor HRD in the absence of gBRCA mutation[123,202–205], as well as up to 25% of advanced prostate tumors also harbor defects in DDR-related genes[206]. Another prevalent mechanism of somatic HRD is the epigenetic silencing of *BRCA1* and also *RAD51C* in those tumors that harbor somatic aberrant promoter methylation[81,207]. Therefore, cancers with these alterations may display HRD and are candidates to exhibit enhanced sensitivity to DNA-damaging agents, including PARPi. The current clinical challenge is the identification of such group of tumors to allow extend PARPi treatment to a wider group of cancers[42].

5. BIOMARKERS OF RESPONSE TO PARPi

Precision medicine approaches have the potential to improve cancer treatments by identifying a priori the subset of patients most likely to benefit from specific targeted therapies, including PARPi[208]. In this sense, the development of biomarkers that interrogate for treatment response provide a robust tool for clinical decision. In the field of PARP inhibitors, although germline or somatic *BRCA1/2* mutations have been used to enrich for responders, there are patients with *BRCA1/2*-mutated cancers that do not respond to PARPi. Moreover, as explained, there is also a substantial number of *BRCA1/2* wild type patients who lack these mutations and may benefit from PARPi monotherapy[128]. Therefore, validated tests that allow predict PARPi antitumor activity are an important clinical need, but there is currently no accurate biomarkers of response to PARPi[144]. Several approaches to predict HRD has been proposed, with differences in their capability in predicting response to PARPi and potential clinical utility (**Table 2**)[144,200,209].

Platinum sensitivity

Because sensitivity to platinum and PARPi are both associated with HRR defects, platinum sensitivity has been used as a surrogate of PARPi response[209] and some trials have demonstrated benefit to PARPi treatment in all platinum-sensitive ovarian cancers[210]. However, it is known that platinum and PARPi responsiveness are not always overlapping[211]. For example, tumors with defects in the nucleotide excision repair (NER) pathway are sensitive to platinum therapy but remain resistant to PARP inhibition[212], and there are also platinum-resistant cancers that respond to PARPi[113].

Biomarkers based on gene mutation analysis

Germline *BRCA1/2* mutations

As tumors with gBRCA mutations has been demonstrated to show PARPi sensitivity, different trials have used sequencing assays to evaluate the presence of this mutations[110,129,213]. The Myriad Genetics BRACAnalysis is an approved, blood-based assay that was used in clinical trials of PARPi to identify ovarian[112,210] and breast cancer[115] patients and establish gBRCA mutation status. However, using this assays based on germline mutations has several limitations, such as the insensitivity to somatic reversion mutations and other mechanisms that recover HRR functionality[214]. This limitations have boosted the development of surrogate biomarkers for PARPi response[200].

Targeted sequencing of HRR-related genes

Targeted sequencing may allow the identification of alterations in various DDR genes that may result in HRR deficiency, so the analysis of a wider number of these genes, and not only the presence of *BRCA1/2* mutation, could help in the identification of HRR-deficient tumors that may respond to PARPi. One example of this approach is the BROCA assay, that analyzes alterations in several HRR-related genes, including *BRCA1, BRCA2, ATM, BARD1, BRIP1, CHEK1, CHEK2, FAM175A, MRE11A, NBN, PALB2, RAD51C,* and *RAD51D*. The presence of damaging alterations in at least one of these genes strongly correlated with platinum sensitivity and overall survival in advanced OC[215]. An alternative approach might be the use of whole-exome sequencing (WES), that provides the sequence of most exons. WES was used in metastatic PC, with high correlation between the presence of HRR alterations and clinical response rate to PARPi[126,127]. However, WES is not commonly applied in clinical practice and the predictive value of alterations in some genes, such as *ATM*, *FANCA* or *CHEK2,* remains to be validated[209]. Other challenges of this approaches are the heterogeneity underlying genome maintenance mechanisms between tumor types, with the effect in HRR capacity of phosphatase and tensin homolog (PTEN) loss being a notable example. Loss of PTEN functionality confers sensitivity to PARPi in glioblastoma and endometrial cancer[216,217], but not in OC or PC[215,218]. Moreover, the interpretation of

mutations in a single gene and its effects HRR capacity may be difficult due to low frequencies or undetermined functional relevance[200].

Genomic scars and mutational signatures

Genomic scars and mutational signatures have been identified to be associated with an HRD phenotype and can define a wider population that may benefit from agents targeting DDR[219]. Genomic scars represent genome-wide patterns of genomic signatures reflecting historical exposures to DNA damage and repair[209]. Tumors with defects in HRR repair DNA lesions using error-prone pathways, such as NHEJ, leading to frequent genomic structural rearrangements that can be identified and quantified by genomic profiling[144,209,220–223]. These characteristic genomic alterations include: large-scale transitions (LST), chromosomal breaks between adjacent regions of ≥ 10Mb; loss of heterozygosity (LOH), loss of one allele at many sites across the genome, via deletion or copy umber neutral LOH; and telomeric allelic imbalance (TAI), allelic imbalance near telomeres[200]. All three patterns are highly correlated with alterations in *BRCA1/2* and other HRR-related genes and with sensitivity to platinum and PARPi[224]. Within various clinical trials with PARPi, different assays designed as companion diagnostics for selecting patients with HRR-deficient tumors who are more likely to benefit from PARPi monotherapy.

The FoundationFocus™CDx$_{BRCA\ LOH}$ tests for germline and somatic mutations in *BRCA1/2* and the proportion of the genome affected by LOH in the tumor. This test has been used as a companion diagnostic to rucaparib, demonstrating the benefit of PARPi maintenance therapy in patients with *BRCA1/2*-mutated and/or LOH-high platinum-sensitive OC[117,225]. However, later clinical trials demonstrated benefit from maintenance with rucaparib even in women classified has HRR-proficient[119].

The Myriad Genetics' myChoice® HRD assay is based on a combination of LOH, TAI and LST[226]. In OC, a high HRD score has been associated with higher benefit from niraparib maintenance, although PARP inhibition also improved progression free survival (PFS) in HRD-negative patients[120]. In TNBC, the myChoice® HRD assay showed to associated with

increased pathological complete response rates after platinum chemotherapy in some trials[227,228] but not it others[123,229]. In the field of PARP inhibitors, the HRD test has been shown to be useful in identifying *BRCA1/2* wild type patients who can benefit from the PARPi talazoparib[121]. Nevertheless, despite it has been demonstrated the efficacy of PARP inhibition in tumors classified as HRD, there are still a proportion of patient that did not respond[115,121], so further research is needed to evaluate the capacity of this assays in predicting PARPi benefit.

In addition to the mentioned assays, mutational signatures of HRD have been developed through whole-exome or whole-genome sequencing of *BRCA1/2*-mutant tumors[128]. This signatures represent mutational patterns, and not only isolated mutations, that are likely acquired through distinct patterns of mutagen exposure and genomic instability[200]. One study catalogued larger-scale genomic alterations across up to 7000 cancers and identified mutational signatures as patterns for specific aberrant cellular pathways, such as "Signature 3" for *BRCA1/2*-inactivating mutations in different tumor types[230]. Subsequently, the HRDetect test was developed by training these data using *BRCA1/2*-mutated tumors to generate a unique somatic mutational profile with high sensitivity and specificity in identifying tumors with deficiencies in the HRR pathway[231]. However, whereas Signature 3 and HRDetect are highly sensitive for the detection of *BRCA1/2*-mutated and BRCAness tumors, they are still unable to identify as HRR-deficient other tumors with functional alterations in several HRR-related genes, including *ATM*, *CHEK* and *ATR*, and has yet to be validated in clinical trials of PARP inhibition[128,200]

Limitations of genomic assays

As explained, genomic scars have some value in enriching for PARPi-sensitive patients but are still unable to identify patients who will not respond[119,210]. Although genomic scars probably reflect the mutational processes that alter the genome in the absence of HRR over the entire lifetime of a tumor, they only provide a historical, static record of genomic alterations present in the tumor at the time of sample collection[128]. Thus, a major limitation of these assays is that they are largely insensitive to reversion of HRR deficiency, which may occur upon development of resistance to platinum and PARPi. When reversion of HRR

deficiency occurs, the cumulative defects that had occurred in the cancer genome from the original HRR deficiency do not reverse. Thus, the genomic assays still detect these scars and interpret these tumors as HRR-deficient, as has been observed in *BRCA1/2*-mutated cell lines upon *BRCA1/2* secondary mutations that restore HRR functionality[223]. Therefore, these assays might not provide an accurate estimate of whether HRR is still defective in tumor cells at the time of treatment decision, or even how plastic or reversible is the specific HRR defect[100], both being important features for a profound and sustained antitumor response to PARPi. Because of these limitations, assays that reported a dynamic readout of HRR functionality in the tumor would be of high interest.

Dynamic biomarkers

Transcriptional profiles and protein expression

Gene-expression profiles of DDR genes have been described to correlate with outcome and platinum response in ovarian, breast and lung cancers[232–234], but studies in the context of PARP inhibition are still absent. The development of platinum resistance was reflected in the change of the BRCAness profile in some patients, highlighting the dynamic nature of these assays[232]. However, this did not always occur and these approaches suffer from poor reproducibility[205].

The expression of HRR proteins, promoter methylation levels or the microRNAs that regulate *BRCA1* expression can be also measured and may be useful in revealing dynamic HRR alterations[235]. However, many studies of HRR protein expression have been limited by small numbers or technical issues, with poor reproducibility or results inconsistent with current models of HRR signaling. Therefore, both gene and protein expression as a biomarker for PARPi requires further research and clinical validation[205].

Functional assays

One way to overcome the relatively poor specificity of the genomic scars is the development of dynamic, functional biomarkers that directly measure HRR functionality in tumor specimens using approaches such as the localization or activity of key DNA repair proteins. The recruitment of DDR factors to sites of DNA damage can be visualized as discrete nuclear foci by microscopy[29,236], so HRR pathway can be mechanistically evaluated by directly assessing by immunoassays the formation of nuclear foci of DNA repair proteins[136,237]. A functional assay should ideally measure a single downstream event that would reflect proficiency of multiple upstream components of HRR[200]. In this sense, RAD51 foci formation had been proposed as a predictive biomarker of PARPi response[238–240], as the inability of cells to form RAD51 foci is a common feature of HRD. RAD51 foci formation potentially provides a global read-out of HRR capacity regardless the mechanisms of HRR deficiency or reversion. This is of special interest as many of the factors that influence HRR are still unknown[200]. Other DNA repair proteins has been also examined, including γH2AX and 53BP1 foci[241,242], as well as nuclear staining of phospho-NBS1 (pNBS1)[243].

Although functional assays may provide the most dynamic, real-time readout of DNA repair, they are clinically hampered. The most important technical challenge is that these assays usually require fresh tissue and/or the exposure of the cancer specimen to some form of DNA damage (radiation or chemotherapy) before the evaluation of DNA repair proteins[144,238,240,241]. This requirement increases the technical complexity, limits the reproducibility and impossibilities the use of formalin-fixed and paraffin-embedded (FFPE) tumor samples. Therefore, at present, RAD51 foci formation remains a biologically useful biomarker of HRR capacity but the implementation of these assays in the routine clinical practice remains difficult[200].

Other biomarkers

There are other potential biomarkers that are being investigated. For example, the activity of PARP enzymes were used as pharmacodynamic marker of PARPi activity both in tumors and in peripheral blood lymphocytes, but there was no correlation with clinical

outcomes[209,244]. PARylation levels have also been used as pharmacodynamic marker and suggested as predictive biomarkers of PARPi response, which may be limited due to the wide variations in PARP activity among patients[241,245–247]. The evaluation of the presence of miRNAs involved in the regulation of BRCA proteins (such as miR182)[248], and levels of 53BP1 expression[249] are also being studied as biomarkers of PARPi response. Finally, as stabilization of replication forks may provide resistance to PARPi, assays for replication stress have been also developed, including the DNA fiber assay[165] and the formation of phosphorylated replication protein A (pRPA), FANCD2 and PTIP nuclear foci[209].

Overall, there is currently no prospectively validated biomarker of HRR that has been incorporated in clinical practice, and this remains an active area of investigation. Therefore, the development of a robust biomarker that adequate captures the diverse genetic and epigenetic mechanisms of HRR deficiency, compatible with FFPE specimens remains elusive[144].

Table 2 | **Biomarkers of patient selection for PARPi treatment.** The main advantages (PROS) and disadvantages (CONS) of different methods are indicated. Based on[200,250]

Biomarker	PROS	CONS
Platinum-sensitivity	Direct Does not require tumor samples	Response do not overlap completely 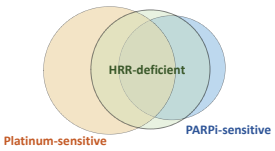
Gene mutation analysis • *BRCA1/2* mutation • HRR-related genes 	Easy and fast Can be performed on archival material	Other mutations that recover HRR remain undetected Undetermined functional relevance
Genomic scars 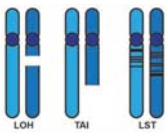	Test consequences of HRR deficiency Also detects BRCAness phenotypes Can be performed on archival material	Insensitive to HRR restoration
Functional assays 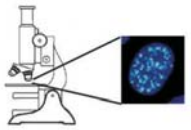	Dynamic detection of HRR capacity; sensitive to HRR restoration Also detects BRCAness phenotypes	Technical complexity Require fresh tumor material Require previous DNA damaging treatment

6. TARGETING DDR IN COMBINATION WITH PARPi

As explained, some patients do not respond or eventually progress to PARP inhibition, which points to primary or acquired mechanisms of resistance to single-agent therapy and highlights the importance of investigating combination treatment strategies that overcome or prevent PARPi resistance. As mentioned above, the ability of PARPi to sensitize tumor cells to DNA-damaging chemotherapies provided the initial rationale for developing clinically useful PARPi drugs. PARP inhibition sensitize cells to the alkylating agent temozolomide by PARP1 trapping, whereas sensitization to topoisomerase poison by PARPi is largely driven by the catalytic inhibition of PARP1 and less dependent upon trapping ability[99,251]. These observations are consistent with the failure of the relatively poor PARP1 trapping PARPi, veliparib, to enhance clinical temozolomide responses in BRCA-mutant BC patients, despite enhancing the effect of a carboplatin/paclitaxel combination[252]. However, clinical experience with therapies that combine PARPi with chemotherapies has been, in general, mixed[100].

Combination with DDR inhibitors

Combination therapies of PARPi with other DDR-targeting agents provides a rational option. As mentioned, DDR integrates the regulation of cell cycle progression and DNA repair, allowing time to repair damaged DNA[100]. There are three cell cycle checkpoints where the cell may be arrested in response to DNA damage, and the specific response pathway will be different depending on the cell cycle status. The key DDR factors that regulate the G1/S checkpoint include ATM, CHK2 and p53 and its activation allow the repair of DNA damage prior to the start of DNA replication[23]. ATR, CHK1, DNA-PK and WEE1 are the checkpoint proteins implicated in the S-phase checkpoint to delay replication origin firing, provide time to deal with DNA damage and prevent under-replicated DNA regions beyond S-phase. Finally, the activity of CHK1 and WEE1 in the G2/M checkpoint represents the major opportunity for preventing DNA damage taken into mitosis, where may result in mitotic catastrophe and cell death[23].

All the mentioned kinases respond to different types of DNA damage and/or regulate specific cell cycle transitions. Therefore, targeting these enzymes could be used in cancer treatment with the goal of maximize DNA damage in G1 and S-phases of the cell cycle and prevent repair in G2 to ensure the damage is taken through into mitosis, ultimately resulting in cell death (**Fig.8**). Thus, the rationale to combine a PARPi with cell cycle inhibitors is to impair tumor cells to stall the cell cycle and limit the time to repair DNA lesion, so DNA damage is not repaired and cell death occurs. In concordance, preclinical evidence suggests that combining agents targeting key components of the DDR can cause or enhance sensitivity to PARPi and overcome acquired resistance to single-agent DDR inhibitors by inducing synthetic lethality[128,253].

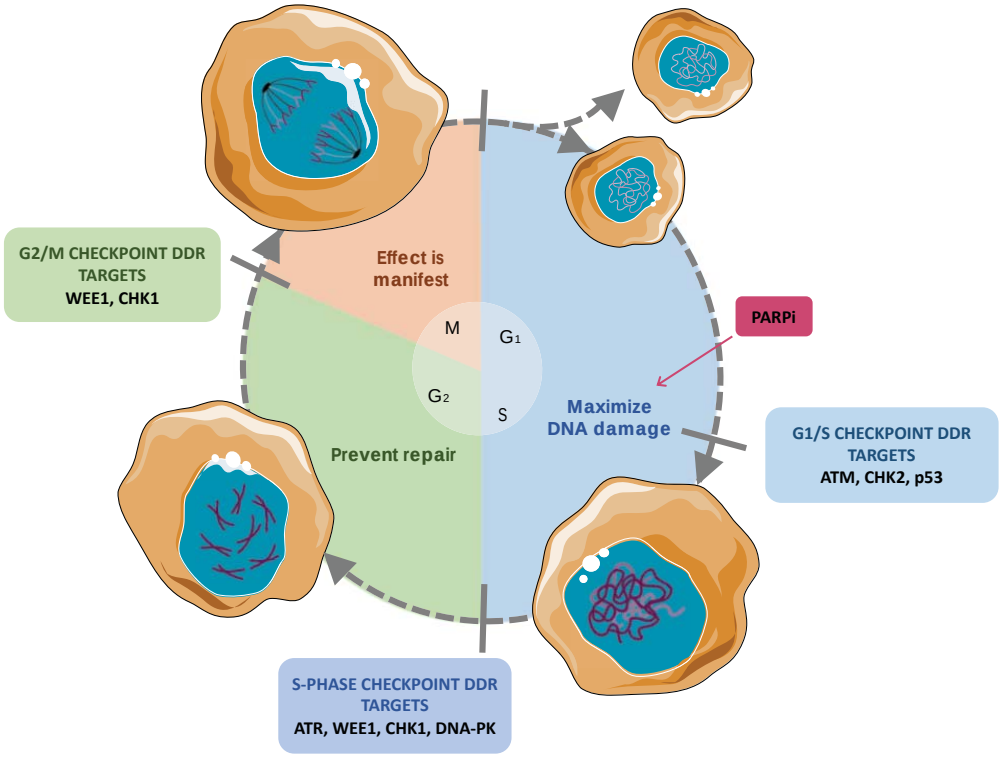

Figure 8 | **Strategy for the use of DDR inhibitors as anticancer agents.** The strategy for the development of DDR-targeted therapies is to maximize the DNA damage during G1 and S phases of the cell cycle (in blue), together with preventing its repair during G2 (in green) by minimizing the time to repair. This strategy leads to maximum amount of DNA damage in mitosis and cell death (in orange). The potential DDR targets that act at the three key cell-cycle checkpoints are represented. Based on[23].

In this sense, inhibitors of the kinases implicated in DDR has gained interest. ATR is a central checkpoint kinase in the response to DNA damage, including the resected ends of DNA DSBs and stalled replication forks. ATR activates different pathways that collectively safeguard the integrity of replication forks and prevent entry into mitosis with incompletely replicated genomes[254]. Thus, ATR is activated by replication stress and it induces origin firing shutdown and slows down replication fork speed and cell cycle progression through the activation of CHEK1 and inactivation of cyclin-dependent kinases CDK1 and CDK2 (CDK1/2)[255,256]. WEE1 kinase similarly plays a critical role in the activation of the G2-M checkpoint through the regulation of CDK1/2[34]. The recent development of ATR, CHK1 and WEE1 inhibitors make the combination of this agents with PARPi a testable hypothesis that is being currently studied in clinical trials for different scenarios[100,128,173]. ATM is another logical therapeutic target in combination with PARPi, given its crucial function as a central regulator of the DDR, especially in DSBs repair[257]. The ATM kinase is activated in response to DNA DSBs, signals to G1/S cell cycle checkpoint and DNA repair pathways, and is reciprocally synthetic lethal with PARP[258]. Finally, effective DNA repair by NHEJ requires the activity of DNA-PK and its inhibition sensitizes cells to DSB-inducing agents, such as radiotherapy and topoisomerase II inhibitors[259]. Different DNA-PK inhibitors have recently entered clinical development[260]. Results from diverse clinical trials will provide important data regarding the ability of cell cycle inhibitors to overcome PARPi resistance.

WEE1 inhibition

As explained, WEE1 is a protein with kinase activity required for physiologic cell cycle progression. CDK1 phosphorylation by WEE1 inhibits CDK1 activity and results in the activation of the G2/M checkpoint and cell cycle arrest, providing time for repair damaged DNA[261]. As a consequence of this important role of WEE1 in cell cycle progression, the predominant mechanism-of-action of WEE1 inhibitors (WEE1i) was initially believed to be failure of the G2/M checkpoint, resulting in mitotic catastrophe[261]. Importantly, the G2/M checkpoint is especially relevant in *TP53*-mutant cells, as this cells also lack G1/S checkpoint and are therefore unable to stop cell cycle and repair damaged DNA at this point. Thus,

there is a rationale to targeting p53-deficient cells with WEE1 blockade and, as approximately 84% of TNBC harbor alterations in *TP53*, it is therefore an attractive disease to study the efficacy of WEE1i[128].

In addition to regulating CDK1 activity at the G2/M checkpoint, WEE1 also phosphorylates CDK2, whose activity is critical in maintaining proper DNA replication during S-phase. CDK2 regulates the expression of ribonucleotide reductase subunit M2 (RRM2) both directly and through the control of E2F1 degradation[262,263]. Thus, increased CDK2 activity results in uncontrolled firing of replication origins and downregulation of RRM2 expression, therefore leading to nucleotide starvation and loss of genomic integrity[262]. Hence, inhibition of WEE1 could be a powerful manner to increase the levels of replication stress in cancer cells. This effect, together with forcing the cells to enter in mitosis prematurely, even before DNA replication is complete, will cause cell death[264].

The first WEE1i AZD1775 has shown antitumor activity as single-agent in preclinical models in addition to potentiate the cytotoxic effects of various DNA-damaging agents[34]. Moreover, there are also preclinical studies combining WEE1i with the PARPi olaparib that revealed an enhanced PARPi-mediated radiosensitazion of pancreatic cancer cells by reducing HRR capacity and abrogating the G2 cell cycle checkpoint[191].

In this scenario, there is now a need to better define the patient populations predicted to respond to WEE1i monotherapy and novel combination regimens[34]. In addition, the examination of potential pharmacodynamic markers for replication fork protection and replication stress (e.g. phosphorylated RPA foci and the DNA fiber assay) will be necessary to improve therapeutic potential of these drugs[173,209]. In addition to p53 deficiency, preclinical data suggest that DDR defects and nucleotide resource starvation that resulted in increased replication stress also increase sensitivity to WEE1 inhibition[263,265,266], with single agent activity observed even in *TP53* wild type cancer cells[128,267].

In sum, the development of inhibitors of key mediators of DNA repair and replication has rapidly expanded, but the differential roles of ATM, ATR, CHK1 and WEE1, among others, in cell cycle, replication forks protection and DNA damage repair could create a clinical barrier to choose the correct combination strategy. As PARPi resistance can be achieve by multiple and independent mechanism, determine the specific clinical scenarios where combining PARPi with other DDR inhibitors result in therapeutic benefit is therefore necessary[268]. Efforts are ongoing to optimize these therapies, including the development of predictive biomarkers of response, assessment of the mechanisms of resistance and evaluation of rational, tolerable combination treatments[128].

HYPOTHESIS AND OBJECTIVES

Hypothesis 1

The restoration of HRR capacity is a frequent mechanism of resistance to PARP inhibitors in germline *BRCA1/2*-mutated tumors.

To test this hypothesis, the following objectives were established:

- Develop a panel of patient derived xenografts (PDX) from breast and ovarian cancer patients with germline mutations in *BRCA1/2* genes (gBRCA)
- Investigate the antitumor activity of the PARPi olaparib in the panel of gBRCA PDX models
- Characterize the mechanisms of resistance to PARPi in the panel of gBRCA PDX models

Hypothesis 2

The restoration of HRR capacity in gBRCA tumors can be measured by the immunodetection of RAD51 nuclear foci and this assay can be used as a functional biomarker of PARPi response.

To test this hypothesis, the following objectives were established:

- Develop an immunofluorescence assay to detect RAD51 nuclear foci formation in formalin fixed paraffin embedded (FFPE) tumor samples
- Validate the capacity of the RAD51 immunoassay to predict PARPi response in tumor samples from PDXs and patients

Hypothesis 3

The RAD51 assay allows the identification of HRR-deficient tumors with no *BRCA1/2* mutations that may benefit from PARP inhibition, allowing to extend the use of PARPi treatment beyond the gBRCA condition.

To test this hypothesis, the following objectives were established:

- Develop a panel of PDXs from BC patients with wild type *BRCA1/2* (non-gBRCA)
- Investigate the antitumor activity of the PARPi olaparib in the panel of non-gBRCA PDX models
- Characterize the mechanisms of sensitivity to PARPi in the panel of non-gBRCA PDX models
- Validate the RAD51 assay as biomarker to predict antitumor response to PARPi
- Compare the prediction capacity of the RAD51 assay with another currently used genomic biomarker of PARPi response
- Study the feasibility of the RAD51 assay in routine tumor samples from patients, including PALB2-related breast tumors

Hypothesis 4

The inhibition of WEE1 and other DDR proteins increases the levels of replication stress and improves antitumor response to PARPi when used as a combination strategy.

To test this hypothesis, the following objectives were established:

- Investigate the antitumor activity of the WEE1 inhibitor AZD1775 as single-agent and in combination with olaparib
- Characterize the mechanisms of action of inhibiting WEE1i in the panel of PDX models
- Investigate the antitumor activity of the ATM inhibitor AZD0156 in combination with olaparib in gBRCA1 mutated tumors that are resistant to WEE1 plus PARP inhibition

METHODS

Generation of patient-derived xenograft (PDX) models

Fresh tumor samples from breast or ovarian cancer patients with (n=11) or without (n=14) gBRCA mutation were collected prospectively for implantation into nude mice at Vall d'Hebron Institute of Oncology (VHIO, Spain) under an institutional review board (IRB)-approved protocol and the associated informed consent, or by the National Research Ethics Service, Cambridgeshire 2 REC (REC reference number: 08/H0308/178). The experiments were conducted following the European Union's animal care directive (2010/63/EU) and were approved by the Ethical Committee of Animal Experimentation of the Vall d'Hebron Research Institute. Fresh primary or metastatic human breast tumors were obtained from patients at time of surgery or biopsy and immediately implanted into the mammary fat pad (surgery samples) or the lower flank (metastatic samples) of 6-week-old female athymic HsdCpb:NMRI-Foxn1nu (Harlan Laboratories) or NOD.Cg-Prkdc^{scid}Il2rg^{tm1Wjl}/SzJ (Charles River) mice. Animals were continuously supplemented with 1 μM 17β-estradiol (Sigma-Aldrich) in their drinking water. Upon growth of the engrafted tumors, the model was perpetuated by serial transplantation onto the lower flank. In each passage, flash-frozen and formalin-fixed paraffin embedded (FFPE) samples were taken for genotyping and histological studies. Three models (2 TNBC, STG139 and STG316 and 1 ER-positive BC, STG201) were generated in CRUK/UCAM, a member of the EurOPDX consortium (http://www.europdx.eu), as previously reported[269]. Four models with acquired PARPi-resistance were generated in the laboratory (see below).

In vivo experiments of PDX sensitivity to PARP, WEE1 and ATM inhibitors

To evaluate the sensitivity to different DDR inhibitors, at least three tumor-bearing mice were equally distributed into treatment groups with tumors ranging 50 to 350 mm^3. When allocating animals to treatment arms we ensured that the mean starting volume between arm was not statistically different by t-test. Olaparib was administered oral (p.o.) 6-days per week at 50 mg/kg in 10%v/v DMSO / 10%w/v Kleptose [HP-β-CD]. AZD1775 was administered oral 6-days per week at 120 mg/kg in 0.5%v/v Methylcellulose. AZD0156 was administered 3-days per week at 2 or 2.5 mg/kg in 10% DMSO plus 90% Captisol (30% w/v).

To generate PDX models with acquired resistance to PARPi, olaparib treatment was maintained in olaparib-sensitive tumors until individual tumors regrew. Tumor growth was measured blinded to the treatment effect with caliper bi-weekly from first day of treatment to day 21 and every 7-10 days in the acquired resistance setting. Mouse weight was recorded twice weekly. The tumor volume was calculated as V = 4π/3/Lxlxl, "L" being the largest diameter and "l" the smallest. Mice were euthanized when tumors reached 1500 mm^3, in accordance with institutional guidelines. The antitumor activity was determined by comparing tumor volume at 21 days to its baseline: % tumor volume change = (Vday21 –Vday1)/Vday1 x100. For sensitive PDXs, the best response was defined as the minimum value of % tumor volume change sustained for at least 10 days. To classify the antitumor response, the Response Evaluation Criteria In Solid Tumors (RECIST) on the % tumor volume change was modified (mRECIST): CR (complete response), best response ≤ -95%; PR (partial response), -95% < best response ≤ -30%; SD (stable disease), -30% < best response ≤ +20%, PD (progressive disease), % tumor volume change at day 21 > +20%[270,271].

Analysis of the *BRCA1/2* genes and loss of heterozygosity in PDX tumors

DNA was extracted from PDX samples using DNeasy Blood & Tissue Kit (Qiagen). All exons and flanking intronic regions of the *BRCA1* and *BRCA2* genes were sequenced by the Multiplicom MASTR T Dx methodology in an Illumina MiSeq Sequencer. Coverage range was 100-2240X. Results were analyzed with Sophia DDM® platform, which integrates PEPPER™, MUSKAT™ and MOKA™ technologies (minimum coverage of 100 reads per base). Pathogenic variants were confirmed by Sanger sequencing using BigDye Terminator v3.1 Cycle Sequencing Kit in a 3130xl sequencer (Applied Biosystems, Foster City, CA, USA). Screening for large genomic rearrangements was done using multiplex ligation-dependent probe amplification (MLPA) commercial kit #P002 for *BRCA1* (MRC-Holland, Amsterdam, The Netherlands), in accordance with the manufacturer's instructions. PCR products were analyzed on an ABI 3130xl capillary sequencer using GeneMapper (Applied Biosystems) and Coffalyser.Net (MRC-Holland, Amsterdam, The Netherlands) software. The deletion of exons 3-7 of *BRCA1* in PDX274 was confirmed by sequencing the PCR product (736bp) after

amplification of cDNA with exon 1 oligonucleotide 5'-ACAGGCTGTGGGGTTTCTC-3' and exon 10 reverse oligonucleotide 5'- TTCATCCCTGGTTCCTTGAG-3'. Nomenclature of variants was according to the Human Genome Variation Society. This analysis was performed in collaboration with the Oncogenetics Group at VHIO.

Analysis of *BRCA1* mRNA expression

RNA was extracted from PDX samples (15-30 mg) by using the PerfectPure RNA Tissue kit (5 Prime). The purity and integrity were assessed by the Agilent 2100 Bioanalyzer system and cDNA was obtained using the PrimeScript RT Reagent kit (Takara). Quantitative RT-PCR was performed in a 7900HT Fast Real-Time PCR System (Applied Biosystems) using TaqMan Universal Master Mix II (Applied Biosystems) and predesigned human specific primers and TaqMan probes (Hs99999908_m1 for GUSB, Hs99999903_m1 for ACTB and Hs01556193_m1 for BRCA1). The comparative CT method was used for data analysis, in which geNorm algorithms were applied to select the most stably expressed housekeeping genes (GUSB and ACTB) and geometric means were calculated to obtain normalized CT values[272].

Exome sequencing (PDXs cohorts 1 and 2)

All laboratory methods were performed using the manufacturer's protocols. Genomic DNA was isolated from fresh frozen PDX tissue using the Promega Maxwell 16® Tissue SEV DNA Purification Kit (catalog #AS1030) and the Maxwell® 16 MDx Instrument (Promega Corp., Madison, WI, USA). Specifically, samples were loaded into well #1 of the Maxwell cartridge, run using the "DNA/tissue" protocol, and genomic DNA was eluted with 300 µl Elution Buffer. All samples were quantified using the Qubit® dsDNA HS Assay Kit (catalog #Q32851) and Qubit 2.0 fluorometer (Thermo Fisher Scientific, Waltham, MA, USA) and sent to AstraZeneca for sequencing. Exome libraries were constructed using the KAPA Hyper Prep Library Preparation Kit (Kapa Biosystems Inc., Wilmington, MA, USA) and genes were captured using the xGen® Exome Research Panel v1.0 (Integrated DNA Technologies,

Coralville, IA, USA). Paired end 150 bp sequencing was performed on an Illumina HiSeq 4000 using TruSeq SBS reagents (Illumina) with approximately 10 Gbp per sample for ~200-fold average sequence depth. Data analysis followed standard methodologies. Briefly, sequencing reads were aligned to both human hg19 and mouse mm10 genomes using Burrows-Wheeler Alignment (BWA), then mouse-derived sequences in the human.bam file were removed using Disambiguate[273]. Variants were called in the human.bam files using VarDirect[274]. Copy number analysis was performed using Seq2C[275].

BRCA1 promoter methylation

DNA was isolated as described and sent to the Division of Molecular Pathology and Cancer Genomics at The Netherlands Cancer Institute. *BRCA1* promoter methylation was measured using Methylation-specific MLPA (MS-MLPA) (MRC Holland, Amsterdam, the Netherlands) according to manufacturer's instructions. The two xenografts generated in CRUK/UCAM (STG139 and STG201) had been previously tested using reduced-representation bisulfite sequencing (RRBS)[269] and further validated using MS-MLPA. Positive controls of *BRCA1* promoter hypermethylated were used[276] (T127 and /162).

Immunofluorescence experiments

The following primary antibodies were used for immunofluorescence (IF): rabbit anti-RAD51 (Santa Cruz Biotechnology sc-8349 1:250), rabbit anti-RAD51 (Abcam ab133534, 1:1000), mouse anti-geminin (NovoCastra NCL-L, 1:100 in PDX samples, 1:60 in patient samples), rabbit anti-geminin (ProteinTech 10802-1-AP, 1:400), mouse anti-BRCA1 (Santa Cruz Biotechnology sc-6954, 1:50), mouse anti-BRCA1 (Abcam ab16780, 1:200), mouse anti-γH2AX (Millipore #05-636, 1:200), rabbit anti-53BP1 (Cell Signalling #4937, 1:100), rabbit anti-phospho-RPA32 S4/S8 (pRPA S4/S8, Bethyl, A300-245A, 1:500), rabbit anti-phospho-DNA-PKc S2056 (pDNA-PKc, Abcam ab18192, 1:200), rabbit anti-phospho-histone H3 S10 (pHH3, Cell Signalling #9701, 1:100). Goat anti-rabbit Alexa fluor 568, goat anti-mouse Alexa fluor 488, donkey anti-mouse Alexa fluor 568 and goat anti-rabbit Alexa fluor

488 (Invitrogen; 1:500) were used as secondary antibodies. For target antigen retrieval, sections were microwaved for 4 minutes at 110°C in DAKO Antigen Retrieval Buffer pH 9.0 (pH 6.0 for 53BP1 and pHH3 staining) in a T/T MEGA multifunctional Microwave Histoprocessor (Milestone). Sections were cooled down in distilled water for 5 minutes, then permeabilized with DAKO Wash Buffer (contains Tween 20) for 5 minutes, followed by incubation in blocking buffer (DAKO Wash Buffer with 1% bovine serum albumin) for 5 minutes. Primary antibodies were diluted in DAKO Antibody Diluent and incubated at room temperature for 1 hour. Sections were washed for 5 minutes in DAKO Wash Buffer followed by 5 minutes in blocking buffer. Secondary antibodies were diluted in blocking buffer and incubated for 30 minutes at room temperature. The 2-step washing was repeated followed by 5 min incubation in distilled water. Dehydration was performed with increasing concentrations of ethanol. Sections were mounted with DAPI ProLong Gold antifading reagent and stored at -20°C. Immunofluorescence images were acquired using Olympus DP72 microscope and generated using CellSens Entry software.

Immunofluorescence scoring

Scoring was performed blindly onto life images using a 60x-immersion oil lens. At least 2 biological replicates of each PDX model and treatment were analyzed. Nuclear foci of 0.42 to 1.15 μm diameter were quantified on FFPE tumor samples. For RAD51 scoring, the percentage of geminin-positive cells with 5 or more RAD51 nuclear foci was quantified. Geminin was used as counterstaining to mark for S/G2-cell cycle phase[277]. One-hundred geminin-positive cells from at least 3 representative areas of each sample were analyzed. For the pharmacodynamic studies, the levels of DNA damage and replication stress was quantified on FFPE tumor samples by scoring the percentage of geminin-positive cells with γH2AX or pRPA32 S4/S8 nuclear foci, respectively, as described for RAD51 scoring. Replication stress levels was also quantified by scoring the percentage of cells with pan-nuclear γH2AX staining. The percentage of cells in mitosis or S/G2-phase of the cell cycle was quantified by scoring the percentage of cells with pHH3 or geminin staining, respectively.

ATM immunohistochemistry

For ATM staining, the same protocol as for IF assay was performed in collaboration with AstraZeneca. Tissues were additionally blocked in endogenous peroxidase block (3% H_2O_2 in dH_2O) for 10 min. Rabbit anti-ATM (Abcam ab32420, 1.2 µg/mL) was used as primary antibody. Antibody detection was performed with DAKO Envision HRP for 30 min with visualization using DAKO DAB solution for 10 min and counterstaining in Carazzi's haematoxylin. ATM was scored by image analysis using Indica Labs HALO, by automated tissue classification of tumor regions and analysis of percentage positive tumor nuclei.

Reverse phase protein array (RPPA) analysis

RPPA analysis was performed in the MD Anderson Cancer Center as described[278,279]. PDX tumor proteins were denatured by 1% (w/v) SDS in the presence of β-mercaptoethanol and adjusted to a final concentration of 1mg/ml. Samples were diluted in five serial 2-fold dilutions in dilution buffer (lysis buffer containing 1% SDS) and arrayed on nitrocellulose-coated slides (Grace Biolab) using an Aushon 2470 Arrayer (Aushon BioSystems). Each slide was probed with a validated primary antibody plus a biotin-conjugated secondary antibody. The signal was amplified using a DakoCytomation–catalyzed system (Dako) and visualized by DAB colorimetric reaction. Slides were scanned, analyzed and quantified using a customized-software Microvigene (VigeneTech Inc.) to generate spot intensity.

PDX for RAD51 assay validation (PDX cohort-3)

PDX from cohort-3 were generated at Curie Institute (Paris, France) and Paoli Calmette Institute (Marseille, France) under approved informed consent. The majority of these PDXs were previously published[280,281]. *In vivo* experiments were performed at Xentech. When tumors reached a size of 70-250 mm^3, mice were randomly assigned to homogeneous groups of 5 to 10 animals and were treated p.o. with niraparib (50 mg/kg or 75 mg/kg), olaparib (50 mg/kg or 100 mg/kg) or veliparib (100 mg/kg) daily for 28 days. Tumor volume was evaluated by measuring biweekly tumor diameters with a caliper.

HRD score

Myriad's myChoice® HRD Test was performed at Myriad Genetics on DNA extracted from PDXs of cohort-3. DNA extraction was performed at Xentech using the NucleoBond AXG100 kit (Macherey-Nagel).

73-gene profiling of PDX cohort-3

Mutation profiling of 73 genes among the most frequently mutated in cancer according to the COSMIC database was performed at BGI (Beijing, China) on genomic DNA by exon trapping with NimbleGen microarray followed by deep sequencing by using Illumina's HiSeq technology, with at least 50X effective mean depth for each sample. This study was performed in collaboration with Xentech.

Cell lines

The following *in vitro* studies were performed at the Genome Stability Laboratory at CHU de Québec Research Center in collaboration with Jean-Yves Mason, Mandy Ducy and Jacques Simard. U2OS osteosarcoma cells (HTB-96) were purchased from American Type Culture Collection (ATCC) and maintained in McCoy's 5A (Gibco) supplemented with 10% Fetal Bovine Serum (FBS) and 1% penicillin/streptomycin (P/S). HeLa cells were maintained in DMEM medium (Corning) supplemented with 10% FBS and 1% P/S. All cell lines were routinely tested to be mycoplasma free.

Cas9/mClover-LMNA homologous recombination assay

The mClover-LMNA homologous recombination assay was adapted from[282,283]. In brief, U2OS cells were seeded at 175,000 cells per well in 6-well plates to be transfected 6 hours later with control or *PALB2* siRNA at a final concentration of 50 nM using Lipofectamine RNAiMAX (Invitrogen). Twenty-four hours post-transfection, $1x10^6$ cells per condition were pelleted and resuspended in 100 µL complete nucleofector solution (SE Cell Line 4D-

Nucleofector™ X Kit, Lonza) to which 1 µg of pCR2.1-CloverLMNAdonor, 1 µg pX330-LMNAgRNA, 1 µg of the indicated *PALB2* construct, 0.1 µg of piRFP670-N1 (used as transfection control), and 200 µmol of siRNA was added. Once transferred to a 100 µl Lonza certified cuvette, cells were transfected using the 4D-Nucleofector X-unit, program CM-104, immediately resuspended in culture media and transferred to a 100 mm dish for 64 hours. Then, 500,000 cells were plated onto glass coverslips while the remaining was lysed for western blotting as described below. Coverslips were fixed with 4% paraformaldehyde and analyzed for Clover expression by fluorescence microscopy a total of 72 h post nucleofection.

Localization of PALB2 to laser-induced DSBs

The experiments were performed as described in[284]. Briefly, HeLa cells were transfected with YFP-PALB2-WT or YFP-PALB2-p.M296Nfs and microirradiated along a track in cell nuclei. The recruitment of YFP-PALB2 to laser-induced DNA damage sites was monitored over time by imaging cells every 2 min for 1 h. The fluorescence intensity of the indicated DNA constructs at DNA damage sites relative to an unirradiated area was quantified and plotted over time.

Protein extraction and western blotting

Flash-frozen pieces of tumor were lysed in ice-cold buffer containing Tris–HCl pH 7.8 20 mmol/L, NaCl 137 mmol/L, EDTA pH 8.0 2 mmol/L, NP40 1%, glycerol 10%, supplemented with NaF 10 mmol/L, Leupeptin 10 mg/mL, Na_2VO_4 200 mmol/L, PMSF 5 mmol/L, and Aprotinin (Sigma-Aldrich). Homogenization was performed on ice with a POLYTRON® system PT 1200 E (Kinematica). Lysates were centrifuged at 13.000 rpm 4ºC during 30 min and the supernatants were collected. Protein concentration was calculated using DCTM Protein Assay (Bio-Rad). A total of 30 µg of protein were separated on 12% SDS-PAGE at 100V and transferred to nitrocellulose membrane for 1.5 h at 100 V. Membranes were blocked for 1 h in 5% milk in Tris-buffered saline (TBS)-Tween and then hybridized using

the primary antibodies in 5% BSA TBS-Tween: rabbit anti-RAD51 (Santa Cruz Biotechnology H-92, 1:500), rabbit anti-human GAPDH (Abcam ab128915, 1:5000), mouse anti-tubulin (Sigma-Aldrich T-9026, 1:5000). Mouse and rabbit horseradish peroxidase (HRP)-conjugated secondary antibodies (GE Helthcare, 1:2000) were diluted in 5% milk in TBS-Tween and proteins were detected with Immobilon Western Chemiluminiscent HRP substrate (Millipore). Images were captured with a FUJIFILM LASS-4000 camera system and quantified with Image J (http://rsb.info.nih.gov/ij/).

For BRCA1, tumor lysates were made in RIPA lysis buffer complemented with 2X Complete protease inhibitor cocktail (Roche) and Pefabloc (Roche; 1mg/ml). Western blots were performed as described[142] by the Division of Molecular Pathology and Cancer Genomics at The Netherlands Cancer Institute. Briefly, protein samples containing 40 µg protein are heated 10 min at 70°C, loaded on to a NuPage 3-8% Tris Acetate gradient gel (Invitrogen EA03752BOX) and run for 2-3 h at 100 V in Novex Tris-acetate running buffer (Invitrogen LA0041) supplied with Nupage antioxidant (NP0005). The protein samples were transferred on a PVDF membrane (Millipore IPVH0001030; 30 s prewetted in methanol) in 50mM Tris, 36mM glycine containing 0.01% SDS, during 16 h at 100 mA. Membranes were blocked for 1 h with 5% ELK non-fat dry milk powder (Campina)/ TBS-Tween and incubated overnight at 4 °C with primary antibody (anti-BRCA1, Cell Signalling #9010, 1:1000 in 1% ELK/TBST). Goat anti rabbit-HRP-conjugated secondary antibody (DAKO, 1:2000) was diluted in 1% ELK/TBST and incubated for 1 h at room temperature. The signal is detected by electrochemiluminescence (ECL)-using ECL Plus (Amersham RPN2132/ Pierce PX0080196).

For PALB2, western blots were performed by the Genome Stability Laboratory at CHU de Québec Research Center. U2OS cells were resuspended in ice-cold lysis buffer (50 mM Tris-HCl, pH 7.4, 500 mM NaCl, 0.5% NP-40) containing protease and phosphatase inhibitors (PMSF (1 mM), aprotinin (4 µg/ml), leupeptin (1 µg/ml), NaF (5 mM) and Na_3VO_4 (1 mM)). Frozen tumors of each PDX (n=1-3 replicates) were lysed in 500 µl of ice-cold lysis buffer (40 mM Tris-HCl pH 7.4, 1% Triton-X-100, 40 mM Beta-glycero phosphate, 5% Glycerol, 100 mM NaCl, 1 mM EDTA, 50 mM NaF, and protease and phosphatase inhibitors as above) per 100 mg and then crushed using a sterile pestle (Axygen). U2OS and PDX lysates were incubated for 30 min on ice and sonicated 30 s ON\OFF for 10 cycles with a Bioruptor

(Diagenode). Insoluble material was removed by high-speed centrifugation at 4°C and protein concentration was determined by the Bradford assay. Total soluble protein extracts were separated by SDS-PAGE and transferred onto nitrocellulose membranes (GE Healthcare). Membranes were blocked for an hour at room temperature with 5% non-fat dry milk in PBST and probed overnight, 4°C, with rabbit anti-PALB2 antibody (Bethyl A301-246A, 1:2000) and mouse anti-GAPDH antibody (Fitzgerald 10R-G109a, 1:160000) in the blocking solution. HRP-conjugated secondary antibodies (Jackson ImmunoResearch, 1:10000) were diluted in PBST for 1 h at room temperature followed by detection using the Western Lighting Chemiluminescence Reagent Plus (PerkinElmer).

gBRCA patient cohort

The cohort consisted of gBRCA metastatic patients treated at the Vall d'Hebron University Hospital within clinical trials testing PARP inhibitors in monotherapy or combination, with FFPE material representative of the disease and signed IRB-approved informed consent form. IF analysis and RAD51 quantification was performed as described for FFPE PDX tumor samples.

HBOC patient cohort

The cohort consisted of breast cancer patients from the Vall d'Hebron University Hospital, with FFPE material representative of the disease and signed IRB-approved informed consent form. Due to personal or family history, and after ruling out *BRCA1/2* mutations, patients were tested for germline mutations linked to breast cancer susceptibility within a research protocol. IF analysis and RAD51 quantification was performed as described for FFPE PDX tumor samples.

Statistical analysis

Regarding the sample size calculation, this exploratory study involved as many samples as possible during the study timeframe. Data was analyzed with GraphPad Prism version 7.0. Error bars represent the Standard Error of the Mean (SEM) of at least two biological replicates, unless otherwise stated. Shapiro-Wilk test was used to assess normality of data distributions. Statistical tests were performed using paired or unpaired two-tailed *t*-test (for two groups comparison of PARP1 and 53BP1 protein levels, YFP intensity (%) in the FRAP assay and the percentage of γH2AX/geminin-positive cells, geminin-positive cells and pHH3-positive cells); Mann-Whitney U-test (for two groups comparison of the percentage of RAD51/geminin-positive cells, pRPA32 S4/S8/geminin-positive cells and pan-γH2AX-positive cells); or one-way ANOVA (for three or more groups comparisons). For treatment efficacy comparisons of the *in vivo* experimental data, two-way ANOVA was used. Pearson correlation was used to analyze the correlation between the RAD51 score and the tumor volume change upon olaparib treatment. For the validation of the two anti-RAD51 antibodies, Spearman correlation was used. The ROC AUC was calculated to estimate the prediction capacity of HRD and RAD51 scores to PARPi response. For ROC curve comparison, a two-sided bootstrap test was used by means of statistical package pROC in R software version 3.4.1. To calculate the association between *PALB2* mutation and the RAD51 score a logistic regression model was fitted to estimate the odds ratio (OR) with CI95%. Levene's test is used to test if groups of comparison have equal variances (homoscedasticity). No evidence has been found to reject the hypothesis of homoscedasticity in our data. Consequently, the statistical comparison has been carried out under the hypothesis of similar variance between groups.

RESULTS

PART 1

A RAD51 assay identifies restoration of homologous recombination repair as the major mechanism of PARP inhibitor resistance in germline *BRCA1/2* mutated breast cancer.

This chapter is based on a published paper[285]

The establishment of a PDX panel from gBRCA patients' tumors

To investigate the mechanisms of PARPi resistance in human tumors, a panel of patient derived xenografts (PDX) from gBRCA mutation carriers with breast or ovarian cancer was developed. For this purpose, fresh tumor samples from patients were prospectively collected and implanted into nude mice. A total of twelve PDX models (11 gBRCA1 and 1 gBRCA2) were established (**Table 3**). Specifically, eight PDXs derived from gBRCA1 metastatic tumors from different organs and four PDXs were established from primary breast tumors. Five engrafted models were derived from patients with metastatic disease participating in clinical trials with PARPi. Of note, three samples were obtained prior to olaparib treatment from patients who showed partial response (PR, n=1) or no response to the treatment (primary resistance, n=2). Two additional samples were derived from metastatic gBRCA1 OC patients who progressed to the PARPi olaparib after showing a sustained partial response (acquired resistance, n=2).

Germline mutations in *BRCA1/2* were confirmed in all models but PDX274, and they were associated with loss of the wild type allele (**Appendix Fig.S1**). Specifically, PDX274 lacked the germline *BRCA1* c.211A>G mutation in exon 5 due to an out-of-frame deletion of exons 3 to 7 of *BRCA1* in the pathogenic allele, unveiled by massively parallel sequencing and MLPA. This detection was confirmed at the somatic level in the original patient's tumor, meaning that it was not acquired in the PDX.

Table 3 | **Characteristics of patients and PDXs from cohort-1.** The patient characteristics are summarized, including the germline *BRCA1/2* mutation, prior therapies and response to PARPi when available. The PDX information include timepoint of implantation, response to PARPi, loss of heterozygosity (LOH) in *BRCA1/2,* genetic reversions in *BRCA1* and mutated relevant genes found in the PDXs. For missense mutations, the variant allele frequency and functional effect is indicated. HGVS, Human Genome Variation Society. TNBC, triple negative BC. Met, metastasis. Pap, papillary. OC, ovarian cancer. ER+BC, estrogen receptor positive BC. Adj, adjuvant; NeoAdj, neoadjuvant. SD, stable disease. PD, progressive disease. CR, complete response.

PATIENT							PDX		Response to Olaparib		PDX											
											BRCA1/2		Genetic alterations in known PARPi-resistance genes									
PARPi treatment		ID	Diagnosis / Sample origin	Germline BRCA1/2 mutation (HGVS)	Predicted BRCA1/2 protein	Prior therapies	ID	Timepoint of implantation	Patient	PDX	mutation (HGVS)	LOH	MLPA BRCA1	Genetic Reversion *BRCA1/2*	*TP53BP1*	*PAXIP1 (PTIP)*	*PRCC*	*C20orf196 (SHLD1)*	*FAM35A (SHLD2)*	*SLFN11*	*RAD51*	*ATM*
PARPi treated	implanted prior to exposure to PARPi	Pt124	TNBC Skin Met	*BRCA1* c.1961delA	BRCA1 p.Lys654Serfs*47	1. NeoAdj doxorubicin + docetaxel; 2. Adj cisplatin + vinorelbin; 3. paclitaxel + bevacizumab; 4. vinorelbine + capecitabine + bevacizumab	PDX124	Prior to cisplatin and PARPi combination	Sensitive (PR)	mSD	*BRCA1* c.1961delA	LOH	n	No	None	(4 copies)	None	None	None	None	6 copies, focal	None
		Pt127	TNBC Skin Met	*BRCA1* c.68_69delAG	BRCA1 p.Glu23Valfs*17	1. NeoAdj doxorubicin + cyclophosphamide → docetaxel	PDX127	Prior to cisplatin and PARPi combination	Primary resistance	mPD	*BRCA1* c.68_69delAG	LOH	cnLOH	No	None	None	p.55T, 0.49, unknown		Complete deletion	None	None	p.I1547T, 0.52, unknown
		Pt179	TNBC sc. Met	*BRCA1* c.68_69delAG	BRCA1 p.Glu23Valfs*17	Bilateral metachronic BC. 1. 1st Adj: epirubicin + cyclophosphamide + 5FU; 2. 2nd. Adj: capecitabine; 3. cisplatin; 4. cisplatin	PDX179	Prior to cisplatin and PARPi combination	Primary resistance	mPD	*BRCA1* c.68_69delAG	LOH	n	No	None	None	None	None	None	None	3 copies, not focal	None
	implanted at progression to PARPi	Pt196	Pap. Serous OC Pericardial Met	*BRCA1* c.1961delA	BRCA1 p.Lys654Serfs*47	1. NeoAdj/Adj carboplatin + paclitaxel; 2. carboplatin + paclitaxel; 3. carboplatin + paclitaxel; 4. pegylated liposomal doxorubicin; 5. olaparib	PDX196	At PARPi progression	Acquired resistance	mPD	*BRCA1* c.1961delA	LOH	cnLOH	No	None	None	None	None	None	None	None	p.V245I, 0.22, unknown; p.C532Y, 0.71, unknown
		Pt280	Pap. Serous OC Lymph node Met	*BRCA1* Complete deletion	BRCA1 p.0	1. Adj carboplatin + paclitaxel; 2. carboplatin + paclitaxel; 3. liposomal doxorubicin; 4. paclitaxel + bevacizumab; 5. cisplatin + olaparib → olaparib monotherapy; 6. carboplatin + pegylated liposomal doxorubicin; 7. gemcitabine; 8. paclitaxel	PDX280	At PARPi progression	Acquired resistance	mPD	*BRCA1* Complete deletion	LOH	null	No	None	None	None	None	None	p.H661D, 0.97, unknown	None	None
PARPi untreated		Pt221	TNBC Primary	*BRCA1* c.5027delT	BRCA1 p.Leu1676*	1. NeoAdj doxorubicin + cyclophosphamide + 5FU → paclitaxel	PDX221	Post-neoadjuvant chemotherapy	Untreated	mPD	*BRCA1* c.5027delT	LOH	cnLOH	No	None	None	None	None	None	None	None	None
		Pt230	TNBC Primary	*BRCA1* c.68_69delAG	BRCA1 p.Glu23Valfs*17	1. NeoAdj non-pegylated liposomal doxorubicin + cyclophosphamide → paclitaxel	PDX230	Post-neoadjuvant chemotherapy	Untreated	mCR	*BRCA1* c.68_69delAG	LOH	n	No	None	None	None	None	None	None	None	None
							PDX230OR	derived from PDX230	NA	mPD		LOH	NA	No	splice; c.5294_5305 +33del45	None	None	None	None	None	None	None
		Pt236	TNBC Skin Met	*BRCA1* c.5194-12G>A	BRCA1 p.His1732Phefs*5	1. NeoAdj doxorubicin + cyclophosphamide + docetaxel; 2. paclitaxel + gemcitabine; 3. capecitabine; 4. pegylated irinotecan (NKTR102)	PDX236	Post-pegylated irinotecan	Untreated	mPD	*BRCA1* c.5194-12G>A	LOH	cnLOH	No	None	None	None	None	None	None	None	None
		Pt252	TNBC Lymph node Met	*BRCA1* c.5123C>A	BRCA1 p.Ala1708Glu	1. NeoAdj epirubicin + docetaxel; 2. carboplatin + gemcitabine; 3. lurbinectedin (PM01183)	PDX252	Post-lurbinectedin	Untreated	mPD	*BRCA1* c.5123C>A	LOH	cnLOH	No	None	None	None	None	None	None	None	p.R919T, 0.29, unknown
		Pt274	TNBC Skin Met	*BRCA1* c.211A>G	BRCA1 p.Cys64X	1. NeoAdj doxorubicin + cyclophosphamide → docetaxel 2. Adj carboplatin + gemcitabine; 3. eribulin; 4. pegylated liposomal doxorubicin	PDX274	Post-pegylated liposomal doxorubicin	Untreated	mPD	*BRCA1* deletion exons 3-7	LOH	n	No	None	None	None	p.D58N, 0.43, unknown	None	None	None	None
		STG316	TNBC Primary	*BRCA1* c.134+3A>C	BRCA1 p.Cys27X	1. NeoAdj docetaxel x3, epirubicin + cyclophosphamide + 5FU x1, cisplatin x1, carboplatin x2	STG316	Post-carboplatin	Untreated	mPD	*BRCA1* c.134+3A>C	LOH	n	No	deletion exons 12-16	None	None	None	None	None	None	None
		Pt71	ER+BC Primary	*BRCA2* c.3264dupT	BRCA2 p.Gln1089Serfs*10	None	PDX071	Treatment naïve	Untreated	mCR	*BRCA2* c.3264dupT	LOH	n	No	None	None	None	None	None	None	None	None

This panel of PDXs allowed us to perform *in vivo* experiments and have unlimited access to tumor material from the pre-PARPi treatment, during-treatment and post-PARPi resistance acquisition scenarios. Using these PDX tumor samples we performed genomic analysis to detect both secondary mutations in *BRCA1/2* and other genomic alterations, functional tests of DNA repair markers (including 53BP1, BRCA1, γH2AX and RAD51 foci) and also proteomic studies of different proteins implicated in PARPi response.

Olaparib antitumor activity in the gBRCA PDX panel distinguishes a subset of PARPi-resistant tumors

The antitumor activity of the PARPi olaparib was assessed in the PDX collection (**Fig.9A**). Three gBRCA models exhibited antitumor activity with olaparib treatment as assessed by mRECIST (see materials and methods): complete response (CR, n=2: PDX071 and PDX230) or stable disease (SD, n=1: PDX124). The remaining nine gBRCA PDX models were resistant to olaparib treatment (PD, progressive disease). Of note, all the PARPi-resistant PDXs are *BRCA1* mutant and seven out of nine came from the advanced metastatic setting. Among the PDX models from gBRCA primary tumors, two out of four (50%) showed CR. The resistance to PARPi-treatment in the PDXs implanted after patient progression to PARPi, namely PDX196 and PDX280, was confirmed in the PDXs (**Fig.9A**). Moreover, the sensitivity to PARPi-treatment in the PDXs from metastatic patients previously treated with PARPi (PDX127, PDX179 and PDX124) mirrored the patients' clinical response (**Fig.9B**).

One additional resistant model was generated after prolonged exposure (>100 days) and steep progression to olaparib (PDX230OR) from its PARPi-sensitive counterpart (PDX230, **Fig.9C**). This new gBRCA1 acquired-resistant PDX was stablished by implanting the tumor overgrowing with olaparib treatment (black triangles in **Fig.9C**). The *in vivo* activity of olaparib was assessed in the PDX230OR, proving that the new model is resistant to PARPi treatment (**Fig.9A**). Altogether, a collection of 13 gBRCA1/2 models (called PDX cohort-1) was generated and, when known, recapitulates patients' response to PARPi. Thus, this PDX panel represents a tool for monitoring the antitumor activity of PARPi and a suitable platform to study clinically relevant mechanisms of PARPi resistance *in vivo*.

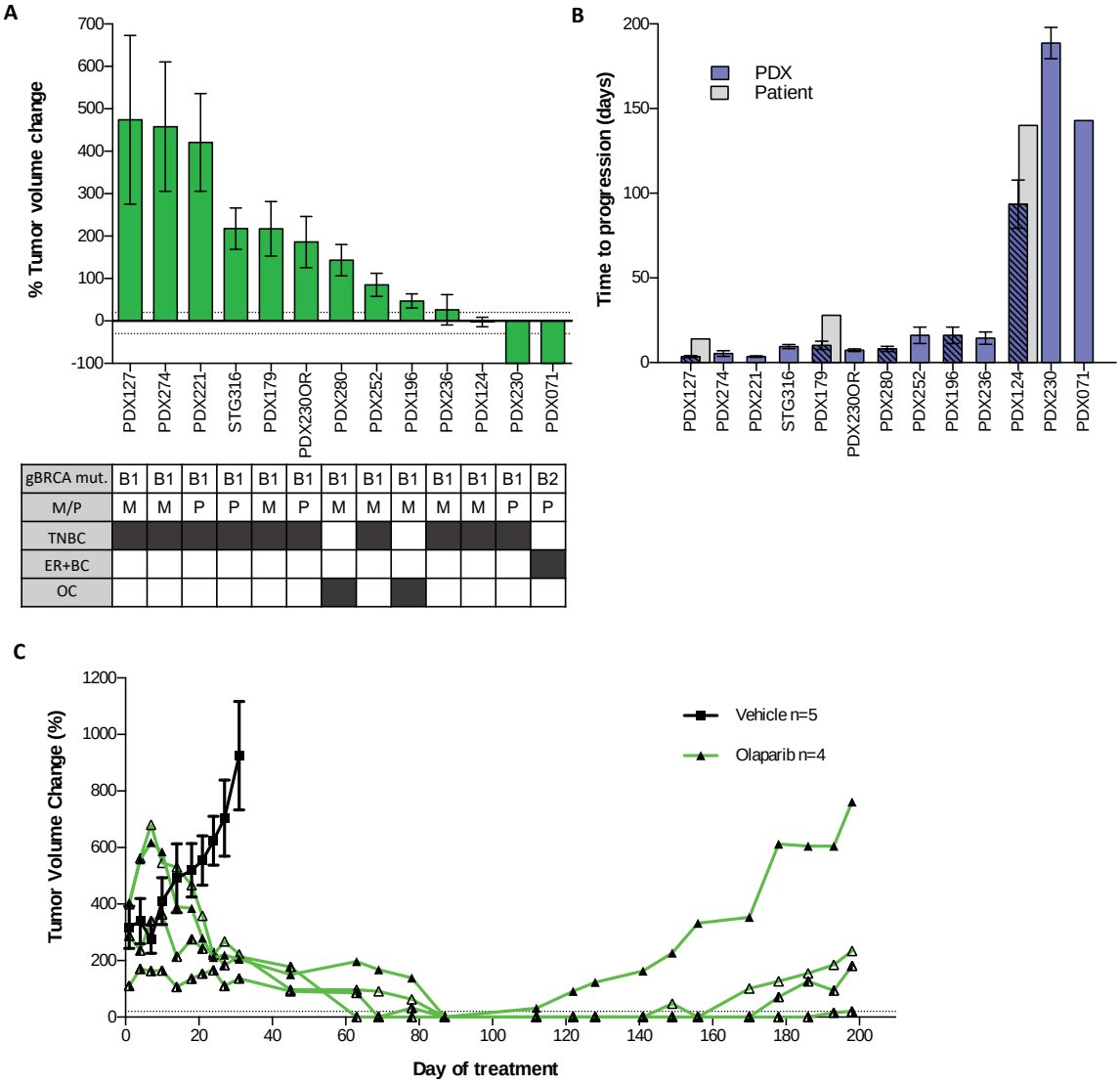

Figure 9 | **The antitumor activity of olaparib in the PDX cohort-1 identifies a subset of gBRCA-mutated PARPi-resistant tumors. A)** Waterfall plot showing the percentage of tumor volume change compared to the tumor volume on day 1. +20% and -30% are marked by doted lines to indicate the range of PR, SD and PD. The box underneath summarizes different characteristics of each model and the clinical context at the moment of PDX implantation. TNBC, Triple Negative Breast Cancer; ER+BC, Estrogen Receptor positive Breast Cancer; OC, Ovarian Cancer; P, primary; M, metastasis. Error bars indicate SEM from independent tumors. **B)** Graph showing the sensitivity of the PDX vs. the patient's clinical response to olaparib. Time to PARPi progression of patients and PDXs is shown. Blue bars, time point at which the % of tumor volume change was ≥20% following olaparib treatment in the PDX models. Patients' time on PARPi therapy until progression is plotted in light grey bars (Pt127, Pt179 and Pt124). Blue bars show mean +/- SEM of at least 3 independent PDX tumors. **C)** Acquisition of PARPi-resistance in PDX230 after prolonged exposure to olaparib. The percentage of tumor volume change during olaparib treatment is plotted. For vehicle-treated tumors, the mean +/- SEM is represented (squares). The individual tumors of the olaparib arm are shown in green lines (different triangle patterns).

PARPi-resistant gBRCA1 PDX models do not harbor target loss or secondary *BRCA1* mutations

Having stablished the panel of gBRCA PDX models and the *in vivo* antitumor activity of olaparib, we aimed to investigate the mechanisms of resistance to PARPi in these PDXs. In order to verify that all tumors express the drug target, PARP1 protein levels were determined by RPPA. Results confirmed that all gBRCA PDXs expressed different levels of PARP1 similar than other tumors with no gBRCA mutation (**Fig.10A**), and olaparib-resistant PDXs did not showed lower levels of PARP1 (**Fig.10B**). Then, in order to investigate whether genetic reversion is a dominant mechanism for clinical resistance to PARPi in our panel of gBRCA PDXs, massively parallel exome sequencing was assessed to study the presence of secondary mutations in *BRCA1/2* genes. Surprisingly, no frameshift-correction nor genetic reversion of the inherited mutation occurred in this population of PARPi-resistant tumors, since all models but PDX274 harbored the expected germline mutation. The out-of-frame deletion of *BRCA1* exons 3-7 in PDX274 was predicted to cause a premature stop codon and truncated protein (**Appendix Fig.S1** and **Table 3**).

Altogether, these results demonstrated that neither target loss nor secondary mutations represented a mechanism of PARPi resistance in PDX cohort-1.

The expression of functional hypomorphic BRCA1 isoforms is associated with PARPi resistance in gBRCA1 PDX models

We next analyze the expression level of *BRCA1* by measuring the levels of *BRCA1* mRNA among the gBRCA PDX panel (**Fig.10C**). As expected, PDX280, which harbored a large deletion encompassing the complete *BRCA1* gene, showed absent *BRCA1* mRNA. All the remaining gBRCA PDX models showed variable *BRCA1* mRNA expression. Having confirmed *BRCA1* mRNA expression in all PDX models but PDX280, we investigated the potential expression of hypomorphic BRCA1 isoforms and its recruitment to DNA damage sites. For this purpose, we conducted an immunofluorescence (IF) staining of DDR proteins in samples from PARPi-resistant *vs* PARPi-sensitive PDXs. DNA DSBs were detected as phosphorylated histone H2AX (γH2AX) nuclear foci[286]; RAD51 nuclear foci was used as

marker of DNA repair by HRR[287]; geminin staining was used as marker of S and G2 phases of the cell cycle, when HRR takes place[288]; to detect BRCA1 protein and potential hypomorphic isoforms, we used two different antibodies against the N-terminus (B1-NT) or the C-terminus (B1-CT) of BRCA1. We set up the conditions for the IF assay in formalin-fixed, paraffin-embedded (FFPE) tumor samples in two non-gBRCA PDX models: one luminal B model, PDX131, and one TNBC model, PDX094. We stained both vehicle- and cisplatin- (in PDX131) or olaparib-treated (in PDX094) FFPE tumor samples and were able to detect nuclear foci of RAD51, γH2AX and BRCA1 with both B1-NT and B1-CT antibodies (**Appendix Fig.S2**). Co-localization of RAD51 and γH2AX foci (**Appendix Fig.S2A**) in addition with the presence of RAD51 and BRCA1 foci only in cells in S/G2-phase of the cell cycle (geminin-positive, **Appendix Fig.S2B**) demonstrated the specificity of the assay.

We then performed the IF assay to detect BRCA1 nuclear foci in the gBRCA PDX panel, using the *BRCA2* mutant PDX071 as a positive control for the assay (BRCA1 nuclear foci were detected with both BRCA1 antibodies) and PDX280 as a negative control due to complete deletion and no mRNA expression of *BRCA1*. With this assay, BRCA1 nuclear foci were also detected in seven additional gBRCA1 PDX models, either by using the B1-NT or the B1-CT antibodies, in concordance with the expression of different hypomorphic BRCA1 isoforms. PDX124 and PDX196 harbor a mutation in the exon 11 of *BRCA1* (c.1961delA) and express the BRCA1-Δ11q splice isoform (p.Ser264_Gly1366del)[145]. As expected, BRCA1 nuclear foci were detected with both B1-NT and B1-CT antibodies (**Fig.11A**). In the N-terminal BRCA1 mutants PDX179, STG316 and PDX274, BRCA1 nuclear foci were observed exclusively with the B1-CT antibody, consistent with a BRCA1 RING-less protein isoform being expressed[143] (**Fig.11A**). Two out of the three C-terminal BRCA1 mutant models, namely PDX221 and PDX236, showed BRCA1 nuclear foci after staining with the B1-NT antibody but not with the B1-CT antibody, consistent with the hypothetical stabilization of the gBRCA1 mutant protein via HSP90[131] (**Fig.11A**). Of note, the BRCA1 foci were always restricted to cells in the S/G2-phase of the cell cycle (geminin-positive). In addition, the different BRCA1 isoforms were detected by western blot at the respective predicted sizes of the truncated proteins (**Fig.11B**). No detection of BRCA1 nuclear foci was seen neither in the gBRCA1 PDX230, that showed CR to PARPi treatment, nor in the three remaining PARPi-resistant PDXs, namely

PDX127, PDX230OR and PDX252, together with PDX280 (**Fig.11A**). In summary, these data showed that a large proportion of PARPi-resistant gBRCA1 PDX models exhibit recruitment of different hypomorphic BRCA1 isoforms to form nuclear foci.

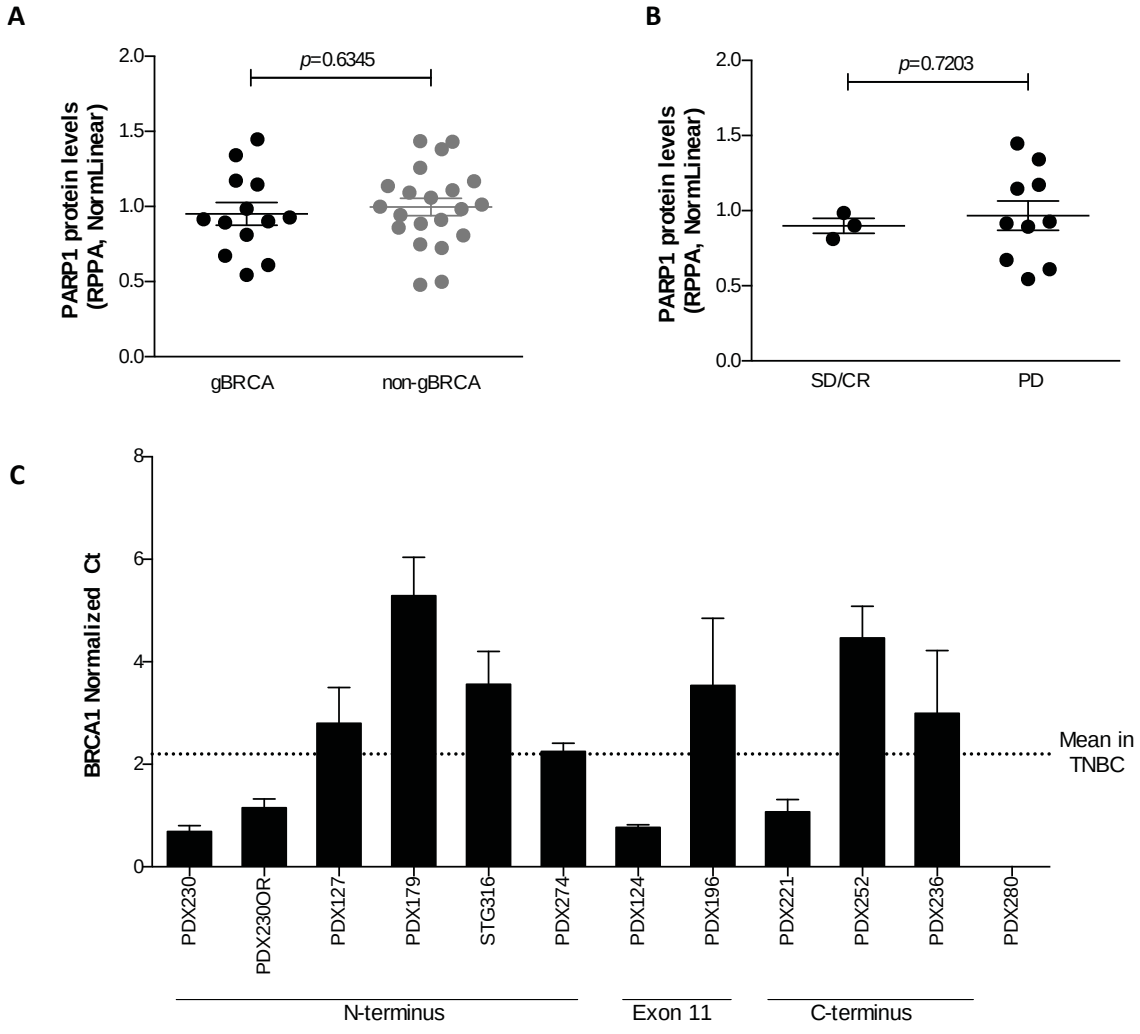

Figure 10 | **Analysis of PARP1 protein levels and BRCA1 mRNA expression in PDX cohort-1. A)** PARP1 protein levels measured by RPPA in the gBRCA PDX models and other cohort of TNBC PDXs with no mutations in *BRCA1/2* (non-gBRCA) (Unpaired *t*-test). **B)** Comparison of PARP1 protein levels between PARPi-resistant vs. PARPi-sensitive PDX models from cohort-1 (Unpaired *t*-test). Each point represents the mean of at least 3 independent PDX tumors. Error bars indicate SEM of different PDXs. **C)** *BRCA1* mRNA levels of the gBRCA PDX models measured by real-time qRT-PCR is represented and compared to the mean of two TNBC PDXs with no mutation in *BRCA1/2*. The domain of the *BRCA1* mutation is indicated. PDX280 harbors a complete deletion in *BRCA1*. Error bars indicate SEM from 3 independent tumors.

Loss of 53BP1 and FAM35A in PARPi-resistant gBRCA1 PDX models

Having shown that four out of eleven olaparib-resistant gBRCA1 PDX models did not express hypomorphic BRCA1 proteins, we further aimed to investigate the mechanisms of PARPi resistance in these models. As PARPi resistance in BRCA1-deficient tumors may also result from loss of end resection barrier, such as 53BP1[148,149], we tested whether this mechanism occurs in our panel of gBRCA PDXs. Exome sequencing was performed to find out somatic mutations in known genes implicated end resection suppression and PARPi resistance (**Table 3**): *TP53BP1*, *MAD2L2* (REV7), *PAXIP1* (PTIP), *Artemis*, *RIF1*, *PRCC*, *c20orf196* (SHLD1), *FAM35A* (SHLD2) and *FLJ26957* (SHLD3). Results showed genetic alterations in *TP53BP1* in two PARPi-resistant models, PDX230OR and STG316. STG316 had acquired a large homozygous deletion encompassing exons 12-16 of *TP53BP1* (**Table 3**). Inactivation of *TP53BP1* in PDX230OR was due to a homozygous deletion of 45 base pairs (bp) encompassing 12 exonic and 33 intronic bp including the splice donor site, which was not present in its PARPi-sensitive counterpart PDX230 (**Table 3**). These results suggest that the acquired mutation in *TP53BP1* was responsible of the acquisition of PARPi resistance in this gBRCA1 PDX. We then analyzed the 53BP1 protein levels by RPPA to ruled out the possibility of epigenetic silencing or low expression of 53BP1 in other PARPi-resistant PDXs. Only the two models with genetic alterations in *TP53BP1,* namely PDX230OR and STG316, showed low 53BP1 protein levels (**Fig.11C**). We then confirmed these results by performing IF analysis to detect 53BP1 in olaparib-treated PDX samples, showing that both PDX230OR and STG316 were unable to form 53BP1 nuclear foci, in comparison with all the other gBRCA PDX models (**Fig.11A**). Interestingly, among the remaining three PDXs models with unknown mechanisms of PARPi resistance (PDX127, PDX252, PDX280), PDX127 harbors a FAM35A loss, which is part of the shieldin complex. The absence of any member of this complex has been recently demonstrated to derive in PARPi resistance similarly to 53BP1 loss[154–157]. An heterozygous unknown mutation in the REV7-interacting domain of PRCC (p.P55T, Variant Allele Frequency (VAF) = 0.49, **Table 3**) is also found in PDX127. Finally, PDX274 showed an unknown, heterozygous mutation in other member of the shieldin complex, C20orf196 (p.D58N, VAF = 0.43, **Table 3**). The remaining PDXs did not harbor any genetic alteration in genes implicated in end resection.

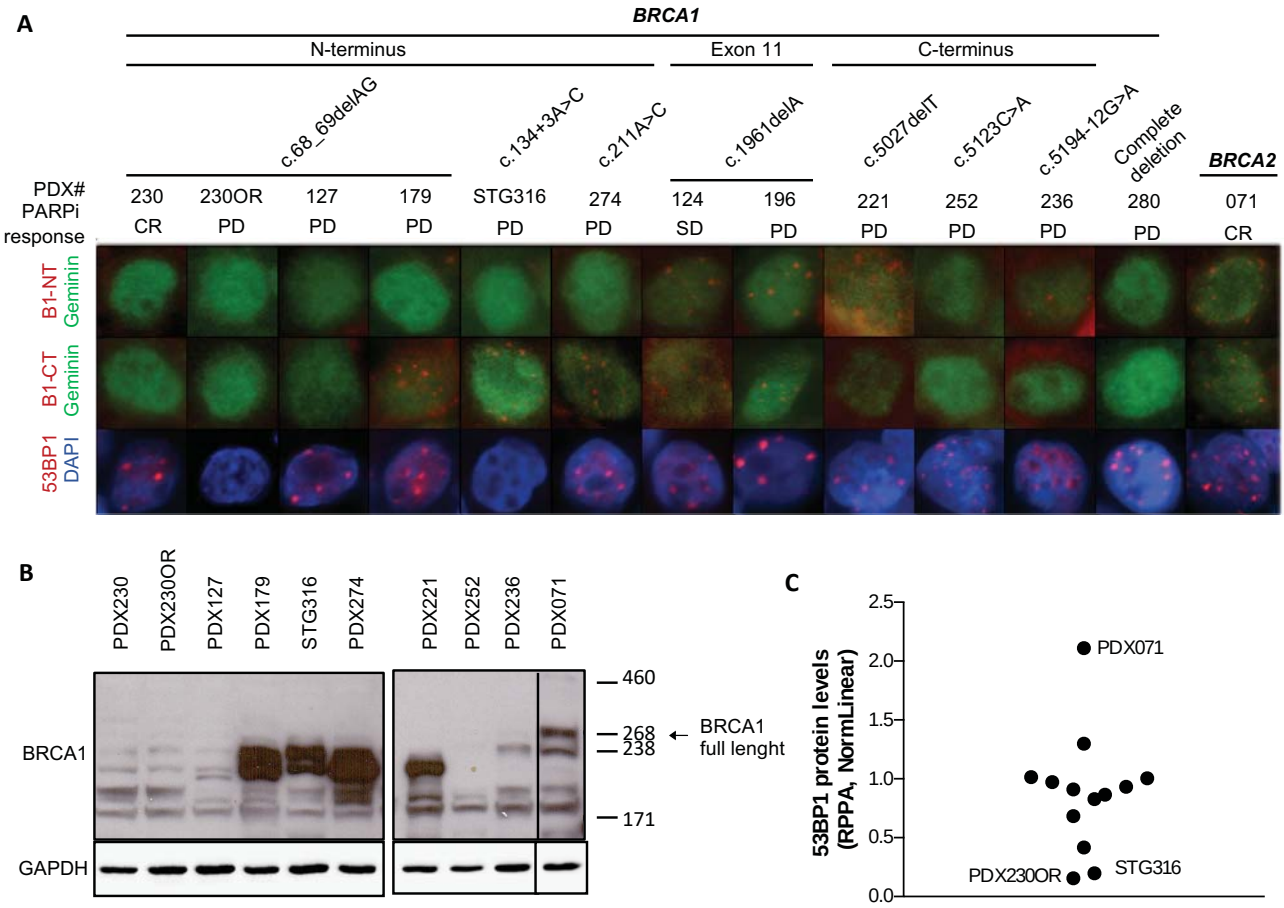

Figure 11 | **Hypomorphic BRCA1 isoforms and 53BP1 loss were associated with PARPi resistance in gBRCA1 PDX models. A)** PARP1 Immunofluorescence staining of BRCA1 [with an antibody toward the N-terminus (B1-NT) or C-terminus (B1-CT) of BRCA1] and 53BP1 nuclear foci in olaparib-treated samples across the PARPi-sensitive and PARPi-resistant gBRCA PDX models. The response to PARPi treatment and the location of the mutation within the *BRCA1* gene is indicated. Nuclei were visualized with DAPI (blue). Green nuclei indicate geminin-positive cells (cells in S/G2-phase of the cell cycle). One cell is shown for each model. **B)** Western blot of hypomorphic BRCA1 isoforms detected with an antibody towards the exon 11 of BRCA1 (B1-exon 11); loading control is human GAPDH. **C)** 53BP1 protein levels measured by RPPA in the gBRCA PDXs models. Each point represents the mean of at least 3 independent PDX tumors.

To study other mechanisms that could explain PARPi-resistance, we then investigated the presence of inactivating mutations in other known PARPi resistance genes, including *PARP1*, *SLFN11* and *CHD4* (**Table 3**). We only found a genetic alteration in these genes in PDX280, which harbors an unknown short variant mutation in SLFN11 (p.H661D, VAF = 0.97, **Table 3**), but it must be further validated as mechanisms of PARPi resistance. We did not observe inactivating mutations in other known PARPi resistance genes described to date.

These data demonstrated that the recovery of DNA end resection capacity through loss of either 53BP1 or FAM35A occurs in our panel of gBRCA1 PARPi-resistant PDX models.

PARPi-resistant gBRCA1 PDXs are able to form RAD51 nuclear foci

Our findings demonstrated the recruitment of hypomorphic BRCA1 isoforms to DNA damage sites and/or the removal of a barrier to DNA end resection (53BP1 and FAM35A) in gBRCA1 PARPi-resistant PDXs, two mechanisms of PARPi resistance that are associated with the recovery of HRR capacity. Therefore, we then studied the capacity to form RAD51 nuclear foci in our gBRCA PDX panel as a functional surrogate of HRR. With this aim, we performed the IF assay to detect geminin-positive cells with RAD51 nuclear foci in olaparib-treated FFPE tumor samples from the PDX cohort-1. RAD51 nuclear foci were detected in all the eleven PARPi-resistant gBRCA PDXs, including all models expressing hypomorphic BRCA1 isoforms and/or lacking 53BP1/FAM35A, but also the two PDXs with unknown mechanism of PARPi resistance, namely PDX252 and PDX280. Interestingly, RAD51 foci co-localized with BRCA1 foci in all PDX expressing the BRCA1 RING-less (PDX179, STG316 and PDX274), BRCA1-Δ11q (PDX196 and PDX124) and C-terminal BRCA1 mutants (PDX221 and PDX236) (**Fig.12A**).

RAD51 nuclear foci formation can be assessed in untreated tumor samples and is associated with PARPi resistance in PDX cohort-1

When assessing for RAD51 nuclear foci formation, we also observed that the model that showed disease stabilization upon olaparib treatment, that is PDX124, showed much stronger pan-nuclear RAD51 staining than the other models. This pattern is consistent with a focal *RAD51* amplification (**Table 3**) and high protein expression (**Fig.12B**). Furthermore, we also noticed that this SD model showed lower levels of cells with RAD51 nuclear foci than the other PD models. For this reason, we ought to investigate this observation by scoring the percentage RAD51-positive cells across the PDX cohort-1. To control for the effect of intertumoral variability in proliferation and to avoid false negatives on RAD51 scoring, we assessed RAD51 foci only in geminin-positive cells, therefore assessing RAD51 foci only among tumor cells in S/G2-phase of the cell cycle. In all tumor analyzed, RAD51 foci were observed only in geminin-positive cells, providing further validation of the staining. To consider a cell as RAD51-positive, 5 or more RAD51 nuclear foci should be quantified[238]. Among the 13 evaluated gBRCA PDX models, the percentage of RAD51-positive cells was significantly higher in PARPi-resistant vs PARPi-sensitive PDXs (35.6 ± 2.4 % in PARPi-resistant *vs.* 5.1 ± 3.3 % in PARPi-sensitive, p=0.0017) (**Fig.13A and B**).

To discard the possibility that there was a different explanation for the lack of RAD51 foci, that is, that tumor samples had not enough DNA damage or there are PARPi pharmacodynamic differences, we examined the levels of cells with γH2AX foci as marker of DSBs in all PDX models, both in vehicle- and olaparib-treated tumor samples. To be consistent with the RAD51 scoring and be sure that DSBs could be repair by HRR, we scored the percentage of cells with γH2AX foci within the geminin-positive cells. As expected, the levels of γH2AX-positive cells increased in the olaparib-treated samples (**Fig.13C**). This analysis showed that lack of DNA damage was not the cause underlying the absence of RAD51 foci in the sensitive models and ruled out both pharmacodynamic differences and drug export as potential reasons for the differential responses to PARPi.

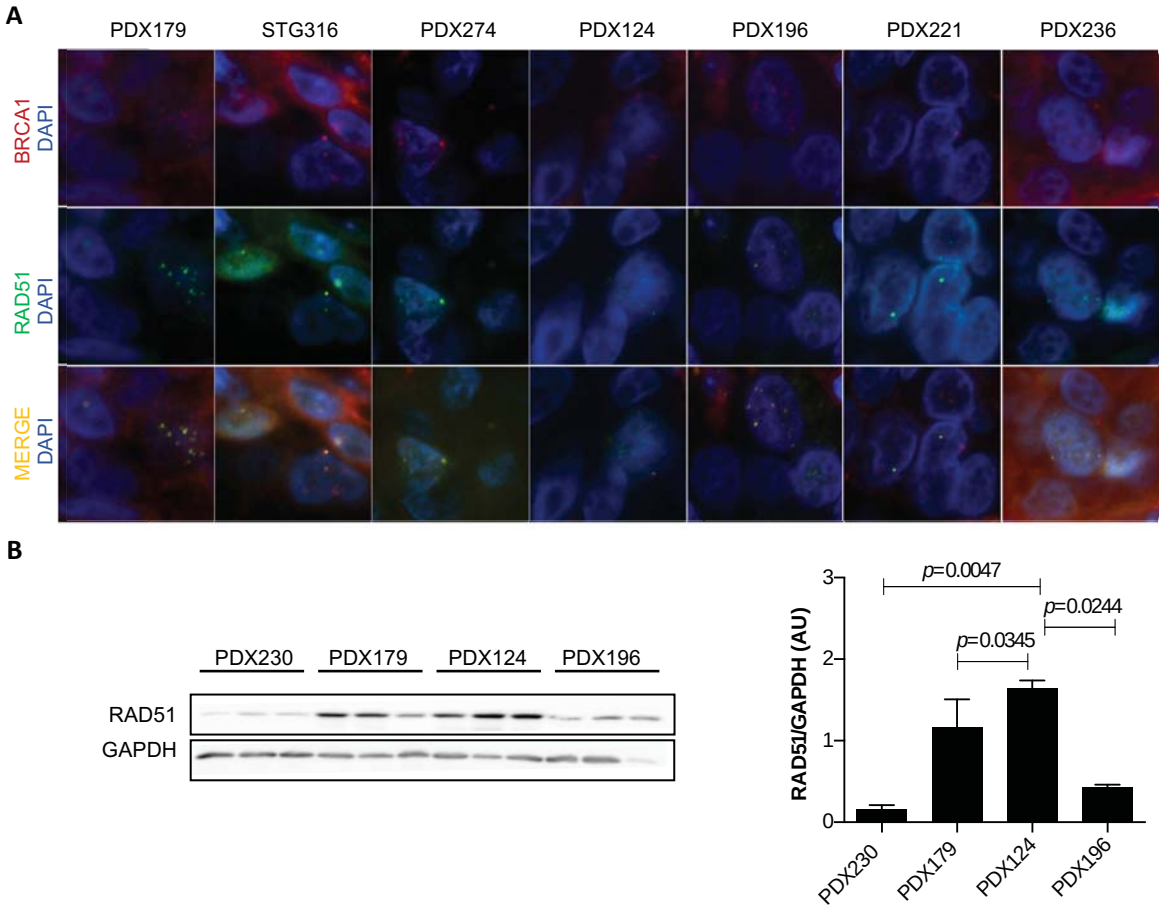

Figure 12 | **RAD51 foci formation in gBRCA1 PDXs expressing BRCA1 isoforms and RAD51 amplification in PDX124. A)** Immunofluorescence staining of BRCA1 (red) and RAD51 (green) showing co-localization of the two HRR markers in FFPE tumor samples from the indicated PDXs. Nuclei were visualized with DAPI (blue). All pictures were taken at 600x magnification. **B)** RAD51 amplification and overexpression in PDX124. Western blot of RAD51 and protein level quantification relative to human GAPDH in PDX124 and other gBRCA models (One-way ANOVA). Last sample from PDX196 was excluded in the analysis due to low band in GAPDH, used as loading control.

While previous studies had reported low levels of DNA damage as potential limitation to evaluate HRR functionality[238,240], we surprisingly observed substantial levels of baseline DNA damage, above 20% (**Fig.13C**). Thus, we also attempted to determine the level of RAD51-positive cells in vehicle-treated tumor samples from the gBRCA PDX cohort (**Fig.13A and B**). As shown with olaparib-treated tumors, PARPi-resistant tumors showed higher baseline percentage of RAD51-positive cells compared to PARPi-sensitive (24.0 ± 1.8 % *vs.* 3.4 ± 2.5 %, p=0.0025).

Finally, as RAD51 nuclear foci are observed during the S/G2-phase of the cell cycle, if a tumor sample lacks proliferating cells, RAD51 foci may not be observed. In order to circumvent this, we incorporated an evaluation of the percentage of geminin-positive cells in each analyzed model, as an indicator of adequate levels of proliferation. The rate of geminin-positive cells in all the 17 analyzed PDX models was between 30-70% in treated and non-treated samples (**Fig.13D**). There was no significant difference in the baseline percentage of geminin-positive cells between RAD51-positive and RAD51-negative groups, although PARPi-resistant models slightly increment the number of cells in S/G2-phase of the cell cycle upon olaparib treatment. This might be related with the capacity to stop cell cycle progression and give time to repair the DNA damage caused by PARP inhibition.

These data support that the differences in the levels of RAD51-positive cells between olaparib-sensitive and olaparib-resistant gBRCA PDXs reflected differences in tumor biology and not in other factors related with the formation of RAD51 foci. Therefore, it can be concluded that retention or restoration of HRR capacity is a common event associated with PARPi resistance in our gBRCA PDX panel and readily detectable with the RAD51 assay in PARPi-treated and untreated tumor samples, regardless of the underlying mechanisms of resistance.

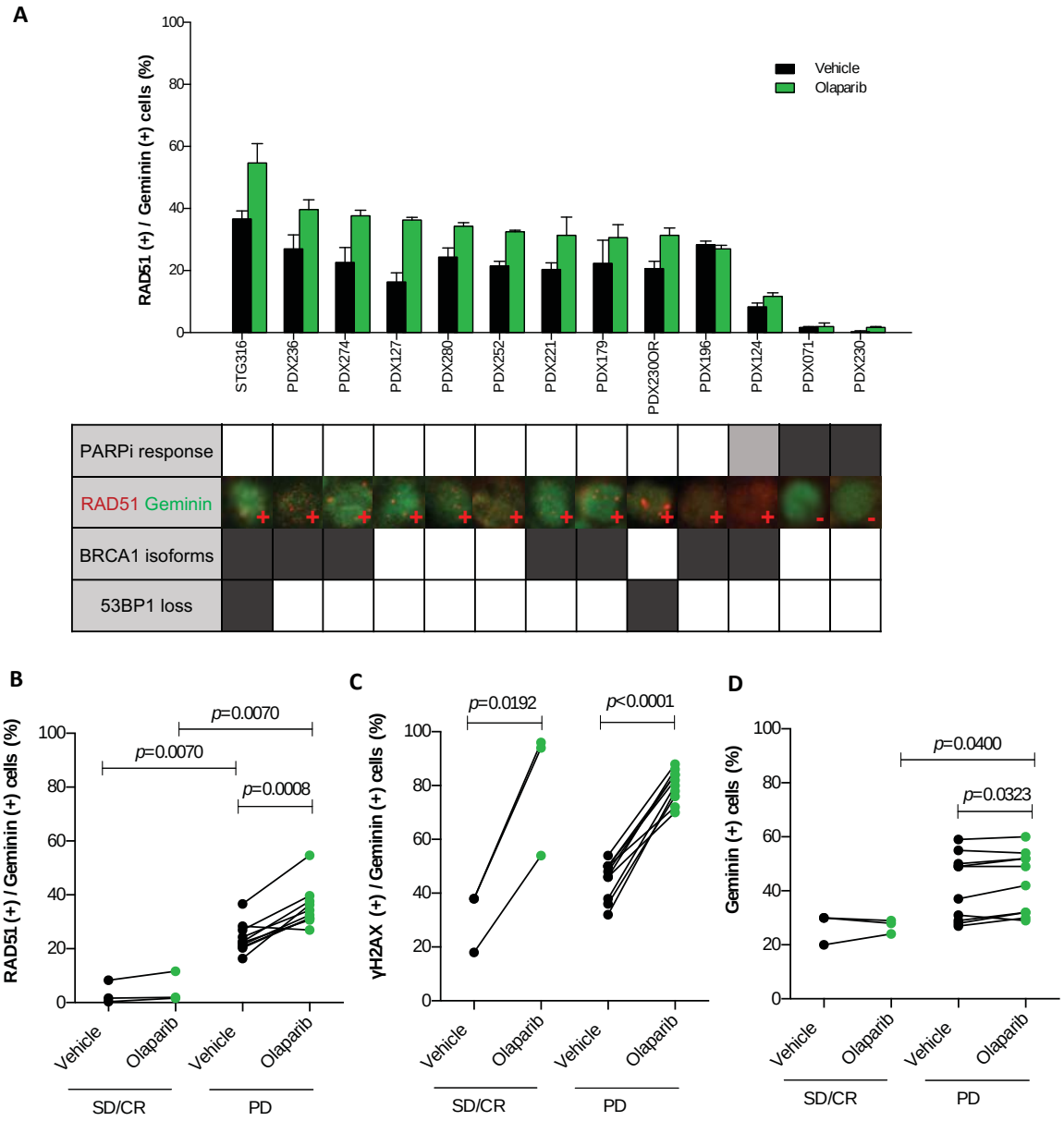

Figure 13 | **The detection of RAD51 nuclear foci identifies PARPi-resistant PDX tumors. A)** Percentage of geminin-positive, RAD51 nuclear foci-containing cells detected by immunofluorescence in FFPE samples from PDX tumors treated with PARPi (green bars) or vehicle (black bars). Error bars indicate SEMs from independent tumors. The correlation with PARPi-response is shown in the summary underneath: white box: PD; grey box: SD; black box: CR. Immunofluorescence staining of RAD51 foci in PARPi-treated PDX tumors is shown; one cell in the S/G2-phase (geminin-positive, green) with or without RAD51 foci (red) is shown for each model. The expression of BRCA1 isoforms and 53BP1 loss are also summarized. **B-D)** Quantification of geminin-positive cells that exhibit **B)** RAD51 (Mann–Whitney U-test) or **C)** γH2AX foci formation and **D)** cells in the S/G2-phase of the cell cycle (geminin-positive) (Paired *t*-test in vehicle- vs PARPi-treated tumors; Unpaired *t*-test in CR/PR vs PD tumors) following treatment with vehicle or olaparib in PARPi-sensitive (SD/CR) and PARPi-resistant (PD) PDXs.

RAD51 foci formation in FFPE tumor samples from patients predicts response to PARPi

To assess the feasibility and clinical applicability of detecting RAD51 foci in clinical samples, we stained for RAD51, γH2AX and geminin in 20 FFPE tumor samples from patients, including seven available samples from patients corresponding to seven gBRCA models of PDX cohort-1 (**Fig.14**). The analyzed tumor samples presented variable levels of RAD51- and γH2AX-positive cells regardless of whether or not patients received prior treatment (**Fig.14A and B**). Surprisingly, high levels of DNA damage were detected in some treatment-naïve tumor samples, specially from gBRCA1 mutation carriers. We also confirmed the presence of RAD51 nuclear foci in the FFPE sections of all the five patients' tumors corresponding to PARPi-resistant PDXs, namely PDX179, PDX221, PDX236, PDX252 and PDX274. Conversely, we were unable to detect RAD51 nuclear foci in the FFPE specimens of the two patients' tumors corresponding to the PARPi-sensitive gBRCA PDX models PDX071 and PDX230 (**Fig.14C**).

These results prompted us to further assess the potential clinical utility of the RAD51 assay as a functional biomarker of PARPi response in a cohort of patients treated with various PARPi at our institution (n=10 samples), including two paired pre/post-PARPi samples (Pt124 and Pt310). This cohort included eight patients with germline mutations in *BRCA1* (n=5) or *BRCA2* (n=3) and diagnosis of either BC (n=6) or OC (n=2). The tumor samples were collected prior to (n=7) or at progression (n=3) to treatment with PARPi. We stained for RAD51 and geminin and scored blindly (**Fig.15**). Importantly, all PARPi-resistant tumor samples, both with primary (n=4) and acquired resistance (n=3), showed higher levels of RAD51-positive cells than PARPi-sensitive tumors (n=2, **Fig.15B**). In Pt310, a *BRCA2* carrier who achieved a sustained PR for 17 months to the PARPi talazoparib, the pre-PARPi tumor sample showed no cells with RAD51 foci (0%) whereas the PARPi-progression sample scored 38%. Similarly, Pt124 scored 1% of RAD51-positive cells in the tumor sample collected before response to PARPi-treatment but scored 32% cells with RAD51 foci in the acquired-resistant tumor sample (**Fig.15B**). These results confirmed an inverse relationship between the RAD51 score and clinical efficacy of PARP inhibition in the overall patient cohort.

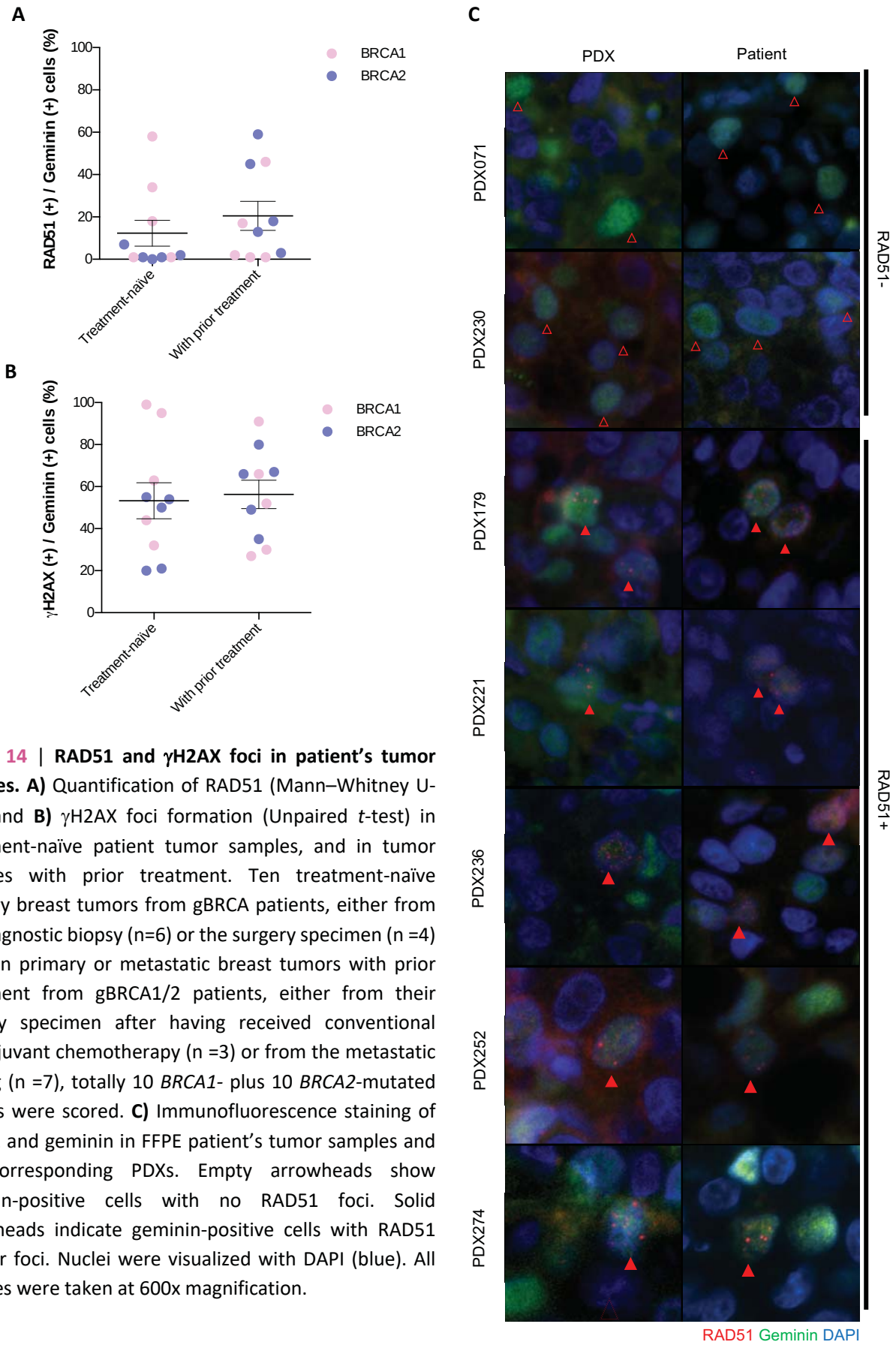

Figure 14 | **RAD51 and γH2AX foci in patient's tumor samples. A)** Quantification of RAD51 (Mann–Whitney U-test) and **B)** γH2AX foci formation (Unpaired *t*-test) in treatment-naïve patient tumor samples, and in tumor samples with prior treatment. Ten treatment-naïve primary breast tumors from gBRCA patients, either from the diagnostic biopsy (n=6) or the surgery specimen (n =4) and ten primary or metastatic breast tumors with prior treatment from gBRCA1/2 patients, either from their surgery specimen after having received conventional neoadjuvant chemotherapy (n =3) or from the metastatic setting (n =7), totally 10 *BRCA1*- plus 10 *BRCA2*-mutated tumors were scored. **C)** Immunofluorescence staining of RAD51 and geminin in FFPE patient's tumor samples and the corresponding PDXs. Empty arrowheads show geminin-positive cells with no RAD51 foci. Solid arrowheads indicate geminin-positive cells with RAD51 nuclear foci. Nuclei were visualized with DAPI (blue). All pictures were taken at 600x magnification.

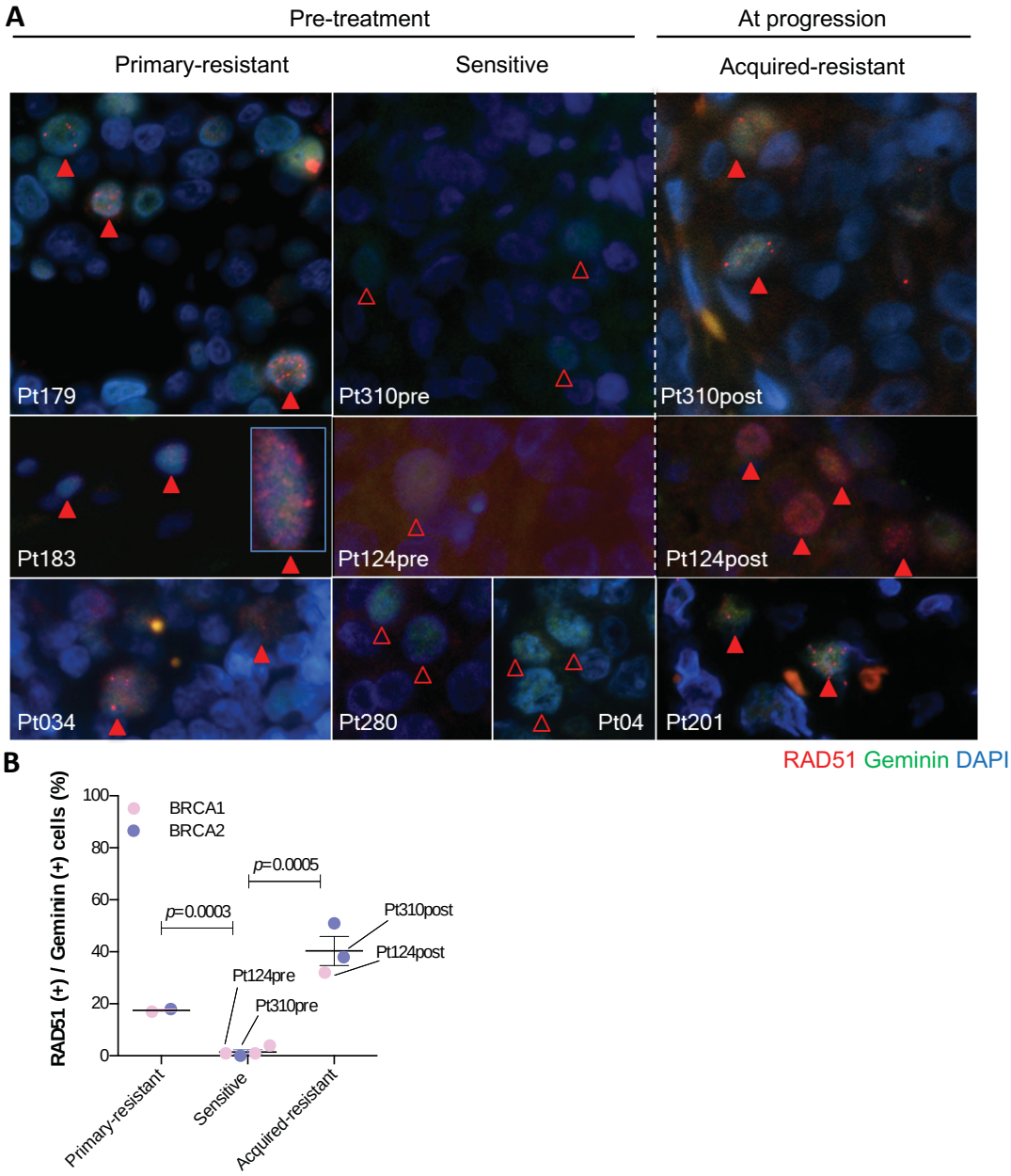

Figure 15 | **RAD51 in patients' tumors is associated with PARPi clinical response. A)** Immunofluorescence staining of RAD51 and geminin in the pretreatment patients' setting using a pretreatment tumor sample (or the most recent metastatic sample). Samples from three PARPi-resistant patients (Pt179, skin metastasis of TNBC; Pt183, dermal lymphatic carcinomatosis of ovarian cancer; Pt034, lymph node metastasis of ER+ BC) and four PARPi-sensitive patients (Pt310pre, liver metastasis of ER+ BC; Pt124pre, primary TNBC; Pt280, peritoneal implant of ovarian cancer; Pt04, lymph node metastasis of TNBC) are shown. For acquired resistance, samples obtained from three patients at PARPi progression (Pt310post, liver metastasis; Pt124post, skin metastasis; Pt201, skin metastasis of ER+ BC) are shown. Empty arrowheads show geminin-positive cells with no RAD51 foci. Solid arrowheads indicate geminin-positive cells with RAD51 nuclear foci. Nuclei were visualized with DAPI (blue). All pictures were taken at 600x magnification. **B)** Quantification of cells in S/G2-phase of the cell cycle (geminin-positive) with RAD51 nuclear foci in patients' tumor samples shown in panel A (Mann–Whitney U-test). Pt183 was not scored as the tumor did not contain enough geminin-positive cells.

PART 2

The RAD51 assay identifies homologous recombination repair deficient sporadic breast tumors with PARP inhibitor sensitivity.

This chapter is based on a published paper[289]

The establishment of a PDX panel from non-gBRCA patient's tumors

As HRR deficiency may occur also in tumors with wild type *BRCA1/2*, we aimed to investigate the antitumor activity of the PARPi olaparib in human tumors from BC patients not carrying germline mutations in *BRCA1* or *BRCA2*. For this purpose, we stablished a collection of thirteen PDX models from triple negative, non-gBRCA BC patients. Two additional models were provided by members of the EuroPDX consortium (1 TNBC and 1 ER-positive BC), yielding a total of fifteen PDX models (14 TNBC and 1 ER-positive BC). Specifically, seven PDX were stablished from triple negative or ER-positive metastatic breast tumors and eight were primary breast tumors (**Table 4**).

Olaparib antitumor activity in the non-gBRCA PDX panel distinguishes a subset of tumor highly sensitive to PARPi

We tested the antitumor activity of olaparib in the non-gBRCA PDXs. Treatment with olaparib exhibited antitumor activity in four PDX models as assessed by mRECIST (see materials and methods): CR (n=2: PDX093 and PDX197) or PR (n=2: STG201 and PDX302). The remaining eleven PDXs were olaparib resistant (PD) (**Fig.16A**). Within the four olaparib-sensitive models, three acquired-resistant PDXs were developed after prolonged exposure and steep progression to olaparib, namely STG201OR, PDX093OR and PDX302OR (**Fig.16B**). These non-gBRCA acquired-resistant PDX models were stablished and the *in vivo* activity of olaparib was assessed, proving the resistance to PARPi (**Fig.16A**). Therefore, a collection of 18 non-gBRCA models was generated (PDX cohort-2) and constituted a platform to validate the RAD51 assay as biomarker of PARPi response beyond gBRCA and study clinically relevant mechanisms of PARPi sensitivity and acquired-resistance *in vivo*.

Table 4 | **Descriptive analysis from available patients of PDX cohort-2.** Median time between diagnosis and first relapse (in years) N=11 because 2 patients had no relapse. Median time between PDX and first relapse (in months) n=8 because 2 patients had no relapse and in 3 cases PDX sample was collected

Variable	N	Mean	Median (Min-Max)	Levels	n	%	Positive	Negative	Result	YES	NO
Median age at cancer diagnosis (in years)	13	57.85	58.19 (31.59-93.53)	-	-	-	-	-	-	-	-
Median time between diagnosis and first relapse (in months)	11	20.27	15 (5-96)	-	-	-	-	-	-	-	-
Median time between PDX and diagnosis (in months)	13	18.92	11 (1-97)	-	-	-	-	-	-	-	-
Median time between PDX and first relapse (in months)	8	6.88	6 (0-15)	-	-	-	-	-	-	-	-
Stage at diagnosis (n=13)	-	-	-	Stage I	2	15.39	-	-	-	-	-
	-	-	-	Stage II	7	53.85	-	-	-	-	-
	-	-	-	Stage III	3	23.08	-	-	-	-	-
	-	-	-	Stage IV	1	7.69	-	-	-	-	-
IHC characterization (n=13)	-	-	-	Estrogen receptor	-	-	4	9	-	-	-
	-	-	-	Progesterone receptor	-	-	2	11	-	-	-
	-	-	-	Her2 status	-	-	0	13	-	-	-
Cancer subtype (n=13)	-	-	-	Luminal A	1	-	-	-	-	-	-
	-	-	-	Luminal B	4	-	-	-	-	-	-
	-	-	-	TNBC	8	-	-	-	-	-	-
Mutational panel assessed (n=13)	-	-	-	Mutation	1	-	-	-	*TP53* Y106X	-	-
	-	-	-	WT	1	-	-	-	NA	-	-
	-	-	-	Not assessed	11	-	-	-	NA	-	-
Patient's therapy exposure previous to PDX (n=13)	-	-	-	Anthracyclines	-	-	-	-	-	8	5
	-	-	-	Taxanes	-	-	-	-	-	9	4
	-	-	-	Platinum	-	-	-	-	-	4	9
	-	-	-	Capecitabine	-	-	-	-	-	3	10
	-	-	-	Gemcitabine	-	-	-	-	-	3	10
	-	-	-	Hormone therapy	-	-	-	-	-	1	12
	-	-	-	Eribuline	-	-	-	-	-	1	12
	-	-	-	Other therapies	-	-	-	-	-	4	9

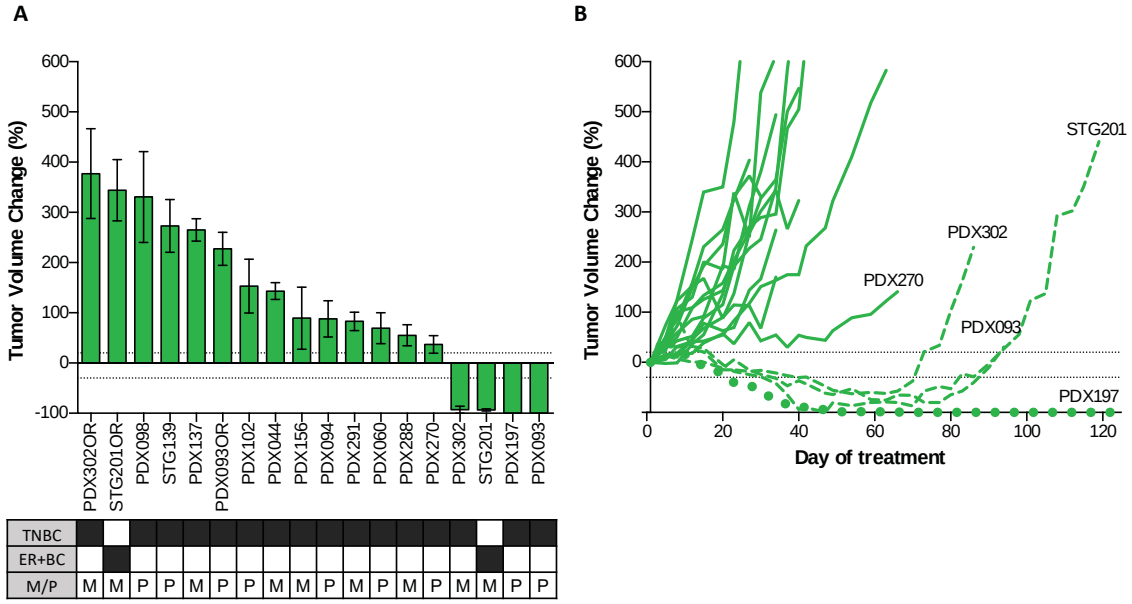

Figure 16 | **The antitumor activity of olaparib in PDXs identifies a subset of PARPi-sensitive tumors. A)** Waterfall plot showing the percentage of tumor volume change compared to the tumor volume on day 1. +20% and -30% are marked by doted lines to indicate the range of PR, SD and PD. The box underneath summarizes different characteristics of each model and the clinical context at the moment of PDX implantation. TNBC, Triple Negative Breast Cancer; ER+BC, Estrogen Receptor positive Breast Cancer; P, primary; M, metastasis. Error bars indicate SEM from independent tumors. **B)** Acquisition of PARPi-resistance in PDX302, STG201 and PDX093 after prolonged exposure to olaparib. The percentage of tumor volume change during olaparib treatment is plotted. Olaparib-sensitive models are represented with discontinuous lines.

PARPi-sensitive PDX models harbor epigenetic silencing of *BRCA1*

We next performed molecular and genetic characterization of PDX models from cohort-2 to identify somatic alterations compatible with HRR deficiency in the PARPi-sensitive models. Given that approximately 10% of sporadic breast cancers are HRR-deficient because of aberrant *BRCA1* promoter methylation[290], we first analyzed the epigenetic silencing of *BRCA1* by measuring the levels of *BRCA1* promoter methylation. MS-MLPA showed that three out of four olaparib-sensitive models, namely PDX302, STG201 and PDX197, and the olaparib-resistant model PDX270 presented *BRCA1* promoter hypermethylation, while the remaining PDX models showed low levels of methylation (**Fig.17A**, grey bars). Of note, this approach validated previously reported results of *BRCA1* promoter methylation from the models STG139 and STG201[269].

To validate these findings, we next analyzed *BRCA1* expression levels and the capacity to form BRCA1 nuclear foci as readout of BRCA1 functionality. Absence of *BRCA1* mRNA and lack of BRCA1 nuclear foci were restricted to the four models that showed *BRCA1* promoter hypermethylation, validating the epigenetic silencing of *BRCA1* in these PDXs (**Fig.17A**). Interestingly, the olaparib acquired-resistant models STG201OR and PDX302OR showed lower levels of *BRCA1* promoter hypermethylation in comparison to their sensitive counterparts, and recovered both *BRCA1* expression and nuclear foci formation (**Fig.17 and Appendix Fig.S3**).

Taken together, these results demonstrated that *BRCA1* epigenetic silencing is a common event among the PARPi-sensitive models of PDX cohort-2, but it did not fully overlap with PARPi sensitivity, as it was present in one PARPi-resistant model (PDX270) and absent in one olaparib-sensitive PDX (PDX093).

Somatic alterations in HRR-related genes within PDX cohort-2

As somatic genetic alterations could be present in other genes related with HRR functionality, we then performed exome sequencing to analyze this possibility in PDX cohort-2 (**Appendix Table S1**). Within the olaparib-sensitive PDX models, we identified frameshift mutations in HRR-related genes in two models: *PALB2* and *FANCD2* in PDX093 and STG201, respectively. PDX270 is a PARPi-resistant model and harbors a somatic frameshift mutation in the HRR-related gene *RAD54L*. The remaining PDX models did not show genetic alterations in HRR-related genes (**Fig.17A**). In summary, neither epigenetic silencing of *BRCA1* nor the presence of HRR-related genetic alterations fully associated with PARPi sensitivity in PDX cohort-2.

We further studied the HRR-related genetic alterations in the PARPi-sensitive models to investigate their relationship with HRR capacity. In STG201, PARPi sensitivity could be explained by the epigenetic silencing of *BRCA1*, but the mutation in *FANCD2* may also impact HRR. However, we discarded this possibility as the *FANCD2* mutation was still present in the acquired resistant model STG201OR (**Fig.17A and Appendix Table S1**).

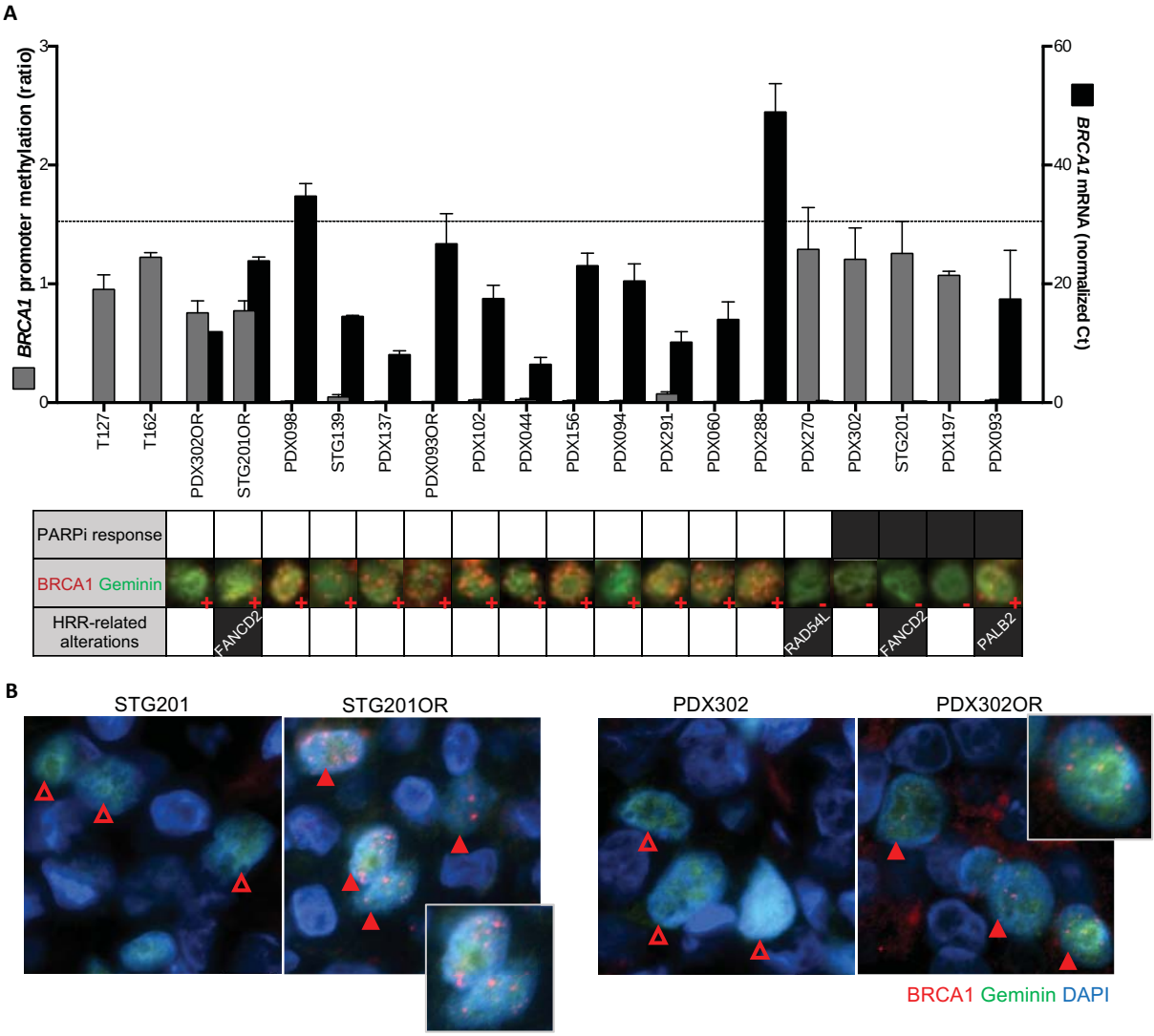

Figure 17 | ***BRCA1* promoter hypermethylation is associated with PARPi sensitivity in PDX cohort-2.** **A)** Levels of *BRCA1* promoter hypermethylation, *BRCA1* mRNA and the presence of BRCA1 nuclear foci are shown. Grey bars represent *BRCA1* promoter methylation levels; black bars show *BRCA1* mRNA levels in the PDX tumors. Error bars indicate SEM from independent tumors. T127 and T162 were used as positive controls for hypermethylated *BRCA1* promoter. Dashed line indicates mean of *BRCA1* mRNA levels in normal breast. PARPi-response is shown in the summary underneath: white box: PD; black box: PR/CR. Immunofluorescence staining of BRCA1 nuclear foci in PDX tumors is shown; one cell in the S/G2-phase (geminin-positive, green) with or without BRCA1 nuclear foci (red) is shown for each model. Alterations in HRR-related genes in PDX are also indicated. **B)** Restoration of BRCA1 foci formation in PARPi acquired-resistant PDXs. Immunofluorescence staining of BRCA1 foci in PARPi-treated tumors from STG201, PDX302 and the corresponding PARPi acquired-resistant models (STG201OR and PDX302OR). Empty arrowheads show geminin-positive cells with no BRCA1 foci. Solid arrowheads indicate geminin-positive cells with BRCA1 nuclear foci. Nuclei were visualized with DAPI (blue). All pictures were taken at 600x magnification. Larger views of positive cells are shown in each case.

We then investigated whether the *PALB2* mutation in PDX093 could explain the sensitivity to PARPi in this model. The *PALB2* mutation (c.886dupA) in PDX093 predicts a truncated PALB2 protein lacking the C-terminus region (p.M296Nfs), as the known germline pathogenic variant *PALB2* c.886del[291]. It has been described that the N-terminal coiled-coil of PALB2 acts as a dominant negative protein in a competition between PALB2 self-interaction and PALB2-BRCA1 interaction, severely affecting HRR capacity[292]. As the *PALB2* mutation in PDX093 was heterozygous in the tumor (VAF=0.44, **Appendix Table S1**) we decided to characterize this alteration in order to know if it may be related with PARPi sensitivity in this model. First, we validated exome sequencing data by Sanger and, as expected, results were consistent with a heterozygous mutation and the presence of mRNA from both the mutated and the wild type alleles (**Fig.18A**). Nevertheless, the PALB2 wild type protein was not detected by western blot in PDX093 (**Fig.18B**).

We then examined the recruitment of PALB2 to DSBs sites after laser-induced DNA damage. The experiment consisted in the microirradiation of HeLa cells transfected with YFP-PALB2-WT or YFP-PALB2-p.M296Nfs. The recruitment of YFP-PALB2 to laser-induced DNA damage sites was monitored over the time showing that PALB2 p.M296Nfs mutant protein was not property recruited (**Fig.18C**).

The second experiment consisted in study the effect of PALB2 p.M296Nfs mutant protein on HRR capacity using a Cas9/mClover-LMNA HRR assay in U2OS cells. In PALB2 siRNA-treated U2OS cells, transfection with wild type PALB2 partly rescued HRR capacity, while cells complemented with PALB2 p-M296Nfs mutant were HRR deficient (**Fig.18D**). We also performed the same experiment but with no PALB2 siRNA treatment to simulate the heterozygous condition in PDX093. Overexpression of PALB2 p.M296Nfs led to a 2-fold reduction of mClover-positive cells, demonstrating that this PALB2 mutant protein causes HRR deficiency despite the presence of endogenous wild type PALB2, in favor of a dominant negative effect[293] (**Fig.18E**). Collectively, all these assays indicate that PARPi sensitivity in PDX093 is probably due to impaired HRR caused by the *PALB2* c.886dupA mutation.

These studies were performed in collaboration with the Genome Stability Laboratory at CHU de Québec Research Center.

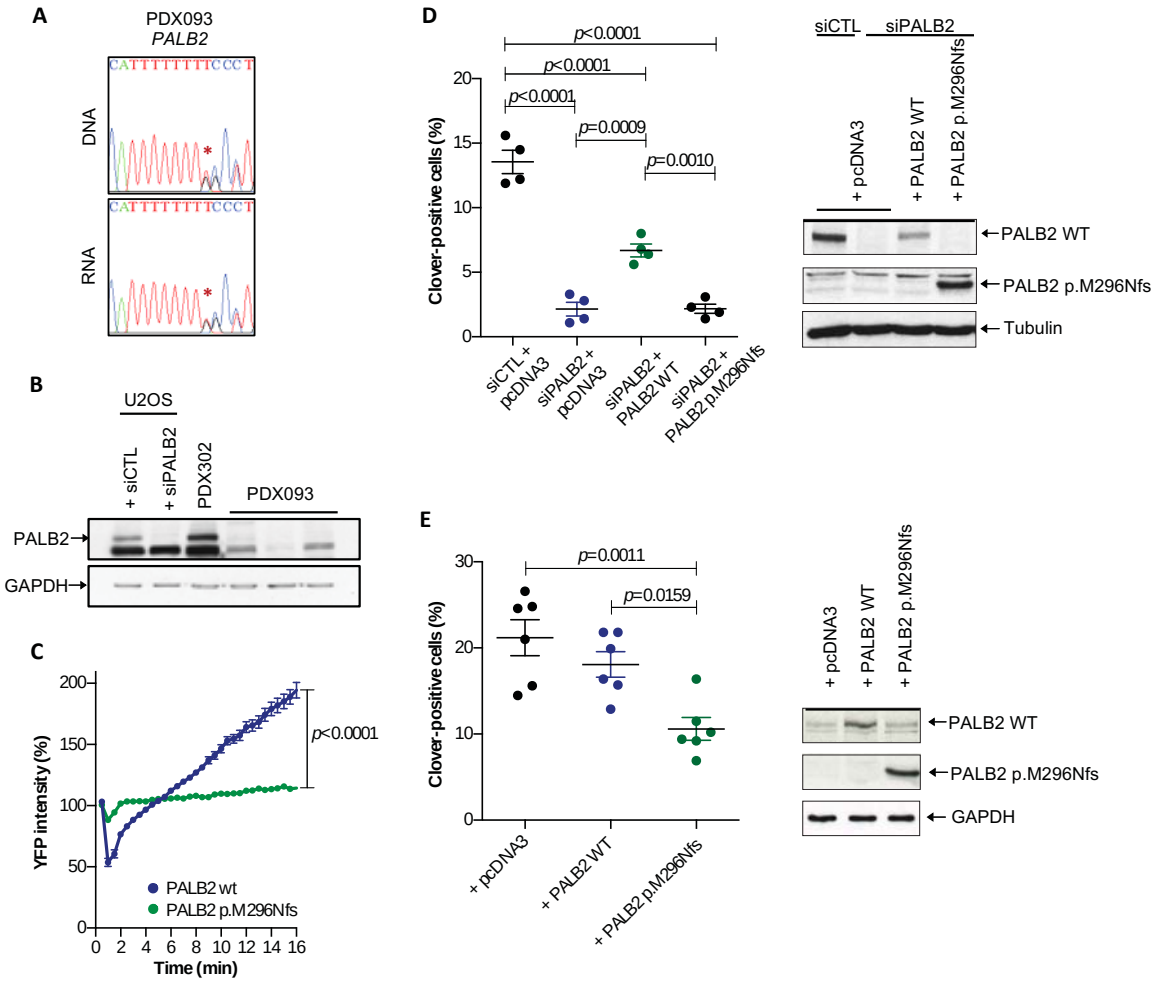

Figure 18 | **PALB2 p.M296Nfs mutation present in PDX093 impairs HRR capacity. A)** Sanger sequencing reverse plots of DNA and RNA from PDX093 showing 1 nt (T) insertion in one *PALB2* allele (*PALB2* c.866dupA). **B)** Western blot of PALB2 detected in U2OS cells and PDXs. Three biological replicates of PDX093 are shown; PDX302 is used as *PALB2* wild type (wt) PDX control. C) YFP-PALB2 recruitment to laser-induced DSBs is impaired in HeLa cells expressing PALB2 p.M296Nfs (Unpaired *t*-test at 16 min). Error bars indicate SEM of >40 cells per condition. **D-E)** Gene-targeting efficiency using Cas9/mClover-LMNA1 homologous recombination assay of **D)** siRNA PALB2 cells or **E**) cells with no *PALB2* depletion complemented with PALB2 wild type and PALB2 p.M296Nfs siRNA-resistant constructs. mClover positive cells were quantified (One-Way ANOVA). Western blots of PALB2 wild type and PALB2 p.M296Nfs for each condition are shown. Error bars indicate SEM from independent experiments.

RAD51 score is a robust biomarker to predict PARPi response in non-gBRCA PDX models

Given that PARPi-sensitive models of PDX cohort-2 harbor genetic alterations related with HRR deficiency, we investigated the capacity of repair DNA by HRR in our collection of non-gBRCA PDXs. With this purpose, we aimed to validate the RAD51 assay as functional biomarker of PARPi response and study its utility to extend PARPi treatment beyond gBRCA.

Firstly, in order to more deeply analyze the RAD51 scoring protocol, we performed an in-depth analysis of absolute RAD51 foci quantification in nine representative PDXs, including six PARPi-resistant (PDX098, PDX060, PDX094, PDX044, PDX102 and PDX270) and three PARPi-sensitive (PDX197, STG201 and PDX302) models. Quantification analysis revealed that, in HRR-deficient tumors, most of the geminin-positive cells exhibited zero RAD51 foci, while the HRR-proficient cells exhibit a bimodal distribution of the number RAD51 foci with the highest peak at 5 foci-per-cell (**Fig.19**). Regarding prediction of PARPi response, we analyzed different foci-per-cell thresholds in the untreated samples proving that the 5 foci-per-cell cut-off is the highest (most stringent) threshold that provides the most accurate and specific prediction (**Fig.20A and B**). These results demonstrated that the 5 RAD51 foci-per-nucleus cut-off was accurate for discrimination purposes.

Finally, we validated our findings by quantifying the RAD51 score with another commercial antibody against RAD51 in both vehicle- and PARPi-treated tumor samples from PDX cohort-2. Correlation analysis of the RAD51 quantifications with the two different antibodies demonstrated the repeatability of the RAD51 assay (**Fig.20C**).

Then, to avoid carrying the risk of technical issues leading to falsely scoring RAD51-negative samples, we stablished a protocol shown in **Fig.21A** that includes several quality controls (QC). Firstly, we used positive and negative external controls with every run of staining. Secondly, we used two internal controls: (i) the number of geminin-positive cells had to be at least 40, to ensure that there are sufficient cells in S/G2-phase of the cell cycle; and (ii) the % of γH2AX/geminin-positive cells had to be at least of 25%, to ensure that the tumor has sufficient endogenous DNA damage. Lack of either geminin- or γH2AX-positive cells (below those thresholds) would preclude scoring of RAD51.

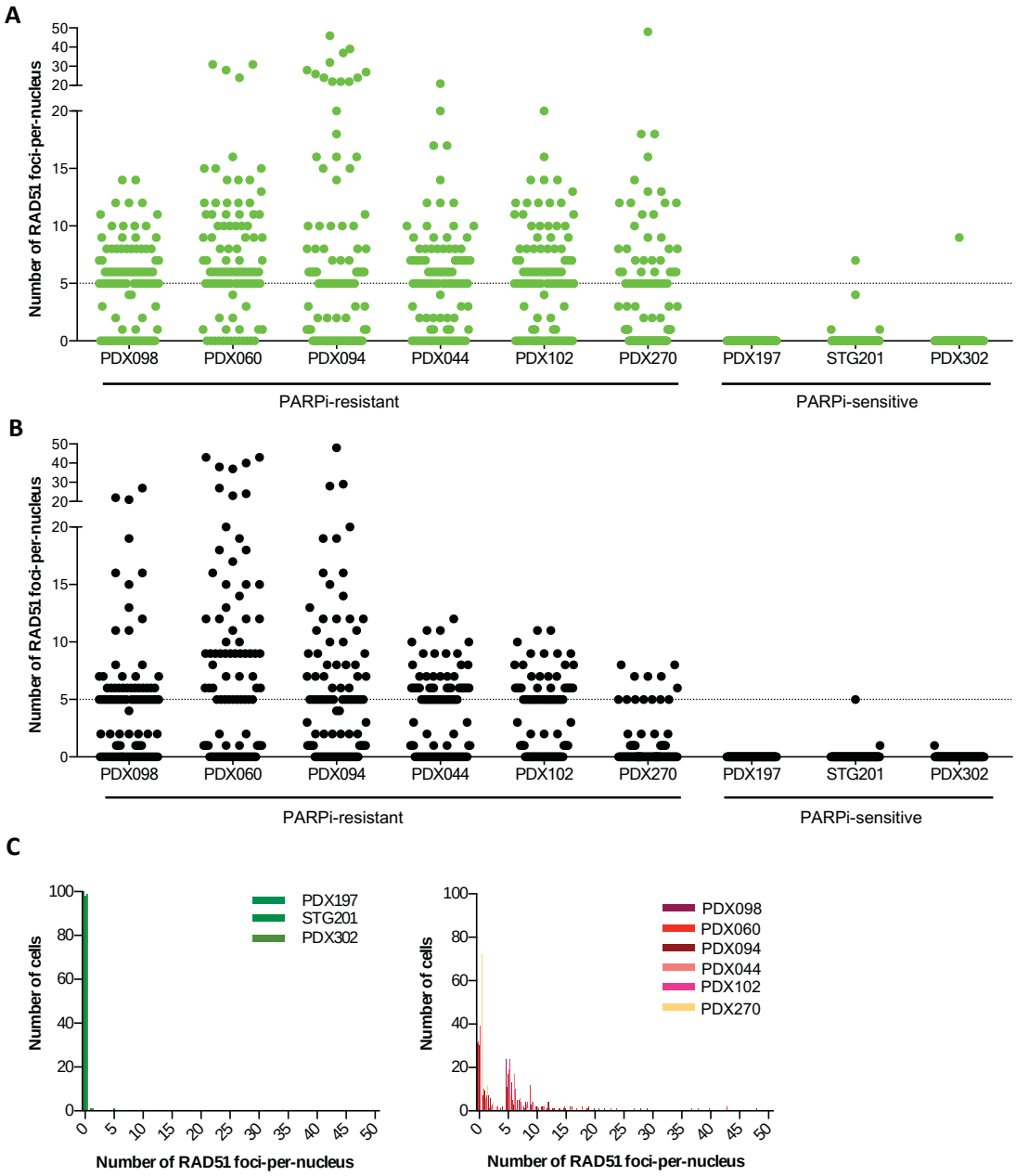

Figure 19 | **The 5 RAD51 foci-per-nucleus cut off differentiates PARPi-sensitive and PARPi-resistant PDXs. A-B)** Scatter plots showing the number of RAD51 foci in each individual geminin-positive cell (100 cells for each model) in **A)** vehicle- or **B)** olaparib-treated samples from six PARPi-resistant and three PARPi-sensitive PDXs models from cohort-2. The dashed line indicates the cut-off of 5 RAD51 foci-per-nucleus. **C)** Histogram distribution of the number of geminin-positive cells with increasing number of RAD51 foci-per-nucleus (0 to 50) in three PARPi-sensitive (left panel) and six PARPi-resistant (right panel) PDXs from cohort-2. Each color represents one PDX model.

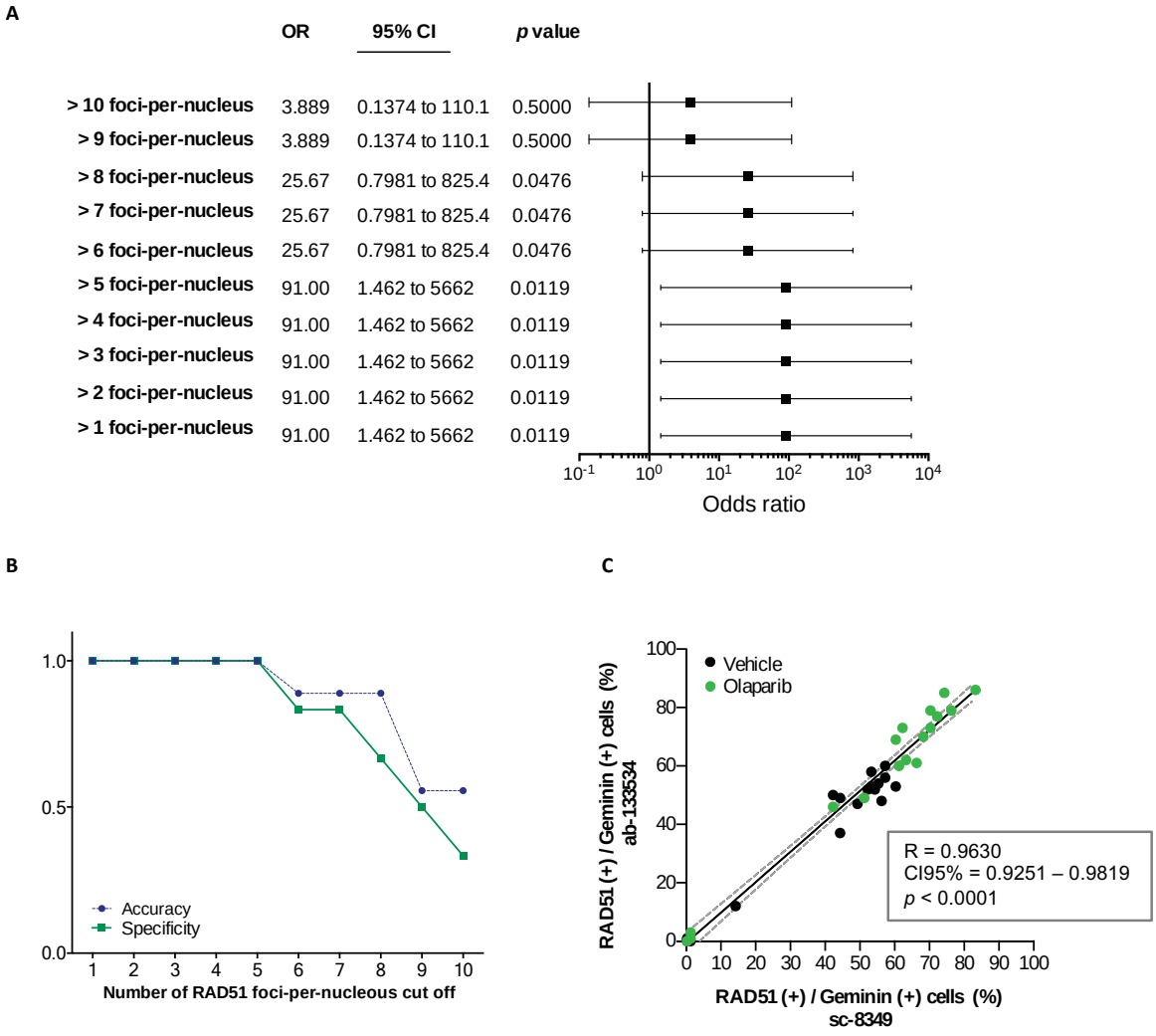

Figure 20 | **Analysis of the RAD51 foci-per-nucleus cut off and validation of RAD51 scoring with two different antibodies. A)** Forest plots and Odd's ratio analysis and **B)** accuracy and specificity of the RAD51 score using different cut offs from 1 to 10 foci per nucleus. **C)** Spearman correlation of the percentage of RAD51 (+)/Geminin (+) cells in PDX cohort-2 assessed with two different antibodies against RAD51 both in vehicle- and PARPi-treated PDX samples.

Following this protocol, the RAD51 assay was performed in the PDX cohort-2. We first studied the PARPi pharmacodynamic effect and the levels of endogenous DNA damage by quantifying the levels of γH2AX-positive cells in the S/G2-phase of the cell cycle (geminin-positive) in tumor samples from PDXs. All models, both in vehicle- and olaparib-treated samples showed levels of γH2AX-positive cells above 25%, and these numbers increased upon olaparib treatment, as expected (**Fig.21B**). These results ruled out pharmacodynamic differences between PARPi-sensitive and PARPi-resistant non-gBRCA PDXs of cohort-2. We then investigated the proliferation levels of these tumors, showing that all the analyzed tumor samples presented percentages of cells in S/G2-phase of the cell cycle (geminin-positive) above 20% (**Fig.21C**).

Having shown that lack of DNA damage or low proliferation rates may not be a limitation to evaluate HRR functionality, we scoring for RAD51 in tumor samples from PDX cohort-2. In olaparib treated tumors, the four PARPi-sensitive models showed significantly lower RAD51 score than the fourteen PARPi-resistant models (1.25 ± 0.25% *vs.* 66.54 ± 2.70 %; $p<0.0001$) (**Fig.22A and B**). This is also true for vehicle-treated samples, where RAD51 could be scored (0.75 ± 0.48% *vs.* 47.08 ± 3.37 %; $p=0.0007$) and correlated with the antitumor activity of olaparib ($p=0.0044$) (**Fig.22C**). Interestingly, immunofluorescence analysis revealed that the three acquired-resistant models STG201OR, PDX302OR and PDX93OR had high levels of RAD51-positive cells, while RAD51 foci are absent in the olaparib-sensitive counterparts (**Fig.22A and Appendix Fig.S4**). This was consistent with the decrease in *BRCA1* promoter methylation and recovery of *BRCA1* mRNA and BRCA1 nuclear foci formation in STG201OR and PDX302OR (**Fig.17 and Appendix Fig.S5**). In PDX93OR HRR recovery is consistent with the loss of the *PALB2* mutation present in the olaparib-sensitive counterpart PDX093 (**Fig.17 and Appendix Table S1**). These data suggested that in the hemicigosis context of PDX093OR, the dominant negative effect of PALB2 p.M296Nfs disappeared, allowing to HRR proficiency and PARPi acquired resistance. Altogether, these data indicate that loss of HRR capacity is a frequent event associated with PARPi sensitivity and demonstrated that the RAD51 score is a robust and highly discriminative biomarker of PARPi sensitivity vs PARPi resistance in the PDX cohort-2.

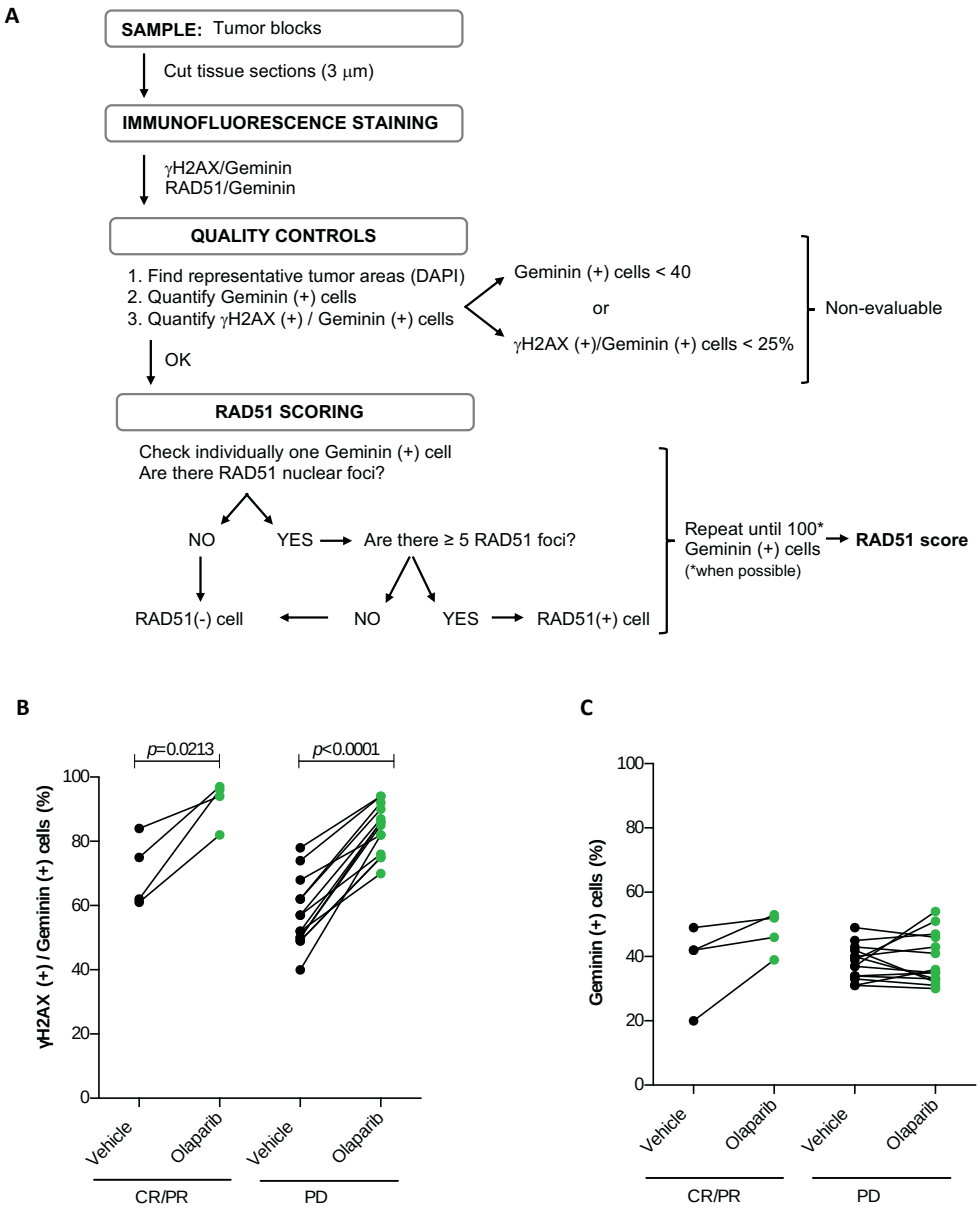

Figure 21 | **Baseline levels of DNA damage or low number of cells in S/G2-phase of the cell cycle did not impairs RAD51 scoring in PDX cohort-2. A)** Flow diagram of the RAD51 scoring criteria and quality controls. **B-C)** Quantification of **B)** cells in S/G2-phase of the cell cycle (geminin-positive) that exhibit γH2AX foci formation and **C)** cells in S/G2-phase of the cell cycle following treatment with vehicle and olaparib in PARPi-sensitive (CR/PR) and PARPi-resistant (PD) PDXs (Paired *t*-test in vehicle- vs PARPi-treated tumors; Unpaired *t*-test in CR/PR vs PD tumors).

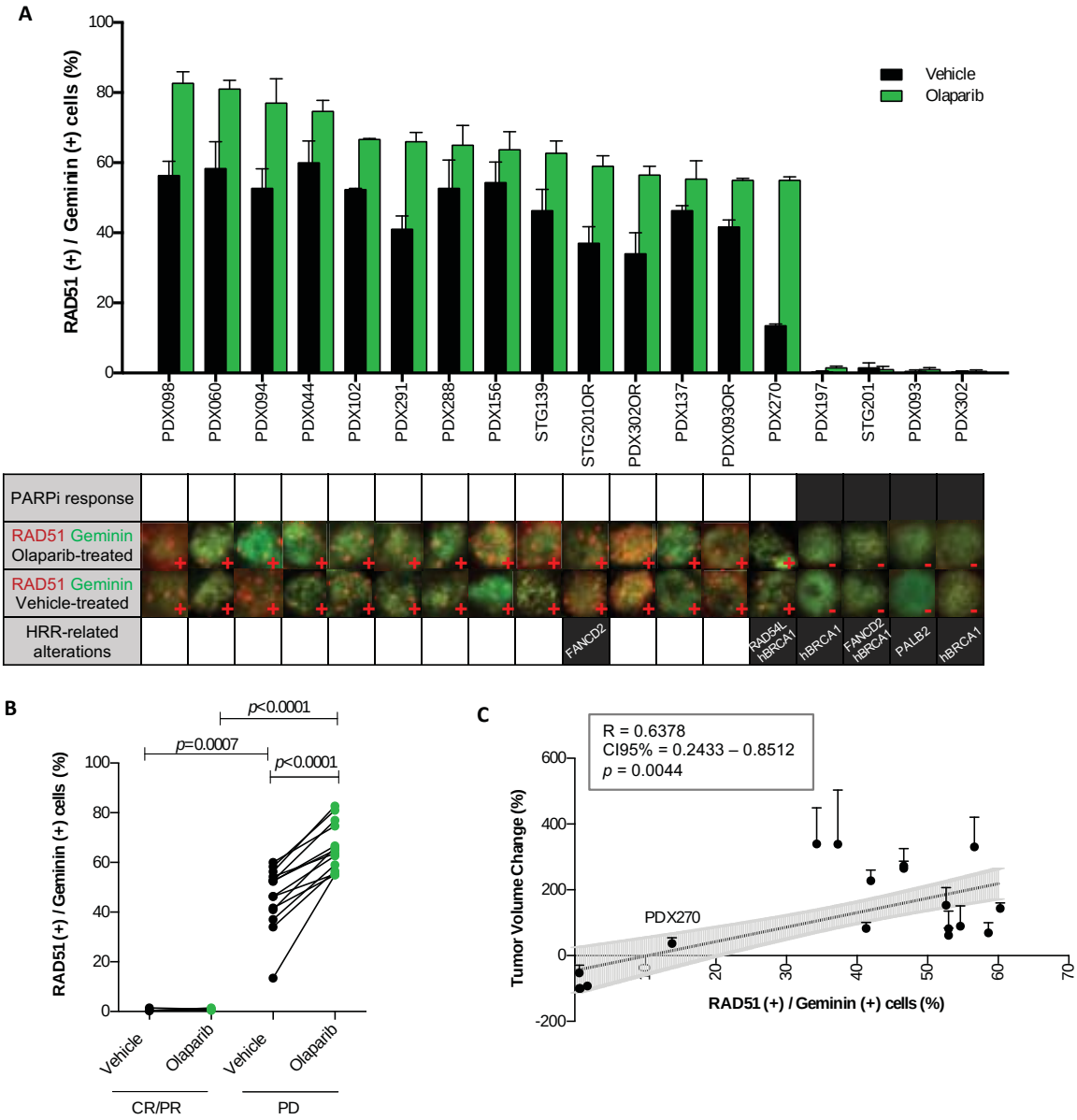

Figure 22 | **Lack of RAD51 nuclear foci identifies PARPi-sensitive PDX tumors. A)** Percentage of geminin-positive, RAD51 nuclear foci-containing cells detected by immunofluorescence in FFPE samples from PDX tumors treated with PARPi (green bars) or vehicle (black bars). Error bars indicate SEMs from independent tumors. The correlation with PARPi-response is shown in the summary underneath: white box: PD; black box: PR/CR. Immunofluorescence staining of RAD51 foci in PARPi- and vehicle-treated PDX tumors is shown; one cell in the S/G2-phase (geminin-positive, green) with or without RAD51 foci (red) is shown for each model. Alterations in HRR-related genes are also summarized: hBRCA1: *BRCA1* promoter hypermethylation and lack of *BRCA1* expression and BRCA1 nuclear foci formation. **B)** Quantification of cells in S/G2-phase of the cell cycle (geminin-positive) that exhibit RAD51 foci formation following treatment with vehicle and olaparib in PARPi-sensitive (CR/PR) and PARPi-resistant (PD) PDXs (Mann–Whitney U-test). **C)** Pearson correlation between the RAD51 score (percentage of RAD51 (+)/Geminin (+) cells, assessed in untreated FFPE tumor samples) and the percentage of tumor volume change in olaparib-treated tumors from PDX cohort-2. Each dot represents one PDX model. Error bars indicate SEM from at least 3 independent tumors treated with olaparib.

RAD51 score predicts response to PARPi in an independent PDX cohort

Having stablished the conditions for RAD51 scoring, we proceeded to further validate the RAD51 assay as biomarker to predict PARPi sensitivity using an independent PDX cohort (PDX cohort-3). The PDX cohort-3 consisted of 28 TNBC models, including eight tumors with pathogenic variants in *BRCA1* (n=5), *BRCA2* (n=2) or *PALB2* (n=1). All these variants were classified as pathogenic by the ClinVar database and their VAFs were consistent with loss of heterozygosity (LOH) (**Appendix Table S2**). The antitumor activity of three different PARPi and doses was assessed in this panel of PDXs (olaparib 50 mg/kg, olaparib 100 mg/kg, niraparib 50 mg/kg, niraparib 75 mg/kg and veliparib 100 mg/kg), giving rise to a panel composed of 21 progressing and 7 regressing PDX models (**Fig.23A**). Following the stablished protocol showed in **Fig.21A**, the RAD51 score was performed blindly in untreated FFPE tumor samples from the PDX cohort-3. Based on PDX cohort-1 and cohort-2 results and previous studies[238] we used a 10%-RAD51 score cutoff to differentiate PARPi-sensitive from PARPi-resistant PDXs. Within the PDX cohort-3, seven models (25%) showed a RAD51 score ≤ 10% and 21 models (75%) showed a RAD51 score above the cutoff, with 100% sensitivity and 100% specificity for PARPi response prediction (**Fig.23A and B**). HRR capacity was also quantified using the Myriad's myChoice® HRD score to compare this genetic biomarker with our functional RAD51 assay in the PDX cohort-3. As in PDX cohort-1 and cohort-2, the RAD51 score showed complete discriminative capacity in predicting PARPi response (ROC AUC=1) in PDX cohort-3, while the HRD score had lower predictive power (ROC AUC = 0.735). These differences in AUC between the two biomarkers were statistically significant (difference between AUC = 0.27; Confidence Interval 95% (CI95%) 0.08-0.46; p=0.005; **Fig.23B**). Of note, we did not observe significant differences in the levels of DNA damage (quantified as the percentage of cells in the S/G2-phase of the cell cycle with γH2AX nuclear foci) between PARPi-sensitive and PARPi-resistant PDXs from cohort-3 (**Fig.23C**).

Within the PDX cohort-3, there are three *BRCA1*-mutated and one *BRCA2*-mutated PDXs that are PARPi-resistant and exhibited RAD51 foci formation. As we have described in PDX cohort-1 that the expression of hypomorphic BRCA1 isoforms and 53BP1 loss are associated with HRR functionality, we further explore these mechanisms of PARPi resistance in these models. IF analysis revealed that loss of 53BP1 did not explain PARPi

resistance in the three *BRCA1*-mutated PDXs that exhibited RAD51 foci (**Fig.24A**). Instead, two of them (HBCx28 and HBCx11) exhibited BRCA1 nuclear foci formation, indicative of functional HRR restoration by the expression of BRCA1 hypomorphic variants (**Fig.24A**). Specifically, HBCx28 harbors a mutation in the N-terminus of *BRCA1* (c.212+3A>G) and BRCA1 nuclear foci were only detected with the antibody against the C-terminus of the protein (B1-CT), consistent with the expression of the BRCA1 RING-less hypomorphic variant[143]. However, this isoform was not expressed in the other N-terminus *BRCA1* mutant and PARPi-resistant model HBCx8. HBCx-11 harbors a mutation in the exon 11 of *BRCA1* (c.1961del) and BRCA1 nuclear foci were detected with both B1-NT and B1-CT antibodies, as expected when the BRCA1-Δ11q splice isoform is expressed[145]. Surprisingly, BRCA1 foci were also present in the PARPi-sensitive model T330, which also harbors a mutation in the exon 11 of *BRCA1* (c.3839_3844delins5), but not in the other PARPi-sensitive BRCA1-mutant T168 (**Fig.24A**).

Within the *BRCA1/2* wild type PARPi-sensitive PDX models from cohort-3 (HBCx14, HBCx6 and HBCx15), we aimed to investigated the epigenetic silencing of *BRCA1* as mechanism of HRR deficiency and PARPi sensitivity. With this aim, we analyzed the capacity to form BRCA1 nuclear foci by IF. We could detect BRCA1 nuclear foci only in one out of three PARPi-resistant PDXs (HBCx14), while HBCx6 and HBCx15 did not show BRCA1 foci, suggesting *BRCA1* epigenetic silencing as being the cause of PARPi sensitivity in these models (**Fig.24B**).

Altogether, these results support the use of the RAD51 score as a predictive biomarker of PARPi response and further demonstrate that this assay allows to correctly capture both BRCA-related tumors that restore HRR-capacity and non-BRCA tumors that are HRR deficient, regardless the mechanism of PARPi resistance and sensitivity.

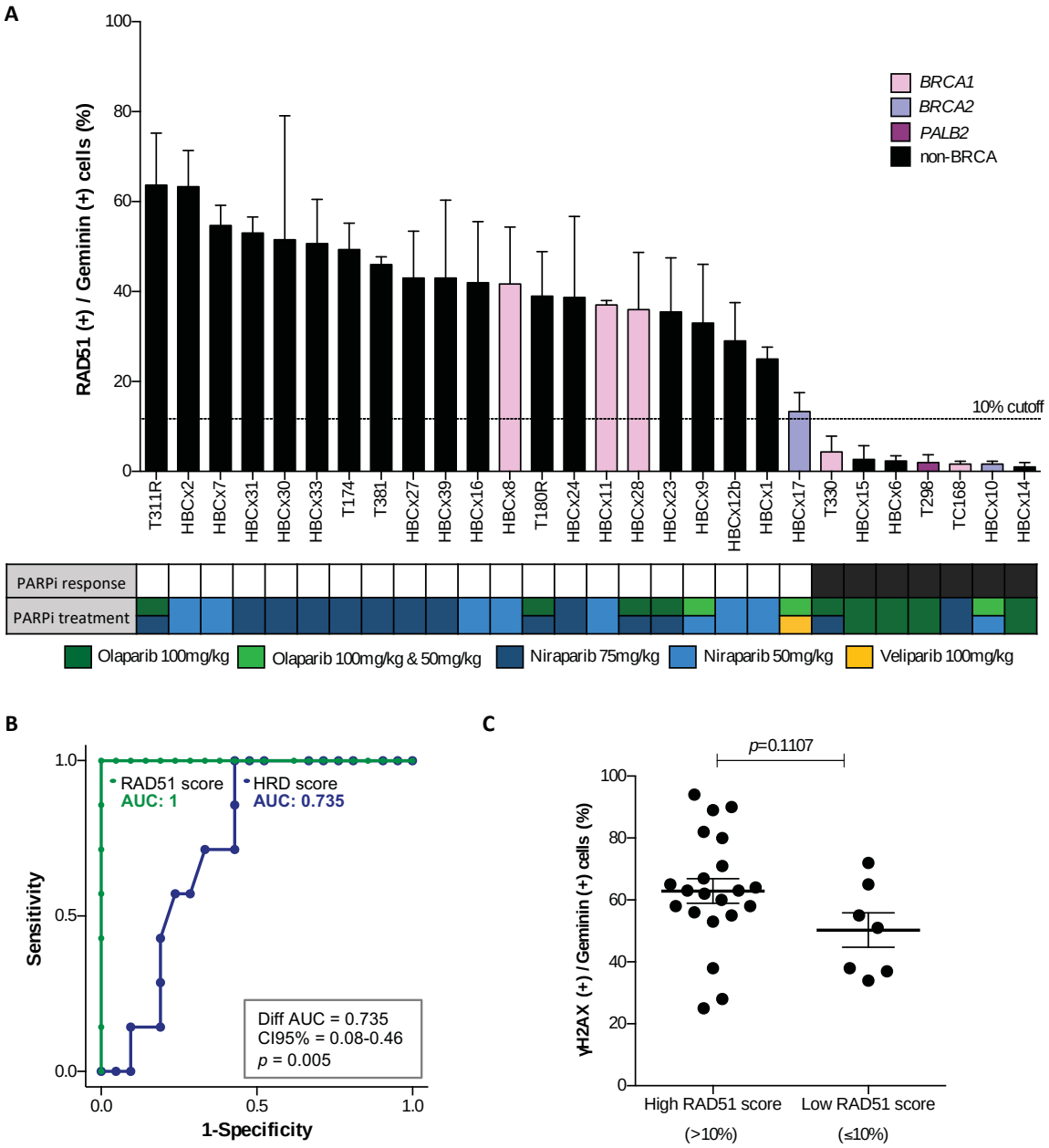

Figure 23 | **RAD51 score predicts PDX tumor response to PARPi in an independent PDX panel (cohort-3). A)** Percentage of geminin-positive, RAD51 nuclear foci-containing cells in FFPE samples from untreated PDX tumors of cohort-3. Color bars indicate the presence of pathogenic variants in the indicated genes. Error bars indicate SEM from independent tumors. PARPi-response is shown in the summary underneath: black box: PR/CR; white box: PD. Box colors indicate the PARP inhibitor treatment. Boxes with two colors indicate the same response to both treatments. Olaparib 100mg/kg & 50mg/kg indicates that both doses were tested and resulted in the same response categorization. **B)** Receiver Operating Characteristic (ROC) curves of the RAD51 score (green) and HRD score (blue) for PARPi response prediction capacity in the PDX cohort-3 (Bootstrap statistical test). **C)** Percentage of geminin-positive cells with γH2AX nuclear foci in untreated tumor samples from PDX cohort-3 (Unpaired *t*-test).

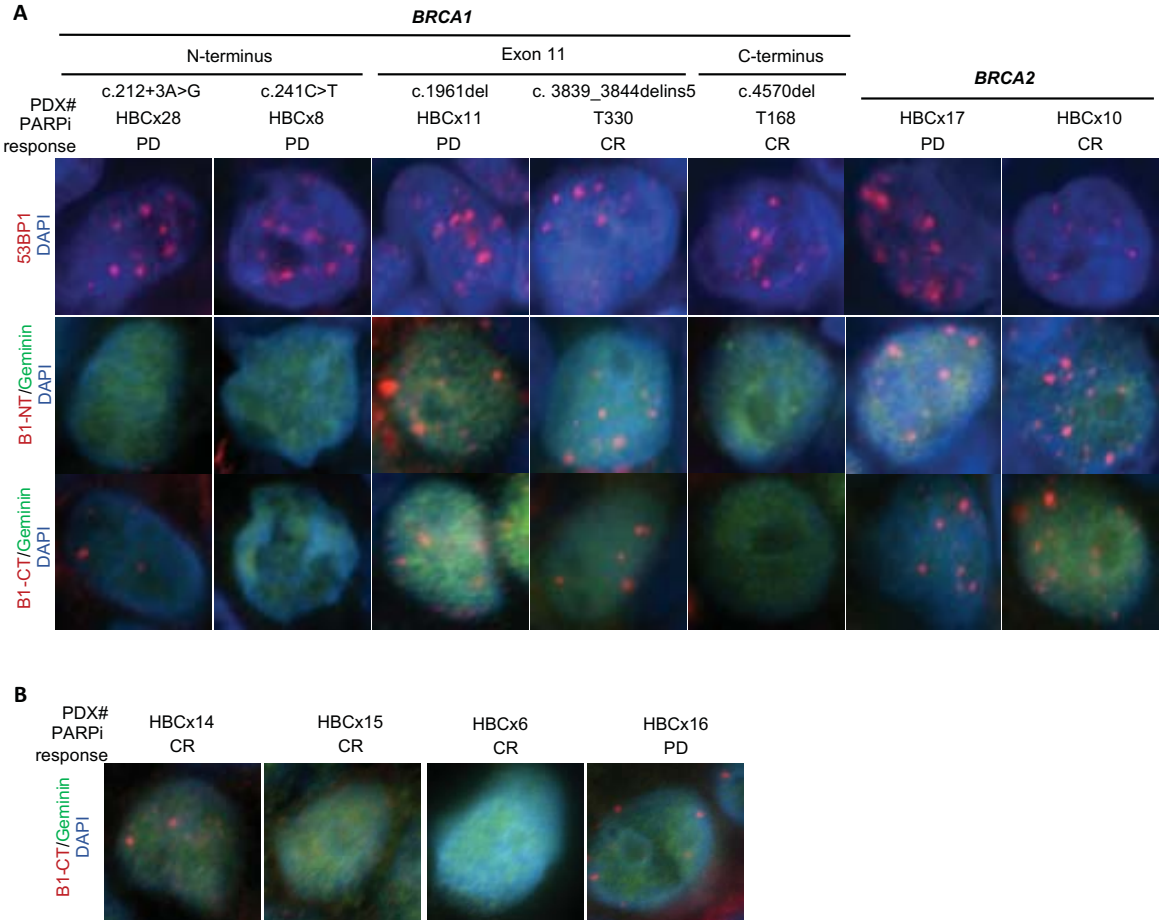

Figure 24 | **Hypomorphic BRCA1 isoforms and lack of BRCA1 nuclear foci in PDX cohort-3. A)** Immunofluorescence staining of 53BP1 and BRCA1 nuclear foci [with an antibody toward the N-terminus (B1-NT) or C-terminus (B1-CT) of BRCA1] in *BRCA1/2*-mutant models from PDX cohort-3. The response to PARPi treatment and the location of the mutation within the *BRCA1* gene is indicated. **B)** Immunofluorescence staining of BRCA1 nuclear foci in four *BRCA1/2* wild type models. The response to PARPi treatment is indicated. Nuclei were visualized with DAPI (blue). Green nuclei indicate geminin-positive cells (S/G2-phase of the cell cycle). One cell is shown for each model.

Scoring RAD51 in clinical samples identifies HRR-deficient tumors among patients with hereditary breast and ovarian cancer (HBOC) syndrome, including PALB2-related tumors

After these encouraging results in PDX models from breast cancer patients, we assessed the ability of the RAD51 assay to identify HRR-deficient tumors beyond gBRCA mutated patients. For this purpose, we collected a total of 29 FFPE tumor samples from a cohort of patients with clinical suspicion of hereditary breast cancer and without gBRCA mutations. Given that two out of two PDXs models with genetic alterations in *PALB2* (PDX093 in cohort-2 and T298 in cohort-3) are PARPi-sensitive and showed low RAD51 score, we aimed to explore the potential association of harboring a mutation in *PALB2* and HRR deficiency. To this aim, we enriched our patient cohort with 11 tumors from patients with germline mutations in *PALB2* (gPALB2) (**Table 5**). We stained for RAD51, γH2AX and BRCA1 in these tumors and RAD51 could be scored in 23 FFPE tumor samples (**Table 5, Fig.25 and Appendix Fig.S6**). Six tumors derived from young patients (≤35 years) and the remaining 17 tumor samples were obtained from 14 patients with family history of BC, including the eleven *PALB2*-related tumors. Fourteen out of 23 tumor samples showed low RAD51 score (≤ 10% cut-off), including all gPALB2 tumor samples (**Fig.25B**). These data showed that carrying a *PALB2* mutation is associated with higher odds of displaying low RAD51 score (odds ratio (OR)=62.4; CI95% 2.852-1367); p=0.0003). The three tumors with low RAD51 score that lacked gPALB2 mutations showed lack of BRCA1 nuclear foci formation, raising the possibility of *BRCA1* epigenetic silencing as being the cause of HRR deficiency (Pt02, Pt07, Pt11; **Fig.25B and Appendix Fig.S6**). Altogether, these results demonstrate that the RAD51 assay is feasible in routine samples from patients and identifies HRR-deficient tumors that are sensitive to PARPi therapy beyond the gBRCA condition.

Table 5 | **Characteristics of HBOC patients' tumors.** Rows 13 to 20 correspond with patients with alterations in *PALB2*. The loss-of-function effect of the *PALB2* c.3201+5G>T splicing variant was confirmed by RNA analysis. IDC: invasive ductal carcinoma.

Patient	Sample	PALB2 ALTERATION	TYPE OF SAMPLE	DIAGNOSIS	AGE OF DIAGNOSIS	H.GRADE	ER STATUS	PR STATUS	Her2 STATUS	Ki67 (%)
01	01	-	Breast surgery	IDC	58	3	+	+	-	20
02	02	-	Tumorectomy	IDC	29	3	-	-	-	90
03	03	-	Core biopsy	IDC	40	3	-	-	-	70, 80
04	04	-	Core biopsy	IDC	48	2	-	-	-	50
05	05	-	Core biopsy	IDC	52	1	+	+	-	8
06	06	-	Core biopsy	IDC	31	2	+	-	-	30
07	07	-	Core biopsy	IDC	27	3	-	+	-	95
08	08	-	Core biopsy	Invasive carcinoma	31	3	-	-	-	70
09	09	-	Core biopsy	IDC	35	2	+	+	+	15
10	10	-	Breast surgery	IDC	28	2	+	+	+	40
11	11	-	Core biopsy	IDC	32	3	-	-	-	85
12	12	-	Breast surgery	IDC	38	2	+	+	-	35
13	13	c.3362delG p.(Gly1121Valfs*3)	Breast surgery	IDC	41	3	+	+	uk	uk
14	14	c.3362delG p.(Gly1121Valfs*3)	Breast surgery	IDC	42	3	+	-	uk	uk
15	15	c.3201+5G>T Splice	Mastectomy	IDC	54	2	+	+	-	22
16	16.1	c.1675C>T p.(Gln559*)	Core biopsy	IDC	51	3	+	+	-	70
	16.2		Core biopsy	IDC		3	+	+	-	60
17	17	c.1111G>T p.(Glu371*)	Core biopsy	ILC	45	2	+	+	-	24
18	18	c.2257C>T p.(Arg753*)	Core biopsy	IDC	46	3	+	+	-	80
19	19	c.1240C>T	Core biopsy	IDC	38	3	-	-	-	90
20	20.1	c.3256C>T p.(Arg1086*)	Core biopsy	IDC	40	3	-	-	-	50
	20.2.1		Core biopsy	IDC		2	-	-	-	55
	20.2.2		Core biopsy	IDC		2	+	+	-	40

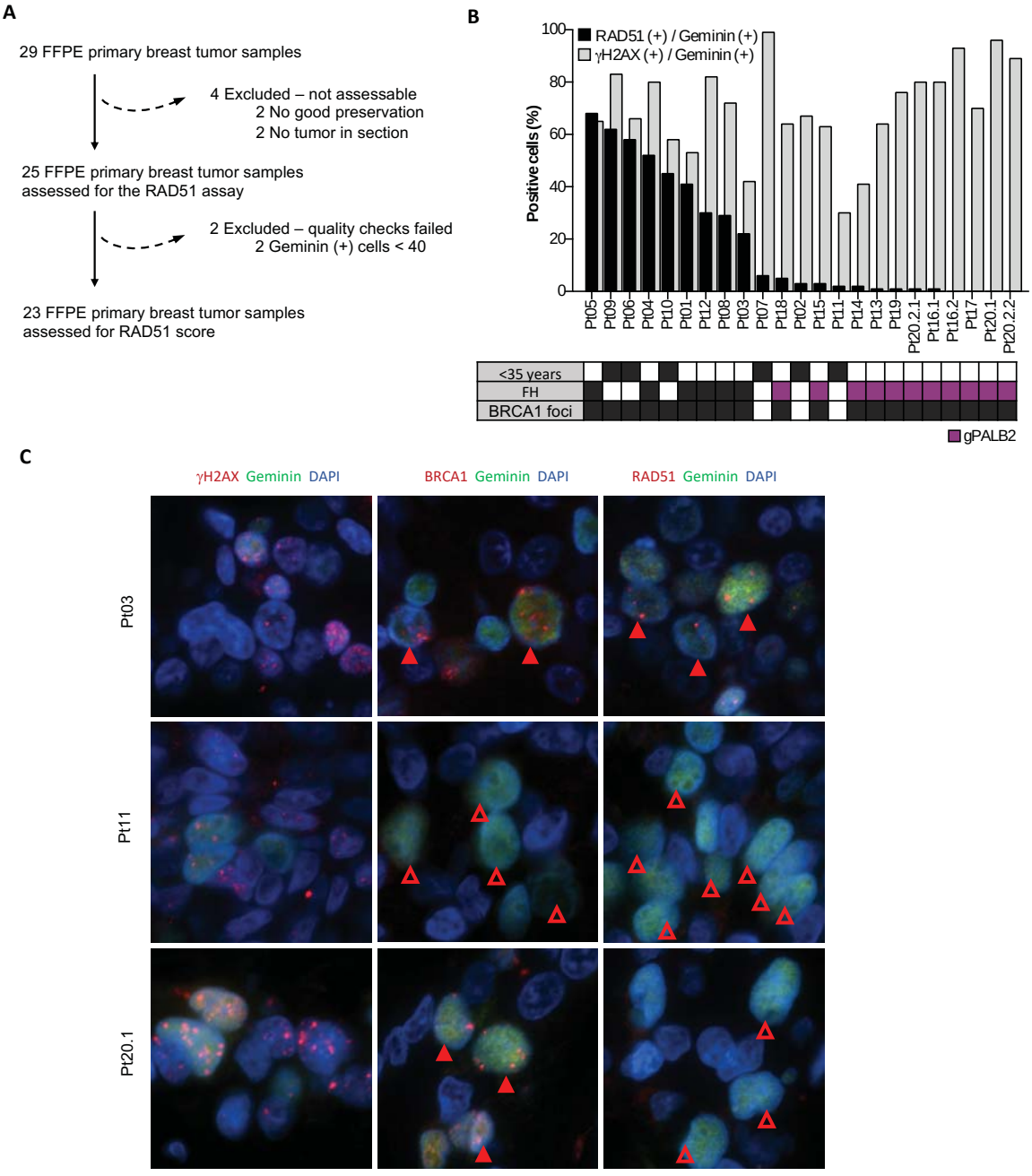

Figure 25 | **RAD51 score in tumors from patients with HBOC syndrome, including germline *PALB2*-mutation carriers. A)** Consort diagram of the FFPE tumor samples from patients with HBOC syndrome following the scoring criteria for the RAD51 assay. **B)** Percentage of geminin-positive, RAD51 (black bars) and γH2AX (grey bars) nuclear foci-containing cells in FFPE tumor samples from patients with HBOC syndrome. The box underneath summarizes the patient's young onset (<35years), her family history (FH, purple box for PALB2-related tumors) and the presence of BRCA1 nuclear foci in the analyzed tumors samples. **C)** Immunofluorescence staining of γH2AX, BRCA1 and RAD51 nuclear foci in FFPE tumors from patients. One RAD51- and BRCA1-positive tumor (Pt03), one RAD51- and BRCA1-negative tumor (Pt11), and one PALB2-related tumor, with BRCA1 but not RAD51 nuclear foci (Pt20.1) are shown. S/G2-phase cells (geminin-positive, green) with or without BRCA1 or RAD51 foci (red) are indicated with filled and empty red arrowheads, respectively. Nuclei were visualized with DAPI (blue). All pictures were taken at 600x magnification.

PART 3

Inhibiting WEE1 and ATM induces replication stress and enhances the antitumor response to PARPi in BRCA1-altered tumors.

AZD1775 antitumor activity in the PDX panel distinguishes a subset of tumors highly sensitive to WEE1 inhibition

Knowing the olaparib-response in two different panels of PDXs (cohort-1 and cohort-2), we then tested the antitumor activity of the WEE1i inhibitor AZD1775 in almost all PDXs, totaling 26 models (**Fig.26A**). One PDX model, namely PDX098, was previously been identified as highly sensitive to the WEE1/CHEK1 inhibitor 681640 (model VHIO098)[269]. This vulnerability was validated *in vivo* using the WEE1 inhibitor AZD1775, in a range of doses and schedules tested in the clinic. At a dose of 120 mg/kg, all tumors regressed (**Fig.26B**). Among the other PDXs, we identified one additional model, PDX236, exhibiting complete response (CR) upon WEE1i treatment (**Fig.26A**). Five additional models showed partial response (PR) (namely PDX280, PDX094, PDX156, PDX060 and STG139), while all other PDXs underwent disease stabilization (SD, n=4, PDX270, STG316, PDX197 and PDX288) or disease progression (PD, n=15). Interestingly, sensitivity to olaparib single agent was mutually exclusive with sensitivity to AZD1775, demonstrating that WEE1i sensitivity does not merely rely on the tumor's deficiency in HRR.

Importantly, single agent treatment with AZD1775 induced durable response, but in four out of six models tested, tumors regrowth and develop acquired response upon continuous treatment (**Fig.26C**).

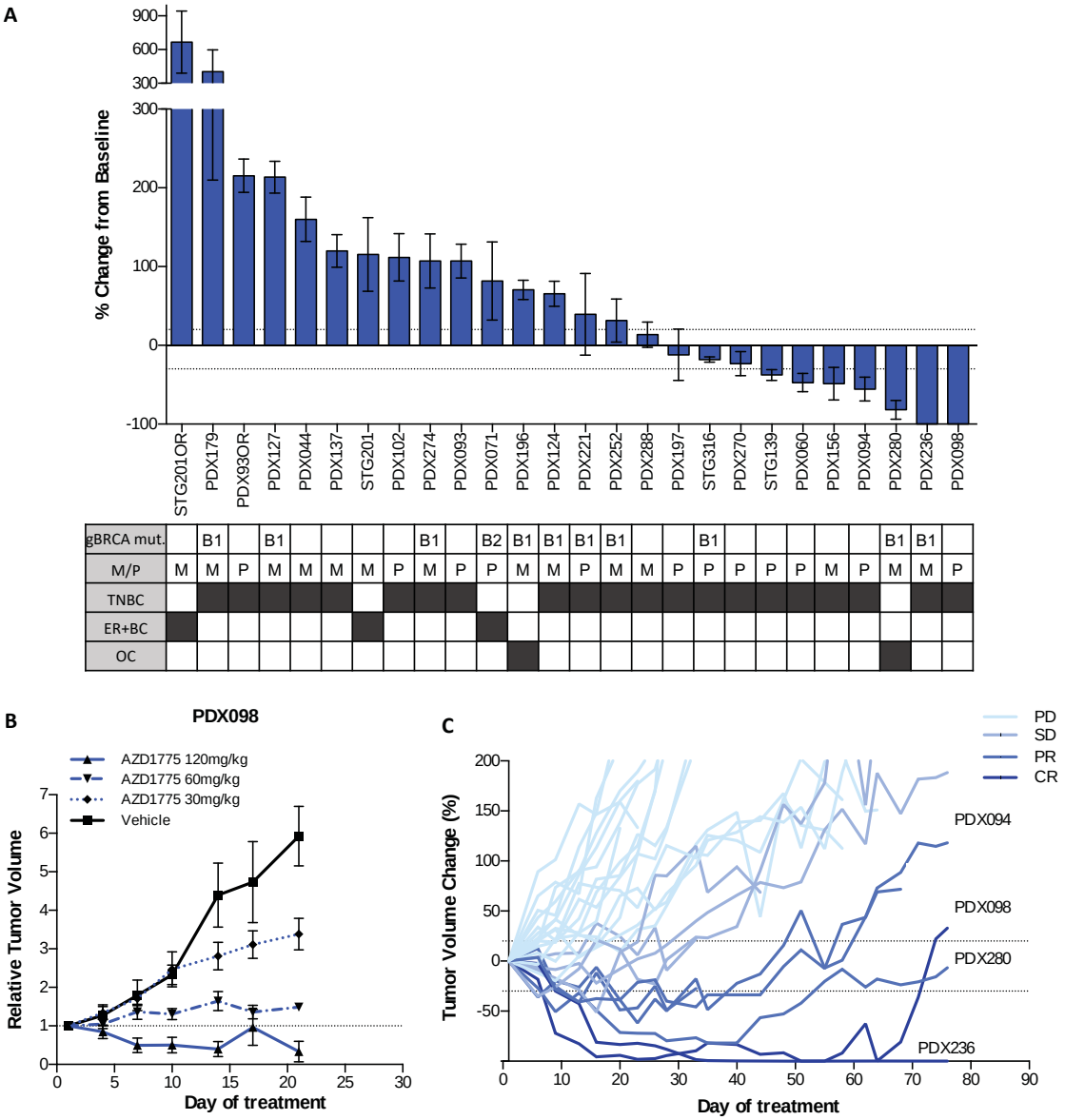

Figure 26 | **The antitumor activity of AZD1775 in PDXs identifies a subset of WEE1i-sensitive tumors.** **A)** Waterfall plot showing the percentage of tumor volume change upon treatment with AZD1775 compared to the tumor volume on day 1. +20% and -30% are marked by doted lines to indicate the range of PR, SD and PD. The box underneath summarizes different characteristics of each model and the presence of germline mutation in *BRCA1/2*. TNBC, Triple Negative Breast Cancer; ER+BC, Estrogen Receptor positive Breast Cancer; OC, Ovarian Cancer. Error bars indicate SEM from independent tumors. **B)** Percentage of tumor volume change during treatment with vehicle and different AZD1775 doses in PDX098. The mean +/- SEM is represented. **C)** Acquisition of WEE1i-resistance in PDX156, PDX098, PDX280 and PDX094 after prolonged exposure to AZD1775. The percentage of tumor volume change during AZD1775 treatment is plotted. Colors indicate the different responses to AZD1775.

Response biomarkers of WEE1 inhibition

We aimed to identify genetic and proteomic markers associated with AZD1775 sensitivity to find candidate biomarkers to better select patient population most likely to respond to WEE1 inhibition. To do this, we conducted exome sequencing and explored a subset of markers at the protein levels, including markers of early entry in S-phase (p16 and pRB S807/811) and markers of replication stress (RS) or abrogated RS response (c-myc, cyclin E1, ATM and phospho-CHK1 S345) (**Appendix Fig.S7**). Taken together, results from this analysis suggest that AZD1775 sensitivity is underlid by a composite of phenotypes including: (i) early entry in S-phase, mediated by *TP53* mutation plus other alterations in the S-phase restriction point; plus (ii) increased RS mediated by *STK11/LKB1* mutations or *CCNE1* amplification and/or (iii) abrogated RS response (e.g. *BRCA1* alterations). This study was performed in collaboration with the DDR team from AstraZeneca.

WEE1 inhibition induces accelerated mitotic entry and replication stress *in vivo*

We then sought to understand if WEE1 inhibition has a dual effect *in vivo* that includes both accelerated mitotic entry and the induction of RS. To this aim, we first tested the effect of AZD1775 in cell cycle progression by quantifying the percentage of cells in G2/M-phase, namely cells with phosphorylated histone H3 S10 nuclear staining (pHH3-positive). WEE1 inhibition resulted in accumulation of pHH3-positive cells, indicative of accelerated mitotic entry (**Fig.27A and B**). However, this effect is not distinctive between PDXs that exhibited tumor regression upon WEE1i treatment (CR/PR, n=7) and PDXs exhibiting tumor growth delay (SD, n=4) or no response (PD, n=15). Therefore, early mitotic entry after treatment with AZD1775 is not indicative of the major phenotype inducing antitumor response.

To study the effects on RS of inhibiting WEE1, we then stained for γH2AX, phosphorylated RPA32 (pRPA32 S4/S8) and geminin in both vehicle- and AZD1775-treated tumor samples from the PDX models. Results showed that AZD1775 markedly induced replication stress *in vivo*, revealed as increased numbers of cells showing pan-nuclear γH2AX staining (**Fig.27C and D**) and cells in S/G2-phase of the cell cycle (geminin-positive) with pRPA32 S4/S8

nuclear foci (**Fig.27E and F**). Most pan-nuclear γH2AX-positive cells were also positive for pRPA 32 S4/S8 (**Fig.28A**) or phosphorylated DNA-PKc (pDNA-PKc, **Fig.28B**), further demonstrating that these markers correspond to RS. In addition, we noticed that both baseline and treatment-induced frequencies of geminin-positive cells with pRPA32 S4/S8 nuclear foci were statistically higher in the WEE1i-resonding PDXs compared with the stabilized and non-responding ones (p=0.0199 and p=0.0065, respectively, **Fig.27F**).

Finally, we examined if the levels of RS changed upon acquired resistance to AZD1775. In all the four PDX models that develop resistance to WEE1 inhibition, namely PDX156, PDX098, PDX280 and PDX094) both markers of replication stress (pan-nuclear γH2AX staining and pRPA32 S4/S8 nuclear foci in S/G2-phase) were reduced upon therapy progression (**Fig.28C and D**). Altogether, these data showed that AZD1775-sensitive tumors exhibited features of high baseline or WEE1i treatment-induced replication stress, suggesting the use of RS biomarkers to predict tumor response to WEE1 inhibition.

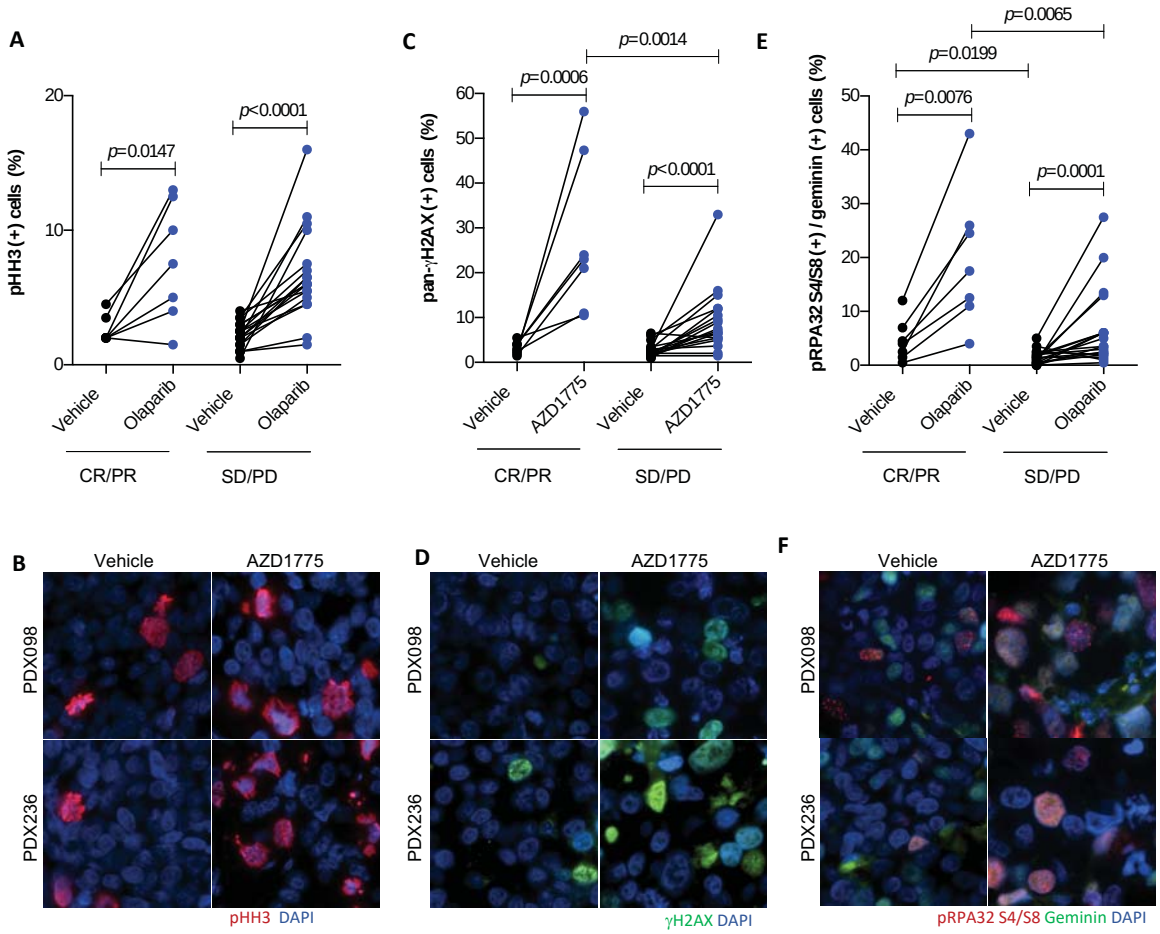

Figure 27 | **Treatment with AZD1775 induces mitotic entry and replication stress. A)** Quantification of cells in G2/M-phase of the cell cycle (pHH3-positive) following treatment with vehicle and AZD1775 in WEE1i-sensitive (CR/PR) and WEE1i-resistant (SD/PD) PDXs (Paired *t*-test in vehicle- vs WEE1i-treated tumors; Unpaired *t*-test in PR/CR vs SD/PD tumors). **B)** Immunofluorescence staining of pHH3 in tumor samples treated with vehicle or AZD1775 of two WEE1i-sensitive PDXs. **C)** Quantification of cells with pan-nuclear γH2AX staining following treatment with vehicle and AZD1775 in WEE1i-sensitive (CR/PR) and WEE1i-resistant (SD/PD) PDXs (Mann–Whitney U-test). **D)** Immunofluorescence staining of γH2AX in tumor samples treated with vehicle or AZD1775 of two WEE1i-sensitive PDXs. **E)** Quantification of geminin-positive cells that exhibit pRPA32 S4/S8 foci formation following treatment with vehicle and AZD1775 in WEE1i-sensitive (CR/PR) and WEE1i-resistant (SD/PD) PDXs (Mann–Whitney U-test). **F)** Immunofluorescence staining of pRPA32 S4/S8 and geminin in tumor samples treated with vehicle or AZD1775 of two WEE1i-sensitive PDXs. Nuclei were visualized with DAPI (blue). All pictures were taken at 600x magnification.

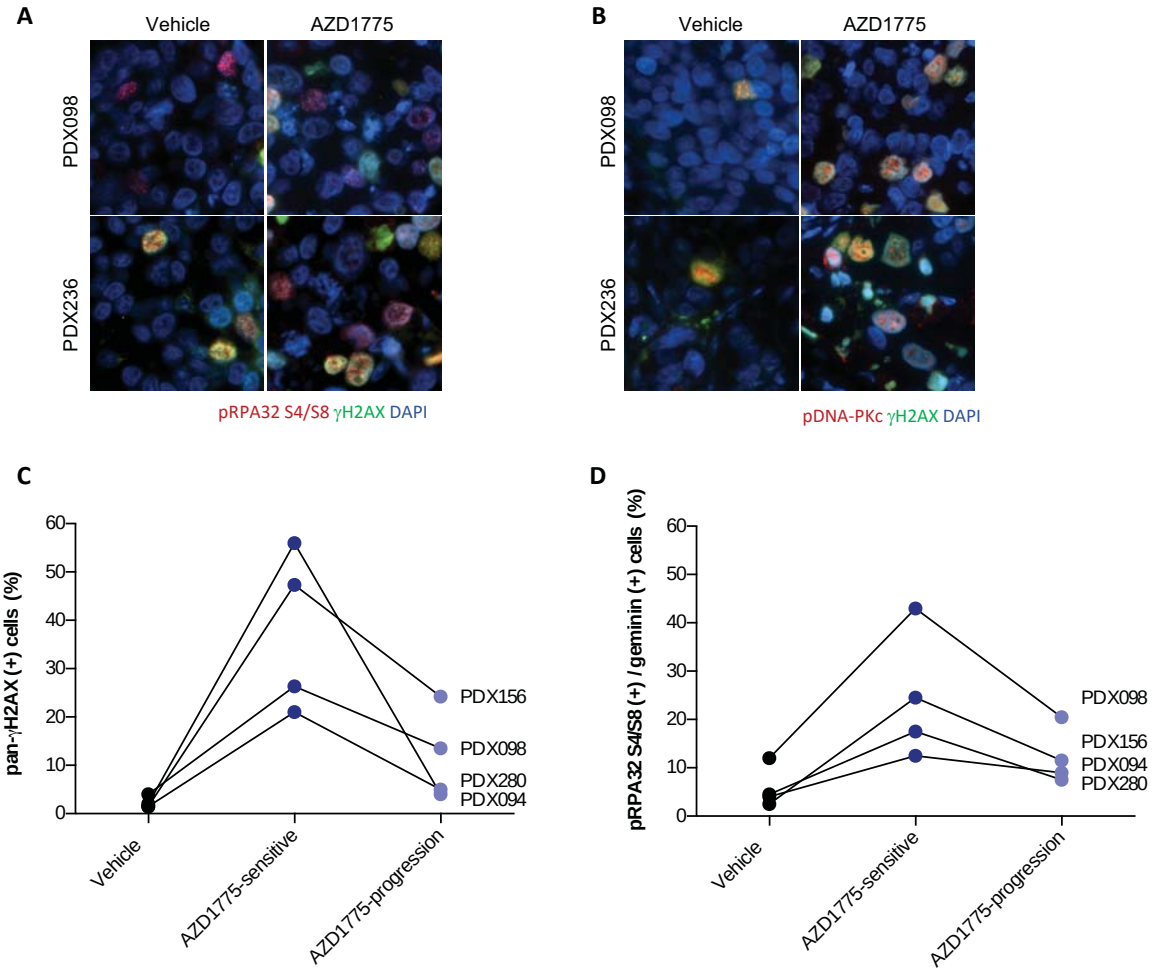

Figure 28 | **Markers of RS upon AZD1775 treatment and decreased levels of RS in WEE1i-acquired resistant PDXs. A-B)** Immunofluorescence staining of γH2AX and **A**) pRPA32 S4/S8 or **B)** pDNA-PKc in tumor samples treated with vehicle or AZD1775 of two WEE1i-sensitive PDXs. Nuclei were visualized with DAPI (blue). All pictures were taken at 600x magnification. **C-D)** Quantification of **C)** cells with pan-nuclear γH2AX staining and **D)** cells in S/G2-phase of the cell cycle (geminin-positive) with pRPA32 S4/S8 nuclear foci following treatment with vehicle or AZD1775 both in responding (dark blue) and acquired resistant (light blue) PDXs. Each dot represents the mean of at least 2 independent PDX tumors.

WEE1 blockade in combination with PARP inhibition sensitizes BRCA1-altered tumors

Currently several clinical trials are ongoing to examine the efficacy of combination therapies with checkpoint inhibitors to broaden the response to PARPi and avoid the emergence of resistance. Thus, we were interested in exploring the combination of the PARP inhibitor olaparib with the WEE1 inhibitor AZD1775 in our panel of PDX models. We examined the antitumor activity of combined olaparib and AZD1775 in all the PDX models (**Fig.29**). The response rate (% of CR+PR) was higher in the combination treatment (62%, 16 out of 26) as that of each single agent AZD1775 (27%, 7 out of 26) or olaparib (15%, 4 out of 26). Interestingly, the two models that partially respond to PARPi, namely PDX124 (a *BRCA1* mutated PDX model that showed disease stabilization) and PDX270 (a *BRCA1* hypermethylated model with limited tumor growth upon PARPi treatment) showed tumor regression when treated with both PARP and WEE1 inhibitors (**Fig.30**). Moreover, in this context of altered BRCA1 function, the addition of AZD1775 to olaparib prevented the acquisition of PARPi resistance and result in long response (>100 days) both in PDX124 and STG201 (another *BRCA1* promoter hypermethylated PDX) (**Fig.30**). Combination treatment also leaded to antitumor response in two additional PDX models with *BRCA1* mutation, namely PDX196 and PDX252 (**Fig.30**).

Previous results have shown that single-biomarker genomic analysis did not help to identify response biomarkers to WEE1i plus PARPi, but we found that the biomarker profiles were more similar to those for single agent AD1775 sensitivity than for olaparib, namely features representative of early entry in S-phase and increased RS.

Therefore, we then study more deeply whether the combination of PARP plus WEE1 inhibition enhance the levels of RS and its relation with combination response in monotherapy-resistant models. Results showed that, in agreement with the observed in the AZD1775 single-agent phenotypic and response biomarkers, tumors that showed tumor regression upon combination treatment (CR/PR, n=4), exhibited higher levels of RS than those PDXs exhibiting tumor growth delay (SD, n=4) or no response (PD, n=5), in terms of pan-nuclear γH2AX staining and pRPA32 S4/S8 nuclear foci containing cells (**Fig.31**).

Altogether, these data demonstrated that PARP plus WEE1 inhibition resulted in exacerbated induction of replication stress in combination-sensitive PDXs and highlights the clinical potential of combining DNA damage repair inhibitors for the treatment of TNBC.

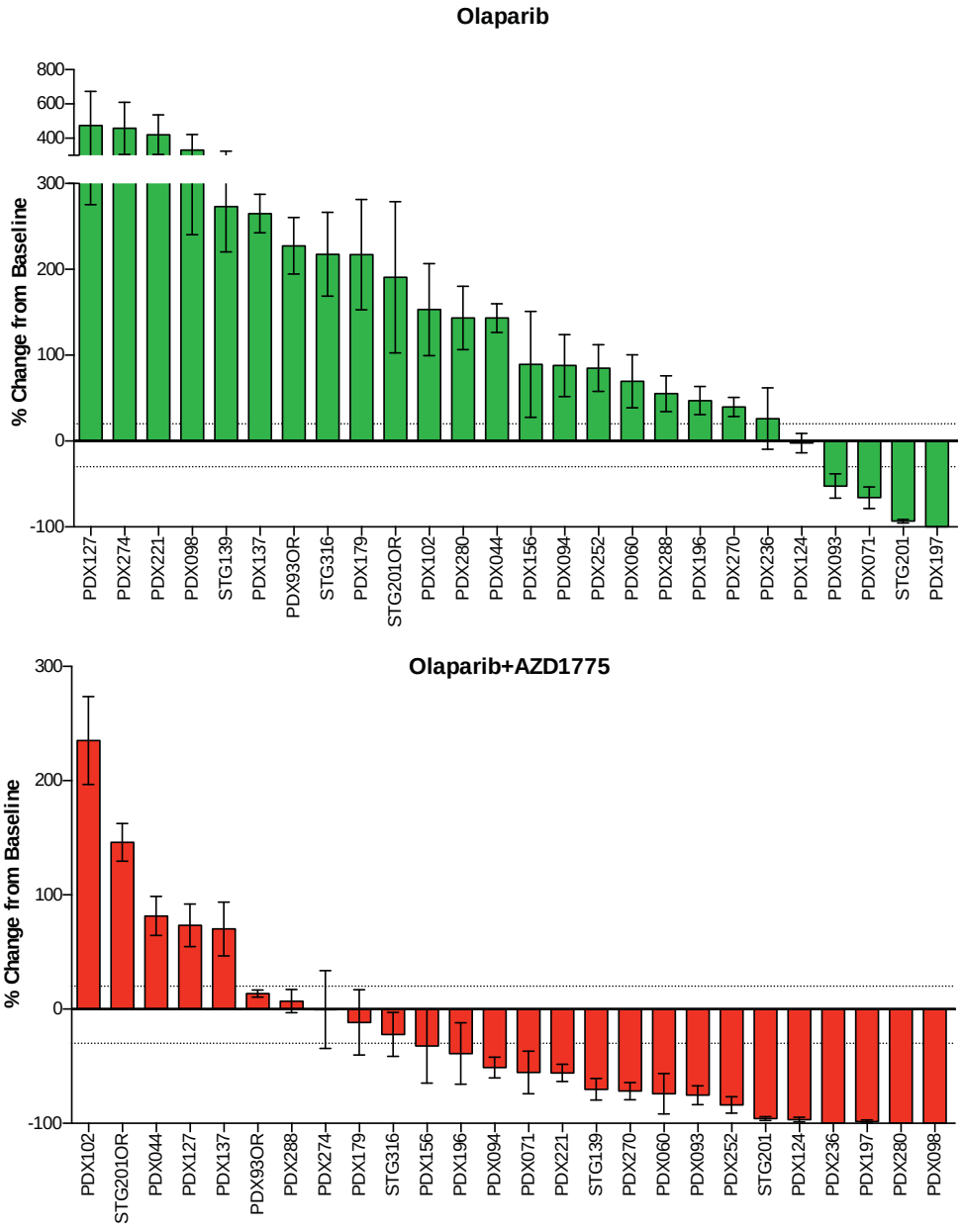

Figure 29 | **WEE1 inhibition enhances PARPi-sensitivity.** Waterfall plot showing the percentage of tumor volume change upon treatment with olaparib (top panel, in green) or olaparib plus AZD1775 (bottom panel, in red) compared to the tumor volume on day 1. +20% and -30% are marked by doted lines to indicate the range of PR, SD and PD.

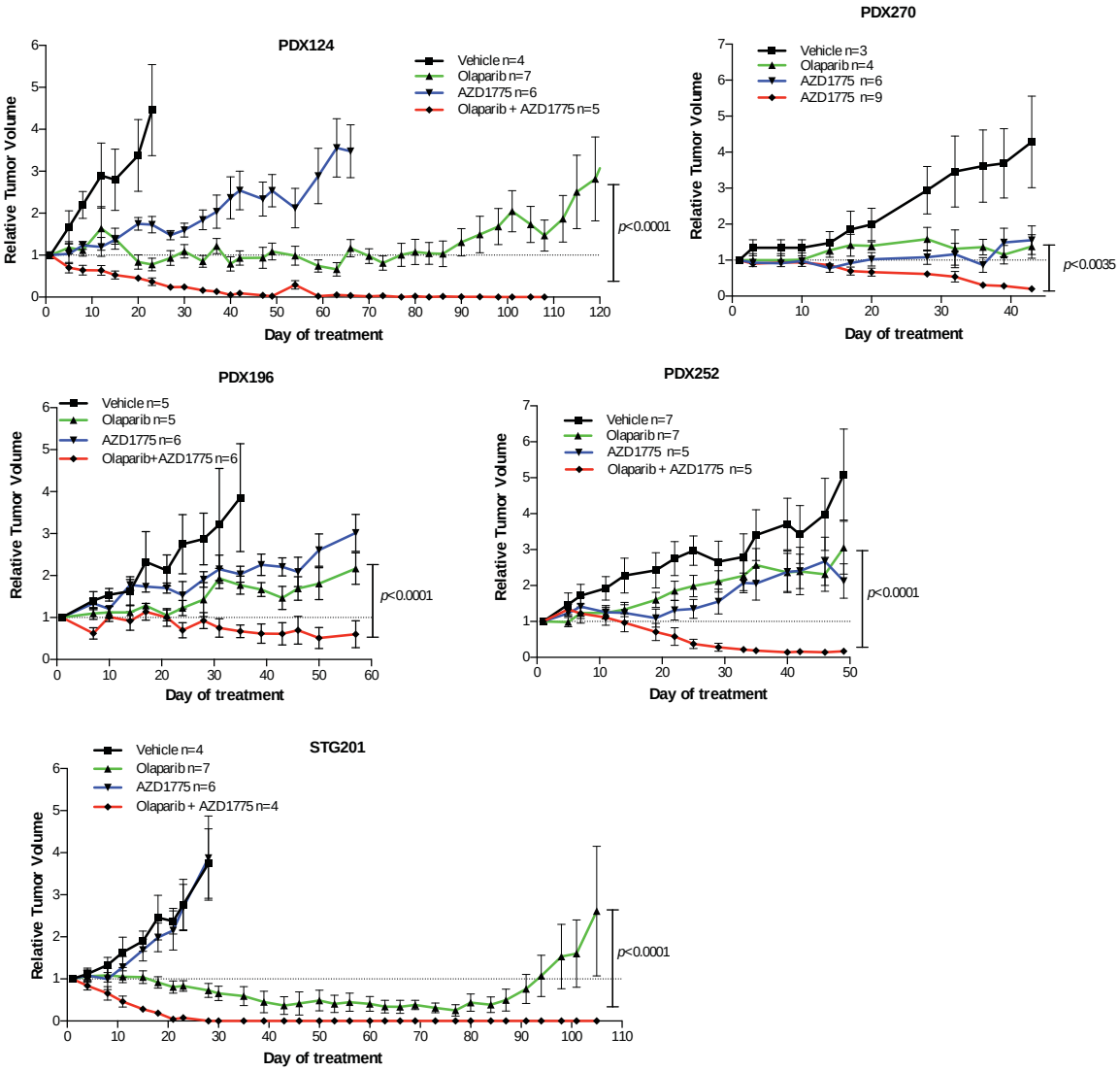

Figure 30 | **WEE1 inhibition enhances PARPi-sensitivity in BRCA1-altered tumors and prevent the acquisition of PARPi resistance.** Percentage of tumor volume change during treatment with vehicle, olaparib, AZD1775 or combination (olaparib + AZD1775) in one PARPi-SD (PDX124), three PARPi-PD (PDX196, PDX270 and PDX252) and one PARPi-CR (STG201) PDXs (Two-way ANOVA). The mean +/- SEM is represented for each arm of treatment.

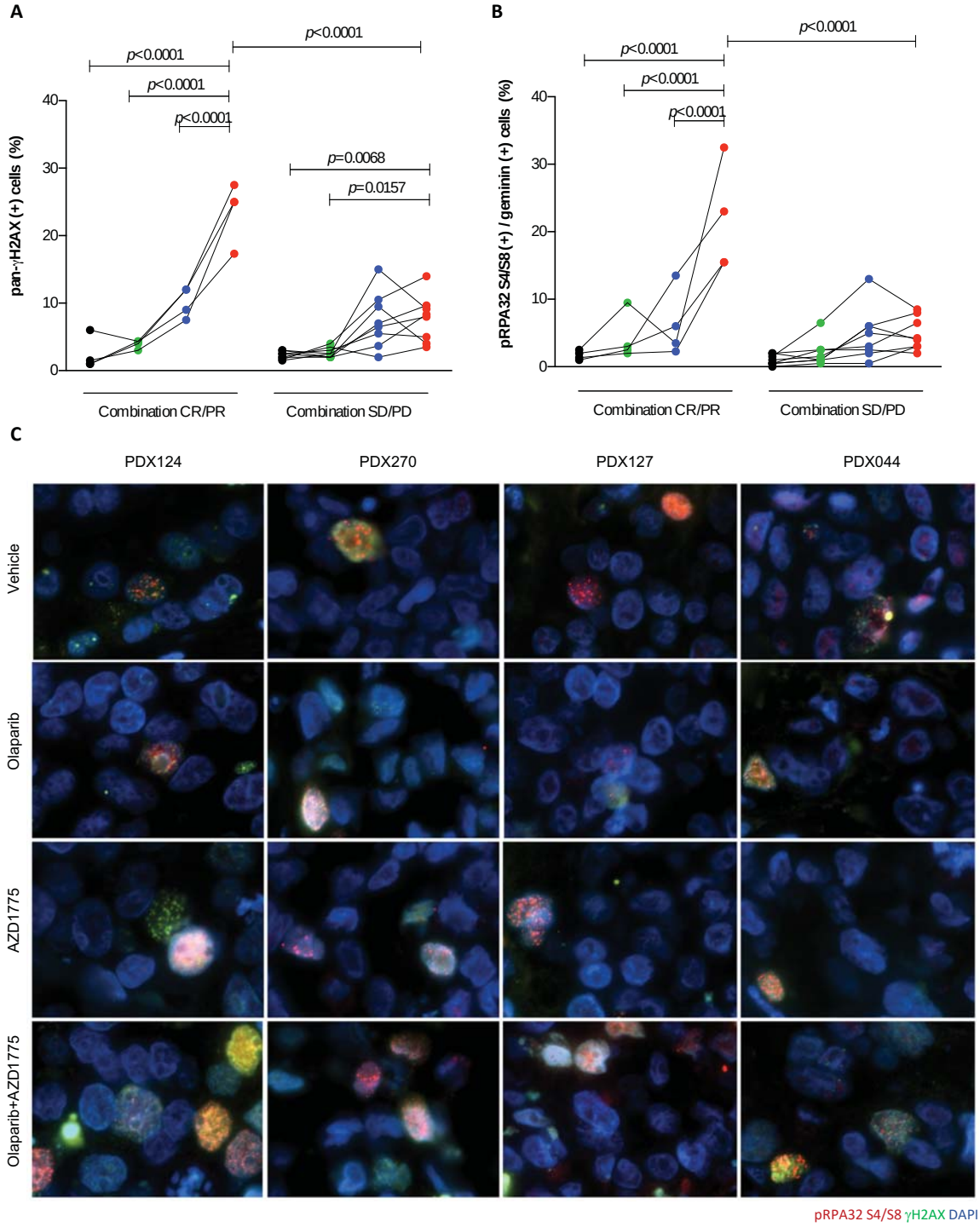

Figure 31 | **Treatment with olaparib plus AZD1775 induces higher levels of replication stress in combination-sensitive PDXs. A-B)** Quantification of **A)** cells with pan-nuclear γH2AX staining and **B)** cells in S/G2-phase of the cell cycle (geminin-positive) with pRPA32 S4/S8 nuclear foci following treatment with vehicle, olaparib, AZD1775 or combination (olaparib + AZD1775) in PDXs showing or not antitumor combination effect (One-way ANOVA). Each dot represents the mean of at least 2 independent PDX tumors. **C)** Immunofluorescence staining of pRPA32 S4/S8 and γH2AX in tumor samples treated with vehicle, olaparib, AZD1775 or combination (olaparib + AZD1775) of two combination-sensitive models (PDX124 and PDX270) and two combination-resistant PDXs (PDX127 and PDX044). Nuclei were visualized with DAPI (blue). All pictures were taken at 600x magnification.

ATM blockade in combination with PARP inhibition sensitizes other BRCA1-altered tumors

Although combining PARPi with WEE1 blockade resulted in tumor regression in most BRCA1-altered PARPi-resistant PDXs, there were still two *BRCA1*-mutated models that progress to this combination therapy, namely PDX127 and STG316. We aimed to further explore the potential of other DDR inhibitors to enhance PARPi antitumor activity in these models. As previously suggested, we hypothesized that ATM blockade is a treatment option for PARPi-resistant BRCA1-deficient tumors that restore HRR through end resection barrier loss by enabling ATM-dependent end resection[138,149]. We tested this hypothesis in the two models of interest, PDX127 and STG316, plus one additional model, PDX280, all of them being ATM-expressing PDXs (**Fig.32A**). STG316 lacks 53BP1 and PDX127 achieve PARPi resistance through loss of FAM35A (**Table 3**). Inhibition of ATM using AZD0156 potentiated olaparib antitumor activity in PDX127 and, to a lesser extent, in STG316 but not in PDX280 (**Fig.32B**). We then investigated whether ATM inhibition resulted in restoration of HRR-deficiency that favored the antitumor response of the combination. To this aim, we assessed the formation of RAD51 and γH2AX nuclear foci in PDX127, which showed the most marked antitumor effect when treated with olaparib plus AZD0156. Unexpectedly, both RAD51 (**Fig.32C**) and γH2AX (**Fig.32D**) foci formation was only marginally reduced in combination-treated tumors, arguing that ATM inhibition may exert a broader effect in signaling the olaparib-induced DDR beyond restoring HRR-deficiency. We then evaluate the induction of replication stress by quantifying pan-nuclear γH2AX staining (**Fig.32E**). Results showed a statistically significant increase of pan-γH2AX-positive cells upon ATMi plus PARPi in comparison with olaparib as single agent only in combination-responders PDX127 and STG316 (**Fig.32E**). These results suggest that the induction of RS is important for combination response and demonstrated that different DDR inhibitors could have similar mechanisms of action but differential responses depending on the genetic background of the tumors.

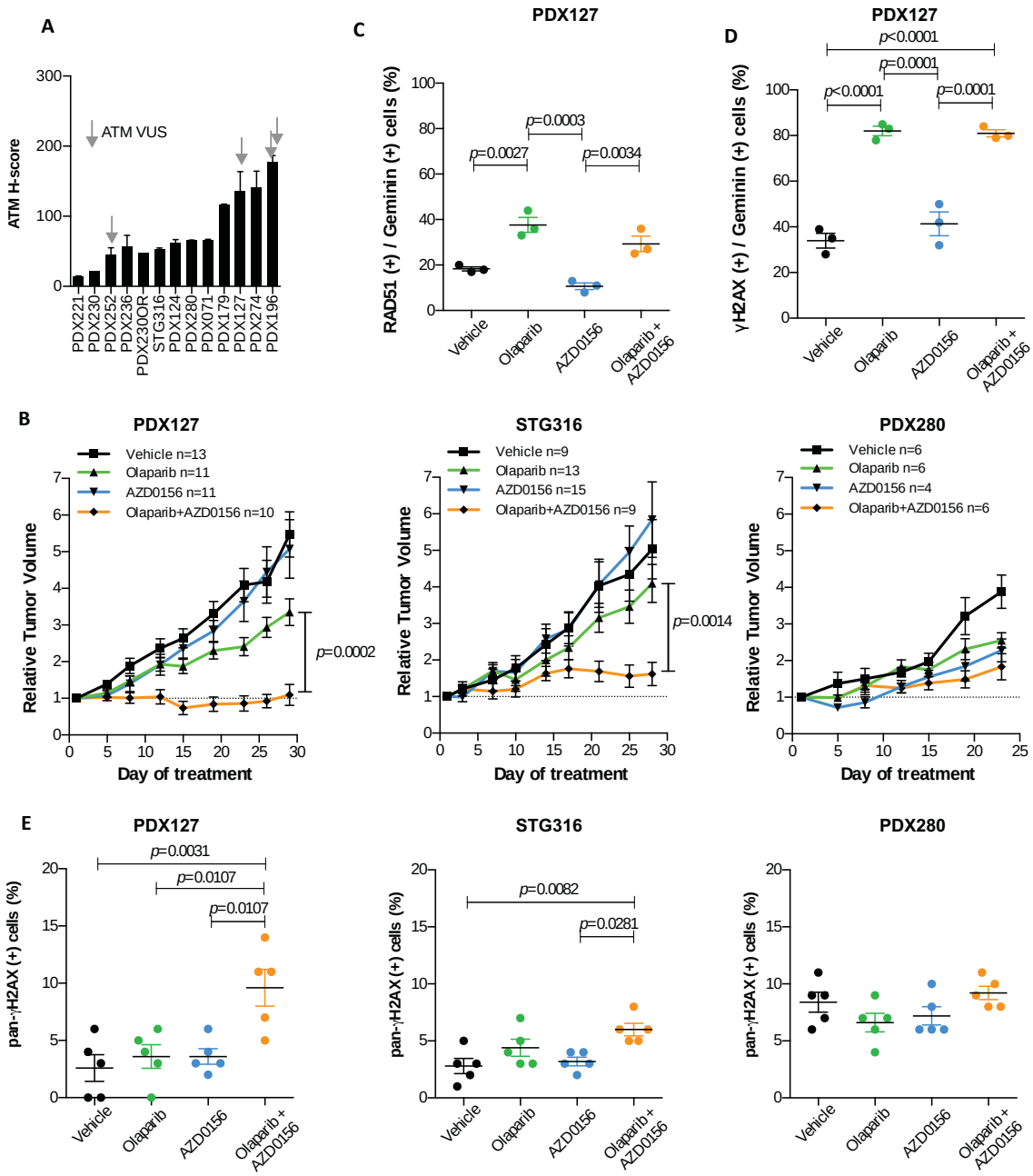

Figure 32 | **ATM inhibition enhances PARPi-sensitivity by inducing replication stress. A)** ATM-expressing tumor cells in the PDXs quantified by immunohistochemistry staining. **B)** Percentage of tumor volume change during treatment with vehicle, olaparib, AZD0156 or combination (olaparib + AZD0156) in PDX127, STG316 and PDX280 (Two-way ANOVA). The mean +/- SEM is represented for each arm of treatment. **C-D)** Quantification of cells in S/G2-phase of the cell cycle (geminin-positive) with **C)** RAD51 and **D)** γH2AX nuclear foci in tumor samples from PDX127 treated with vehicle, olaparib, AZD0156 or combination (olaparib + AZD0156) (One-way ANOVA). **E)** Quantification of cells with pan-nuclear γH2AX staining in tumor samples treated with vehicle, olaparib, AZD0156 or combination (olaparib + AZD0156) from PDX127, STG316 and PDX280. Error bars indicate SEM from independent tumors (One-way ANOVA).

DISCUSSION

PARP inhibitors have become the paradigm of drug-mediated synthetic lethality and, through this concept, were designed as new tailored drugs to selectively kill cancer cells with impaired HRR, initially those with germline mutations in *BRCA1* or *BRCA2* (gBRCA). In the gBRCA scenario, the combination of a functional genetic defect in HRR and pharmacological inhibition of PARP1 leads to cell death through unrepaired DNA damage[128]. PARPi have shown clinical efficacy in patients with *BRCA1/2*-related breast and ovarian cancers[109,113,115,129,130] and have been demonstrated to be beneficial as maintenance treatment in OC patients with platinum-sensitive relapse[114,119,294]. Nevertheless, there are critical questions that still remain in terms of optimizing and widening the clinical efficacy and utility of PARPi.

It is now clear that the efficacy of PARP inhibition is not restricted to the gBRCA population, as other tumors display the "BRCAness" phenotype, meaning that they harbor HRD with wild type *BRCA1/2* genes[295]. As a consequence, the therapeutic landscape of PARPi is now rapidly expanding. On the other hand, however, patients with gBRCA-related tumors frequently do not respond to PARPi and they could inevitably develop acquired resistance, especially in the advanced setting where there is still a need to find additional treatment strategies[128,139]. Therefore, there are at least three important areas of study in the field of PARP inhibition that will improve the success of individualized therapy: (i) to better select patients within the gBRCA population that most benefit from PARPi by recognizing those tumors that will not respond to the treatment; (ii) to investigate the molecular features of PARPi-sensitive tumors that can serve for the selection of patients with *BRCA1/2* wild type tumors candidate to receive PARPi treatment, thereby expanding the use of PARPi beyond the BRCA condition; (iii) and the development of combination treatment strategies to overcome PARPi resistance. In this sense, the development of robust and clinically feasible biomarkers that adequately capture the diverse genetic and epigenetic mechanisms that may impact treatment response is vital to appropriately select patients for PARPi treatment, both as monotherapy and combination strategies. This work contributes in the three mentioned fields to improve the use of PARPi by developing a robust functional biomarker of PARPi response and helping in understand the mechanisms of HRR rewiring and combination treatment options.

The first part of this thesis strengthens the evidence in favor of the restoration of HRR functionality as a frequent mechanism of PARPi resistance among gBRCA breast and ovarian cancers. HRR-restoration is one of the general mechanisms that clinical and preclinical studies have shown to cause PARPi resistance, along with decreasing replication stress and cell cycle progression and other miscellaneous alterations not related with DDR. Restoration of HRR can be achieved by secondary mutations that restore protein function and may be captured by sequencing techniques, albeit their frequency after treatment with PARPi is currently unknown[100]. Most work in gBRCA clinical samples has focused on ovarian cancers[132,296], but whether genetic reversion is also a dominant mechanism for clinical resistance to PARPi in BC remains to be determined[104]. In this work, with the current methodology we did not identify in-frame secondary mutations in *BRCA1* within our panel of gBRCA PDXs, which includes both ovarian and breast tumors. This observation is in line with data that highlights that only a small subset (approximately 20-25%) of patients with PARPi resistance harbors reversion mutations[297]. However, studies in larger clinical data sets are needed to better understand the prevalence of secondary mutations and their influence on PARPi resistance.

Among the different mechanisms of PARPi resistance that has been described, our data suggest that hypomorphic BRCA1 isoforms may contribute to HRR restoration in germline *BRCA1* mutated breast and ovarian cancers. We have developed an immunofluorescence assay with two antibodies against different regions of the BRCA1 protein that allowed to detect nuclear foci formation of hypomorphic BRCA1 isoforms. With this assay, we further demonstrated the functionality of these hypomorphic proteins, including those that form through downstream translation initiation (RING-less BRCA1[143]) and exon-skipping (BRCA1-Δ11q splice isoform[145]), as well as stabilized C-terminal mutant BRCA1 proteins[131]. The presence of these hypomorphic BRCA1 isoforms is associated with PARPi resistance in the PDX cohort-1 and also in an independent PDX panel (cohort-3). Nevertheless, this mechanism of PARPi resistance did not fully overlap with response, as there are gBRCA1 PARPi-resistant models that do not express hypomorphic BRCA1 isoforms (PDX127, PDX280, PDX252, HBCx8). Additionally, in a contrary way, there are also two *BRCA1*-mutated PDXs (both with the mutation within the exon 11 of *BRCA1*) that showed marked

growth delay or antitumor activity upon PARPi treatment but harbored BRCA1 foci formation (PDX124, T330). These data reveal that although the presence of hypomorphic BRCA1 proteins is frequently associated with PARPi resistance in *BRCA1*-mutated breast and ovarian tumors, BRCA1 nuclear foci formation might not always correctly select patients for PARPi treatment. Further studies are needed to help understand the impact of different BRCA1 hypomorphs in PARPi response.

Within our study of PARPi resistance in the panel of gBRCA PDXs, we also reported the presence of other known mechanism of resistance, which is the recovery of DNA end resection capacity. Loss of 53BP1 has been shown to influence in PARPi resistance, probably by shifting the balance of DNA repair from NHEJ to HRR[135]. Here we found that two PARPi-resistant gBRCA1 PDXs (PDX230OR and STG316) harbored genetic alterations in *TP53BP1*. As expected, all PDXs but these two models showed 53BP1 nuclear foci formation by IF. Thus, our data demonstrated that this mechanism of PARPi resistance can occur *in vivo* both in primary- and acquired-resistant gBRCA1 breast tumors. In the same way, we also reported loss of FAM35A in PDX127, another *BRCA1*-mutant and PARPi-resistant PDX with no expression of hypomorphic BRCA1 protein. FAM35A, also known as RINN2, is of special interest as, along with RINN1 and RINN3, compose the shieldin complex, which has been recently identified as a downstream effector of 53BP1-RIF1 in retraining DNA end resection and sensitizing *BRCA1*-deficent cells to PARP inhibition[154–157]. Depletion of shieldin components have shown to reverts PARPi sensitivity in BRCA1-depleted cells by recovering HRR capacity, as shown by the restoration of RAD51 foci formation[157]. Moreover, it was also reported that FAM35A is absent in a common used BRCA1-mutant cell line (HCC1937) that is resistant to PARP inhibition[298,299]. These findings are consistent with our results and support that FAM35A loss modulates PARPi response in PDX127, which showed RAD51 nuclear foci in the absence of BRCA1 function. Therefore, our data further demonstrated that impaired function of FAM35A occurs *in vivo* and is associated with PARPi resistance, which may be important in the novel investigation of the clinical relevance of alterations in the shieldin proteins on HRR capacity and PARPi response. These studies, in fact, can be of especial interest as the chromosomal region encoding *RINN1* and *FAM35A* is frequently deleted in PC (TCGA) and in many cases it is alongside with alterations in other HRR-related

genes[154]. Specifically, *FAM35A* alterations are frequent in PC and significantly less expressed in metastatic cases[299]. Thus, this work could help in better understanding the implication of shieldin components as a therapeutically relevant cancer gen.

We also wanted to examine in our panel of gBRCA PDXs the potential presence of genetic alterations in other known PARPi-resistance genes, including *PARP1*, *MAD2L2*, *PRCC, c20orf196, RIF1, FLJ26957, PAXIP1*, *Artemis*, *SLFN11*, *CHD4*, *RAD51* and *ATM*. With this analysis, we reported an unknown mutation in *SLFN11* in PDX280, a PARPi-resistant ovarian cancer model with complete deletion of *BRCA1*. As mentioned, SLFN11 has been proposed as predictive biomarker of sensitivity to PARPi monotherapy and its inactivation can confer PARPi resistance[179,183]. However, there is an important discrepancy between our findings and previous data, which is the implication of SLFN11 alteration in HRR-capacity. Although it has been reported that PARPi resistance in SLFN11-deficient cells was no caused by activation of HRR[183], the capacity of PDX280 to form RAD51 nuclear foci strongly suggests that the recovery of HRR is the most likely explanation for PARPi resistance in this model. Hence, more studies are needed to understand the effect of SLFN11 p.H661D mutation in protein functionality, HRR-capacity and PARPi response.

Altogether, our PDX cohort-1 enriched with metastatic gBRCA1 breast tumors unveils HRR functionality as the only characteristic that is common in all PARPi-resistant tumors. The recovery of HRR functionality could be achieved through different mechanisms and we also demonstrated the co-existence of multiple of them in one individual tumor, such as PDX124 and STG316 harboring hypomorphic BRCA1 isoforms as well as RAD51 amplification or 53BP1 loss, respectively[269,300]. These findings further highlight that measuring HRR activity with functional assays, such as the RAD51 score, would be a better strategy to select patients who can benefit most from PARPi monotherapy. This is because our data strongly suggest that a high RAD51 score discriminates tumors that will fail PARPi monotherapy independently of the underlying mechanism of HRR restoration. Moreover, the RAD51 assay may capture the dynamic changes in DNA repair that occur throughout tumor evolution and PARPi resistance, therefore contributing to identify more effectively the HRR-proficient *BRCA1/2*-mutated tumors. Therefore, this work supports the use of the

RAD51 functional biomarker to predict response to single agent PARPi and help in appropriate inform treatment strategies and overcome or prevent PARPi resistance within the gBRCA population.

In the second part of this thesis, we focused on expanding the use of this targeted therapy beyond the BRCA condition. This is important because a substantial number of patients who lack *BRCA1/2* mutation may benefit from PARPi monotherapy as they displayed an HRR-deficient condition that can arise through various genomic, epigenetic or post-translation alterations[82,128]. In this sense, there is a clear need to develop robust and clinically feasible biomarkers of HRR functionality correlating with treatment response. Recent advances towards the development of biomarkers of response and resistance to PARPi have been based on targeted sequencing of DNA repair genes, genomic scars, or gene and protein expression[144]. Nevertheless, some of these biomarkers have pitfalls. For example, genomic signatures have a limited capacity to capture restoration of HRR functionality that may occur during tumor evolution or after drug pressure. Instead, functional assays of HRR status provide a more comprehensive and dynamic readout of tumor HRR capacity throughout disease evolution and at the specific moment of treatment decision[144,222]. In these sense, RAD51 foci formation had been examined as biomarker of PARPi response, but previous assays used to quantify RAD51 foci formation are difficult to implement in the clinical practice[238,240].

Here we report on the performance of the RAD51 assay in FFPE cancer samples without prior patient treatment or exogenous DNA damage induction. While previous studies reported low levels of baseline DNA damage as a potential limitation to evaluate HRR[238,240] we were able to consistently detect endogenous DNA damage and RAD51 foci in untreated samples, both from PDX and patients. We demonstrated that the RAD51 score was able to capture the HRR functionality in untreated tumors and correlated with PARPi response. In *BRCA1/2*-mutated and wild type TNBC PDXs, a RAD51 score cut-off of 10% predicted the response to different PARP inhibitors and doses with high specificity and sensitivity, outperforming the HRD score. This represents a novel comparison of the predicting capacities of PARPi response between a functional and a genomic-based assay.

We also tested the feasibility of the RAD51 assay in routine clinical samples from patients with HBOC syndrome, including gPALB2-related tumors, further demonstrating the feasibility of the RAD51 assay in untreated clinical samples. Importantly, the RAD51 assay classified as HRR-deficient all the tumors from patients with deleterious germline *PALB2* mutations, along with three tumors from young-onset BC patients with absent BRCA1 foci formation. Altogether, our data highlighted the utility of the RAD51 score to identify several populations that might be sensitive to PARPi. First, the germline population with HRR alterations, including *BRCA1/2*, *PALB2* and probably other genes, such as *RAD51C* or *RAD51D*. In these patients, the RAD51 assay could be used as an enrichment biomarker to better predict sensitivity to PARPi, since restoration of the HRR pathway might have occurred and result in PARPi-resistance[144,285]. Second, tumors with somatic alterations in HRR-related genes, such as the *PALB2* mutations described in 4% of metastatic BC[293,301]. And third, tumors with epigenetic HRR silencing, such as *BRCA1* or *RAD51C* promoter hypermethylation. Additional work is needed to define the sensitivity and specificity of the assay to predict PARPi benefit, as well as to establish the RAD51 score cut-off that differentiates responders from non-responders to PARPi monotherapy in the clinic. With this purpose, our results will be validated in large patient cohorts of multicenter clinical trials as well as in prospective studies.

The use of the RAD51 assay in other tumor types remains to be explored. Ongoing studies in our laboratory have demonstrated the feasibility of the assay in different cancers, including endometrial, pancreatic and prostate tumors. In this scenario, the RAD51 score, may further cover the current need to enlarge the population eligible for PARPi treatment and to identify other PARPi sensitive tumors beyond the actual selection criteria.

Nevertheless, it is necessary to be aware that the RAD51 assay has some limitations. Firstly, when PARPi sensitivity occurs via mechanisms that do not directly impact on the ability of cells to perform HRR, e.g. alterations in ATM[231,302,303] or in the RNASEH2 complex[304]. Secondly, when PARPi sensitivity occurs via mechanisms that preserve RAD51 foci formation, e.g. alterations in the MRN complex, RAD51AP1, polymerase eta or ERCC1[199,305–307]. Thirdly, when HRR-deficient tumors have acquired PARPi resistance via RAD51-

independent mechanisms such as loss of PARG, mutations in *PARP1* or those that involve replication fork stabilization[160,174,308–312]. Fourthly, when a tumor has low proliferation index or low endogenous DNA damage, in which cases the assay would not be feasible. In this sense, understanding innate tumor genomics and combining this knowledge with the information from functional assays such as the RAD51 score may improve patient selection for PARPi treatment.

The RAD51 score might have other potential uses. For example, it could help in providing functional validation of both tumor and germline genomic variants of unknown significance (VUS). Multigene panel sequencing for breast, ovarian and prostate cases has resulted in increased identification of numerous gene VUS that represent a clinical challenge for risk assessment, genetic counselling and treatment choice[313]. To date, different efforts have been made to standardize the clinical interpretation of these genetic variants and there is a need for highly sensitive and specific assays to improve VUS classification and implement specific preventive measures for healthy carriers as well as therapeutic guidance[314]. The RAD51 assay could, therefore, represent a tool to classify the impact in HRR capacity of VUS in DDR genes, including *BRCA1*, *BRCA2* and *PALB2*, among others. In fact, we have recently reported a study that support a pathogenic classification for a *PALB2* mutation (c.3201+5G>T) present in a RAD51-negative tumor[315]. Specially in the *PALB2*-mutated setting, the RAD51 assay could be of special interest, as some tumors retain the wild type *PALB2* allele and it has been shown that both breast tumors with *PALB2* bi-allelic inactivation and those that retains the wild type *PALB2* allele had high HRD scores[316]. Moreover, heterozygous *PALB2* deletions and other alterations in DDR genes were found in metastatic CRPC (mCRPC) patients, and most of them responded to olaparib[317]. Therefore, the RAD51 assay might be useful in understanding the impact of heterozygous mutations in HRR capacity.

In line with the previous paragraph, the RAD51 assay might also help in the constantly expanded knowledge of genes with direct or indirect roles in HRR capacity and, therefore, in knowing the potential relationship of these genes with PARPi response. For example, *ARID1A* is a gene implicated in chromatin remodeling and one of the most frequently

mutated in cancer[128]. ARID1A deficiency sensitize tumors to various DDR inhibitors in preclinical models, including PARPi[318]. Similarly, as it is also implicated in chromatin remodeling, BAP1 deficiency is associated with PARPi sensitivity[319,320]. These examples demonstrate that the discovery of genes that play distinct roles in DDR, cell-cycle regulation and chromatin remodeling is increasing. In this scenario, a functional test, such as the RAD51 assay, that inform about the potential effect in HRR capacity of aberrations in these genes, could be very helpful. The RAD51 assay could therefore inform about new opportunities to expand the therapeutic landscape of PARP inhibitors. But not only this, because better understanding the proteins involved in DDR in a mutation-specific manner might also help in the identification of treatment strategies to overcome or prevent PARPi resistance. A high RAD51 score may encourage the use of combination therapies with PARPi that enhance DNA damage, such as platinum salts, followed by maintenance with a PARPi[112,321,322]. Moreover, new therapeutic options to overcome PARPi resistance include the use of other targeted agents such as inhibitors of DDR proteins. This work additionally propose that a subset of PARPi-resistant tumors may benefit from combined PARP blockade with other DDR inhibitors.

In this context we tested the inhibition of WEE1 and ATM to enhance antitumor response to PARPi in PDXs. Our work could help in the characterization of TNBC tumors that will benefit from WEE1 inhibition as single agent and in combination with PARPi, in addition to helping in elucidating the mechanisms of action of these compounds *in vivo* and identifying potential biomarkers of response with clinical application.

To study the effects of WEE1 blockade in tumor cells, we investigated both cell-cycle progression and replication stress induction. Although previous studies with AZD1775 in various cell lines and patients with *BRCA* mutation showed an induction of γH2AX with no increase in pHH3[266,323,324], our results showed a dual effect of inhibiting WEE1i *in vivo*, including the reported increase in replication stress but also in the proportion of pHH3-positive cells. Nevertheless, our results showed that the induction of mitotic entry did not discriminates WEE1i-sensitive to -resistant tumors, further demonstrating that premature entry in mitosis may not be the major mechanisms of WEE1i sensitivity[324].

Having shown these mechanisms of action of WEE1 blockade, we also realized that levels of RS, measured as the percentage of cells with pRPA S4/S8 nuclear foci, are higher in WEE1i-sensitive tumors both upon treatment with WEE1i or vehicle. These results are in consistence with the model of "replication catastrophe"[325]. This model proposes that fork stability depends on the protection of ssDNA by RPA and there are tumors with high baseline levels of replication stress in which, although RPA is an abundant protein, its exhaustion may occur because the firing of excessive replication forks after checkpoint inhibition. Forcing cells with high levels of RS to enter mitosis may cause replication catastrophe and cell death[264]. Therefore, our data suggest that the measurement of baseline levels of RS could predict for WEE1i monotherapy response. Previous results have also shown a good correlation between the levels of ssDNA and response to WEE1 and ATR inhibitors using diffuse large B-cell lymphoma (DLBCL) cell lines[326], which highlights the opportunity to test our assay for predict response to other DDR inhibitors. Furthermore, the lack of optimized assays to measure ssDNA or RPA foci represents an actual barrier to use these assays in the clinical practice[310] and our IF assay for pRPA S4/S8 nuclear foci detection could help in this current limitation.

As it has been reported that a genetic background compatible with higher RS predispose to PARP plus WEE1 inhibition sensitivity[327], we then focused on this combination strategy to study the effect of increasing RS to enhance PARPi response. In concordance, we reported that combination-sensitive PDXs harbor exacerbated induction of RS upon WEE1 plus PARP blockade. All the gBRCA1 PDXs that progress to PARPi monotherapy showed antitumor response with this combination treatment but two models, PDX127 and STG316. However, these two BC models showed antitumor activity when combining PARP plus ATM blockade, demonstrating that a subset of PARPi-resistant gBRCA1 tumors could also benefit from this combination strategy[149,258,328,329]. Interestingly, when examined the effects of ATM inhibition in these models, we showed that induction of RS is again the feature that differentiates combination-sensitive from -resistant models. Although further research is needed to confirm these findings, our data suggest that inhibiting ATM did not affects HRR-capacity, but target replication stress response. Altogether, our results support the potential of exploiting replicative stress to treat cancer and combat PARPi resistance,

particularly in *BRCA1*-altered tumors, and suggested that response to combination strategies might depend on different tumor characteristics, such as the mechanisms of PARPi resistance.

In addition to the two DDR inhibitors studied in this thesis, there are other emerging ways and therapeutic potential inhibitors to enhance replicative stress as anticancer treatment, including inhibitors of CHK1, CHK2, ATR or DNA-PK as single agent and in combination with PARPi[23,330] (**Fig.33**). Studies with these compounds are currently underway and some of them have reached advanced stages of preclinical and clinical development[264]. Other interesting targets to increase replicative stress include NEDD8-activating enzyme (NAE)[331] or maternal embryonic leucine zipper kinase (MELK). Preliminary results from our lab showed non-overlapping activity between WEE1, ATR or ATM inhibition, which again demonstrates the importance of characterizing the biomarkers of response to these targeted therapies, where the number of potential targets continuously grows. The efficacy of the use of DDR-inhibitors as anticancer drugs will depend on identifying the susceptibility factors associated with the specific DDR-inhibitor, combination treatments and limiting toxicities.

Another rational combination approach is the use of inhibitors of BET proteins or the PI3K, RAS and AR signaling pathways, which can induce a state of HRR deficiency as they can regulate the expression of HRR genes[332,333] (**Fig.33**). Thus, target these proteins has the potential to induce synthetic lethality with a DDR-inhibitor, such as PARPi, as already shown in preclinical studies[253,334–337]. In this scenario, the work presented in this thesis can also be helpful, as the RAD51 assay could confirm the effect of inducing an HRR deficiency state by targeting these proteins, thereby working both as a functional biomarker in the development of new drugs and as a predictive biomarker for combination treatments with PARPi.

Finally, multiple evidence has provided a biological rationale for combining DDR inhibitors with immunotherapies, as immune-checkpoints inhibitors (ICIs), and the potential use of DDR defects as predictive biomarkers of response to ICIs. Genomic instable tumors as those

with *BRCA1/2* mutation and others with DDR deficiency, are characterized by lymphocytic infiltration[82]. It has been suggested that, as DDR proteins maintain the integrity of the genome, defects in these pathways might increase the tumor mutational burden (TMB), leading to higher neoantigen production and enhanced activation of antitumoral T cells[338–341]. On the other hand, tumors with DDR gene aberrations seem to accumulate cytosolic DNA, which represent a stimulus to the activation of the innate immune system through the cGAS-STING pathway that does not require the recognition of neoantigens[341,342]. In addition, paradoxically, the STING pathway also activates the expression of PD-L1 in tumor cells, therefore limiting the cytotoxic immune response, but giving the opportunity to sensitize the tumor to PD-L1 blockade (**Fig.33**)[343]. Although the rationale of using ICIs in tumors with DDR deficiencies seems clear, evidence is only beginning to emerge[344]. The RAD51 assay may also have place in this scenario, where the correct characterization of HRR-deficient tumors is important to determine the effect of this phenotype in the immune response. Moreover, the combination of the RAD51 assay with others as PD-L1 expression might serve as biomarker to select those tumors that will benefit from ICIs as single agent or in combination with PARP inhibitors.

To conclude, this thesis points out that the RAD51 assay is highly sensitive and specific in predicting antitumor response to PARP inhibition and, taken some considerations into account, it may be implemented in routine clinical diagnostics to provide an accurate measurement of HRR status at the time of treatment decision-making, therefore improving patient selection for PARPi treatment in the field of personalized medicine. We also provide here an improved understanding of the resistance mechanisms to PARPi and their implication in the selection of correct combination strategies with DDR inhibitors, providing novel information that will facilitate patient stratification for DDR-targeting therapies. Key questions for the near future include the characterization of the level of HRD, how to incorporate predictive biomarkers of sensitivity into clinically relevant platforms, and how the molecular heterogeneity within tumors impact treatment regimens and resistance mechanisms. Altogether, this works highlighted that comprehensive functional tests for identifying the biological background of tumors that better respond to targeted therapies

are needed and will be pivotal in developing the right combination strategy and improve patient selection to finally achieve more efficient and durable clinical responses.

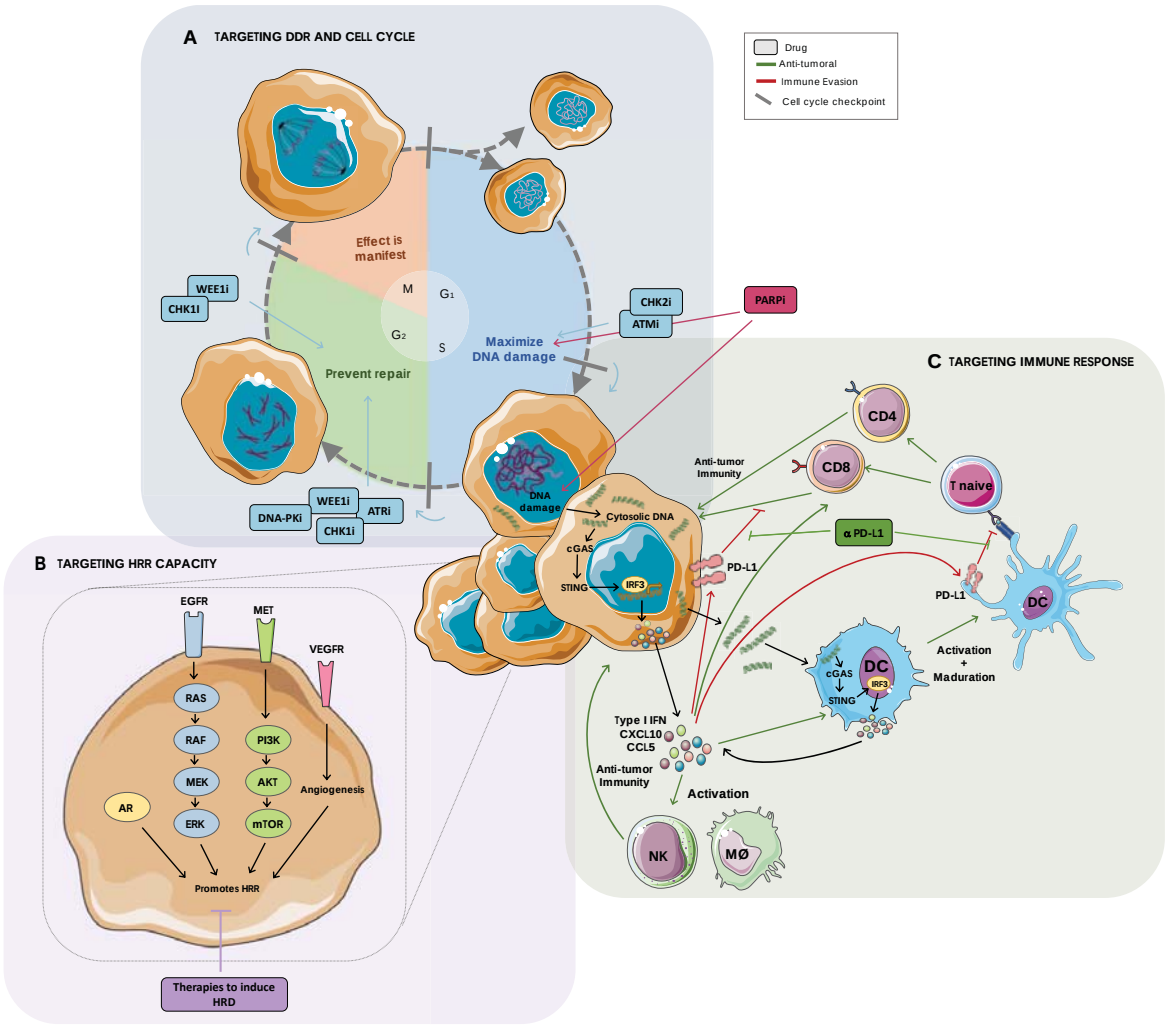

Figure 33 | **Therapies in combination with PARPi.** The different options of therapies that can be combined with PARPi are represented, including **A)** the strategy for the development of DDR-targeted therapies, **B)** the use of inhibitors of proteins of the PI3K, RAS, VEGFR and AR signaling pathways, which can induce a state of HRR deficiency as the can regulate the expression of HRR genes, and **C)** the rationale for combining PARPi with immunotherapies. Tumors with DDR alterations accumulate cytosolic DNA, which represent a stimulus to the activation of the innate immune system through the cGAS-STING pathway that induces the production of type I interferons (IFN) and chemoattractant and pro-inflammatory cytokines (CXCL10, CCL5, IL-1). This cascade result in both the activation of NK cells and macrophages and the infiltration, proliferation and anti-tumor response of CD4+ and CD8+ T cells into the tumor. Paradoxically, the STING pathway also activates the expression of PD-L1 in tumor cells, therefore limiting the cytotoxic immune response, but giving the opportunity to sensitize the tumor to PD-L1 blockade. DC, dendritic cell; M∅, macrophage; NK, natural killer cell; Treg, regulatory T cell.

CONCLUSIONS

PART 1

- Patient derived xenografts (PDX) from germline *BRCA1/2*-mutated (gBRCA) breast and ovarian cancer patients recapitulate the patient's response to PARPi and represent a suitable platform to study *in vivo* antitumor activity of PARPi
- Restoration of HRR functionality is frequent among gBRCA PDXs that do not respond to PARPi treatment
- HRR recovery in the gBRCA PDXs is achieved by several mechanisms including the expression of hypomorphic BRCA1 proteins and loss of an end resection barrier, including 53BP1 and FAM35A
- Detection of RAD51 foci in gBRCA tumors from PDXs and patients correlates with PARPi resistance regardless of the underlying mechanisms of HRR restoration
- The RAD51 assay is a promising biomarker to be used in the clinic for better select gBRCA patients that will benefit from PARPi monotherapy

PART 2

- There are PDXs from *BRCA1/2* wild type (non-gBRCA) breast cancer (BC) patients that showed antitumor activity upon PARP inhibition
- *BRCA1* promoter hypermethylation and genetic alterations in HRR-related genes are associated with PARPi sensitivity in non-gBRCA BC PDXs
- The RAD51 score is a functional biomarker with complete discriminative capacity in predicting PARPi antitumor response in BC PDXs and outperformed the HRD genomic test
- The RAD51 assay is feasible in routine clinical samples without prior exposure to DNA damaging agents
- In clinical samples from patients with HBOC syndrome, carrying a *PALB2* mutation is associated with a low RAD51 score
- The RAD51 score is a functional biomarker that enables the identification of PARPi-sensitive BC and broadens the population who may benefit from this targeted therapy beyond BRCA-related cancers

PART 3

- WEE1 inhibition induces accelerated mitotic entry and enhances replication stress levels in PDX from gBRCA and non-gBRCA breast and ovarian cancers
- Antitumor response to single agent WEE1i is associated with a higher induction of replication stress *in vivo*
- High levels of baseline replication stress correlate with antitumor response to WEE1i single-agent in PDXs
- WEE1 inhibition enhances PARPi antitumor activity in BRCA1-altered PDXs
- WEE1 plus PARP1 blockade leads to exacerbated induction of replication stress in combination-sensitive PDXs
- PARPi resistance in gBRCA1 mutated BC PDXs can be also reverted by combining PARP plus ATM inhibition

REFERENCES

1. World Cancer Research Fund/ American Institute for Cancer Research. *The cancer process*. *Food, Nutrition, Physical Activity and the Prevention of Cancer: A Global Perspective* (2018).

2. Lodish, H. *et al.* Proto-Oncogenes and Tumor-Suppressor Genes. (2000).

3. Croce, C. M. Oncogenes and Cancer. *N. Engl. J. Med.* **358**, 502–511 (2008).

4. Hanahan, D. & Weinberg, R. A. Hallmarks of Cancer: The Next Generation. *Cell* **144**, 646–674 (2011).

5. Vogelstein, B. *et al.* Cancer Genome Landscapes. *Science (80-.).* **339**, 1546–1558 (2013).

6. Ryan, B. M. & Faupel-Badger, J. M. The hallmarks of premalignant conditions: a molecular basis for cancer prevention. *Semin. Oncol.* **43**, 22–35 (2016).

7. Stratton, M. R., Campbell, P. J. & Futreal, P. A. The cancer genome. *Nature* **458**, 719–724 (2009).

8. Tabassum, D. P. & Polyak, K. Tumorigenesis: it takes a village. *Nat. Rev. Cancer* **15**, 473–483 (2015).

9. Hanahan, D. & Weinberg, R. A. The Hallmarks of Cancer. *Cell* **100**, 57–70 (2000).

10. Lazebnik, Y. What are the hallmarks of cancer? *Nat. Rev. Cancer 2010 104* (2010).

11. Santisteban, M. *et al.* Ki67: a time-varying biomarker of risk of breast cancer in atypical hyperplasia. *Breast Cancer Res. Treat.* **121**, 431–437 (2010).

12. Shaaban, A. M., Sloane, J. P., West, C. R. & Foster, C. S. Breast cancer risk in usual ductal hyperplasia is defined by estrogen receptor-alpha and Ki-67 expression. *Am. J. Pathol.* **160**, 597–604 (2002).

13. Raica, M., Cimpean, A. M. & Ribatti, D. Angiogenesis in pre-malignant conditions. *Eur. J. Cancer* **45**, 1924–1934 (2009).

14. Sharma, R. A., Harris, A. L., Dalgleish, A. G., Steward, W. P. & O'Byrne, K. J. Angiogenesis as a biomarker and target in cancer chemoprevention. *Lancet Oncol.* **2**, 726–732 (2001).

15. Block, K. I. *et al.* Designing a broad-spectrum integrative approach for cancer prevention and treatment. *Semin. Cancer Biol.* **35**, S276–S304 (2015).

16. Turley, S. J., Cremasco, V. & Astarita, J. L. Immunological hallmarks of stromal cells in the tumour microenvironment. *Nat. Rev. Immunol.* **15**, 669–682 (2015).

17. Yang, L., Pang, Y. & Moses, H. L. TGF-β and immune cells: an important regulatory axis in the tumor microenvironment and progression. *Trends Immunol.* **31**, 220–227 (2010).

18. Shields, J. D., Kourtis, I. C., Tomei, A. A., Roberts, J. M. & Swartz, M. A. Induction of Lymphoidlike Stroma and Immune Escape by Tumors That Express the Chemokine CCL21. *Science (80-.).* **328**, 749–752 (2010).

19. Khanna, R. Tumour surveillance: Missing peptides and MHC molecules. *Immunol. Cell Biol.* **76**, 20–26 (1998).

20. Bubeník, J. MHC class I down-regulation: tumour escape from immune surveillance? (review). *Int. J. Oncol.* **25**, 487–91 (2004).

21. Negrini, S., Gorgoulis, V. G. & Halazonetis, T. D. Genomic instability — an evolving hallmark of cancer. *Nat. Rev. Mol. Cell Biol.* **11**, 220–228 (2010).

22. Salk, J. J., Fox, E. J. & Loeb, L. A. Mutational Heterogeneity in Human Cancers: Origin and Consequences. *Annu. Rev. Pathol. Mech. Dis.* **5**, 51–75 (2010).

23. O'Connor, M. J. Targeting the DNA Damage Response in Cancer. *Mol. Cell* **60**, 547–560 (2015).

24. Aguilera, A. & Gómez-González, B. Genome instability: a mechanistic view of its causes and consequences. *Nat. Rev. Genet.* **9**, 204–217 (2008).

25. DeNardo, D. G., Andreu, P. & Coussens, L. M. Interactions between lymphocytes and myeloid cells regulate pro- versus anti-tumor immunity. *Cancer Metastasis Rev.* **29**, 309–316 (2010).

26. Grivennikov, S. I., Greten, F. R. & Karin, M. Immunity, Inflammation, and Cancer. *Cell* **140**, 883–899 (2010).

27. Qian, B.-Z. & Pollard, J. W. Macrophage Diversity Enhances Tumor Progression and Metastasis. *Cell* **141**, 39–51 (2010).

28. Karnoub, A. E. & Weinberg, R. A. Chemokine networks and breast cancer metastasis. *Breast Dis.* **26**, 75–85

29. Ciccia, A. & Elledge, S. J. The DNA Damage Response: Making It Safe to Play with Knives. *Mol. Cell* **40**, 179–204 (2010).

30. Jackson, S. P. & Bartek, J. The DNA-damage response in human biology and disease. *Nature* **461**, 1071–1078 (2009).

31. Rouse, J. & Jackson, S. P. Interfaces between the detection, signaling, and repair of DNA damage. *Science* **297**, 547–51 (2002).

32. Harper, J. W. & Elledge, S. J. The DNA damage response: ten years after. *Mol. Cell* **28**, 739–45 (2007).

33. Hoeijmakers, J. H. J. Genome maintenance mechanisms for preventing cancer. *Nature* **411**, 366–374 (2001).

34. Brown, J. S., O'Carrigan, B., Jackson, S. P. & Yap, T. A. Targeting DNA Repair in Cancer: Beyond PARP Inhibitors. *Cancer Discov.* **7**, 20–37 (2017).

35. Pearl, L. H., Schierz, A. C., Ward, S. E., Al-Lazikani, B. & Pearl, F. M. G. Therapeutic opportunities within the DNA damage response. *Nat. Rev. Cancer* **15**, 166–180 (2015).

36. Shrivastav, M., De Haro, L. P. & Nickoloff, J. A. Regulation of DNA double-strand break repair pathway choice. *Cell Res.* **18**, 134–147 (2008).

37. Khanna, K. K. & Jackson, S. P. DNA double-strand breaks: signaling, repair and the cancer connection. *Nat. Genet.* **27**, 247–254 (2001).

38. Moynahan, M. E. & Jasin, M. Mitotic homologous recombination maintains genomic stability and suppresses tumorigenesis. *Nat. Rev. Mol. Cell Biol.* **11**, 196–207 (2010).

39. Lieber, M. R. The Mechanism of Double-Strand DNA Break Repair by the Nonhomologous DNA End-Joining Pathway. *Annu. Rev. Biochem.* **79**, 181–211 (2010).

40. Radhakrishnan, S. K., Jette, N. & Lees-Miller, S. P. Non-homologous end joining: Emerging themes and unanswered questions. *DNA Repair (Amst).* **17**, 2–8 (2014).

41. Ceccaldi, R. *et al.* Homologous-recombination-deficient tumours are dependent on Polθ-mediated repair. *Nature* **518**, 258–62 (2015).

42. Roy, R., Chun, J. & Powell, S. N. BRCA1 and BRCA2: different roles in a common pathway of genome protection. *Nat. Rev. Cancer* **12**, 68–78 (2012).

43. Huen, M. S. Y., Sy, S. M. H. & Chen, J. BRCA1 and its toolbox for the maintenance of genome integrity. *Nat. Rev. Mol. Cell Biol.* **11**, 138–148 (2010).

44. Miki, Y. *et al.* A strong candidate for the breast and ovarian cancer susceptibility gene BRCA1. *Science (80-.).* **266**, 66–71 (1994).

45. Meza, J. E., Brzovic, P. S., King, M. C. & Klevit, R. E. Mapping the functional domains of BRCA1. Interaction of the ring finger domains of BRCA1 and BARD1. *J. Biol. Chem.* **274**, 5659–65 (1999).

46. Wang, Y. *et al.* RING domain-deficient BRCA1 promotes PARP inhibitor and platinum resistance. *J. Clin. Invest.* **126**, 3145–3157 (2016).

47. Billing, D. *et al.* The BRCT Domains of the BRCA1 and BARD1 Tumor Suppressors Differentially Regulate Homology-Directed Repair and Stalled Fork Protection. *Mol. Cell* **72**, 127-139.e8 (2018).

48. Wu, L. C. *et al.* Identification of a RING protein that can interact in vivo with the BRCA1 gene product. *Nat. Genet.* **14**, 430–440 (1996).

49. Sato, K. *et al.* Nucleophosmin/B23 Is a Candidate Substrate for the BRCA1-BARD1 Ubiquitin Ligase. *J. Biol. Chem.* **279**, 30919–30922 (2004).

50. Nishikawa, H. *et al.* Mass Spectrometric and Mutational Analyses Reveal Lys-6-linked Polyubiquitin Chains Catalyzed by BRCA1-BARD1 Ubiquitin Ligase. *J. Biol. Chem.* **279**, 3916–3924 (2004).

51. Christensen, D. E., Brzovic, P. S. & Klevit, R. E. E2–BRCA1 RING interactions dictate synthesis of mono- or specific polyubiquitin chain linkages. *Nat. Struct. Mol. Biol.* **14**, 941–948 (2007).

52. Brzovic, P. S., Lissounov, A., Christensen, D. E., Hoyt, D. W. & Klevit, R. E. A UbcH5/Ubiquitin Noncovalent Complex Is Required for Processive BRCA1-Directed Ubiquitination. *Mol. Cell* **21**, 873–880 (2006).

53. Anderson, S. F., Schlegel, B. P., Nakajima, T., Wolpin, E. S. & Parvin, J. D. BRCA1 protein is linked to the RNA polymerase II holoenzyme complex via RNA helicase A. *Nat. Genet.* **19**, 254–256 (1998).

54. Scully, R. *et al.* BRCA1 is a component of the RNA polymerase II holoenzyme. *Proc. Natl. Acad. Sci. U. S. A.* **94**, 5605–10 (1997).

55. Bochar, D. A. *et al.* BRCA1 is associated with a human SWI/SNF-related complex: linking chromatin remodeling to breast cancer. *Cell* **102**, 257–65 (2000).

56. Yarden, R. I. & Brody, L. C. BRCA1 interacts with components of the histone deacetylase complex. *Proc. Natl. Acad. Sci. U. S. A.* **96**, 4983–8 (1999).

57. Jiang, Q. & Greenberg, R. A. Deciphering the BRCA1 Tumor Suppressor Network. *J. Biol. Chem.* **290**, 17724–17732 (2015).

58. Zhao, G. Y. *et al.* A Critical Role for the Ubiquitin-Conjugating Enzyme Ubc13 in Initiating Homologous Recombination. *Mol. Cell* **25**, 663–675 (2007).

59. Cantor, S. B. *et al.* BACH1, a novel helicase-like protein, interacts directly with BRCA1 and

contributes to its DNA repair function. *Cell* **105**, 149–60 (2001).

60. Yu, X., Wu, L. C., Bowcock, A. M., Aronheim, A. & Baer, R. The C-terminal (BRCT) domains of BRCA1 interact in vivo with CtIP, a protein implicated in the CtBP pathway of transcriptional repression. *J. Biol. Chem.* **273**, 25388–92 (1998).

61. Sy, S. M. H., Huen, M. S. Y. & Chen, J. PALB2 is an integral component of the BRCA complex required for homologous recombination repair. *Proc. Natl. Acad. Sci.* **106**, 7155–7160 (2009).

62. Zhang, F., Fan, Q., Ren, K. & Andreassen, P. R. PALB2 functionally connects the breast cancer susceptibility proteins BRCA1 and BRCA2. *Mol. Cancer Res.* **7**, 1110–8 (2009).

63. Zhang, F. *et al.* PALB2 Links BRCA1 and BRCA2 in the DNA-Damage Response. *Curr. Biol.* **19**, 524–529 (2009).

64. Ghimenti, C. *et al.* Germline mutations of the BRCA1-associated ring domain (BARD1) gene in breast and breast/ovarian families negative for BRCA1 and BRCA2 alterations. *Genes. Chromosomes Cancer* **33**, 235–42 (2002).

65. Thai, T. H. *et al.* Mutations in the BRCA1-associated RING domain (BARD1) gene in primary breast, ovarian and uterine cancers. *Hum. Mol. Genet.* **7**, 195–202 (1998).

66. Capasso, M. *et al.* Common variations in BARD1 influence susceptibility to high-risk neuroblastoma. *Nat. Genet.* **41**, 718–723 (2009).

67. Friedman, L. S. *et al.* Confirmation of BRCA1 by analysis of germline mutations linked to breast and ovarian cancer in ten families. *Nat. Genet.* **8**, 399–404 (1994).

68. Couch, F. J. & Weber, B. L. Mutations and Polymorphisms in the familial early-onset breast cancer (BRCA1) gene. *Hum. Mutat.* **8**, 8–18 (1996).

69. Shattuck-Eidens, D. *et al.* A collaborative survey of 80 mutations in the BRCA1 breast and ovarian cancer susceptibility gene. Implications for presymptomatic testing and screening. *JAMA* **273**, 535–41 (1995).

70. Koboldt, D. C. *et al.* Comprehensive molecular portraits of human breast tumours. *Nature* **490**, 61–70 (2012).

71. Parkin, D. M., Bray, F., Ferlay, J. & Pisani, P. Global Cancer Statistics, 2002. *CA. Cancer J. Clin.* **55**, 74–108 (2005).

72. Lacroix, M. Stable 'portrait' of breast tumors during progression: data from biology, pathology and genetics. *Endocr. Relat. Cancer* **11**, 497–522 (2004).

73. Simpson, P. T., Reis-Filho, J. S., Gale, T. & Lakhani, S. R. Molecular evolution of breast cancer. *J. Pathol.* **205**, 248–54 (2005).

74. Brenton, J. D. Molecular Classification and Molecular Forecasting of Breast Cancer: Ready for Clinical Application? *J. Clin. Oncol.* **23**, 7350–7360 (2005).

75. Reis-Filho, J. S., Westbury, C. & Pierga, J.-Y. The impact of expression profiling on prognostic and predictive testing in breast cancer. *J. Clin. Pathol.* **59**, 225–31 (2006).

76. Perou, C. M. Molecular Stratification of Triple-Negative Breast Cancers. *Oncologist* **15**, 39–48 (2010).

77. Sorlie, T. *et al.* Repeated observation of breast tumor subtypes in independent gene expression data sets. *Proc. Natl. Acad. Sci.* **100**, 8418–8423 (2003).

78. Rouzier, R. *et al.* Breast cancer molecular subtypes respond differently to preoperative chemotherapy. *Clin. Cancer Res.* **11**, 5678–85 (2005).

79. Visvader, J. E. & Stingl, J. Mammary stem cells and the differentiation hierarchy: current status and perspectives. *Genes Dev.* **28**, 1143–1158 (2014).

80. Lehmann, B. D. B. *et al.* Identification of human triple-negative breast cancer subtypes and preclinical models for selection of targeted therapies. *J. Clin. Invest.* **121**, 2750–2767 (2011).

81. Lips, E. H. *et al.* Triple-negative breast cancer: BRCAness and concordance of clinical features with BRCA1-mutation carriers. *Br. J. Cancer* **108**, 2172–2177 (2013).

82. Turner, N., Tutt, A. & Ashworth, A. Opinion: Hallmarks of 'BRCAness' in sporadic cancers. *Nat. Rev. Cancer* **4**, 814–819 (2004).

83. Venkitaraman, A. R. Cancer Suppression by the Chromosome Custodians, BRCA1 and BRCA2. *Science (80-.).* **343**, 1470–1475 (2014).

84. Wooster, R. *et al.* Identification of the breast cancer susceptibility gene BRCA2. *Nature* **378**, 789–792 (1995).

85. Mavaddat, N. *et al.* Cancer risks for BRCA1 and BRCA2 mutation carriers: results from prospective analysis of EMBRACE. *J. Natl. Cancer Inst.* **105**, 812–22 (2013).

86. Hellebrand, H. *et al.* Germline mutations in the PALB2 gene are population specific and occur with low frequencies in familial breast cancer. *Hum. Mutat.* **32**, E2176–E2188 (2011).

87. Bhattacharyya, A., Ear, U. S., Koller, B. H., Weichselbaum, R. R. & Bishop, D. K. The breast cancer susceptibility gene BRCA1 is required for subnuclear assembly of Rad51 and survival following treatment with the DNA cross-linking agent cisplatin. *J. Biol. Chem.* **275**, 23899–903 (2000).

88. Bryant, H. E. *et al.* Specific killing of BRCA2-deficient tumours with inhibitors of poly(ADP-ribose) polymerase. *Nature* **434**, 913–7 (2005).

89. Farmer, H. *et al.* Targeting the DNA repair defect in BRCA mutant cells as a therapeutic strategy. *Nature* **434**, 917–21 (2005).

90. Rottenberg, S. *et al.* High sensitivity of BRCA1-deficient mammary tumors to the PARP inhibitor AZD2281 alone and in combination with platinum drugs. *Proc. Natl. Acad. Sci.* **105**, 17079–17084 (2008).

91. Jackson, S. P. & Helleday, T. Drugging DNA repair. *Science (80-.).* **352**, 1178–1179 (2016).

92. Schreiber, V., Dantzer, F., Ame, J.-C. & de Murcia, G. Poly(ADP-ribose): novel functions for an old molecule. *Nat. Rev. Mol. Cell Biol.* **7**, 517–528 (2006).

93. Pascal, J. M. The comings and goings of PARP-1 in response to DNA damage. *DNA Repair (Amst).* **71**, 177–182 (2018).

94. Caldecott, K. W. DNA single-strand break repair. *Exp. Cell Res.* **329**, 2–8 (2014).

95. Frit, P., Barboule, N., Yuan, Y., Gomez, D. & Calsou, P. Alternative end-joining pathway(s): Bricolage at DNA breaks. *DNA Repair (Amst).* **17**, 81–97 (2014).

96. Ronson, G. E. *et al.* PARP1 and PARP2 stabilise replication forks at base excision repair intermediates through Fbh1-dependent Rad51 regulation. *Nat. Commun.* **9**, 746 (2018).

97. Rehman, F. L., Lord, C. J. & Ashworth, A. Synthetic lethal approaches to breast cancer therapy. *Nat. Rev. Clin. Oncol.* **7**, 718–724 (2010).

98. Helleday, T. The underlying mechanism for the PARP and BRCA synthetic lethality: Clearing up the misunderstandings. *Mol. Oncol.* **5**, 387–393 (2011).

99. Murai, J. *et al.* Trapping of PARP1 and PARP2 by Clinical PARP Inhibitors. *Cancer Res.* **72**, 5588–99 (2012).

100. Lord, C. J. & Ashworth, A. PARP inhibitors: Synthetic lethality in the clinic. *Science (80-.).* **355**, 1152–1158 (2017).

101. Dedes, K. J. *et al.* Synthetic lethality of PARP inhibition in cancers lacking BRCA1 and BRCA2 mutations. *Cell Cycle* **10**, 1192–9 (2011).

102. Ashworth, A., Lord, C. J. & Reis-Filho, J. S. Genetic Interactions in Cancer Progression and Treatment. *Cell* **145**, 30–38 (2011).

103. Plummer, E. Inhibition of poly(ADP-ribose) polymerase in cancer. *Curr. Opin. Pharmacol.* **6**, 364–368 (2006).

104. Bouwman, P. & Jonkers, J. Molecular pathways: How can BRCA-mutated tumors become resistant to PARP inhibitors? *Clin. Cancer Res.* **20**, 540–547 (2014).

105. Lord, C. J. & Ashworth, A. Mechanisms of resistance to therapies targeting BRCA-mutant cancers. *Nat. Med.* **19**, 1381–8 (2013).

106. Farmer, H. *et al.* Targeting the DNA repair defect in BRCA mutant cells as a therapeutic strategy. *Nature* **434**, 917–921 (2005).

107. Bryant, H. E. *et al.* Specific killing of BRCA2-deficient tumours with inhibitors of poly(ADP-ribose) polymerase. *Nature* **434**, 913–917 (2005).

108. Domchek, S. M. *et al.* Efficacy and safety of olaparib monotherapy in germline BRCA1/2 mutation carriers with advanced ovarian cancer and three or more lines of prior therapy. *Gynecol. Oncol.* **140**, 199–203 (2016).

109. Fong, P. C. *et al.* Inhibition of Poly(ADP-Ribose) Polymerase in Tumors from *BRCA* Mutation Carriers. *N. Engl. J. Med.* **361**, 123–134 (2009).

110. Fong, P. C. *et al.* Poly(ADP)-Ribose Polymerase Inhibition: Frequent Durable Responses in *BRCA* Carrier Ovarian Cancer Correlating With Platinum-Free Interval. *J. Clin. Oncol.* **28**, 2512–2519 (2010).

111. Faraoni, I. & Graziani, G. Role of BRCA Mutations in Cancer Treatment with Poly(ADP-ribose) Polymerase (PARP) Inhibitors. *Cancers (Basel).* **10**, 487 (2018).

112. Ledermann, J. *et al.* Olaparib maintenance therapy in patients with platinum-sensitive relapsed serous ovarian cancer: a preplanned retrospective analysis of outcomes by BRCA status in a randomised phase 2 trial. *Lancet Oncol.* **15**, 852–861 (2014).

113. Kaufman, B. *et al.* Olaparib Monotherapy in Patients With Advanced Cancer and a Germline BRCA1/2 Mutation. *J. Clin. Oncol.* **33**, 244–50 (2014).

114. Pujade-Lauraine, E. *et al.* Olaparib tablets as maintenance therapy in patients with platinum-sensitive, relapsed ovarian cancer and a BRCA1/2 mutation (SOLO2/ENGOT-Ov21): a double-blind, randomised, placebo-controlled, phase 3 trial. *Lancet. Oncol.* **18**, 1274–1284 (2017).

115. Robson, M. *et al.* Olaparib for Metastatic Breast Cancer in Patients with a Germline *BRCA* Mutation. *N. Engl. J. Med.* NEJMoa1706450 (2017). doi:10.1056/NEJMoa1706450

116. Moore, K. *et al.* Maintenance Olaparib in Patients with Newly Diagnosed Advanced Ovarian Cancer. *N. Engl. J. Med.* **379**, 2495–2505 (2018).

117. Swisher, E. M. *et al.* Rucaparib in relapsed, platinum-sensitive high-grade ovarian carcinoma (ARIEL2 Part 1): an international, multicentre, open-label, phase 2 trial. *Lancet Oncol.* **18**, 75–87 (2017).

118. Oza, A. M. *et al.* Antitumor activity and safety of the PARP inhibitor rucaparib in patients with high-grade ovarian carcinoma and a germline or somatic BRCA1 or BRCA2 mutation: Integrated analysis of data from Study 10 and ARIEL2. *Gynecol. Oncol.* **147**, 267–275 (2017).

119. Coleman, R. L. *et al.* Rucaparib maintenance treatment for recurrent ovarian carcinoma after response to platinum therapy (ARIEL3): a randomised, double-blind, placebo-controlled, phase 3 trial. *Lancet* **390**, 1949–1961 (2017).

120. Mirza, M. R. *et al.* Niraparib Maintenance Therapy in Platinum-Sensitive, Recurrent Ovarian Cancer. *N. Engl. J. Med.* **375**, 2154–2164 (2016).

121. Litton, J. K. *et al.* Talazoparib in Patients with Advanced Breast Cancer and a Germline *BRCA* Mutation. *N. Engl. J. Med.* **379**, 753–763 (2018).

122. Litton, J. K. *et al.* A feasibility study of neoadjuvant talazoparib for operable breast cancer patients with a germline BRCA mutation demonstrates marked activity. *npj Breast Cancer* **3**, 49 (2017).

123. Loibl, S. *et al.* Survival analysis of carboplatin added to an anthracycline/taxane-based neoadjuvant chemotherapy and HRD score as predictor of response—final results from GeparSixto. *Ann. Oncol.* **29**, 2341–2347 (2018).

124. Rugo, H. S. *et al.* Adaptive Randomization of Veliparib–Carboplatin Treatment in Breast Cancer. *N. Engl. J. Med.* **375**, 23–34 (2016).

125. Tutt, A. *et al.* 216TiPOlympiA: A randomized phase III trial of olaparib as adjuvant therapy in patients with high-risk HER2-negative breast cancer (BC) and a germline BRCA1/2 mutation (gBRCAm). *Ann. Oncol.* **28**, (2017).

126. Mateo, J. *et al.* DNA-Repair Defects and Olaparib in Metastatic Prostate Cancer. *N. Engl. J. Med.* **373**, 1697–1708 (2015).

127. Abida W, Bryce AH, Vogelzang NJ, et al. Preliminary results from TRITON2: a phase 2 study of rucaparib in patients with metastatic castration-resistant prostate cancer (mCRPC) associated with homologous recombination repair (HRR) gene alterations. *Present. Eur. Soc. Med. Oncol. (ESMO), Munich, Ger. 19–23 October, 2018*

128. Pilié, P. G., Tang, C., Mills, G. B. & Yap, T. A. State-of-the-art strategies for targeting the DNA damage response in cancer. *Nat. Rev. Clin. Oncol.* (2018). doi:10.1038/s41571-018-0114-z

129. Audeh, M. W. *et al.* Oral poly(ADP-ribose) polymerase inhibitor olaparib in patients with BRCA1 or BRCA2 mutations and recurrent ovarian cancer: a proof-of-concept trial. *Lancet (London, England)* **376**, 245–51 (2010).

130. Tutt, A. *et al.* Oral poly(ADP-ribose) polymerase inhibitor olaparib in patients with BRCA1 or BRCA2 mutations and advanced breast cancer: a proof-of-concept trial. *Lancet* **376**, 235–244 (2010).

131. Johnson, N. *et al.* Stabilization of mutant BRCA1 protein confers PARP inhibitor and platinum resistance. *Proc. Natl. Acad. Sci. U. S. A.* **110**, 17041–6 (2013).

132. Barber, L. J. *et al.* Secondary mutations in BRCA2 associated with clinical resistance to a PARP inhibitor. *J. Pathol.* **229**, 422–429 (2013).

133. Boersma, V. *et al.* MAD2L2 controls DNA repair at telomeres and DNA breaks by inhibiting 5' end resection. *Nature* **521**, 537–40 (2015).

134. Edwards, S. L. *et al.* Resistance to therapy caused by intragenic deletion in BRCA2. *Nature* **451**, 1111–5 (2008).

135. Jaspers, J. E. *et al.* Loss of 53BP1 Causes PARP Inhibitor Resistance in Brca1-Mutated Mouse Mammary Tumors. *Cancer Discov.* **3**, 68–81 (2012).

136. Norquist, B. *et al.* Secondary Somatic Mutations Restoring *BRCA1/2* Predict Chemotherapy Resistance in Hereditary Ovarian Carcinomas. *J. Clin. Oncol.* **29**, 3008–3015 (2011).

137. Sakai, W. *et al.* Functional Restoration of BRCA2 Protein by Secondary BRCA2 Mutations in BRCA2-Mutated Ovarian Carcinoma. *Cancer Res.* **69**, 6381–6386 (2009).

138. Xu, G. *et al.* REV7 counteracts DNA double-strand break resection and affects PARP inhibition. *Nature* **521**, 541–544 (2015).

139. D'Andrea, A. D. Mechanisms of PARP inhibitor sensitivity and resistance. *DNA Repair (Amst).* **71**, 172–176 (2018).

140. Sakai, W. *et al.* Secondary mutations as a mechanism of cisplatin resistance in BRCA2-mutated cancers. *Nature* **451**, 1116–20 (2008).

141. Kondrashova, O. *et al.* Secondary Somatic Mutations Restoring *RAD51C* and *RAD51D* Associated with Acquired Resistance to the PARP Inhibitor Rucaparib in High-Grade Ovarian Carcinoma. *Cancer Discov.* **7**, 984–998 (2017).

142. Bouwman, P. *et al.* A High-Throughput Functional Complementation Assay for Classification of BRCA1 Missense Variants. *Cancer Discov.* **3**, 1142–1155 (2013).

143. Drost, R. *et al.* BRCA1185delAG tumors may acquire therapy resistance through expression of RING-less BRCA1. *J. Clin. Invest.* **126**, 2903–2918 (2016).

144. Konstantinopoulos, P. A., Ceccaldi, R., Shapiro, G. I. & D'Andrea, A. D. Homologous Recombination Deficiency: Exploiting the Fundamental Vulnerability of Ovarian Cancer. *Cancer Discov.* **5**, 1137–1154 (2015).

145. Wang, Y. *et al.* The BRCA1- 11q Alternative Splice Isoform Bypasses Germline Mutations and Promotes Therapeutic Resistance to PARP Inhibition and Cisplatin. *Cancer Res.* **76**, 2778–2790 (2016).

146. Tammaro, C., Raponi, M., Wilson, D. I. & Baralle, D. BRCA1 exon 11 alternative splicing, multiple functions and the association with cancer. *Biochem. Soc. Trans.* **40**, 768–72 (2012).

147. Patch, A.-M. *et al.* Whole–genome characterization of chemoresistant ovarian cancer. *Nature* **521**, 489–494 (2015).

148. Bouwman, P. *et al.* 53BP1 loss rescues BRCA1 deficiency and is associated with triple-negative and BRCA-mutated breast cancers. *Nat. Struct. Mol. Biol.* **17**, 688–695 (2010).

149. Bunting, S. F. *et al.* 53BP1 Inhibits Homologous Recombination in Brca1-Deficient Cells by Blocking Resection of DNA Breaks. *Cell* **141**, 243–254 (2010).

150. Xu, G. *et al.* REV7 counteracts DNA double-strand break resection and affects PARP inhibition. *Nature* **521**, 541–544 (2015).

151. Feng, L., Fong, K.-W., Wang, J., Wang, W. & Chen, J. RIF1 Counteracts BRCA1-mediated End Resection during DNA Repair. *J. Biol. Chem.* **288**, 11135–11143 (2013).

152. Callen, E. *et al.* 53BP1 Mediates Productive and Mutagenic DNA Repair through Distinct Phosphoprotein Interactions. *Cell* **153**, 1266–1280 (2013).

153. Wang, J. *et al.* PTIP associates with Artemis to dictate DNA repair pathway choice. *Genes Dev.* **28**, 2693–2698 (2014).

154. Gupta, R. *et al.* DNA Repair Network Analysis Reveals Shieldin as a Key Regulator of NHEJ and PARP Inhibitor Sensitivity. *Cell* **173**, 972-988.e23 (2018).

155. Ghezraoui, H. *et al.* 53BP1 cooperation with the REV7–shieldin complex underpins DNA structure-specific NHEJ. *Nature* **560**, 122–127 (2018).

156. Noordermeer, S. M. *et al.* The shieldin complex mediates 53BP1-dependent DNA repair. *Nature* **560**, 117–121 (2018).

157. Dev, H. *et al.* Shieldin complex promotes DNA end-joining and counters homologous recombination in BRCA1-null cells. *Nat. Cell Biol.* **20**, 954–965 (2018).

158. Barazas, M. *et al.* The CST Complex Mediates End Protection at Double-Strand Breaks and Promotes PARP Inhibitor Sensitivity in BRCA1-Deficient Cells. *Cell Rep.* **23**, 2107–2118 (2018).

159. Chapman, J. R. *et al.* RIF1 Is Essential for 53BP1-Dependent Nonhomologous End Joining and Suppression of DNA Double-Strand Break Resection. *Mol. Cell* **49**, 858–871 (2013).

160. Chaudhuri, R. A. *et al.* Replication fork stability confers chemoresistance in BRCA-deficient cells. *Nature* **535**, 382–387 (2016).

161. Errico, A. & Costanzo, V. Mechanisms of replication fork protection: a safeguard for genome stability. *Crit. Rev. Biochem. Mol. Biol.* **47**, 222–235 (2012).

162. Bhat, K. P. & Cortez, D. RPA and RAD51: fork reversal, fork protection, and genome stability. *Nat. Struct. Mol. Biol.* **25**, 446–453 (2018).

163. Quinet, A., Lemaçon, D. & Vindigni, A. Replication Fork Reversal: Players and Guardians. *Mol. Cell* **68**, 830–833 (2017).

164. Meghani, K. *et al.* Multifaceted Impact of MicroRNA 493-5p on Genome-Stabilizing Pathways Induces Platinum and PARP Inhibitor Resistance in BRCA2-Mutated Carcinomas. *Cell Rep.* **23**, 100–111 (2018).

165. Schlacher, K. *et al.* Double-Strand Break Repair-Independent Role for BRCA2 in Blocking Stalled Replication Fork Degradation by MRE11. *Cell* **145**, 529–542 (2011).

166. Schlacher, K., Wu, H. & Jasin, M. A Distinct Replication Fork Protection Pathway Connects Fanconi

Anemia Tumor Suppressors to RAD51-BRCA1/2. *Cancer Cell* **22**, 106–116 (2012).

167. Lomonosov, M., Anand, S., Sangrithi, M., Davies, R. & Venkitaraman, A. R. Stabilization of stalled DNA replication forks by the BRCA2 breast cancer susceptibility protein. *Genes Dev.* **17**, 3017–3022 (2003).

168. Lemaçon, D. *et al.* MRE11 and EXO1 nucleases degrade reversed forks and elicit MUS81-dependent fork rescue in BRCA2-deficient cells. *Nat. Commun.* **8**, 860 (2017).

169. Mijic, S. *et al.* Replication fork reversal triggers fork degradation in BRCA2-defective cells. *Nat. Commun.* **8**, 859 (2017).

170. Berti, M. *et al.* Human RECQ1 promotes restart of replication forks reversed by DNA topoisomerase I inhibition. *Nat. Struct. Mol. Biol.* **20**, 347–354 (2013).

171. Amé, J. C. *et al.* PARP-2, A novel mammalian DNA damage-dependent poly(ADP-ribose) polymerase. *J. Biol. Chem.* **274**, 17860–8 (1999).

172. Rondinelli, B. *et al.* EZH2 promotes degradation of stalled replication forks by recruiting MUS81 through histone H3 trimethylation. *Nat. Cell Biol.* **19**, 1371–1378 (2017).

173. Haynes, B., Murai, J. & Lee, J. M. Restored replication fork stabilization, a mechanism of PARP inhibitor resistance, can be overcome by cell cycle checkpoint inhibition. *Cancer Treat. Rev.* **71**, 1–7 (2018).

174. Yazinski, S. A. *et al.* ATR inhibition disrupts rewired homologous recombination and fork protection pathways in PARP inhibitor-resistant BRCA-deficient cancer cells. *Genes Dev.* **31**, 318–332 (2017).

175. Ray Chaudhuri, A. *et al.* Replication fork stability confers chemoresistance in BRCA-deficient cells. *Nature* **535**, 382–387 (2016).

176. Choi, Y. H. & Yu, A.-M. ABC transporters in multidrug resistance and pharmacokinetics, and strategies for drug development. *Curr. Pharm. Des.* **20**, 793–807 (2014).

177. Pettitt, S. J. *et al.* A Genetic Screen Using the PiggyBac Transposon in Haploid Cells Identifies Parp1 as a Mediator of Olaparib Toxicity. *PLoS One* **8**, e61520 (2013).

178. Liu, X. *et al.* Acquired Resistance to Combination Treatment with Temozolomide and ABT-888 Is Mediated by Both Base Excision Repair and Homologous Recombination DNA Repair Pathways. *Mol. Cancer Res.* **7**, 1686–1692 (2009).

179. Lok, B. H. *et al.* PARP Inhibitor Activity Correlates with *SLFN11* Expression and Demonstrates Synergy with Temozolomide in Small Cell Lung Cancer. *Clin. Cancer Res.* **23**, 523–535 (2017).

180. Pietanza, M. C. *et al.* Randomized, Double-Blind, Phase II Study of Temozolomide in Combination With Either Veliparib or Placebo in Patients With Relapsed-Sensitive or Refractory Small-Cell Lung Cancer. *J. Clin. Oncol.* **36**, 2386–2394 (2018).

181. Byers, L. A. *et al.* Proteomic Profiling Identifies Dysregulated Pathways in Small Cell Lung Cancer and Novel Therapeutic Targets Including PARP1. *Cancer Discov.* **2**, 798–811 (2012).

182. Mu, Y. *et al.* SLFN11 inhibits checkpoint maintenance and homologous recombination repair. *EMBO Rep.* **17**, 94–109 (2016).

183. Murai, J. *et al.* Resistance to PARP inhibitors by SLFN11 inactivation can be overcome by ATR inhibition. *Oncotarget* **7**, 76534–76550 (2016).

184. Cerrato, A., Morra, F. & Celetti, A. Use of poly ADP-ribose polymerase [PARP] inhibitors in cancer cells bearing DDR defects: the rationale for their inclusion in the clinic. *J. Exp. Clin. Cancer Res.* **35**, 179 (2016).

185. Sonnenblick, A., de Azambuja, E., Azim, H. A. & Piccart, M. An update on PARP inhibitors—moving to the adjuvant setting. *Nat. Publ. Gr.* **12**, 27–41 (2014).

186. Metzger-Filho, O. *et al.* Dissecting the Heterogeneity of Triple-Negative Breast Cancer. *J. Clin. Oncol.* **30**, 1879–1887 (2012).

187. Wang, Z. C. *et al.* Loss of heterozygosity and its correlation with expression profiles in subclasses of invasive breast cancers. *Cancer Res.* **64**, 64–71 (2004).

188. Turner, N. C. *et al.* BRCA1 dysfunction in sporadic basal-like breast cancer. *Oncogene* **26**, 2126–2132 (2007).

189. Joosse, S. A. *et al.* Genomic signature of BRCA1 deficiency in sporadic basal-like breast tumors. *Genes. Chromosomes Cancer* **50**, 71–81 (2011).

190. Silver, D. P. *et al.* Efficacy of Neoadjuvant Cisplatin in Triple-Negative Breast Cancer. *J. Clin. Oncol.* **28**, 1145–1153 (2010).

191. Lord, C. J. & Ashworth, A. BRCAness revisited. *Nat. Rev. Cancer* **16**, 110–120 (2016).

192. McCabe, N. *et al.* Deficiency in the repair of DNA damage by homologous recombination and sensitivity to poly(ADP-ribose) polymerase inhibition. *Cancer Res.* **66**, 8109–8115 (2006).

193. O'Sullivan, C. C., Moon, D. H., Kohn, E. C. & Lee, J.-M. Beyond Breast and Ovarian Cancers: PARP Inhibitors for BRCA Mutation-Associated and BRCA-Like Solid Tumors. *Front. Oncol.* **4**, 42 (2014).

194. Lee, J. -m., Ledermann, J. A. & Kohn, E. C. PARP Inhibitors for BRCA1/2 mutation-associated and BRCA-like malignancies. *Ann. Oncol.* **25**, 32–40 (2014).

195. Blazek, D. *et al.* The Cyclin K/Cdk12 complex maintains genomic stability via regulation of expression of DNA damage response genes. *Genes Dev.* **25**, 2158–2172 (2011).

196. Joshi, P. M., Sutor, S. L., Huntoon, C. J. & Karnitz, L. M. Ovarian Cancer-associated Mutations Disable Catalytic Activity of CDK12, a Kinase That Promotes Homologous Recombination Repair and Resistance to Cisplatin and Poly(ADP-ribose) Polymerase Inhibitors. *J. Biol. Chem.* **289**, 9247–9253 (2014).

197. Bajrami, I. *et al.* Genome-wide profiling of genetic synthetic lethality identifies CDK12 as a novel determinant of PARP1/2 inhibitor sensitivity. *Cancer Res.* **74**, 287–97 (2014).

198. Cheng, H. *et al.* PARP inhibition selectively increases sensitivity to cisplatin in ERCC1-low non-small cell lung cancer cells. *Carcinogenesis* **34**, 739–749 (2013).

199. Postel-Vinay, S. *et al.* A high-throughput screen identifies PARP1/2 inhibitors as a potential therapy for ERCC1-deficient non-small cell lung cancer. *Oncogene* **32**, 5377–5387 (2013).

200. Hoppe, M. M., Sundar, R., Tan, D. S. P. & Jeyasekharan, A. D. Biomarkers for Homologous Recombination Deficiency in Cancer. *JNCI J. Natl. Cancer Inst.* **110**, 704–713 (2018).

201. Heeke, A. L., Baker, T., Lynce, F., Pishvaian, M. J. & Isaacs, C. Prevalence of homologous recombination deficiency among all tumor types. *J. Clin. Oncol.* **35**, 1502–1502 (2017).

202. Bell, D. *et al.* Integrated genomic analyses of ovarian carcinoma. *Nature* **474**, 609–615 (2011).

203. Akashi-Tanaka, S. *et al.* BRCAness Predicts Resistance to Taxane-Containing Regimens in Triple Negative Breast Cancer During Neoadjuvant Chemotherapy. *Clin. Breast Cancer* **15**, 80–85 (2015).

204. van 't Veer, L. J. *et al.* Gene expression profiling predicts clinical outcome of breast cancer. *Nature* **415**, 530–536 (2002).

205. Vollebergh, M. A. *et al.* Genomic patterns resembling BRCA1- and BRCA2-mutated breast cancers predict benefit of intensified carboplatin-based chemotherapy. *Breast Cancer Res.* **16**, R47 (2014).

206. Robinson, D. *et al.* Integrative Clinical Genomics of Advanced Prostate Cancer. *Cell* **161**, 1215–1228 (2015).

207. Swisher, E. M. *et al.* BRCA1 and RAD51C promoter hypermethylation confer sensitivity to the PARP inhibitor rucaparib in patients with relapsed, platinum-sensitive ovarian carcinoma in ARIEL2 Part 1. *Gynecol. Oncol.* **145**, 5 (2017).

208. Ganguly, B., Dolfi, S. C., Rodriguez-Rodriguez, L., Ganesan, S. & Hirshfield, K. M. Role of Biomarkers in the Development of PARP Inhibitors. *Biomark. Cancer* **8**, 15–25 (2016).

209. Stover, E. H., Konstantinopoulos, P. A., Matulonis, U. A. & Swisher, E. M. Biomarkers of response and resistance to DNA repair targeted therapies. *Clin. Cancer Res.* **22**, 5651–5660 (2016).

210. Mirza, M. R. *et al.* Niraparib Maintenance Therapy in Platinum-Sensitive, Recurrent Ovarian Cancer. *N. Engl. J. Med.* **375**, 2154–2164 (2016).

211. Gelmon, K. A. *et al.* Olaparib in patients with recurrent high-grade serous or poorly differentiated ovarian carcinoma or triple-negative breast cancer: a phase 2, multicentre, open-label, non-randomised study. *Lancet Oncol.* **12**, 852–861 (2011).

212. Ceccaldi, R. *et al.* A Unique Subset of Epithelial Ovarian Cancers with Platinum Sensitivity and PARP Inhibitor Resistance. *Cancer Res.* **75**, 628–634 (2015).

213. Fong, P. C. *et al.* Inhibition of poly(ADP-ribose) polymerase in tumors from BRCA mutation carriers. *N. Engl. J. Med.* **361**, 123–34 (2009).

214. Sakai, W. *et al.* Secondary mutations as a mechanism of cisplatin resistance in BRCA2-mutated cancers. *Nature* **451**, 1116–1120 (2008).

215. Pennington, K. P. *et al.* Germline and Somatic Mutations in Homologous Recombination Genes Predict Platinum Response and Survival in Ovarian, Fallopian Tube, and Peritoneal Carcinomas. *Clin. Cancer Res.* **20**, 764–775 (2014).

216. McEllin, B. *et al.* PTEN Loss Compromises Homologous Recombination Repair in Astrocytes: Implications for Glioblastoma Therapy with Temozolomide or Poly(ADP-Ribose) Polymerase Inhibitors. *Cancer Res.* **70**, 5457–5464 (2010).

217. Dedes, K. J. *et al.* PTEN Deficiency in Endometrioid Endometrial Adenocarcinomas Predicts Sensitivity to PARP Inhibitors. *Sci. Transl. Med.* **2**, 53ra75-53ra75 (2010).

218. Fraser, M. *et al.* PTEN Deletion in Prostate Cancer Cells Does Not Associate with Loss of RAD51 Function: Implications for Radiotherapy and Chemotherapy. *Clin. Cancer Res.* **18**, 1015–1027 (2012).

219. O'Kane, G. M., Connor, A. A. & Gallinger, S. Characterization, Detection, and Treatment Approaches for Homologous Recombination Deficiency in Cancer. *Trends Mol. Med.* **23**, 1121–1137 (2017).

220. Alexandrov, L. B. & Stratton, M. R. Mutational signatures: the patterns of somatic mutations hidden in cancer genomes. *Curr. Opin. Genet. Dev.* **24**, 52–60 (2014).

221. Helleday, T., Eshtad, S. & Nik-Zainal, S. Mechanisms underlying mutational signatures in human cancers. *Nat. Rev. Genet.* **15**, 585–598 (2014).

222. Watkins, J. a, Irshad, S., Grigoriadis, A. & Tutt, A. N. Genomic scars as biomarkers of homologous recombination deficiency and drug response in breast and ovarian cancers. *Breast cancer Res.* **16**, 211 (2014).

223. Abkevich, V. *et al.* Patterns of genomic loss of heterozygosity predict homologous recombination repair defects in epithelial ovarian cancer. *Br. J. Cancer* **107**, 1776–1782 (2012).

224. Timms, K. M. *et al.* Association of BRCA1/2defects with genomic scores predictive of DNA damage repair deficiency among breast cancer subtypes. *Breast Cancer Res.* **16**, 475 (2014).

225. González Martín, A. Progress in PARP inhibitors beyond BRCA mutant recurrent ovarian cancer? *Lancet. Oncol.* **18**, 8–9 (2017).

226. Watkins, J. a, Irshad, S., Grigoriadis, A. & Tutt, A. N. J. Genomic scars as biomarkers of homologous recombination deficiency and drug response in breast and ovarian cancers. *Breast Cancer Res.* **16**, 211 (2014).

227. Telli, M. L. *et al.* Homologous Recombination Deficiency (HRD) Score Predicts Response to Platinum-Containing Neoadjuvant Chemotherapy in Patients with Triple-Negative Breast Cancer. *Clin. Cancer Res.* **22**, 3764–3773 (2016).

228. Isakoff, S. J. *et al.* TBCRC009: A Multicenter Phase II Clinical Trial of Platinum Monotherapy With Biomarker Assessment in Metastatic Triple-Negative Breast Cancer. *J. Clin. Oncol.* **33**, 1902–1909 (2015).

229. Tutt, A. *et al.* Carboplatin in BRCA1/2-mutated and triple-negative breast cancer BRCAness subgroups: the TNT Trial. *Nat. Med.* (2018). doi:10.1038/s41591-018-0009-7

230. Alexandrov, L. B. *et al.* Signatures of mutational processes in human cancer. *Nature* **500**, 415–421 (2013).

231. Davies, H. *et al.* HRDetect is a predictor of BRCA1 and BRCA2 deficiency based on mutational signatures. *Nat. Med.* **23**, 517–525 (2017).

232. Konstantinopoulos, P. A. *et al.* Gene expression profile of BRCAness that correlates with responsiveness to chemotherapy and with outcome in patients with epithelial ovarian cancer. *J. Clin. Oncol.* **28**, 3555–61 (2010).

233. Kang, J., D'Andrea, A. D. & Kozono, D. A DNA repair pathway-focused score for prediction of outcomes in ovarian cancer treated with platinum-based chemotherapy. *J. Natl. Cancer Inst.* **104**, 670–81 (2012).

234. Pitroda, S. P. *et al.* DNA Repair Pathway Gene Expression Score Correlates with Repair Proficiency and Tumor Sensitivity to Chemotherapy. *Sci. Transl. Med.* **6**, 229ra42-229ra42 (2014).

235. Moskwa, P. *et al.* miR-182-Mediated Downregulation of BRCA1 Impacts DNA Repair and Sensitivity to PARP Inhibitors. *Mol. Cell* **41**, 210–220 (2011).

236. Bekker-Jensen, S. *et al.* Spatial organization of the mammalian genome surveillance machinery in response to DNA strand breaks. *J. Cell Biol.* **173**, 195–206 (2006).

237. Polo, S. E. & Jackson, S. P. Dynamics of DNA damage response proteins at DNA breaks: a focus on protein modifications. *Genes Dev.* **25**, 409–433 (2011).

238. Graeser, M. *et al.* A marker of homologous recombination predicts pathologic complete response to neoadjuvant chemotherapy in primary breast cancer. *Clin. Cancer Res.* **16**, 6159–6168 (2010).

239. Mukhopadhyay, A. *et al.* Development of a Functional Assay for Homologous Recombination Status in Primary Cultures of Epithelial Ovarian Tumor and Correlation with Sensitivity to Poly(ADP-Ribose) Polymerase Inhibitors. *Clin. Cancer Res.* **16**, 2344–2351 (2010).

240. Naipal, K. A. T. *et al.* Functional Ex Vivo Assay to Select Homologous Recombination-Deficient Breast Tumors for PARP Inhibitor Treatment. *Clin. Cancer Res.* **20**, 4816–4826 (2014).

241. Redon, C. E. *et al.* Histone H2AX and Poly(ADP-Ribose) as Clinical Pharmacodynamic Biomarkers. *Clin. Cancer Res.* **16**, 4532–4542 (2010).

242. Willers, H. *et al.* DNA Damage Response Assessments in Human Tumor Samples Provide Functional Biomarkers of Radiosensitivity. *Semin. Radiat. Oncol.* **25**, 237–250 (2015).

243. LoRusso, P. M. *et al.* Phase I Safety, Pharmacokinetic, and Pharmacodynamic Study of the Poly(ADP-ribose) Polymerase (PARP) Inhibitor Veliparib (ABT-888) in Combination with Irinotecan in Patients with Advanced Solid Tumors. *Clin. Cancer Res.* **22**, 3227–3237 (2016).

244. Ji, J. *et al.* Modeling Pharmacodynamic Response to the Poly(ADP-Ribose) Polymerase Inhibitor ABT-888 in Human Peripheral Blood Mononuclear Cells. *PLoS One* **6**, e26152 (2011).

245. Gottipati, P. *et al.* Poly(ADP-Ribose) Polymerase Is Hyperactivated in Homologous Recombination–Defective Cells. *Cancer Res.* **70**, 5389–5398 (2010).

246. Michels, J. *et al.* Cisplatin Resistance Associated with PARP Hyperactivation. *Cancer Res.* **73**, 2271–2280 (2013).

247. Zaremba, T. *et al.* Poly(ADP-ribose) polymerase-1 (PARP-1) pharmacogenetics, activity and expression analysis in cancer patients and healthy volunteers. *Biochem. J.* **436**, 671–679 (2011).

248. Schoppy, D. W. *et al.* Oncogenic stress sensitizes murine cancers to hypomorphic suppression of ATR. *J. Clin. Invest.* **122**, 241–252 (2012).

249. Flynn, R. L. *et al.* Alternative lengthening of telomeres renders cancer cells hypersensitive to ATR inhibitors. *Science (80-.).* **347**, 273–277 (2015).

250. Talens, F., Jalving, M., Gietema, J. A. & Van Vugt, M. A. Therapeutic targeting and patient selection for cancers with homologous recombination defects. *Expert Opin. Drug Discov.* **12**, 565–581 (2017).

251. Murai, J. *et al.* Stereospecific PARP Trapping by BMN 673 and Comparison with Olaparib and Rucaparib. *Mol. Cancer Ther.* **13**, 433–443 (2014).

252. Isakoff, S. J. *et al.* A randomized Phase II study of veliparib with temozolomide or carboplatin/paclitaxel versus placebo with carboplatin/paclitaxel in *BRCA1* / *2* metastatic breast cancer: design and rationale. *Futur. Oncol.* **13**, 307–320 (2017).

253. Ibrahim, Y. H. *et al.* PI3K Inhibition Impairs BRCA1/2 Expression and Sensitizes BRCA-Proficient Triple-Negative Breast Cancer to PARP Inhibition. *Cancer Discov.* **2**, 1036–1047 (2012).

254. Lecona, E. & Fernandez-Capetillo, O. Targeting ATR in cancer. *Nat. Rev. Cancer* **18**, 586–595 (2018).

255. Yekezare, M., Gomez-Gonzalez, B. & Diffley, J. F. X. Controlling DNA replication origins in response to DNA damage - inhibit globally, activate locally. *J. Cell Sci.* **126**, 1297–1306 (2013).

256. Méchali, M. Eukaryotic DNA replication origins: many choices for appropriate answers. *Nat. Rev. Mol. Cell Biol.* **11**, 728–738 (2010).

257. Weber, A. M. & Ryan, A. J. ATM and ATR as therapeutic targets in cancer. *Pharmacol. Ther.* **149**, 124–138 (2015).

258. Bryant, H. E. & Helleday, T. Inhibition of poly (ADP-ribose) polymerase activates ATM which is required for subsequent homologous recombination repair. *Nucleic Acids Res.* **34**, 1685–1691 (2006).

259. Zhao, Y. *et al.* Preclinical Evaluation of a Potent Novel DNA-Dependent Protein Kinase Inhibitor NU7441. *Cancer Res.* **66**, 5354–5362 (2006).

260. Tsuji, T. *et al.* CC-115, a dual inhibitor of mTOR Kinase and DNA-PK, blocks DNA damage repair pathways and selectively inhibits ATM-deficient cell growth <i>in vitro</i> *Oncotarget* **8**, 74688–74702 (2017).

261. Aarts, M. *et al.* Forced Mitotic Entry of S-Phase Cells as a Therapeutic Strategy Induced by Inhibition of WEE1. *Cancer Discov.* **2**, 524–539 (2012).

262. Buisson, R., Boisvert, J. L., Benes, C. H. & Zou, L. Distinct but Concerted Roles of ATR, DNA-PK, and Chk1 in Countering Replication Stress during S Phase. *Mol. Cell* **59**, 1011–1024 (2015).

263. Pfister, S. X. *et al.* Inhibiting WEE1 Selectively Kills Histone H3K36me3-Deficient Cancers by dNTP Starvation. *Cancer Cell* **28**, 557–568 (2015).

264. Dobbelstein, M. & Sørensen, C. S. Exploiting replicative stress to treat cancer. *Nat. Rev. Drug Discov.* **14**, 405–423 (2015).

265. Richer, A. L. *et al.* WEE1 Kinase Inhibitor AZD1775 Has Preclinical Efficacy in LKB1-Deficient Non–Small Cell Lung Cancer. *Cancer Res.* **77**, 4663–4672 (2017).

266. Guertin, A. D. *et al.* Preclinical Evaluation of the WEE1 Inhibitor MK-1775 as Single-Agent Anticancer Therapy. *Mol. Cancer Ther.* **12**, 1442–1452 (2013).

267. Mizuarai, S. *et al.* Discovery of gene expression-based pharmacodynamic biomarker for a p53 context-specific anti-tumor drug Wee1 inhibitor. *Mol. Cancer* **8**, 34 (2009).

268. Duma, N., Gast, K. C., Choong, G. M., Leon-Ferre, R. A. & O'Sullivan, C. C. Where Do We Stand on the Integration of PARP Inhibitors for the Treatment of Breast Cancer? *Curr. Oncol. Rep.* **20**, (2018).

269. Bruna, A. *et al.* A Biobank of Breast Cancer Explants with Preserved Intra-tumor Heterogeneity to Screen Anticancer Compounds. *Cell* **167**, 260-274.e22 (2016).

270. Gao, H. *et al.* High-throughput screening using patient-derived tumor xenografts to predict clinical trial drug response. *Nat. Med.* **21**, 1318–1325 (2015).

271. Therasse, P. *et al.* New guidelines to evaluate the response to treatment in solid tumors. European Organization for Research and Treatment of Cancer, National Cancer Institute of the United States, National Cancer Institute of Canada. *J. Natl. Cancer Inst.* **92**, 205–16 (2000).

272. Vandesompele, J. *et al.* Accurate normalization of real-time quantitative RT-PCR data by geometric averaging of multiple internal control genes. *Genome Biol.* **3**, RESEARCH0034 (2002).

273. Ahdesmäki, M. J., Gray, S. R., Johnson, J. H. & Lai, Z. Disambiguate: An open-source application for disambiguating two species in next generation sequencing data from grafted samples. *F1000Research* **5**, 2741 (2016).

274. Lai, Z. *et al.* VarDict: a novel and versatile variant caller for next-generation sequencing in cancer research. *Nucleic Acids Res.* **44**, e108–e108 (2016).

275. Reznik, E. *et al.* Mitochondrial DNA copy number variation across human cancers. *Elife* **5**, (2016).

276. ter Brugge, P. *et al.* Mechanisms of Therapy Resistance in Patient-Derived Xenograft Models of BRCA1-Deficient Breast Cancer. *J. Natl. Cancer Inst.* **108**, djw148 (2016).

277. Ballabeni, A., Zamponi, R., Moore, J. K., Helin, K. & Kirschner, M. W. Geminin deploys multiple mechanisms to regulate Cdt1 before cell division thus ensuring the proper execution of DNA replication. *Proc. Natl. Acad. Sci.* **110**, E2848–E2853 (2013).

278. Deng, W. *et al.* Role and therapeutic potential of PI3K-mTOR signaling in de novo resistance to BRAF inhibition. *Pigment Cell Melanoma Res.* **25**, 248–258 (2012).

279. Gopal, Y. N. V. *et al.* Basal and Treatment-Induced Activation of AKT Mediates Resistance to Cell Death by AZD6244 (ARRY-142886) in Braf-Mutant Human Cutaneous Melanoma Cells. *Cancer Res.* **70**, 8736–8747 (2010).

280. Marangoni, E. *et al.* A New Model of Patient Tumor-Derived Breast Cancer Xenografts for Preclinical Assays. *Clin. Cancer Res.* **13**, 3989–3998 (2007).

281. Charafe-Jauffret, E. *et al.* ALDH1-Positive Cancer Stem Cells Predict Engraftment of Primary Breast Tumors and Are Governed by a Common Stem Cell Program. *Cancer Res.* **73**, 7290–7300 (2013).

282. Pinder, J., Salsman, J. & Dellaire, G. Nuclear domain 'knock-in' screen for the evaluation and identification of small molecule enhancers of CRISPR-based genome editing. *Nucleic Acids Res.* **43**, 9379–9392 (2015).

283. Pauty, J. *et al.* Cancer-causing mutations in the tumor suppressor PALB2 reveal a novel cancer mechanism using a hidden nuclear export signal in the WD40 repeat motif. *Nucleic Acids Res.* **45**, 2644–2657 (2017).

284. Couturier, A. M. *et al.* Roles for APRIN (PDS5B) in homologous recombination and in ovarian cancer prediction. *Nucleic Acids Res.* **44**, 10879–10897 (2016).

285. Cruz, C. *et al.* RAD51 foci as a functional biomarker of homologous recombination repair and PARP inhibitor resistance in germline BRCA-mutated breast cancer. *Ann. Oncol.* **29**, 1203–1210 (2018).

286. Petermann, E., Orta, M. L., Issaeva, N., Schultz, N. & Helleday, T. Hydroxyurea-Stalled Replication Forks Become Progressively Inactivated and Require Two Different RAD51-Mediated Pathways for Restart and Repair. *Mol. Cell* **37**, 492–502 (2010).

287. Raderschall, E., Golub, E. I. & Haaf, T. Nuclear foci of mammalian recombination proteins are located at single-stranded DNA regions formed after DNA damage. *Proc. Natl. Acad. Sci. U. S. A.* **96**, 1921–6 (1999).

288. McGarry, T. J. & Kirschner, M. W. Geminin, an inhibitor of DNA replication, is degraded during mitosis. *Cell* **93**, 1043–53 (1998).

289. Castroviejo-Bermejo, M. *et al.* A RAD51 assay feasible in routine tumor samples calls PARP inhibitor response beyond BRCA mutation. *EMBO Mol. Med.* **10**, e9172 (2018).

290. Shakeri, H., Fakhrjou, A., Nikanfar, A. & Mohaddes-Ardebili, S. M. Methylation Analysis of BRCA1 and APC in Breast Cancer and It's Relationship to Clinicopathological Features. *Clin. Lab.* **62**, 2333–2337 (2016).

291. Antoniou, A. C. *et al.* Breast-cancer risk in families with mutations in PALB2. *N. Engl. J. Med.* **371**, 497–506 (2014).

292. Buisson, R. *et al.* Cooperation of breast cancer proteins PALB2 and piccolo BRCA2 in stimulating homologous recombination. *Nat. Struct. Mol. Biol.* **17**, 1247–1254 (2010).

293. Lee, J. E. A. *et al.* Molecular analysis of PALB2 -associated breast cancers. *J. Pathol.* **245**, 53–60 (2018).

294. Mirza, M. R. *et al.* Niraparib Maintenance Therapy in Platinum-Sensitive, Recurrent Ovarian Cancer. *N. Engl. J. Med.* **375**, 2154–2164 (2016).

295. Brown, J. S., Kaye, S. B. & Yap, T. A. PARP inhibitors: the race is on. *Br. J. Cancer* **114**, 713–715 (2016).

296. Wästberg, B. A., Erlandsson, L. K. & Eklund, M. Client perceptions of a work rehabilitation programme for women: The Redesigning Daily Occupations (ReDO) project. *Scand. J. Occup. Ther.* **20**, 118–126 (2013).

297. Domchek, S. M. Reversion Mutations with Clinical Use of PARP Inhibitors: Many Genes, Many Versions. *Cancer Discov.* **7**, 937–939 (2017).

298. Findlay, S. *et al.* SHLD2/FAM35A co-operates with REV7 to coordinate DNA double-strand break repair pathway choice. *EMBO J.* **37**, e100158 (2018).

299. Tomida, J. *et al.* FAM35A associates with REV7 and modulates DNA damage responses of normal and BRCA1-defective cells. *EMBO J.* **37**, e99543 (2018).

300. Martin, R. W. *et al.* RAD51 Up-regulation Bypasses BRCA1 Function and Is a Common Feature of BRCA1-Deficient Breast Tumors. *Cancer Res.* **67**, 9658–9665 (2007).

301. Lefebvre, C. *et al.* Mutational Profile of Metastatic Breast Cancers: A Retrospective Analysis. *PLoS Med.* **13**, 1–18 (2016).

302. Chen, C.-C. *et al.* ATM loss leads to synthetic lethality in BRCA1 BRCT mutant mice associated with exacerbated defects in homology-directed repair. *Proc. Natl. Acad. Sci.* **114**, 7665–7670 (2017).

303. Balmus, G. *et al.* ATM orchestrates the DNA-damage response to counter toxic non-homologous end-joining at broken replication forks. *bioRxiv* 330043 (2018). doi:10.1101/330043

304. Zimmermann, M. *et al.* CRISPR screens identify genomic ribonucleotides as a source of PARP-trapping lesions. *Nature* **559**, 285–289 (2018).

305. Oplustilova, L. *et al.* Evaluation of candidate biomarkers to predict cancer cell sensitivity or resistance to PARP-1 inhibitor treatment. *Cell Cycle* **11**, 3837–3850 (2012).

306. Wiese, C. *et al.* Promotion of Homologous Recombination and Genomic Stability by RAD51AP1 via RAD51 Recombinase Enhancement. *Mol. Cell* **28**, 482–490 (2007).

307. Kawamoto, T. *et al.* Dual Roles for DNA Polymerase η in Homologous DNA Recombination and Translesion DNA Synthesis. *Mol. Cell* **20**, 793–799 (2005).

308. Gogola, E. *et al.* Selective Loss of PARG Restores PARylation and Counteracts PARP Inhibitor-Mediated Synthetic Lethality. *Cancer Cell* **33**, 1078-1093.e12 (2018).

309. Michelena, J. *et al.* Analysis of PARP inhibitor toxicity by multidimensional fluorescence microscopy reveals mechanisms of sensitivity and resistance. *Nat. Commun.* **9**, 2678 (2018).

310. Pettitt, S. J. *et al.* Genome-wide and high-density CRISPR-Cas9 screens identify point mutations in PARP1 causing PARP inhibitor resistance. *Nat. Commun.* **9**, 1849 (2018).

311. Kais, Z. *et al.* FANCD2 Maintains Fork Stability in BRCA1/2-Deficient Tumors and Promotes Alternative End-Joining DNA Repair. *Cell Rep.* **15**, 2488–2499 (2016).

312. Guillemette, S. *et al.* Resistance to therapy in BRCA2 mutant cells due to loss of the nucleosome remodeling factor CHD4. *Genes Dev.* **29**, 489–94 (2015).

313. Eccles, D. M. *et al. BRCA1* and *BRCA2* genetic testing—pitfalls and recommendations for managing variants of uncertain clinical significance. *Ann. Oncol.* **26**, 2057–2065 (2015).

314. Spurdle, A. B. *et al.* ENIGMA-Evidence-based network for the interpretation of germline mutant alleles: An international initiative to evaluate risk and clinical significance associated with sequence variation in BRCA1 and BRCA2 genes. *Hum. Mutat.* **33**, 2–7 (2012).

315. Duran-Lozano, L. *et al.* Alternative transcript imbalance underlying breast cancer susceptibility in a family carrying PALB2 c.3201+5G>T. *Breast Cancer Res. Treat.* (2018). doi:10.1007/s10549-018-05094-8

316. Lee, J. E. A. *et al.* Molecular analysis of PALB2 associated breast cancers. *J. Pathol.* (2018). doi:10.1002/path.5055

317. Mateo, J. *et al.* DNA-Repair Defects and Olaparib in Metastatic Prostate Cancer. *N. Engl. J. Med.* **373**, 1697–1708 (2015).

318. Shen, J. *et al.* ARID1A Deficiency Impairs the DNA Damage Checkpoint and Sensitizes Cells to PARP Inhibitors. *Cancer Discov.* **5**, 752–767 (2015).

319. Yu, H. *et al.* Tumor suppressor and deubiquitinase BAP1 promotes DNA double-strand break repair. *Proc. Natl. Acad. Sci.* **111**, 285–290 (2014).

320. Parrotta, R. *et al.* A Novel BRCA1-Associated Protein-1 Isoform Affects Response of Mesothelioma Cells to Drugs Impairing BRCA1-Mediated DNA Repair. *J. Thorac. Oncol.* **12**, 1309–1319 (2017).

321. Lee, J.-M. *et al.* Phase I/Ib Study of Olaparib and Carboplatin in BRCA1 or BRCA2 Mutation-Associated Breast or Ovarian Cancer With Biomarker Analyses. *JNCI J. Natl. Cancer Inst.* **106**, dju089 (2014).

322. Balmaña, J. *et al.* Phase I trial of olaparib in combination with cisplatin for the treatment of patients with advanced breast, ovarian and other solid tumors. *Ann. Oncol.* **25**, 1656–1663 (2014).

323. Kreahling, J. M. *et al.* MK1775, a Selective Wee1 Inhibitor, Shows Single-Agent Antitumor Activity against Sarcoma Cells. *Mol. Cancer Ther.* **11**, 174–182 (2012).

324. Do, K. *et al.* Phase I Study of Single-Agent AZD1775 (MK-1775), a Wee1 Kinase Inhibitor, in Patients With Refractory Solid Tumors. *J. Clin. Oncol.* **33**, 3409–3415 (2015).

325. Toledo, L., Neelsen, K. J. & Lukas, J. Replication Catastrophe: When a Checkpoint Fails because of Exhaustion. *Mol. Cell* **66**, 735–749 (2017).

326. Young, L. A. *et al.* Abstract 2826: Differential activity of ATR and WEE1 inhibitors in DLBCL subtypes is linked to replication stress and differences in mode of action. *Cancer Res.* **78**, 2826–2826 (2018).

327. Lallo, A. *et al.* The Combination of the PARP Inhibitor Olaparib and the WEE1 Inhibitor AZD1775 as a New Therapeutic Option for Small Cell Lung Cancer. *Clin. Cancer Res.* **24**, 5153–5164 (2018).

328. Weston, V. J. *et al.* The PARP inhibitor olaparib induces significant killing of ATM-deficient lymphoid tumor cells in vitro and in vivo. *Blood* **116**, 4578–4587 (2010).

329. Williamson, C. T. *et al.* ATM Deficiency Sensitizes Mantle Cell Lymphoma Cells to Poly(ADP-Ribose) Polymerase-1 Inhibitors. *Mol. Cancer Ther.* **9**, 347–357 (2010).

330. Toledo, L. I. *et al.* A cell-based screen identifies ATR inhibitors with synthetic lethal properties for cancer-associated mutations. *Nat. Struct. Mol. Biol.* **18**, 721–7 (2011).

331. Soucy, T. A. *et al.* An inhibitor of NEDD8-activating enzyme as a new approach to treat cancer. *Nature* **458**, 732–736 (2009).

332. Yang, L. *et al.* Repression of BET activity sensitizes homologous recombination–proficient cancers to PARP inhibition. *Sci. Transl. Med.* **9**, eaal1645 (2017).

333. Sun, C. *et al.* BRD4 Inhibition Is Synthetic Lethal with PARP Inhibitors through the Induction of Homologous Recombination Deficiency. *Cancer Cell* **33**, 401-416.e8 (2018).

334. Mo, W. *et al.* mTOR Inhibitors Suppress Homologous Recombination Repair and Synergize with PARP Inhibitors via Regulating SUV39H1 in BRCA-Proficient Triple-Negative Breast Cancer. *Clin. Cancer Res.* **22**, 1699–1712 (2016).

335. Sun, C. *et al.* Rational combination therapy with PARP and MEK inhibitors capitalizes on therapeutic liabilities in *RAS* mutant cancers. *Sci. Transl. Med.* **9**, eaal5148 (2017).

336. Li, L. *et al.* Androgen receptor inhibitor–induced “BRCAness” and PARP inhibition are synthetically lethal for castration-resistant prostate cancer. *Sci. Signal.* **10**, eaam7479 (2017).

337. Juvekar, A. *et al.* Combining a PI3K Inhibitor with a PARP Inhibitor Provides an Effective Therapy for BRCA1-Related Breast Cancer. *Cancer Discov.* **2**, 1048–1063 (2012).

338. Le, D. T. *et al.* PD-1 Blockade in Tumors with Mismatch-Repair Deficiency. *N. Engl. J. Med.* **372**, 2509–2520 (2015).

339. Le, D. T. *et al.* Mismatch repair deficiency predicts response of solid tumors to PD-1 blockade. *Science (80-.).* **357**, 409–413 (2017).

340. Germano, G. *et al.* Inactivation of DNA repair triggers neoantigen generation and impairs tumour growth. *Nature* **552**, 116–120 (2017).

341. Woo, S.-R., Corrales, L. & Gajewski, T. F. Innate Immune Recognition of Cancer. *Annu. Rev. Immunol.* **33**, 445–474 (2015).

342. Parkes, E. E. *et al.* Activation of STING-Dependent Innate Immune Signaling By S-Phase-Specific DNA Damage in Breast Cancer. *J. Natl. Cancer Inst.* **109**, djw199 (2017).

343. Tutt, A. The TNT trial: A randomized phase III trial of carboplatin (C) compared with docetaxel (D) for patients with metastatic or recurrent locally advanced triple negative or BRCA1/2 breast cancer (CRUK/07/012). *SABCS Annu. Meet.* **S3**-**01**, (2014).

344. Brown, J. S., Sundar, R. & Lopez, J. Combining DNA damaging therapeutics with immunotherapy: more haste, less speed. *Br. J. Cancer* **118**, 312–324 (2018).

Pictures used to make Figures 1, 7, 8 and 33 were downloaded and adapted from https://smart.servier.com.

APPENDIX

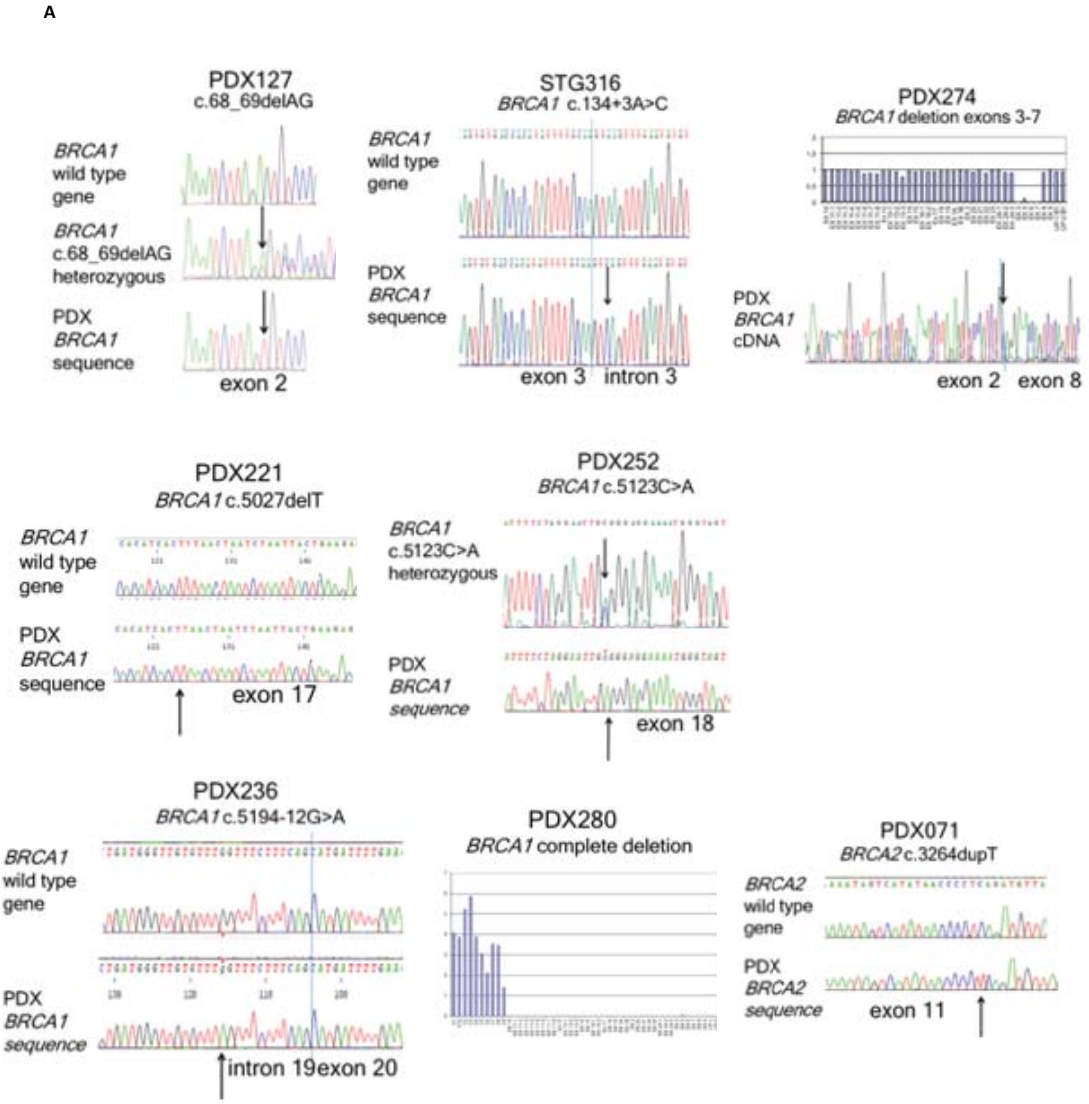

Figure S1 | **Confirmation of the germline *BRCA1/2* mutations in the PDX models of cohort-1.** Orthogonal validation of the germline *BRCA1/2* mutations identified by MiSeq using Sanger sequencing and/or MLPA is shown. PDX127 is shown as an example for the *BRCA1* mutation c.68_69delAG, also identified in PDX179 and PDX230. Of note, PDX274 lacks the germline *BRCA1* c.211A>G mutation in exon 5 due to an out-of-frame deletion of exons 3-7 of *BRCA1* in the pathogenic allele, unveiled by massively parallel sequencing and MLPA. This deletion was confirmed at the somatic level in the original patient´s tumor and thus was not acquired in the PDX. The out-of-frame deletion of *BRCA1* exons 3-7 in PDX274 was predicted to cause a premature stop codon and a non-functional protein, thus it is not a secondary mutation restoring the open reading frame. Electropherograms are shown. Arrows indicate the specific mutations. Vertical lines indicate exon-intron boundaries, when applicable.

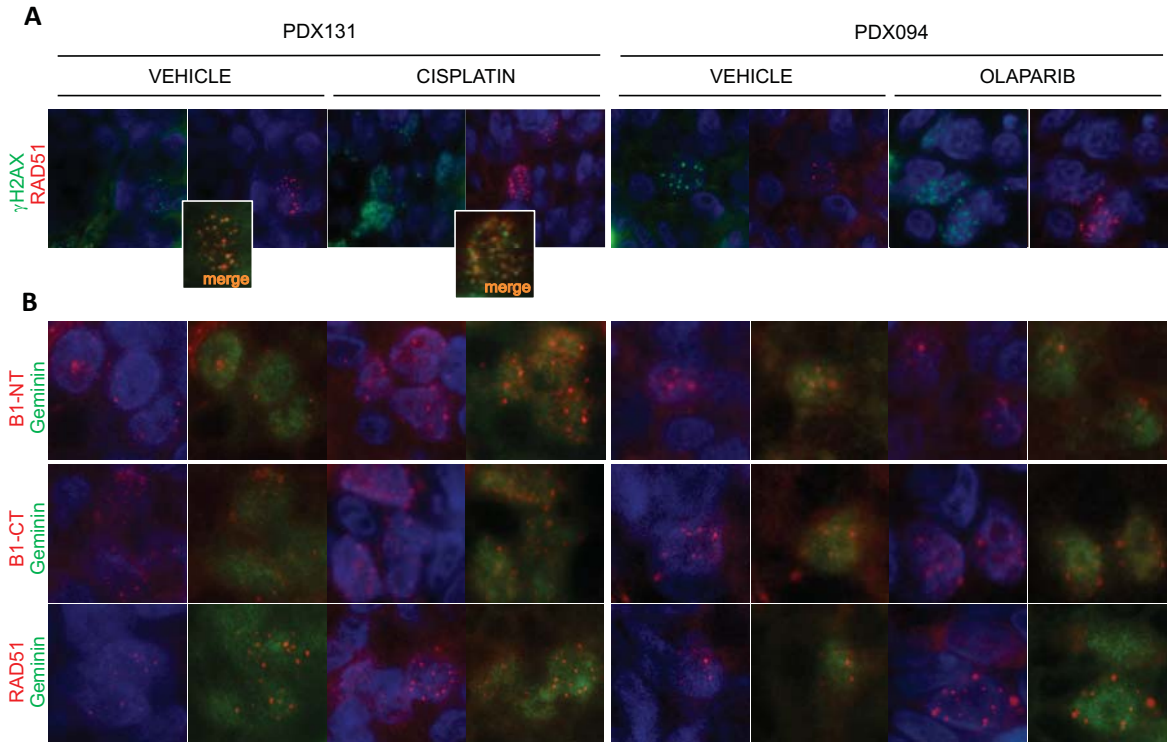

Figure S2 | **Setup of HRR markers by IF in FFPE samples from breast cancer PDX tumors. A)** Immunofluorescence staining of γH2AX and RAD51 following cisplatin or olaparib treatment in a luminal B *BRCA1/2* wild type breast cancer model (PDX131) and a triple negative *BRCA1/2* wild type breast cancer model (PDX094) **B)** Assessment of the HRR markers BRCA1 [with an antibody toward the N-terminus (B1-NT) or C-terminus (B1-CT) of BRCA1] and RAD51 in cells in the S/G2-phase of the cell cycle (geminin-positive) by immunofluorescence in FFPE samples of PDX131 and PDX094. Nuclei were visualized with DAPI (blue). All pictures were taken at 600x magnification.

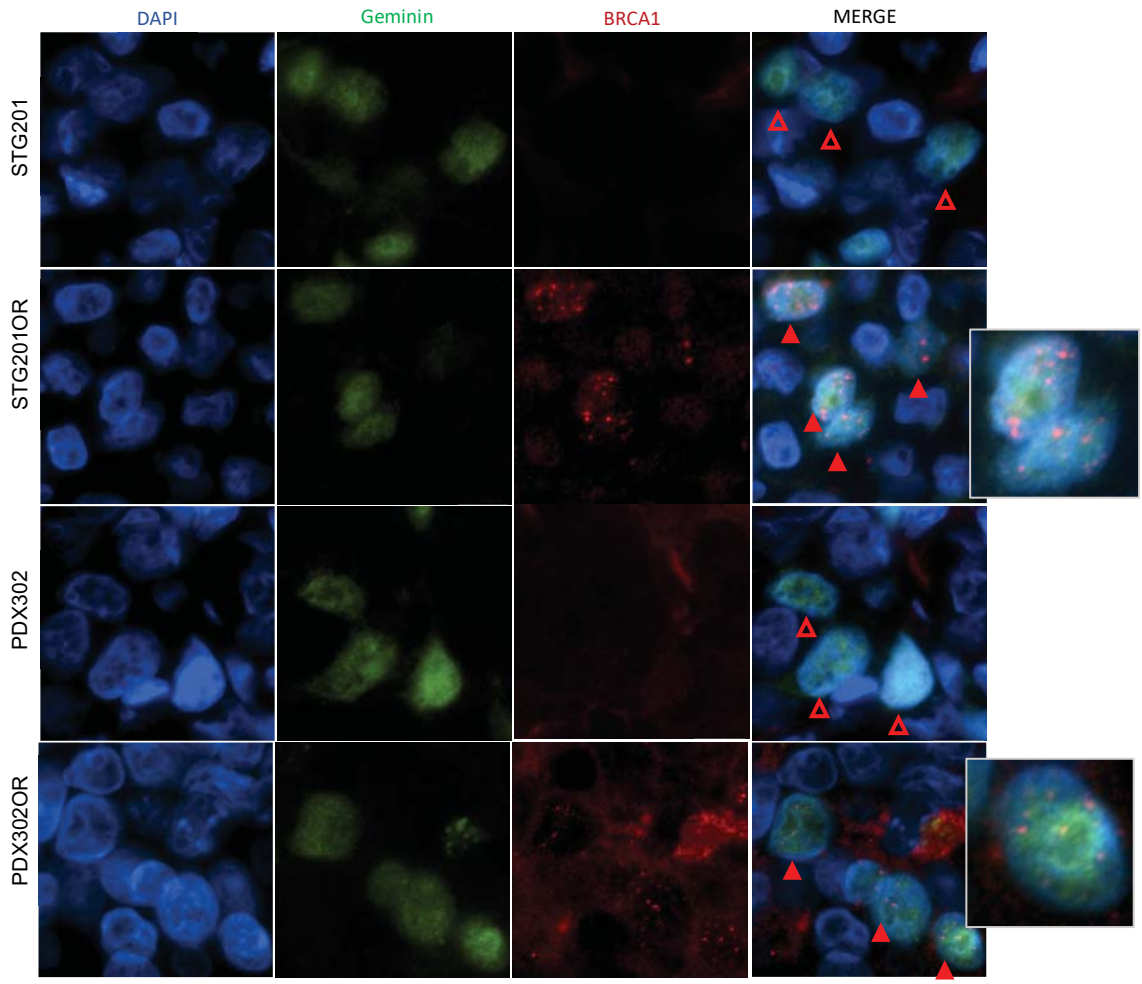

Figure S3 | **Restoration of BRCA1 foci formation in PARPi acquired-resistant PDXs.** Immunofluorescence staining of BRCA1 foci in PARPi-treated tumors from STG201, PDX302 and the corresponding PARPi acquired-resistant models (STG201OR and PDX302OR). Empty arrowheads show geminin-positive cells with no BRCA1 foci. Solid arrowheads indicate geminin-positive cells with BRCA1 nuclear foci. Nuclei were visualized with DAPI (blue). All pictures were taken at 600x magnification. Larger views of positive cells are shown in each case.

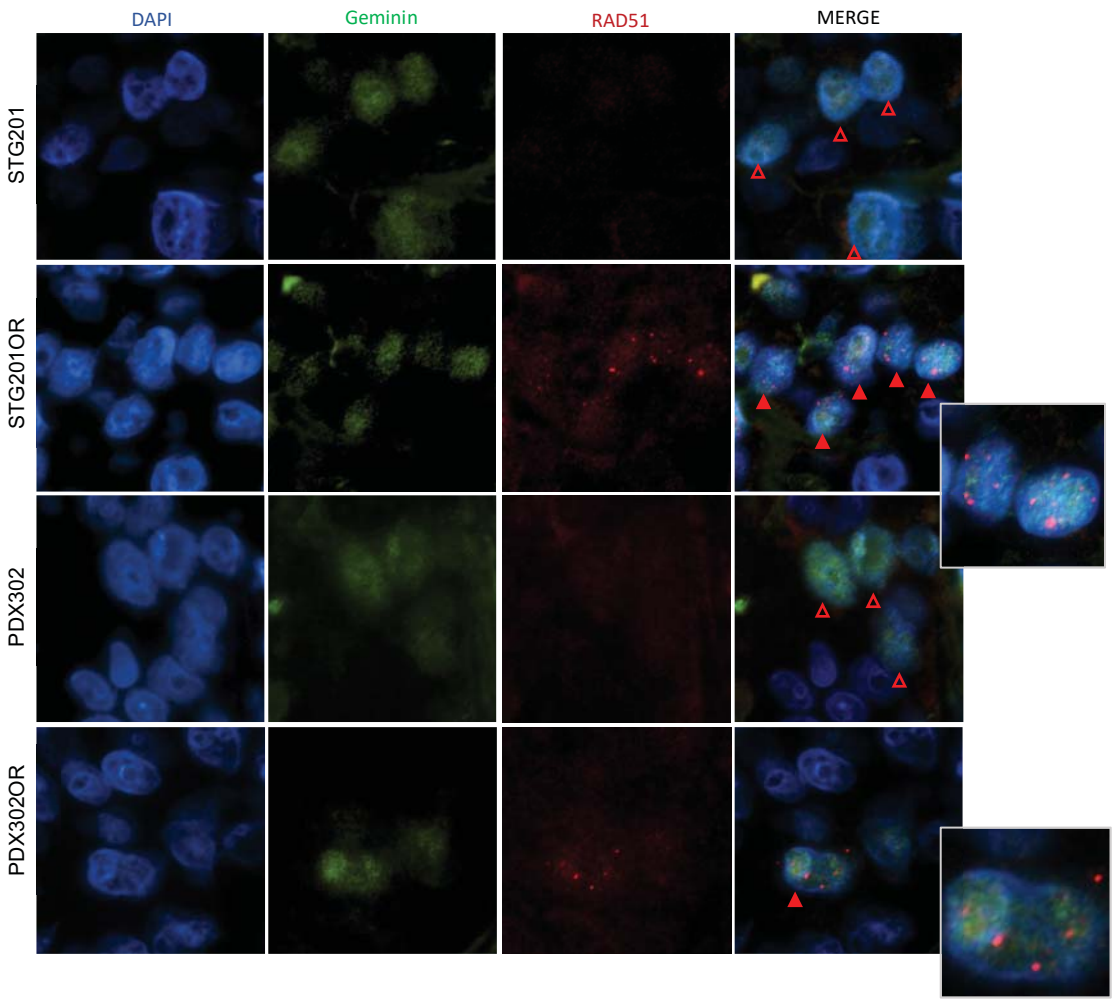

Figure S4 | Restoration of RAD51 foci formation in PARPi acquired-resistant PDXs. Immunofluorescence staining of RAD51 foci in PARPi-treated tumors from STG201, PDX302 and the corresponding PARPi acquired-resistant models (STG201OR and PDX302OR). Empty arrowheads show geminin-positive cells with no RAD51 foci. Solid arrowheads indicate geminin-positive cells with RAD51 nuclear foci. Nuclei were visualized with DAPI (blue). All pictures were taken at 600x magnification. Larger views of positive cells are shown in each case.

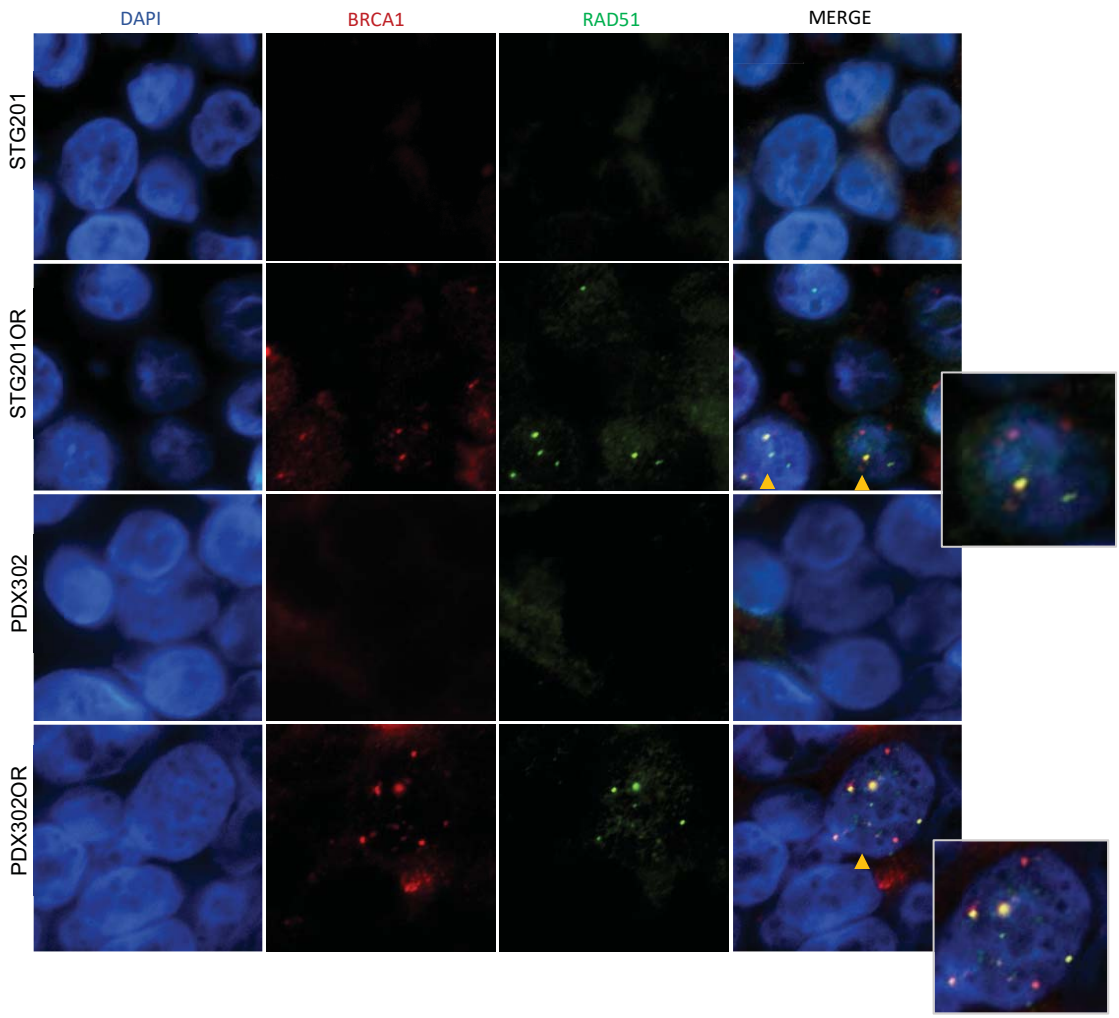

Figure S5 | **Restoration of RAD51 and BRCA1 foci formation in PARPi acquired-resistant PDXs.** Immunofluorescence staining of RAD51 and BRCA1 foci in PARPi-treated tumors from STG201, PDX302 and the corresponding PARPi acquired-resistant models (STG201OR and PDX302OR). Yellow arrowheads show cells with both RAD51 and BRCA1 nuclear foci. Nuclei were visualized with DAPI (blue). All pictures were taken at 600x magnification. Larger views of positive cells are shown in each case.

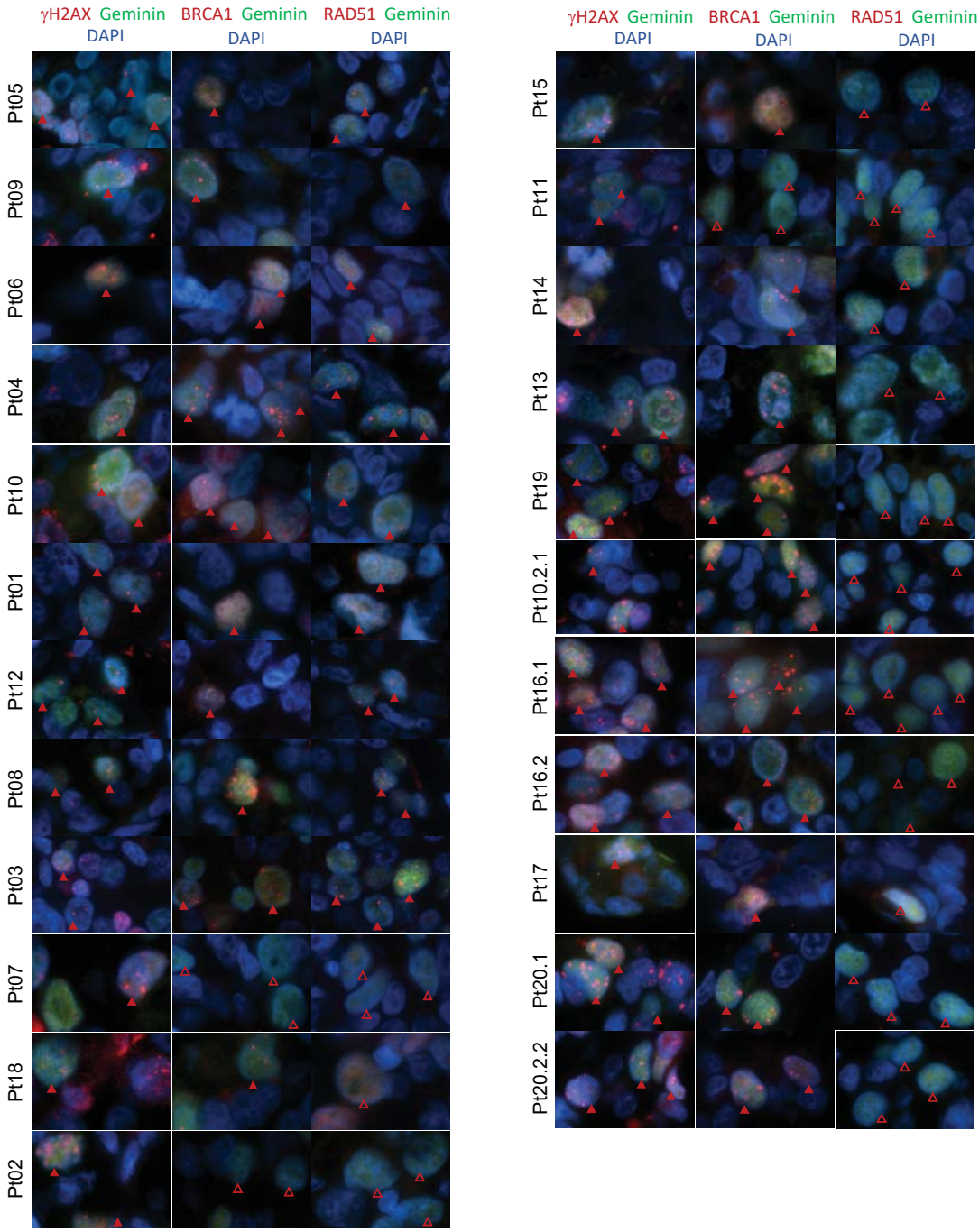

Figure S6 | γH2AX, RAD51 and BRCA1 foci in tumors from patients with HBOC syndrome, including germline *PALB2*-mutation carriers. Immunofluorescence staining of γH2AX, BRCA1 and RAD51 nuclear foci in FFPE tumors from patients. S/G2-phase cells (geminin-positive, green) with or without γH2AX, BRCA1 or RAD51 foci (red) are indicated with filled and empty red arrowheads, respectively. Nuclei were visualized with DAPI (blue). All pictures were taken at 600x magnification.

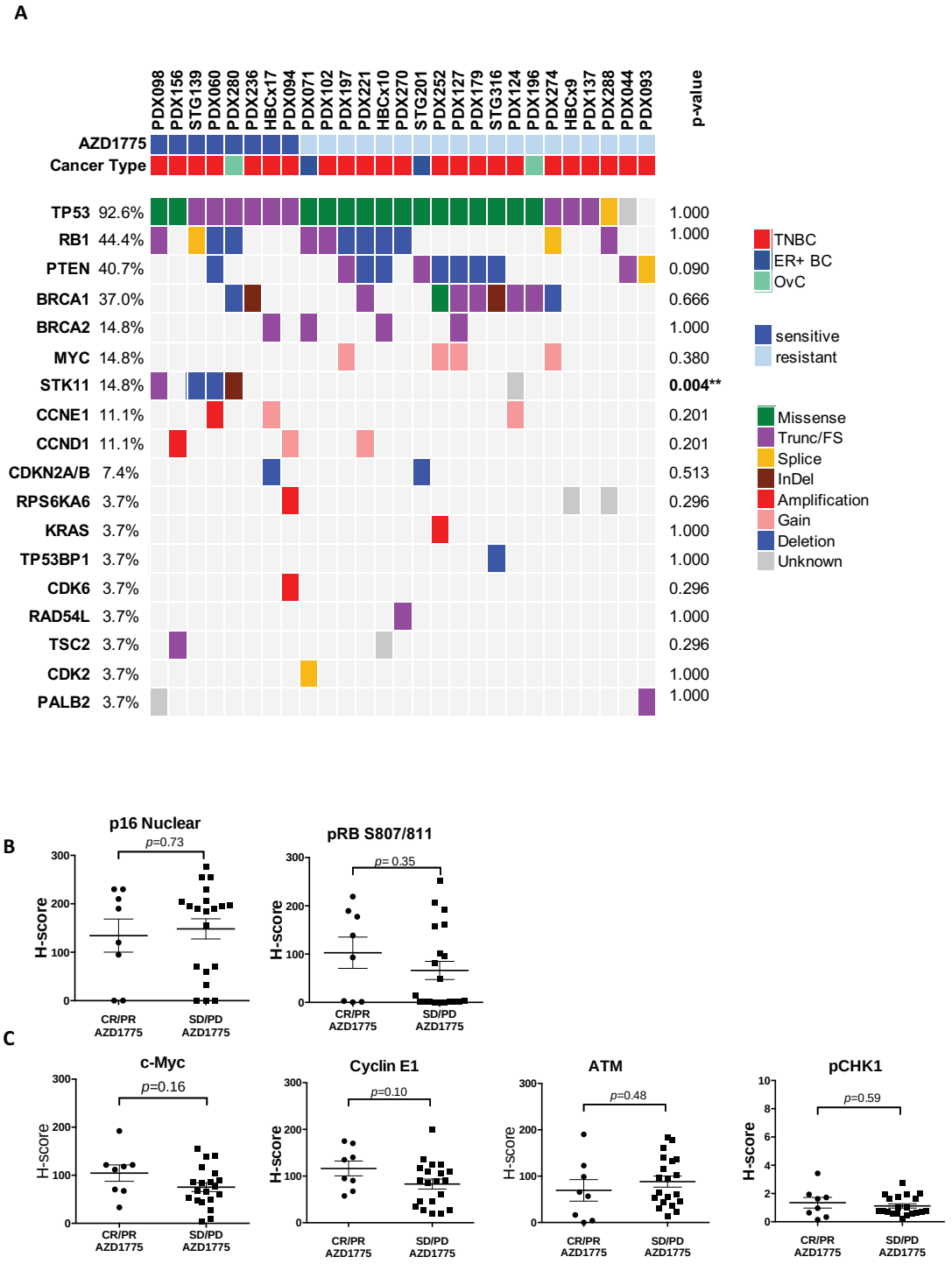

Figure S7 | **Biomarkers of response to WEE1 inhibition.** Results from **A)** exome sequencing and **B-C)** western blot analysis of different markers related with WEE1i response, including **B)** early entry in S-phase and **C)** RS response.

Table S1 | **Exome sequencing results of HRR-related genes in PDX cohort-2.** CNA, Copy number alteration.

PDX#	GENE	SV-PROTEIN-CHANGE	SV-CDS-CHANGE	SOMATIC STATUS/ FUNCTIONAL IMPACT	VAF	CNA-TYPE	known-Other
PDX044	***PTEN***	C211fs	c.631dupT	likely	1,00	-	Trunc/FS
	TP53	V272_R273delinsG	c.815_817delTGC	unknown	0,99	-	unknown-InDel
PDX060	***CCNE1***	-	-	NA	-	amplification	amplification
	MSH6	D763H	c.2287G>C	unknown	0,33	-	unknown-Missense
	PMS2	G857A	c.2570G>C	likely	0,34	-	known-Missense
	POLD2	L132M	c.394C>A	unknown	0,45	-	unknown-Missense
	PTEN	-	-	NA	-	loss	Deletion
	RAD50	-	-	NA	-	loss	Deletion
	SHPRH	R878*	c.2632C>T	likely	0,72	-	Trunc/FS
	TDG	splice	c.408+1_409-1del	likely	0,09	-	Splice
	TP53	R306*	c.916C>T	known	1,00	-	Trunc/FS
PDX093	***FAM175B***	-	-	NA	-	loss	Deletion
	PALB2	M296Nfs	c.886dupA	likely	0,44	-	Trunc/FS
	PMS2	G857A	c.2570G>C	likely	0,42	-	known-Missense
	POLB	V177_R182delinsG	c.530_544delTCTGTGGCAGTTTCA	unknown	1,00	-	unknown-InDel
	PTEN	splice	c.209+2delT	likely	1,00	-	Splice
	RAD50	R365Q	c.1094G>A	unknown	0,93	-	unknown-Missense
	RIF1	G389C	c.1165G>T	unknown	0,52	-	unknown-Missense
	RTEL1	A435T	c.1303G>A	unknown	0,49	-	unknown-Missense
	TDG	splice	c.23+1_24-1del	likely	0,09	-	Splice
PDX093OR	***FAM175B***	-	-	NA	-	loss	Deletion
	FANCI	-	-	NA	-	amplification	amplification
	PMS2	G857A	c.2570G>C	likely	0,52	-	known-Missense
	POLB	V177_R182delinsG	c.530_544delTCTGTGGCAGTTTCA	unknown	0,32	-	unknown-InDel
	POLG	-	-	NA	-	amplification	amplification

	PTEN	splice	c.209+2delT	likely	0,98	-	Splice
	RAD50	R365Q	c.1094G>A	unknown	0,98	-	unknown-Missense
	RIF1	G389C	c.1165G>T	unknown	0,54	-	unknown-Missense
	RTEL1	A435T	c.1303G>A	unknown	0,45	-	unknown-Missense
PDX094	***ATM***	E2294D	c.6882A>T	unknown	0,99	-	unknown-Missense
	BLM	F194fs	c.581_582delTT	known	0,30	-	Trunc/FS
	DDX11	E201K	c.601G>A	unknown	0,09	-	unknown-Missense
	FANCL	I40V	c.118A>G	unknown	0,33	-	unknown-Missense
	GTF2H3	-	-	NA	-	amplification	amplification
	MAD2L1	-	-	NA	-	amplification	amplification
	PARP2	E350D	c.1050G>C	unknown	0,40	-	unknown-Missense
	PMS2	G857A	c.2570G>C	likely	0,40	-	known-Missense
	TP53	G266*	c.796G>T	known	1,00	-	Trunc/FS
PDX098	***ATM***	V1912L	c.5734G>C	unknown	1,00	-	unknown-Missense
	DNTTIP2	T640fs	c.1918dupA	likely	0,37	-	Trunc/FS
	MPG	R246C	c.736C>T	unknown	0,26	-	unknown-Missense
	PALB2	V78I	c.232G>A	unknown	0,34	-	unknown-Missense
	TP53	R249S	c.747G>T	known	1,00	-	known-Missense
	XRCC5	M427I	c.1281G>A	unknown	0,36	-	unknown-Missense
	ZW10	D615N	c.1843G>A	unknown	1,00	-	unknown-Missense
PDX102	***FANCB***	-	-	NA	-	amplification	amplification
	POLA1	-	-	NA	-	amplification	amplification
	RAD54B	K721I	c.2162A>T	unknown	0,11	-	unknown-Missense
	TOP3B	S767P	c.2299T>C	unknown	0,09	-	unknown-Missense
	TP53	Q331H	c.993G>C	known	0,99	-	known-Missense

PDX137	***ATR***	A901P	c.2701G>C	unknown	0,15	-	unknown-Missense
	ERCC2	R616P	c.1847G>C	unknown	0,66	-	unknown-Missense
	PARP4	V458I	c.1372G>A	unknown	0,15	-	unknown-Missense
	PMS2	G857A	c.2570G>C	likely	0,69	-	known-Missense
	POLB	L11fs	c.32_33delTC	likely	0,45	-	Trunc/FS
	REV1	-	-	NA	-	amplification	amplification
	TP53	S166*	c.497C>G	known	1,00	-	Trunc/FS
STG139	***CUL4A***	-	-	NA	-	amplification	amplification
	ERCC5	-	-	NA	-	amplification	amplification
	GTF2H2	-	-	NA	-	amplification	amplification
	LIG4	-	-	NA	-	amplification	amplification
	PER1	-	-	NA	-	amplification	amplification
	PMS2	G857A	c.2570G>C	likely	0,78	-	known-Missense
	RNASEH2A	-	-	NA	-	amplification	amplification
	SHPRH	D1673E	c.5019C>G	unknown	0,40	-	unknown-Missense
	SLX4	P763S	c.2287C>T	unknown	0,42	-	unknown-Missense
	SLX4	P763S	c.2287C>T	unknown	0,42	-	unknown-Missense
	SMARCA4	-	-	NA	-	amplification	amplification
	TP53	E258*	c.772G>T	known	0,99	-	Trunc/FS
	TREX2	G169V	c.506G>T	unknown	0,27	-	unknown-Missense
PDX156	***MSH3***	A57P	c.169G>C	unknown	0,22	-	unknown-Missense
	POLB	-	-	NA	-	amplification	amplification
	POLG	Q53dup	c.156_158dupGCA	unknown	0,74	-	unknown-Other
	TOP3B	S767P	c.2299T>C	unknown	0,08	-	unknown-Missense
	TP53	R280K	c.839G>A	known	1,00	-	known-Missense
PDX197	***CLK2***	Y430C	c.1289A>G	unknown	0,48	-	unknown-Missense
	CUL4A	-	-	NA	-	amplification	amplification

	ERCC5	-	-	NA	-	amplification	amplification
	GTF2H1	K60T	c.179A>C	unknown	0,27	-	unknown-Missense
	LIG1	R643H	c.1928G>A	unknown	0,95	-	unknown-Missense
	LIG4	G120E	c.359G>A	unknown	0,11	-	unknown-Missense
	MSH2	N596S	c.1787A>G	unknown	0,98	-	unknown-Missense
	MSH3	A57_A65del	c.169_195delGCCGCAGCGGCCGCAGCGCCCCCAGCG	unknown	0,10	-	unknown-InDel
	NBN	K223E	c.667A>G	unknown	0,17	-	unknown-Missense
	PTEN	S229*	c.686C>G	likely	1,00	-	Trunc/FS
	RECQL5	A757P	c.2269G>C	unknown	0,38	-	unknown-Missense
	TP53	R175H	c.524G>A	known	0,98	-	known-Missense
STG201	***FANCD2***	S64fs	c.192_195delTCAG	likely	0,98	-	Trunc/FS
	GTF2H4	-	-	NA	-	loss	Deletion
	POLG	Q53dup	c.156_158dupGCA	unknown	0,79	-	unknown-Other
	POLH	S512fs	c.1535_1559delCACCATCCAAGCCCTCATTACCTTT	likely	0,95	-	Trunc/FS
	PTEN	G165fs	c.495_516delAGTAACTATTCCCAGTCAGAGG	likely	1,00	-	Trunc/FS
	TP53	M237I	c.711G>A	known	0,90	-	known-Missense
STG201OR	***FANCD2***	S64fs	c.192_195delTCAG	likely	1,00	-	Trunc/FS
	POLD1	V866V	c.2598G>C	unknown	0,53	-	unknown-Other
	POLG	Q53dup	c.156_158dupGCA	unknown	0,78	-	unknown-Other
	POLH	S512fs	c.1535_1559delCACCATCCAAGCCCTCATTACCTTT	likely	1,00	-	Trunc/FS
	PTEN	V166fs	c.495_516delAGTAACTATTCCCAGTCAGAGG	likely	0,95	-	Trunc/FS
	RAD17	K535fs	c.1605_1605+2delGGT	likely	0,39	-	Trunc/FS
	RECQL5	splice	c.1586-3_1586-2dupCA	likely	0,73	-	Splice
	TDG	-	c.-78402696_793-7del	unknown	0,20	-	unknown-Other
	TP53	M237I	c.711G>A	known	1,00	-	known-Missense
PDX270	***CHAF1A***	G197V	c.590G>T	unknown	0,40	-	unknown-Missense
	RAD54L	V516fs	c.1546delG	likely	1,00	-	Trunc/FS

	RECQL5	K931N	c.2793G>C	unknown	0,08	-	unknown-Missense
	SMC1B	R1210P	c.3629G>C	unknown	0,31	-	unknown-Missense
	TP53	S241A	c.721T>G	known	0,96	-	known-Missense
	TP73	T188A	c.562A>G	unknown	0,09	-	unknown-Missense
PDX288	***ERCC5***	S1097C	c.3290C>G	unknown	0,23	-	unknown-Missense
	POLB	-	-	NA	-	amplification	amplification
	TP53	splice	c.993+1G>A	known	0,99	-	Splice
PDX291	***RECQL5***	splice	c.1586-3_1586-2dupCA	likely	0,47	-	Splice
	SMARCAL1	C562F	c.1685G>T	unknown	0,08	-	unknown-Missense
	TDG	-	c.-78402712_793-5del	unknown	0,77	-	unknown-Other
	TP53	Y107fs	c.321delC	known	0,99	-	Trunc/FS
	UNG	P172T	c.514C>A	unknown	0,45	-	unknown-Missense
PDX302	***CLSPN***	E43D	c.129A>C	unknown	0,22	-	unknown-Missense
	DCLRE1A	R138*	c.412C>T	likely	1,00	-	Trunc/FS
	DDB2	splice	c.1024-5_1077delCCTAGGCAGCCTGGCATCCTCGCTACAACCTCATTGTTGTGGGCCGATACCCAGATCCT	likely	0,18	-	Splice
	RAD17	splice	c.1605_1605+2delGGTinsAAA	likely	0,14	-	Splice
	REV1	A1090_S1091insSA	c.3264_3269dupCAGCGC	unknown	0,52	-	unknown-InDel
	TOP1MT	A88V	c.263C>T	unknown	1,00	-	unknown-Missense
	TP53	T256fs	c.766dupA	known	1,00	-	Trunc/FS
PDX302OR	***CLSPN***	E43D	c.129A>C	unknown	0,30	-	unknown-Missense
	DCLRE1A	R138*	c.412C>T	likely	1,00	-	Trunc/FS
	DDB2	splice	c.1024-5_1077delCCTAGGCAGCCTGGCATCCTCGCTACAACCTCATTGTTGTGGGCCGATACCCAGATCCT	likely	0,38	-	Splice
	REV1	A1090_S1091insSA	c.3264_3269dupCAGCGC	unknown	0,47	-	unknown-InDel
	TOP1MT	A88V	c.263C>T	unknown	1,00	-	unknown-Missense
	TP53	T256fs	c.766dupA	known	1,00	-	Trunc/FS

Table S2 | **73-gene profiling results of PDX cohort-3.**

PDX#	GENE	SV-PROTEIN-CHANGE	SV-CDS-CHANGE	SOMATIC STATUS/ FUNCTIONAL IMPACT	HOMOZYGOSITY
HBCx1	*TP53*	L188 fs35aaTer		known	homozygous
HBCx2	*AKT1*	E17K		known	homozygous
	RB1	del from ex18		known	
	TP53	A276D		known	homozygous
HBCx3	*PTEN*	P246 fs8aa		known	homozygous
	TP53	Q144Ter		known	homozygous
HBCx6	*NF1*	S1030Ter		new	heterozygous
	RB1	del ex1-17		known	
	TP53	T102 fs19aaTer		known	homozygous
HBCx7	*ARID1A*	M1673Ter		new	heterozygous
	ATM	D1853N		known	heterozygous
	CDKN2A	-		deletion	
	EP300	D1713Ter		new	heterozygous
	KDR	chr4-55976819-A->G-(spliceSite)		new	heterozygous
	MLL3	Q2054Ter		new	
	ROS1	Q1369Ter		new	homozygous
HBCx8	*BRCA1*	Q81*	c.241C>T	likely	homozygous
	NRAS	Q61K		known	heterozygous
HBCx9	*ATM*	Q1128R		new	homozygous
	CDH1	A617T		known	heterozygous
	TP53	V143 fs25aaTer		known	homozygous
HBCx10	*BRCA2*	Q3036*	c.9106C>T	likely	homozygous
	PTEN	del ex3		known	
	RB1	deleted gen		known	
	TP53	V157F		known	homozygous
HBCx11	*BRCA1*	K654Sfs*47	c.1961del	likely	homozygous
	ARID1A	E1924 Ter		known	heterozygous
	KDM6A	P807fs 26aa (ins 19nt)		new	heterozygous
	MLL2	E2186 fs73aa (del 16 nt)		new	heterozygous
	PI3KR1	del P568-D569-L570-I571		known	homozygous

	STK11	F354L		known	homozygous
	TP53	R249 fs96aaTer		known	homozygous
HBCx12b	***NF1***	V1764fs 9aa		new	heterozygous
	TP53	del G108-G109		known	homozygous
HBCx14	***HRAS***	E98Ter		new	heterozygous
	NOTCH1	loss		known	
	RB1	del ex1		known	
	TP53	Y163C		known	homozygous
HBCx15	***KIT***	T594I		known	heterozygous
	PITCH1	D39H		known	heterozygous
	TP53	P151H		known	homozygous
HBCx16	***PTEN***	del ex3-4-5		known	
	TP53	E180 ins in frame 6aa (GAAPTM)		known	homozygous
HBCx17	***BRCA2***	S2012Qfs*5	c.6033_6034del	likely	homozygous
	AKT1	D46E		known	homozygous
	CDKN2A	deleted gene		known	
	KDM6A	partially deleted gene		known	
	TP53	H193 fs53aaTer		known	homozygous
HBCx23	***CDKN2A***	deleted gene		known	
	TP53	del N131		known	homozygous
HBCx24	***TP53***	K292 fs11aaTer		known	homozygous
HBCx27	***ATM***	D1853N		known	heterozygous
	CDKN2A	deleted gene		known	
	KDM6A	Q1248Ter		new	homozygous
	TP53	V274D		known	homozygous
HBCx28	***BRCA1***	F46_R71del;C64*	c.212+3A>G	likely	homozygous
	PTEN	loss		known	
	TP53	R175H		known	homozygous
HBCx30	***CDKN2A***	deleted gene		known	
	PTEN	loss		known	
	TP53	F134L		known	homozygous
HBCx31	***AKT1***	E17K		known	homozygous
	TP53	R175H		known	homozygous

HBCx33	*ATRX*	M1800K		known	heterozygous
	TP53	V218E		known	homozygous
HBCx39	*TP53*	Y220C		known	homozygous
T168	*BRCA1*	S1524Lfs*24	c.4570del	likely	homozygous
	TP53	R196Ter		known	homozygous
T174	*CDKN2A*	deleted gene		known	
	PIK3CA	H1047Q		known	homozygous
	TP53	T256P		known	homozygous
T180R	*CREBBP*	deleted gene		known	
	TP53	R175H		known	heterozygous
	TP53	L130 fs38		new	heterozygous
	TSC1	deleted exons 1 to 5		known	
T298	*PALB2*	S475*	c.1424C>G	likely	homozygous
	CREBBP	P1096 fs13aa (TACAGTGCTTCTAGGGTTGG/C)		new	heterozygous
	NOTCH1	E1447 inframe del 116aa		new	homozygous
	PIK3CA	H1047Q		known	homozygous
T311R	*ATM*	N1739R		known	heterozygous
	MLL3	R2139Ter		new	heterozygous
	NF1	Q83Ter		known	homozygous
	PIK3CA	H1047Q		known	homozygous
	TP53	D259V		known	homozygous
T330	*BRCA1*	S1280*	c.3839_3844delins5	likely	homozygous
	NRAS	P185S		known	heterozygous
	TP53	E204Ter		known	homozygous
T381	*TP53*	chr17-7578370-C->T/T-(spliceSite)		known	

Your work is going to fill a large part of your life, and the only way to be truly satisfied is to do what you believe is great work. And the only way to do great work is to love what you do. If you haven't found it yet, keep looking. Don't settle. As with all matters of the heart, you'll know when you find it.

Steve Jobs

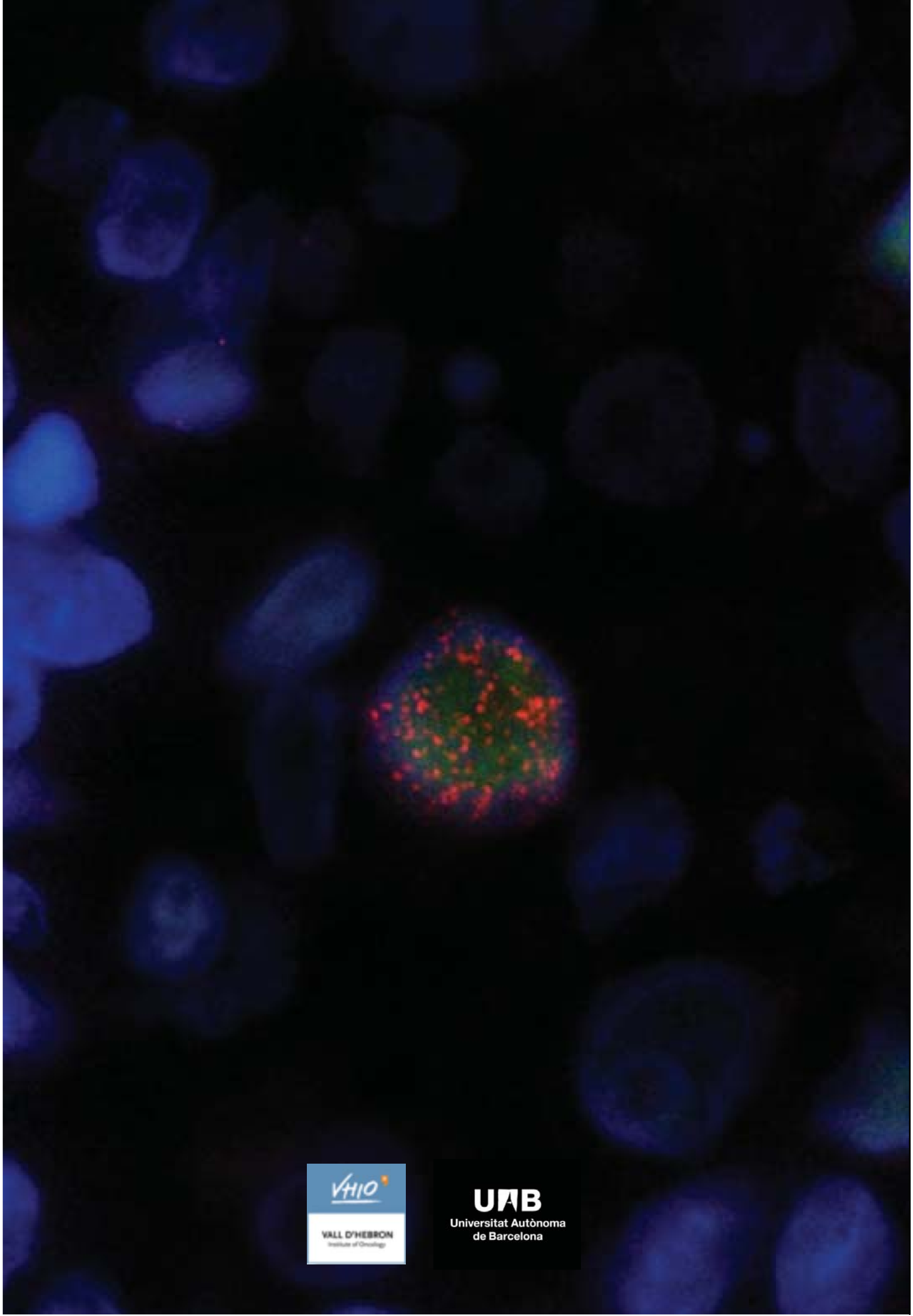
VHIO
VALL D'HEBRON
Institute of Oncology
UAB
Universitat Autònoma
de Barcelona